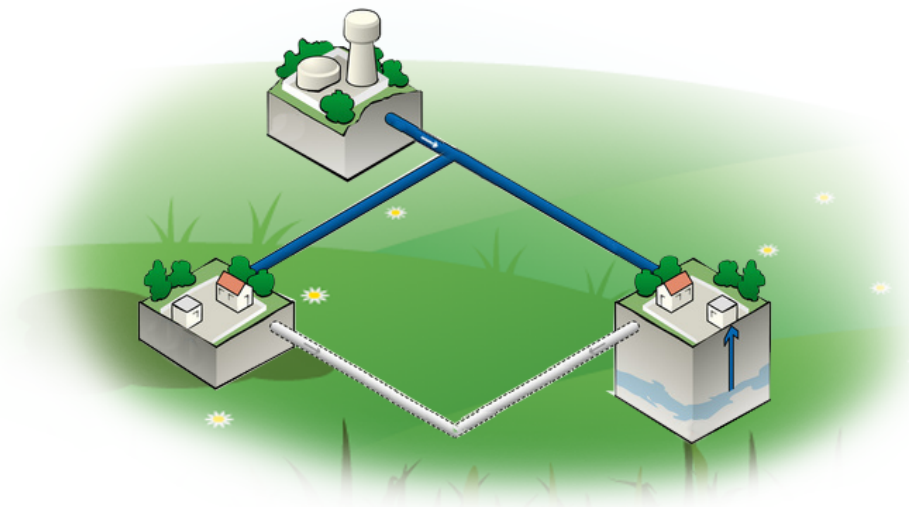


AALBORG UNIVERSITY

Pressure management in Interconnected Water Distribution Networks



Electronics and IT:
Bachelor project

Group:
16gr634



AALBORG UNIVERSITY STUDENT REPORT

Theme:

Control Engineering

Project:

Bachelor project

Projectperiod:

February 2016 - May 2016

Projectgroup:

16gr634

Participants:

Steffen Raaheide
Jacob Naundrup Pedersen
Jonatan Fuglsang Jensen

Councelers:

Tom Nørgaard Jensen
Carsten Skovmose Kallesøe

Copies: 5

Pages: 94

Appendix: 174

Completed: 25-05-2016

Sixth semester of study at The school of information and communication and technology

Electronics and IT

Fredrik Bajers Vej 7

DK-9220 Aalborg Ø, Danmark

<http://www.es.aau.dk>

Abstract:

This report addresses the work with pressure management in a potable water supply network. To supply water to the consumers, a large amount of energy is needed to maintain the correct pressure in the water distribution network. Unfortunately the high pressure leads to water leakages, typically caused by the wear and tear. To partially mitigate this problem the network is divided into smaller interconnect areas, with pressure control. Therefore it is examined how to regulate the pressure in these areas, which leads to the following problem statement:

How can multiple pressure management areas be regulated when these are interconnected and still maintaining a certain water pressure at the critical points?

A dynamic model of a physical system was derived and used to design a cascade controller, to regulate the pressure in two interconnected pressure management areas.

The cascade controller were implemented in Simulink RealTime workshop and tested on the system. The tests showed that the system were slower than calculated, but were still able to keep a reference value at the critical points.

Preface

This report is drafted by group 16gr634, a sixth semester group consisting of three persons studying EIT at Aalborg university. The purpose of this report is to document the work of the design and development of a control system for a water distribution network. It is a Bachelor project in Control Engineering and started on February 1. with a submission deadline on May 25. The group has parallel with the project participated in the following courses: "Matrix computations and Convex optimization", "Introduction to probability theory and Statistics" and "Control Engineering".

This report investigates the possibility to regulate a system of interconnected pressure management area using classic controllers. An analysis of a physical system leads to a dynamic model. Based on a requirement specification, a system design for a regulator, to control the physical system is implemented, and is held against the requirement specification in the final accepttest.

The report is drafted in cooperation with the supervisor:

- Carsten Skovmose Kallesøe, professor at Aalborg university.
- Tom Nørgaard Jensen, post doc at Aalborg university.

The figures in the report is produced by the group unless a source is specified. Sources are indicated by [author,year] and can be found in the bibliography. Appendix is indicated by A.number or [Appendix/filename] on the CD. The paper is structured in chapters, sections and subsection. Every figure, table, equation and code is separately numbered continuously. Figures can be diagrams, flowcharts and graphs. The following is placed on the CD:

- Calculations
- Datasheet
- MATLAB files
- Sources

Steffen Raahede

Jacob Naundrup Pedersen

Jonatan Fuglsang Jensen

Contents

Nomenclature	ix
1 Introduction	1
1.1 Introduction	1
1.2 Pressure management	2
1.3 Project focus	4
2 System analysis	5
2.1 Water system	5
2.2 The physical system	7
2.3 Model of components	13
2.4 Electrical equivalent	19
2.4.1 Kirchhoff's Voltage Law	21
2.4.2 Linearization	22
2.5 Determination of water flow in the operating point	25
2.6 Multiple Input and Multiple Output	29
2.7 System approximation	32
2.8 Analysis of the physical system	41
2.9 Model verification	46
3 System requirement	49
3.1 Requirement	49
3.2 Test specification	50
4 System design	51
4.1 Cascade control	51
4.2 Design of pump controller	52
4.3 Decoupling	58
4.4 Design of hydraulic controller	65
5 Implementation	73
6 Acceptttest	75
6.1 Test of steady state error	75
6.2 System response	79
7 Conclusion	85
8 Optimization	87
9 Perspective	89
10 Discussion	91
Bibliography	93
A Appendix	95
A.1 System analysis	95

A.1.1	Calculation of the pipes	95
A.1.2	Calculation of the water flow	99
A.1.3	Linear model of the centrifugal pump	103
A.1.4	KVL equations	112
A.1.5	Linearization	114
A.1.6	Multivariable equations	116
A.1.7	Rearrange of first order transfer function	119
A.2	System design	121
A.2.1	Decoupling of the TITO system	121
A.2.2	Hydraulic controller	126
A.3	Journals	130
A.3.1	Interconnection test	130
A.3.2	Step response	134
A.3.3	The water flow	143
A.3.4	Relation between differential pressure and velocity	147
A.3.5	Step response with different gains for pump	154
A.3.6	Test of steady state error	157
A.3.7	System response	163

Nomenclature

Symbols

Symbol	Description	Units
A	Area	m^2
D	Diameter	m
f	Surface resistance coefficient	.
F_{in}	Force going in	N
F_{out}	Force pushing out	N
F_r	Resistance force	N
g	Gravitational acceleration	m/s^2
h_f	Head loss for a surface resistance	m
h_m	Head loss for a form resistance	m
i_i	Current	A
k_f	Form loss coefficient	.
K_v	Conductivity of a valve	.
l	Length	m
L_i	Inductance	H
m	Mass	kg
p_{in}	Input pressure	Pa
p_{out}	Output pressure	Pa
q	Volumetric rate flow	m^3/s
R_i	Resistance	Ω
v	Velocity	m/s
V	Volume	m^3
V_i	Voltage	V
Δp	Pressure drop	Pa
ω	Angular velocity	RPM
ρ	Density	kg/m^3
J	Inertia	kg/m^3
K_{vs}	Conductivity of a fully open valve	m^3/h
\mathbf{R}	Reynolds number	.
v_f	The kinematic viscosity of fluid	m/s^2

Notation

Symbol	Description
r	Nonlinear resistance
$AN1 + AN0$	Linear pump model
V_{cc}	Main pump C_2
V_a	PMA pump C_{18}
V_b	PMA pump C_{25}
R_{17}	Electronic valve C_{20}
R_{18}	Electronic valve C_{24}

R_{19}	Electronic valve C_{27}
R_{20}	Electronic valve C_{31}
$L_1 + R_1$	Pipe C_4
$L_2 + R_2$	Pipe C_9
$L_3 + R_3$	Pipe C_8
$L_4 + R_4$	Pipe C_{13}
$L_5 + R_5$	Pipe C_{11}
$L_6 + R_6$	Pipe C_{12}
$L_7 + R_7$	Pipe C_{22}
$L_8 + R_8$	Pipe C_{21}
$L_9 + R_9$	Pipe C_{19}
$L_{10} + R_{10}$	Pipe C_{23}
$L_{11} + R_{11}$	Pipe C_{28}
$L_{12} + R_{12}$	Pipe C_{29}
$L_{13} + R_{13}$	Pipe C_{30}
$L_{14} + R_{14}$	Pipe C_{26}
$L_{15} + R_{15}$	Pipe C_{42}
$L_{16} + R_{16}$	Pipe C_{10}

Introduction 1

This chapter include the introduction for the project Pressure management in Interconnected Water Distribution Networks. A short study on existing pressure management technologies, which leads to the focus of the project being established.

1.1 Introduction

Water is a natural part of the daily life for both human, human industries and animals. The average human body loses around 2.5 to 3 liter of water every day as a result of normal body functions. If a person is not properly hydrated, one's brain can feel the effects of headache, difficulty concentrating and short-term memory loss. [Water, 2016] Even numeracy skills can be reduced, therefore, it is important that water is always accessible. That is the case in many cities and countries via water distribution networks: the consumers are supplied with water from the network, which maintain a positive and constant water pressure in the network. For the consumers to be able to use water in their daily life, the pressure in the network must be maintained at a sufficiently high minimum water pressure to be able to reach all parts of the distributing network and at the same time keep a minimum water pressure for the consumers. Therefore water distribution network is a crucial part of infrastructures in towns and cities around the globe.

To supply the consumers with safe drinking water the infrastructure needs energy to deliver it. The water supply systems are consuming a massive amount of energy. From the groundwater being extracted, to the water going through the treating process and being delivered to the consumers. Providing households with safe drinking water is thus an energy-intensive process. In the U.S., about 4 % of the total power generation is used for water supply and treatment, and in certain parts of the U.S. the number is far higher [Council, 2009].

In this process, some energy is lost due to a number of factors (e.g. ineffective pumps, resistances within the pipes and badly designed infrastructure) [Feldman, 2009]. Another factor to energy losses is water leakages which are a large contributor to energy consumption. The worldwide average water loss is estimated to be 30 % which means that the same amount of energy is lost [Feldman, 2009]. These leaks do not only cause water loss but also an economical loss because of the high cost of energy wasted on the pumping and treatment process. In extreme cases it would also pose a risk to the infrastructure such as buildings and roads [Maninder Pal and Flint, 2010]. This gives a valid reason to reduced these leaks to save energy and to minimize these risks.

Furthermore to accommodate for the water leaks the pressure is increased, therefore the energy consumption is also increased due to the friction that grows within the pipes with the increased water flow. When there is a leak in an iron or steel pipe, if e.g. one doubled

the pressure in the network then it would result in a approximately 41 % increased leakage [Wegelin, 2009].

The energy consumption could be lowered in multiple ways e.g. replacing old equipment, replacing old pumps with newer and more energy efficient pumps, replacing old pipes with newer pipes that have a lower friction or by repairing old damaged pipes. These examples are all expensive processes since most of the water distribution network is located in the underground of cities or towns and therefore it is often required that the traffic be shut down in places where the renovation is taking place which could be for a long period of time and therefore, these approaches are not deemed as a good solution to the problem.

An alternative to these solutions could be pressure management to reduce the energy consumption. Pressure management can be used to control the pressure throughout the distributed network which will ensure that the consumer has the correct pressure at the households, which at the same time reduced the pressure in the entire part of the distributed network to the minimum required pressure. It is particularly useful at night, where the demand for water is lower than it is during the daily hours. Furthermore a lower water pressure in the distribution network, result in an energy saving because the pumps deliver less hydraulic pressure to the water which is reducing the energy consumption. Additionally, a lower pressure will also decrease the leakage and minimize the probability of any new bursts or leaks in the network [Wegelin, 2009].

1.2 Pressure management

As mentioned previously, pressure management is a method that ensures the customers with the minimum water pressure, while reducing the excessive pressure on the pipes from the water supply network. Which will reduce the probability of leakage or new pipe bursts.

In pressure management there exist several systems and technologies. The system is usually set up by dividing the distribution network into smaller areas, which are called pressure management areas (PMA). PMAs can either cover a city block, an industrial area or any other area that needs to be supplied from the distribution network. A PMA is connected to the distribution network via a pressure reduction valve (PRV), which reduces the pressure inside the PMA. The PRV has the purpose of maintaining a minimum pressure at the critical point (CP) inside the PMA. The CP is defined as the end user in the PMA and requires a certain minimum pressure, so the end user at the CP, can use the water [GIZ, 2011].

The PRVs exist in many variants from more advanced PRVs, which can be time dependent to accommodate for daily variation in water use or remote controlled by a operator from a monitor to a more basic one that works like a pressure drop from the distribution network to the PMA.

In the next part, two examples for pressure reduction in a PMA will be presented, one of which is using a basic PRV and another one using pumps.

Figure 1.1 illustrates a distribution network leading into a PMA which has a PRV to regulate the water pressure into the CP.

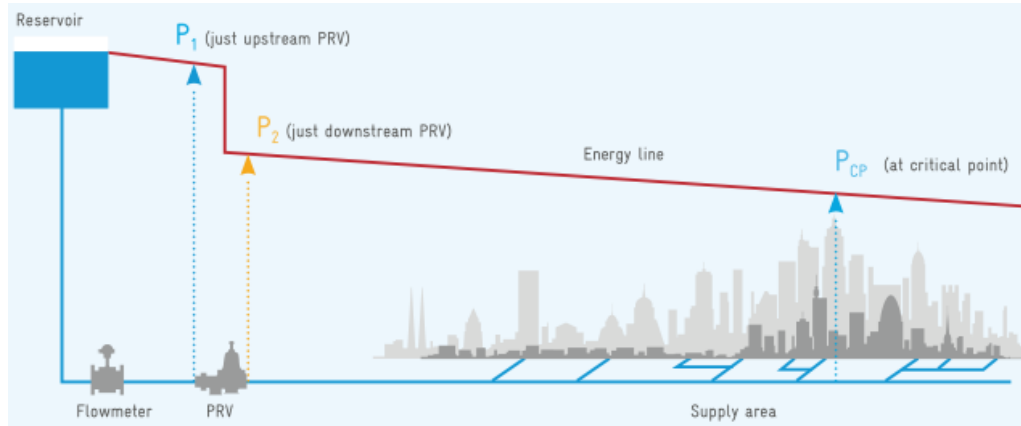


Figure 1.1: Show that the pressure from the distribution network to the PMA is reduced by a PRV [GIZ, 2011].

As shown on figure 1.1, the pressure drops after the PRV and therefore the pressure into the PMA at the CP gets lowered, which means that the pressure is lower than it would have been if the water came directly from the reservoir. If the water came directly from the reservoir, the pressure would have been much higher at the CP and it could have caused increased water loss and damage to the distribution network. A downside of PRV is that it reduces the pressure which means that it consumes the energy that has been used in the water reservoir to increase the pressure.

Figure 1.2 illustrates the same network as figure 1.1 but with a pump instead of a PRV.

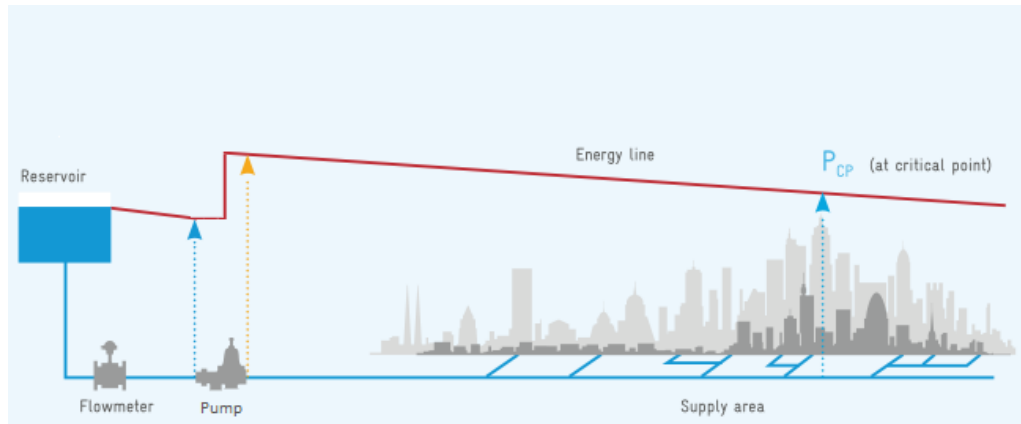


Figure 1.2: The pressure from the distribution network to the PMA is increased by a pump. The figure is from [GIZ, 2011] but with changes, that have been made to illustrate the point of pressure management with a pump. The original figure [GIZ, 2011] has been modified to fit the needs of the report.

The pump on figure 1.2 is used to boost the pressure into the PMA which enables the water reservoir able to use less energy on creating a certain amount of water pressure. A problem arises when using pumps instead of PRV: when several pumps are connected to the same network, instability can occur when feedback control is used for the pump.

1.3 Project focus

In this section the focus of this project will be established, based on the previous section.

The focus of this project will be to regulate a system of interconnected pumps, valves and pipes, which could have instability problems when feedback control is used. The goal is to find a solution for this instability problem, so the system is stable and will be able to keep a certain pressure inside the interconnected PMA's.

The problem statement has been deducted from previous sections:

How can multiple pressure management areas be regulated when these are interconnected and still maintaining a certain water pressure at the critical points?

In the next chapter, an existing system at Aalborg University will be elaborated and analysed.

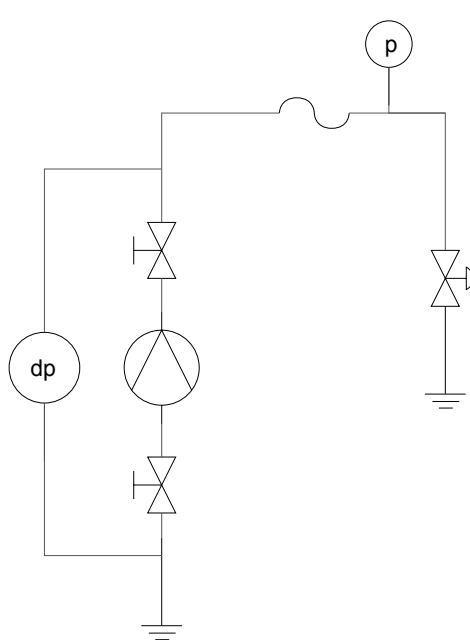
System analysis 2

This chapter includes the introduction of the physical system and its component. A model for each of the component is derived, which leads to a linearisation of the system based on an electrical equivalent. Furthermore the concept of multiple input and multiple output and a method to obtain the transfer function of the system is explained, which leads a first order approximation of the model. Finally is an approximated model for the physical system is derived, which leads to a verification of the two approximated models.

2.1 Water system

In this section, an analysis of a smaller system is used to elaborate the components, inside a water distribution network. A diagram of the water distribution network, which is available at Aalborg University and a simplification thereof will be shown.

In figure 2.1, a simple water distribution network can be seen, this will be used to elaborate which components that are inside such a system. These components are shown in table 2.1 with a description.



Symbol	Description
	Pump.
	Electronic control valve.
	Manaul valve.
	Pressure sensor.
	Differential pressure sensor.
	Pipeline.
	Gnd.

Figure 2.1: Simplified distribution network.

Table 2.1: Description of the symbols.

In the simplified distribution network, the pump is increasing the pressure into the system.

The water is flowing through the pipeline and will end up at a valve, which illustrate the point, where the consumer is using the water. Pressure sensor is measuring the pressure at a certain point and the differential pressure sensor is measuring the pressure across a pump. In figure 2.2, a diagram of the water distribution network that is available at Aalborg University can be seen.

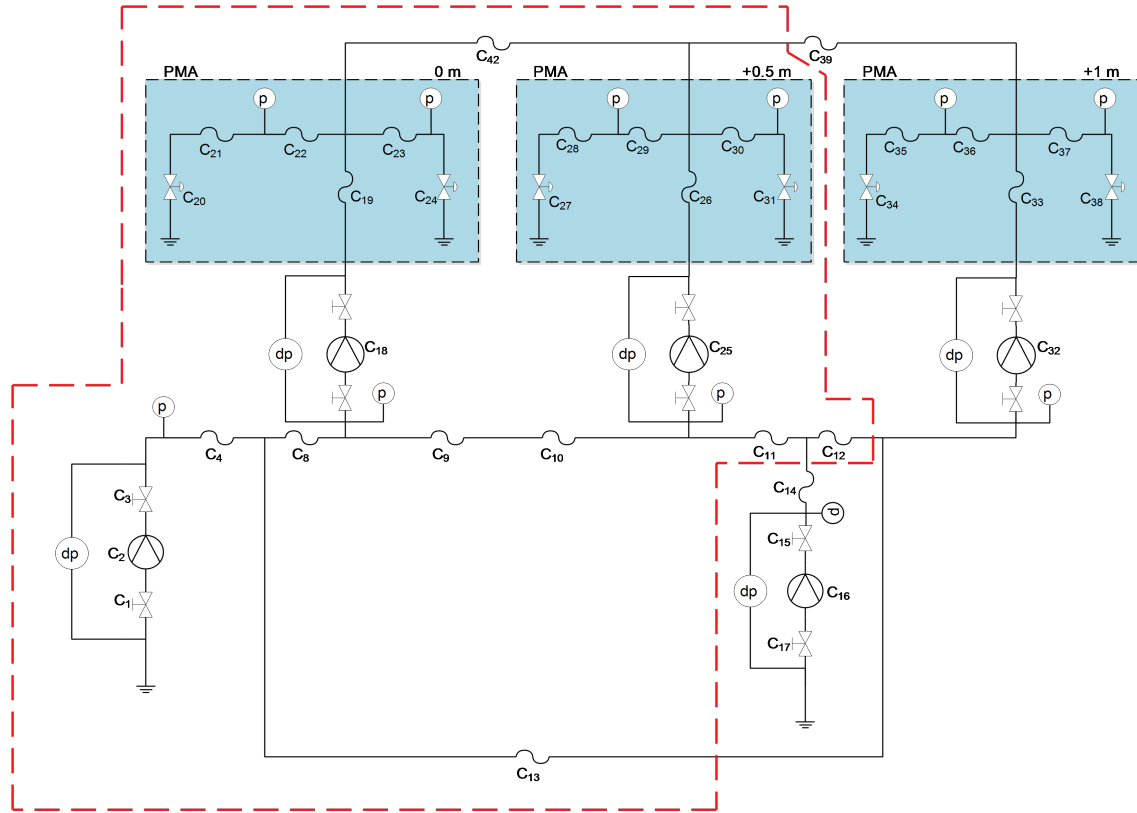


Figure 2.2: Diagram of the distribution network available at Aalborg University.

In the figure 2.2, there is marked three areas with blue. These areas are lifted above the pump, that is pumping water into the respective area at 0 m, 0,5 m and 1 m. The pump C_2 in figure 2.2 is the main pump, which is pumping water into the distribution network, where the three pumps are placed. These three pumps are pumping water into their respective PMA area and is increasing the pressure inside these areas. The last pump C_{16} has the same purpose as the main pump. The red dotted line represent the distribution system, that this report will be focusing on. The reduced network diagram is also shown in figure 2.3.

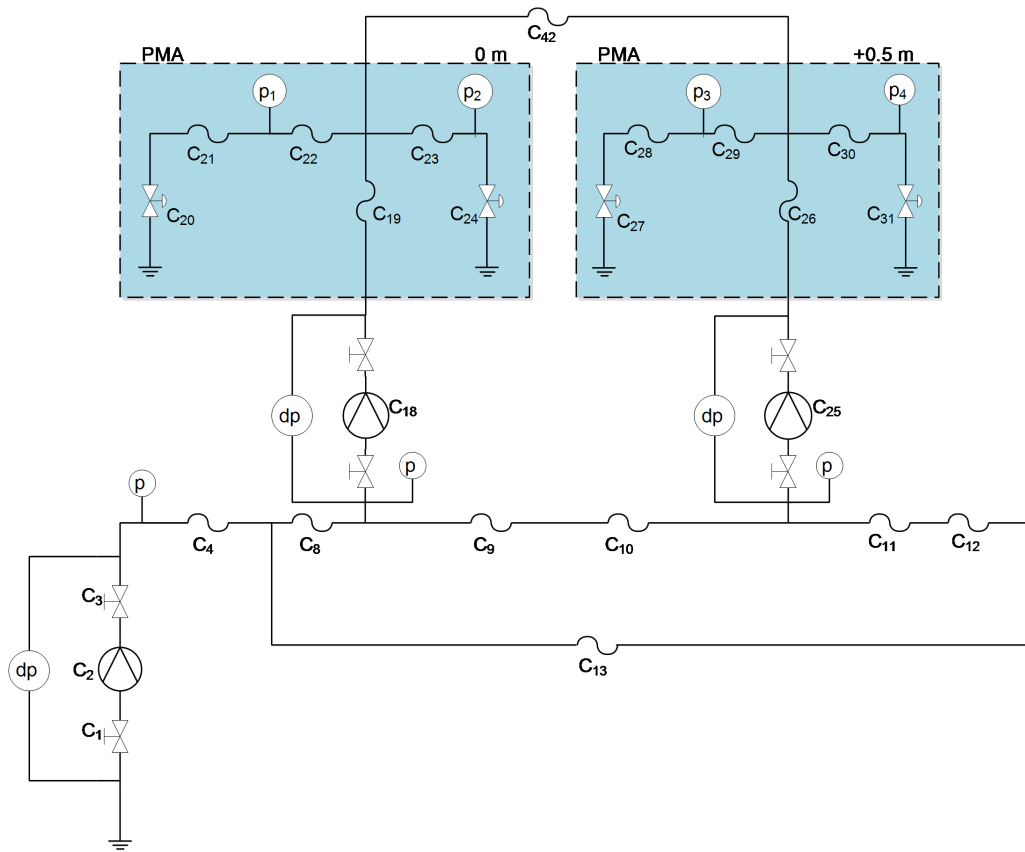


Figure 2.3: Diagram of the reduced distribution network.

In figure 2.3, the reduced network that will be studied in this project is shown. The actual physical system can now be examined in greater detail

2.2 The physical system

This section will introduce the physical system which is located at Aalborg University in The Department of Electronic Systems, Section for Automation and Control. The section will also cover the different components of the system and how to use them. Furthermore, a test will be conducted on it to see how the system reacts to changes.

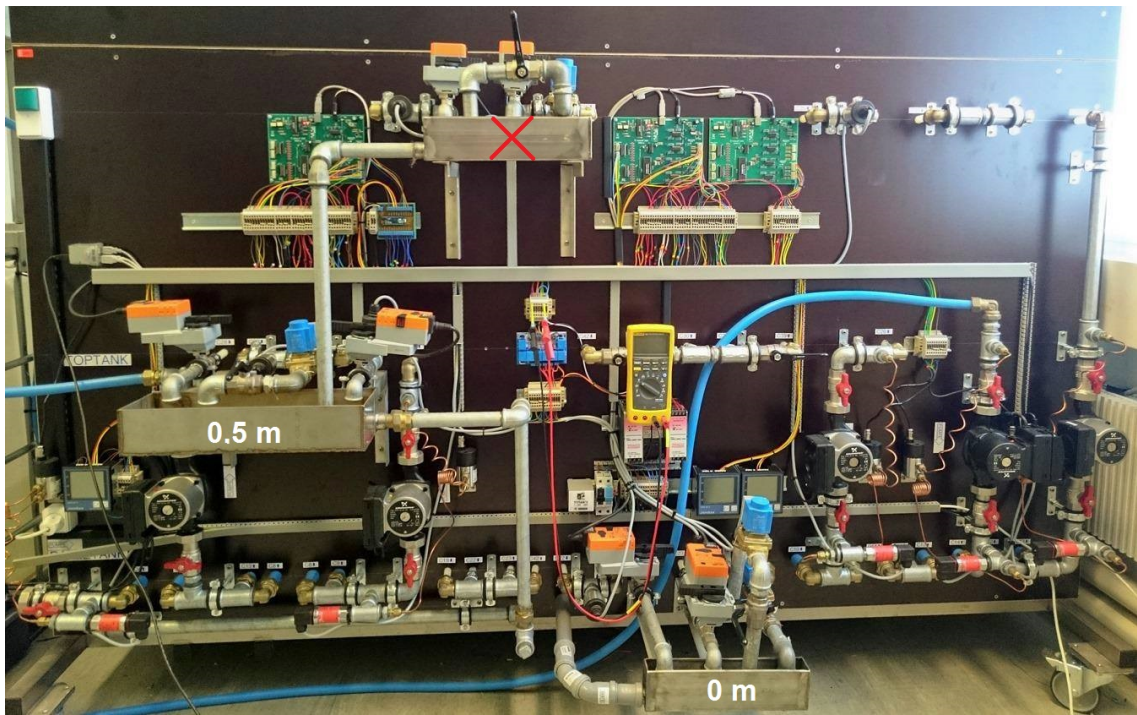


Figure 2.4: The physical system placed at Aalborg University in The Department of Electronic Systems, Section for Automation and Control.

Figure 2.4 shows the physical system that will be studied in this project. It has been chosen to limit the project to the two sub-networks which are placed at 0 m and 0,5 m and therefore the sub-network at 1 m will not be a part of this project. A list of the pipes that are used in this system can be seen in table 2.2.

Type	Component No.
Pipe, PEM, $\phi 20$, Length: 10 m, ϵ : 0.01 mm	$C_8, C_9, C_{10}, C_{11}, C_{12}, C_{13}$
Pipe, PEM, $\phi 20$, Length: 5 m, ϵ : 0.01 mm	C_4
Pipe, PEX, $\phi 10$, Length: 1 m, ϵ : 0.007 mm	$C_{21}, C_{22}, C_{28}, C_{29}$
Pipe, PEX, $\phi 10$, Length: 2 m, ϵ : 0.007 mm	$C_{19}, C_{23}, C_{30}, C_{42}$
Pipe, PEX, $\phi 10$, Length: 3 m, ϵ : 0.007 mm	C_{26}

Table 2.2: Tabel of pipe type, size, length and ϵ , which is the average roughness of a pipe wall found from [Wavin, 2015] PEX and [Wavin, 2012] PEM.

The component numbers are used to refer to a specific component, which can be seen on figure 2.3, and will be used in figures in later sections. PEM and PEX pipes are shown on the figure 2.5:



Figure 2.5: (a) PEX pipe. (b) PEM pipe.

In table 2.3, the pumps that are used in this system are shown. The datasheet for the pumps can be found on CD [Datasheet/Grundfosliterature-UPM2-pumper] and [Datasheet/UPML_XL_GB].

Type	Component No.
Pump, Grundfos UPM 25-60	C_{18}, C_{25}
Pump, Grundfos UPMXL 25-125	C_4

Table 2.3: Pumps.

The UPMXL is the main pump in the system, and the UPMs are pumping water into the PMA's. The pumps are shown in figure 2.6.



Figure 2.6: (a) Grundfos UPM 25-60. (b) Grundfos UPMXL 25-125.

In table 2.4, the valves used in this system can be seen, the datasheet for the manual valve can be found on the CD [Datasheet/R2015-1-S1_valve] and [Datasheet/LRQ24A-SR_SR_1_0_en] for the Belimo valve.

Type	Component No.
Manaul valve	C_1, C_3
Belimo valve	$C_{20}, C_{24}, C_{27}, C_{31}$

Table 2.4: Manual valves.

In figure 2.7, the manual valves that are used to close a section off in the distribution network and the Belimo valves, which are electrically controlled using the actuator, is shown. The Belimo vales are used as the critical point and the opening degree for the valve can be controlled in MATLAB Simulink Realtime workshop, which will be explained later.

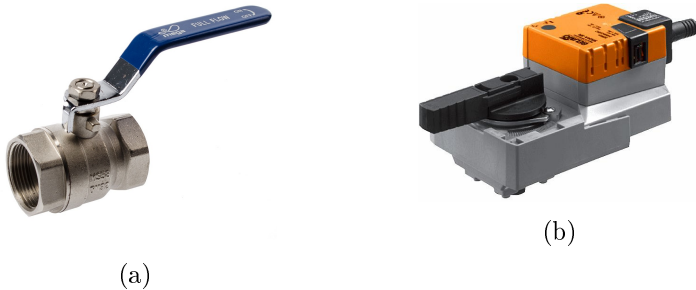


Figure 2.7: (a) Manual valve. (b) Belimo valve.

There are three types of pressure sensors in the system. Six jumo sensors (refer to CD [Datasheet/Jumo_sensor]), which are placed at the critical points. These sensors excels at measuring in small pressure ranges. A Jumo sensor can be seen in figure 2.8 (a). To measure the differential pressure over the pumps the Grundfos Direct SensorTM, type DPI is used and is a differential pressure sensor (refer to CD [Datasheet/Grundfosliterature-pressure-sensor]). A Grundfos Direct sensor can be seen in figure 2.8 (b). To measure the pressure at the pumps the MBS 32/33 from Danfoss is used (refer to CD [Datasheet/Danfoss]). A Danfoss MBS 32/33 sensor can be seen in figure 2.8 (c).

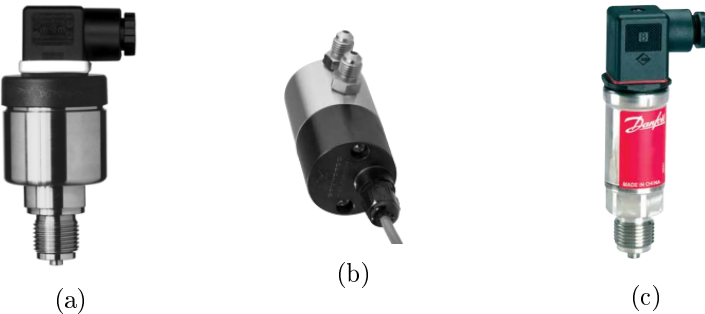


Figure 2.8: (a) Jumo sensor. (b) Grundfos Direct sensor. (c) Danfoss mbs32/33.

The system is controlled using a Realtime workshop, within MATLAB and Simulink. It is able to run Simulink models in realtime and therefore it is possible to change the constant for either the pumps or the Belimo valves when the system is running. To regulate the opening degree of the valves, a parameter from zero to one is used, where zero correspond to a closed valve and one to an open valve. For the pump one corresponds to full speed and zero means that the pump is off. A figure of the system, inside the Realtime workshop is shown in figure 2.9.

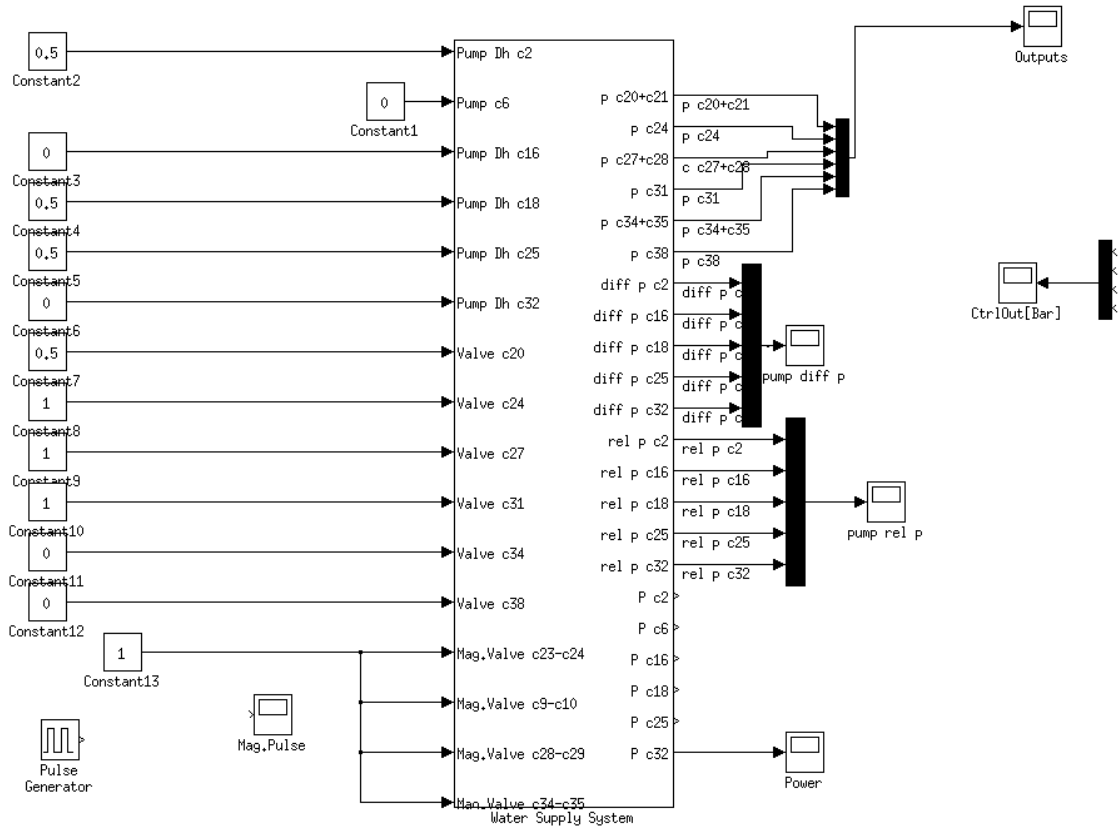
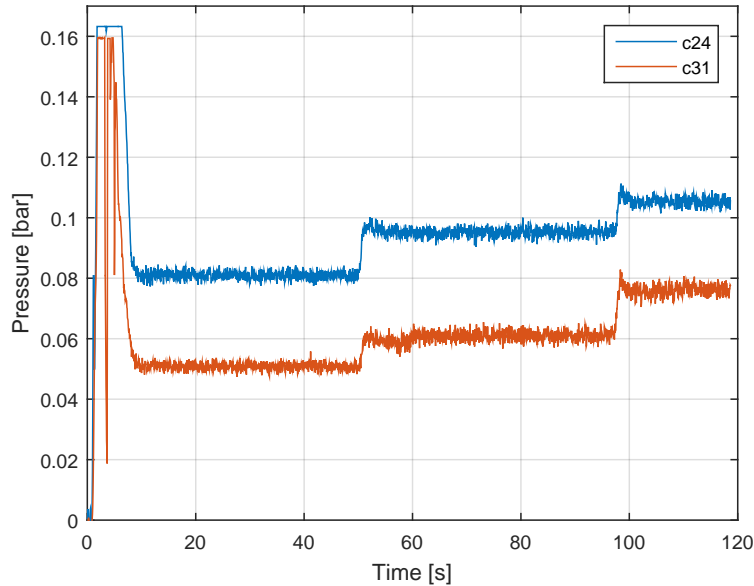
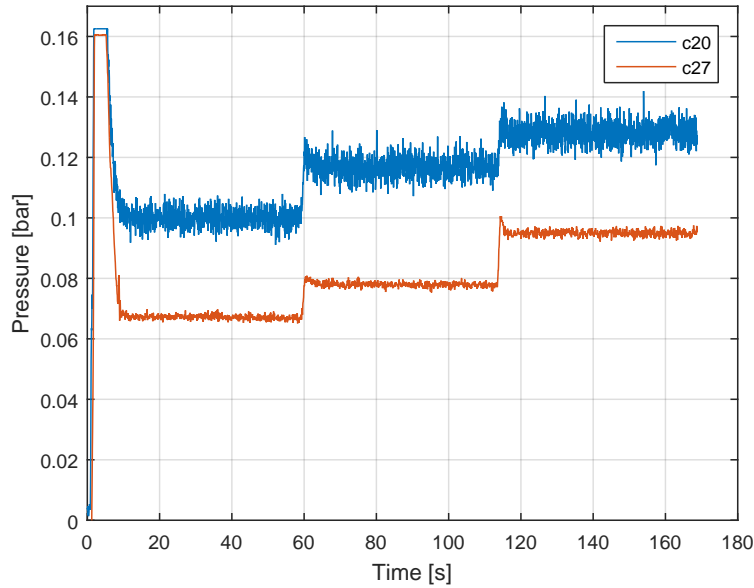


Figure 2.9: Realtime workshop.

To alter the speed or opening degree, the block which contain the constant should be changed. E.g. if the pump C_{18} needs an increase in speed, then the block that points into pump C_{18} , needs to be increased. The pressure at the valves can be seen at the output scope, which shows the pressure for all four valves. Furthermore, there is a scope for the pressure across the pumps, and for the pressure at the pumps.

In figures 2.10 and 2.11, the measured data from the laboratory test is shown. The journal for the measurement can be found in appendix A.3.1.

Figure 2.10: Test for valve C_{24} and C_{31} .Figure 2.11: Test for valve C_{20} and C_{27} .

The figures show, that the pressure increases when one of the two pumps velocity is increased after 50 seconds. And after approximately 100 seconds the second pump's velocity is increased. From both figures it can be seen that when the velocity for one pump is increased, it will result in a pressure boost in both PMA's. This is because the PMA's are interconnected and therefore a pressure increase in one PMA, will result in a pressure increase in the other PMA. It can also be seen that the pressure increases the most in the PMA closest to the main pump. The pressure for C_{20} and C_{27} is measured across a pipe and a valve. The pressure is therefore higher than across C_{24} and C_{31} , where the pressure is only measured across a valve. That is why there is a pressure difference, as shown in figure 2.3.

Through this section, the physical system and its components have been described. Furthermore, a short elaboration on the operation of the system has been given. This leads to the next section that will focus on deriving a model for the component of the pipes, the valves and the pumps.

2.3 Model of components

In this section the goal is to derive a model for each of the components. The models will be used in the later sections, to obtain the parameters for the components in the water distribution network.

The water system will be analysed in steady-state, meaning that there is a constant water flow in the system.

Pipe model

In the system, the pipes connect all the different devices (valves, pumps, etc) and forwards water where needed, therefore a model of the pipes is needed. Although the shape of the pipes in the network varies, the model will be based on one model to simplify the equations and therefore the model will be based on pipes, without curves or bends. The expression can be used to calculate the parameter, for the pressure over the pipes. Refer to appendix A.1.1 for the calculation of the parameter.

The pipes that are used in this distribution system varies from 1 m to 10 m in length and the ones that are below 5 m has a diameter of 10 mm and those that are 5 m and higher has a diameter of 20 mm, this can also be seen on table A.1 in appendix A.1.1



Figure 2.12: The pipe model represents the forces of a pipe.

The derivation of the pipe model is based on figure 2.12, the pipe model is made, with three different forces, F_{in} which is the pressure force going into the pipe, F_r which is the resistance force in the pipe also known as drag force and lastly F_{out} which represents the pressure force pushing to the left.

From these three forces of the pipe, Newton's second law can be applied [Pedersen, 2010], to put up an equation for the pipe:

$$m \cdot \frac{d}{dt}v = F_{in} - F_{out} - F_r \quad [N] \quad (2.1)$$

Where:

m is the mass of the water. [kg]

v is the velocity of the water. [m/s]

F_{in} is the pressure force going into the pipe. [N]

F_{out} is the pressure force pushing to the left. [N]
 F_r is the resistance force in the pipe. [N]

The equation 2.1 is expressing that the water mass multiplied with the water acceleration is equal to the resultant force.

The mass of the water can be expressed as [Pedersen, 2010]:

$$m = \rho \cdot V \quad [\text{kg}] \quad (2.2)$$

Where:

ρ is the density of the water. $[\text{kg}/\text{m}^3]$
 V is the volume of the pipe. $[\text{m}^3]$

Assuming the pipe is a cylinder, with a constant cross sectional area along the length of the pipe, the volume of the pipe can be derived as:

$$V = \pi \cdot r^2 \cdot l \quad \Rightarrow \quad V = A \cdot l \quad (2.3)$$

Where:

A is the area of a circle. $[\text{m}^2]$
 l is the pipe length. $[\text{m}]$

Inserting the new expressions in equation 2.1:

$$\rho \cdot A \cdot l \cdot \frac{d}{dt}v = F_{in} - F_{out} - F_r \quad [\text{N}] \quad (2.4)$$

The average flow velocity over a cross section, can be written as:

$$v = \frac{q}{A} \quad [\text{m}/\text{s}] \quad (2.5)$$

Where:

q is the volumetric rate of flow. $[\text{m}^3/\text{s}]$

The input force and output force can be written as $F = p \cdot A$ [Pedersen, 2010]:

$$F_{in} = p_{in} \cdot A \quad [\text{N}] \quad (2.6)$$

$$F_{out} = p_{out} \cdot A \quad [\text{N}] \quad (2.7)$$

Where:

p_{in} is the pressure at the input. $[\text{Pa}]$
 p_{out} is the pressure at the output. $[\text{Pa}]$

The following expressions can now be inserted in equation 2.4:

$$\rho \cdot A \cdot l \cdot \frac{d}{dt} \left(\frac{q}{A} \right) = p_{in} \cdot A - p_{out} \cdot A - F_r \quad [\text{N}] \quad (2.8)$$

Because the pressure difference is expressed as $\Delta p = p_{in} - p_{out}$, the equation is divided with A on both sides, which gives:

$$\frac{\rho \cdot l}{A} \cdot \frac{d}{dt}q = p_{in} - p_{out} - \frac{F_r}{A} \quad [\text{Pa}] \quad (2.9)$$

Where Δp can be included:

$$\frac{\rho \cdot l}{A} \cdot \frac{d}{dt}q = \Delta p - \frac{F_r}{A} \quad [\text{Pa}] \quad (2.10)$$

The resistance force can now be expressed as form resistance and the surface resistance, where the head losses are given by the Darcy - Weisbach equation [Prabhata K. Swamee, 2008].

For surface resistance:

$$h_f = \frac{8 \cdot f \cdot l \cdot |q| \cdot q}{\pi^2 \cdot g \cdot D^5} \quad [\text{m}] \quad (2.11)$$

Where:

- h_f is the head loss for the surface resistance of the pipe. [m]
- f is the coefficient of surface resistance, friction factor. [·]
- l is the length of the pipe. [m]
- g is the gravitational acceleration. [m/s^2]
- D is the diameter of a circular pipe. [m]

For form resistance:

$$h_m = k_f \frac{8 \cdot |q| \cdot q}{\pi^2 \cdot g \cdot D^5} \quad [\text{m}] \quad (2.12)$$

Where:

- h_m is the head loss for the form resistance of the pipe. [m]
- k_f is the form-loss coefficient. [·]

The resistance force can be expressed as $F = p \cdot A$, [Pedersen, 2010], which gives:

$$F_r = p_r \cdot A \quad [\text{N}] \quad (2.13)$$

When inserted in equation 2.10:

$$\frac{\rho \cdot l}{A} \cdot \frac{d}{dt}q = \Delta p - p_r \quad [\text{Pa}] \quad (2.14)$$

The pressure difference, which is the pressure resistance in the pipe, [Pedersen, 2010], can be expressed as:

$$p_r = \rho \cdot g \cdot h \quad [\text{Pa}] \quad (2.15)$$

By substituting p_r in equation 2.14:

$$\frac{\rho \cdot l}{A} \cdot \frac{d}{dt}q = \Delta p - \rho \cdot g \cdot h \quad [\text{Pa}] \quad (2.16)$$

With equation 2.16, the head loss from form and surface resistance, can be used:

$$\frac{\rho \cdot l}{A} \cdot \frac{d}{dt}q = \Delta p - \rho \cdot g \cdot h_m - \rho \cdot g \cdot h_f \quad [\text{Pa}] \quad (2.17)$$

A height difference across a pipe can be described as $\Delta z \cdot g \cdot \rho$ where Δz is the difference in height, g is the gravitation constant and ρ is the density of the water. This needs to be subtracted from the Δp .

$$\frac{\rho \cdot l}{A} \cdot \frac{d}{dt}q = \Delta p - \rho \cdot g \cdot h_m - \rho \cdot g \cdot h_f - \Delta z \cdot g \cdot \rho \quad [\text{Pa}] \quad (2.18)$$

By inserting both form resistance from equation 2.12 and surface resistance from equation 2.11 into equation 2.17 will result in the following equation:

$$\frac{\rho \cdot l}{A} \cdot \frac{d}{dt}q = \Delta p - \left(k_f \frac{\rho \cdot 8}{\pi^2 \cdot D^4} + \frac{8 \cdot f \cdot \rho \cdot l}{\pi^2 \cdot D^5} \right) \cdot |q| \cdot q \quad [\text{Pa}] \quad (2.19)$$

Isolating Δp which is the pressure difference over the pipe from input to output and substitute with a k_v -factor, and the pipe inertance J , the final pipe model is expressed:

$$\Delta p = J \cdot \frac{d}{dt}q + k_v \cdot |q| \cdot q \quad [\text{Pa}] \quad (2.20)$$

Where:

k_v is a factor published by the manufacturer $[(\text{Pa} \cdot \text{s}^2)/\text{m}^6]$
 J is the inertance in the pipe $[(\text{Pa} \cdot \text{s}^2)/\text{m}^3]$

By inspecting the final pipe model, it can be seen that the first term corresponds to a linear inductor and the second term corresponds to a non-linear resistance.

Valve model

The following model is made for the valves in the distribution network.

The model for a valve can be derived from the following equation 2.21 [Grundfos, 2015].

$$K_{vs} = \frac{q}{\sqrt{\Delta P}} \quad [\text{m}^3/\text{s}] \quad (2.21)$$

Where:

K_{vs} is the conductivity of a valve. $[\text{m}^3/\text{s}]$

ΔP is the pressure drop over the valve. $[\text{Pa}]$

q is the water flow. $[\text{m}^3/\text{s}]$

The K_{vs} factor specifies the water flow in m^3 through a fully-open valve with a pressure across the valve of 1 bar [Grundfos, 2015]. The K_v factor is determined through experiments by the manufacturer and can be found in the datasheet for the valve (refer to CD [Datasheet/R2015-1-S1_valve]).

To find the pressure drop over the valve equation 2.21 must be solved for Δp as in equation 2.22:

$$\Delta p = \left(\frac{q}{K_v} \right)^2 \quad [\text{Pa}] \quad (2.22)$$

Equation 2.22 can be rewritten on the same form, as the equation for the pipe model 2.20:

$$\Delta p = \frac{1}{K_v^2} \cdot |q| \cdot q \quad [\text{Pa}] \quad (2.23)$$

Equation 2.23 describes the model for a valve.

The following figure represents the inner of a ball valve. In this case, the water runs from the left to the right and the flow is regulated by the ball inside the valve. This ball is controlled by an actuator which regulates the opening degree of the valve.

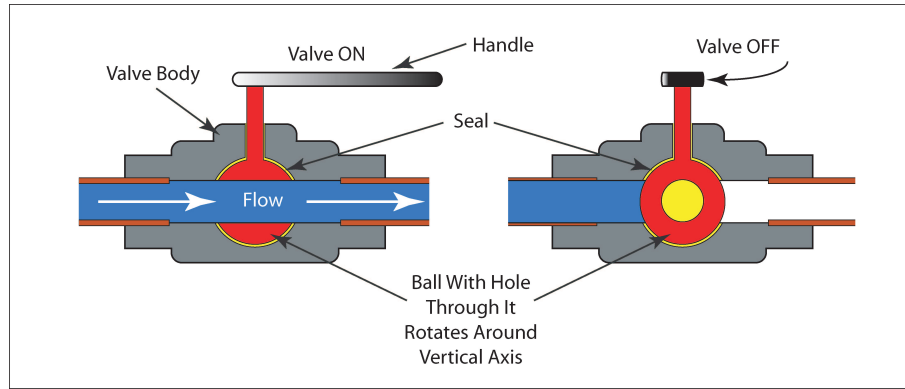


Figure 2.13: Scheme of a ball valve from a side view [Fuchs, 2012].

Pump model

The pumps are being used to regulate the pressure in the networks. The pump model gives the pressure across the pump in terms of the flow through and the rotational speed of the pump.

The pump can be expressed as [Kallesøe, 2005]:

$$\Delta p = -a_{n2}q^2 + a_{n1}q\omega + a_{n0}\omega^2 \quad [\text{Pa}] \quad (2.24)$$

Where:

a_{n2} , a_{n1} and a_{n0} are the constant parameters of the pump.

q are the water flow.

ω are the angular velocity.

[.]
[m³/s]
[m/s]

Figure 2.14 shows how the water is flowing inside a centrifugal pump. The water arrives in the middle of the pump and is driven by the blades in a rotary movement, where the centrifugal force providing energy to the water. The result is that the water will flow out from the outlet of the centrifugal pump.

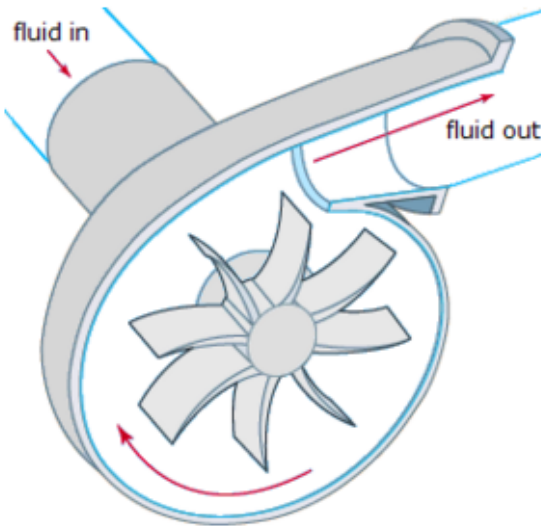


Figure 2.14: Scheme of a pump [Wermac, 2016]

The linear transfer function of the pump is found to be (see appendix A.1.3):

$$C(s) = \frac{Out(s)}{In(s)} = \frac{\Delta P(s)}{\omega(s)} = AN1 + AN0 \quad [\cdot] \quad (2.25)$$

This is under assumption that the water flow, q is constant, where ω are seen as a variable input and ΔP is seen as a variable output, this leads to the linearized term $AN1 + AN0$ that contains the parameters of the pump in the operation point. The linear function is shown in figure 2.15, where the blue line is the difference pressure measured across the pump at a certain angular velocity, this was measured doing a step response test on the physical system in the laboratory. The yellow line is the linear model calculated from the model parameters, as shown on figure 2.15, there is a big deviation between measured output and output from the linearized model. Therefore a new slope have been calculated from two points that is observed to be the operation area, linearized around the operation point at $\omega = 0.5$. The operation area vary with $\omega \pm 0.1$, that is $\omega = 0.4$ and $\omega = 0.6$, which corresponds to a difference pressure across V_a from 0.2683 to 0.4961 bar and for V_b from 0.2615 to 0.4802 bar, these points are found on the measured curve. The new linear function is shown as the red line on the figure and is used further on.

For calculating of the slope the following equation is used:

$$a = \frac{\Delta P_2 - \Delta P_1}{\omega_2 - \omega_1} = \frac{0.2683 - 0.4961}{0.6 - 0.4} = 1.139 \quad [\cdot] \quad (2.26)$$

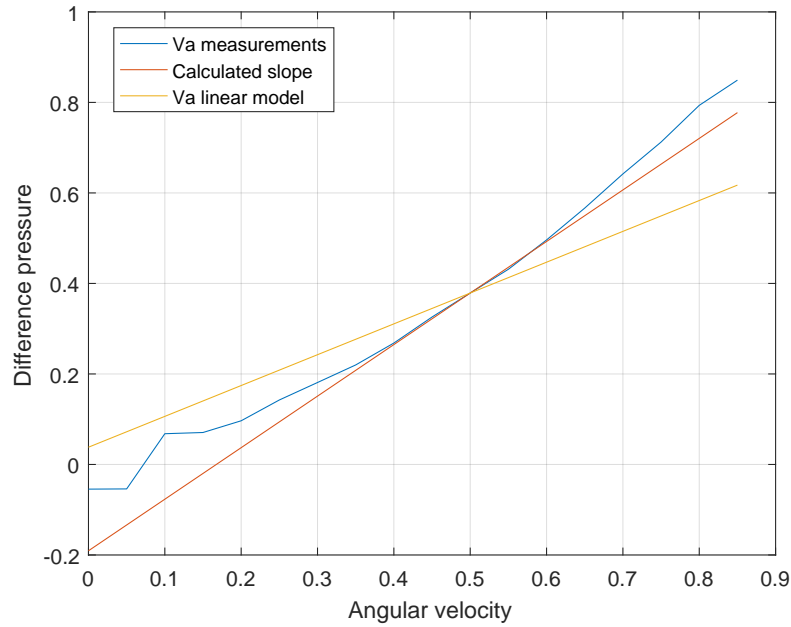


Figure 2.15: Physical measurements against the linear model and calculated slope.

The new slope from the linear function shown as the red line on figure 2.15, is calculated to be 1.139 and is going to be used as the gain for the pump.

The models derived in this section, will be used to calculate the parameters of components, an electric equivalent of the network is therefore needed, which leads to the next section.

2.4 Electrical equivalent

This section will contain an analysis of the water system as seen in section 2.1. To make this analysis of the water system, the system will be translated from water circuit analogy to an electrical circuit analogy by doing the translation, basic electrical circuit analysis can be done on the system. The symbols are now translated as seen in table 2.5.

Fluid symbol	Electrical symbol	Description
		Pump are seen as a voltage supply.
		Electronic control valve are seen as a resistor.
		Manaul valve are removed from the electrical equivalent.
		Pipeline are seen as a inductor in series with a resistor.
		Ground.

Table 2.5: Description of the symbols in the electrical equivalent.

The symbols are defined, and the water system from figure 2.3 can be translated into a electrical circuit as seen in figure 2.16.

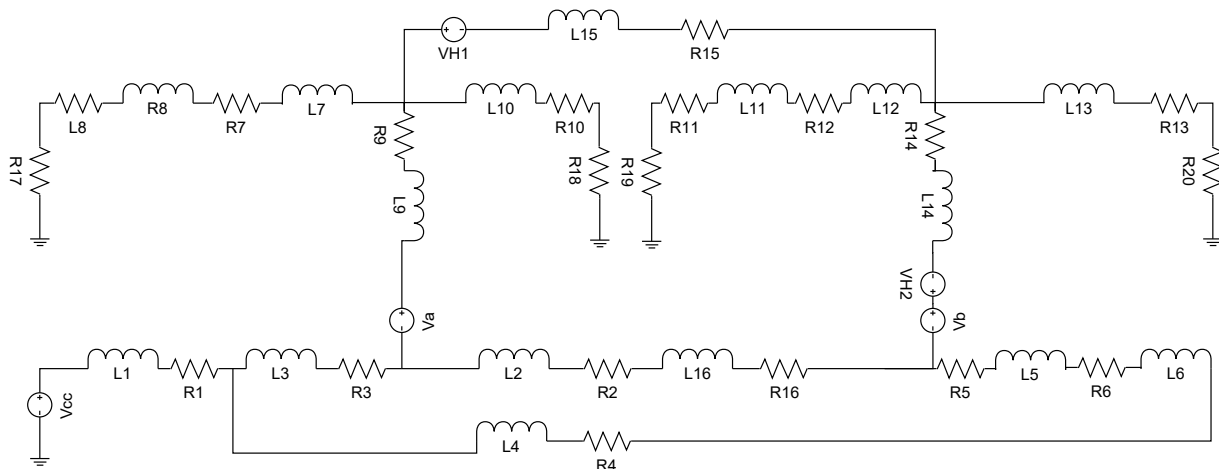


Figure 2.16: Electric equivalent for the water supply system.

The figure 2.16 represents the water supply system, where the pumps, valves and pipelines are seen as electrical components.

In order to derive the electrical equivalent into a transfer function of the system and Laplace transform into the frequency domain, the system equations have to be determined. To be able to Laplace transform, the nonlinear terms have to be linearized. This is done by doing a step of analysis' as listed:

1. Find the mesh loops and define the equations for each loop in the circuit, this can be done using Kirchhoff's Voltage Law (KVL).
2. Determine the operating point of the model by solving the steady state nonlinear algebraic model equations [Modelling and Control, 2015].
3. Rewrite all linear terms in the mathematical model as the sum of their nominal operating point values and incremental variables, noting that the derivatives of constant terms are zero [Modelling and Control, 2015].
4. Replace all nonlinear terms with zero'th and first order terms of their Taylor series expansions. The Taylor series is developed around the operating point, and will include constant [Modelling and Control, 2015].
5. Use the algebraic equation(s) defining the operating point to cancel the constant terms in the differential equation leaving only the linear terms involving incremental variables. terms expressed in operating point variables and linear terms in incremental variables [Modelling and Control, 2015].

2.4.1 Kirchhoff's Voltage Law

In this subsection a circuit analysis will be done by using Kirchhoff's Voltage Law (KVL) step 1 from section 2.4. By doing a circuit analysis with KVL, the voltage through each component can be determined. Where the directed sum of voltages around each loop is equal to zero.

The first step is to identify each mesh loop in the circuit, this is done by looking at a starting point and see which components the loop is crossing, to reach the ending point (see figure 2.17).

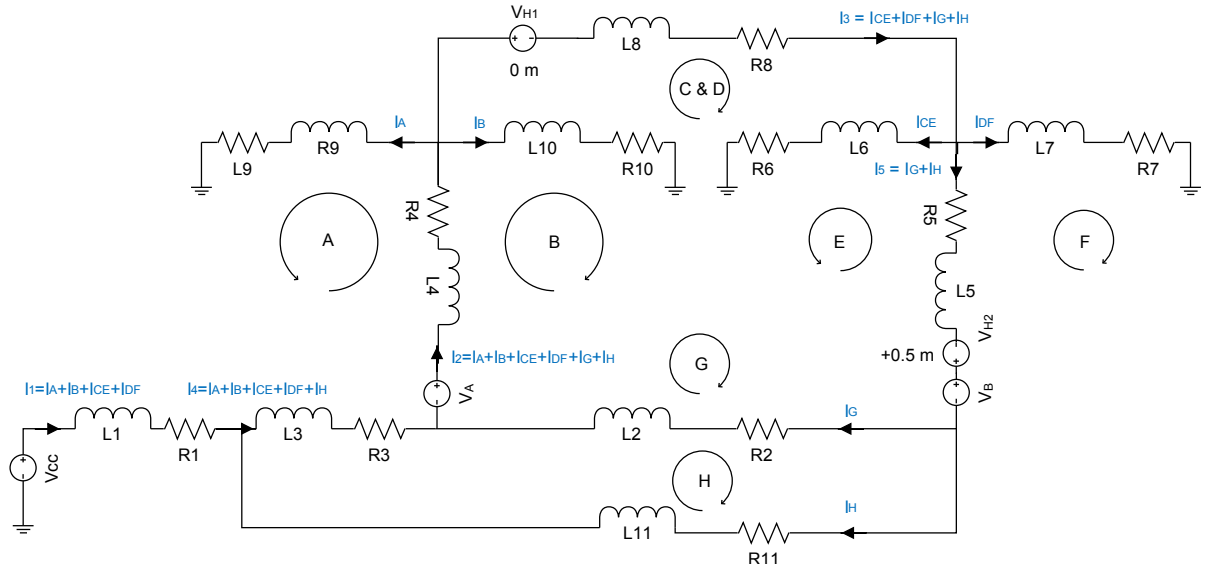


Figure 2.17: Reduced equivalent for the water supply system.

Where:

V_{CC} is the main pump (Pump 1).	[V]
V_A is the pump to network 1 (Pump 4).	[V]
V_{H1} present the height of network 1.	[V]
V_B is the pump to network 2 (Pump 5).	[V]
V_{H2} present the height of network 2.	[V]
I_1 is the current going through loop A,B,C to E and D to F.	[A]
I_2 is the current going through loop A,B,C to E, D to F, G and H.	[A]
I_3 is the current going through loop C to E, D to F, G and H.	[A]
I_4 is the current going through loop A,B,C to E, D to F and H.	[A]
I_5 is the current going through loop G and H.	[A]

The first loop is found from the main pump (V_{CC}), which are going through the elements; V_{CC} , L_1 , R_1 , L_3 , R_3 , $-V_a$, L_4 , R_4 , R_9 and out of L_9 .

From this inspection, by setting the sum of components to zero, the KVL equation for loop A can be determined.

Loop A:

$$-V_{cc} + R_1 \cdot i_1 + L_1 \frac{d(i_1)}{dt} + R_3 \cdot i_4 + L_3 \frac{di_4}{dt} - V_a + L_4 \frac{d(i_2)}{dt} + R_4 \cdot (i_2) + R_9 \cdot i_A + L_9 \frac{di_A}{dt} = 0 \quad (2.27)$$

The other mesh loops in the circuit is determined by the same method and can be found in appendix A.1.4.

For simplification the currents are determined as:

$I_1 = I_A + I_B + I_{CE} + I_{DF}$	[A]
$I_2 = I_A + I_B + I_{CE} + I_{DF} + I_G + I_H$	[A]
$I_3 = I_{CE} + I_{DF} + I_G + I_H$	[A]
$I_4 = I_A + I_B + I_{CE} + I_{DF} + I_H$	[A]
$I_5 = I_G + I_H$	[A]

Now, by having determined each mesh loops in the circuit and their KVL equations, they can now be further analyzed.

From the translation from a fluid system to electrical analogy the resistance in the pipes is nonlinear and therefore needs to be linearized.

2.4.2 Linearization

In order to Laplace transform the electrical equation found by KVL, into frequency domain the nonlinear terms in the equation need to be linearized.

Step 2 from section 2.4, is used to solve the steady state nonlinear equation.

Loop A:

$$\begin{aligned} -V_{cc} + R_1 \cdot i_1 + L_1 \frac{d(i_1)}{dt} + R_3 \cdot i_4 + L_3 \frac{d(i_4)}{dt} - V_a + L_4 \frac{d(i_2)}{dt} + R_4 \cdot (i_2) + R_9 \cdot i_A \\ + L_9 \frac{di_A}{dt} = 0 \end{aligned} \quad (2.28)$$

In steady state:

$$0 = -\bar{V}_a + R_1|\bar{i}_1|\bar{i}_1 + R_3|\bar{i}_4|\bar{i}_4 + R_4|\bar{i}_2|\bar{i}_2 + R_9|\bar{i}_A|\bar{i}_A + c \quad (2.29)$$

As the focus in this project are on the input V_a and V_b , the main pump V_{CC} is seen as a constant.

Step 3 from section 2.4 will be used to rewrite all the linear terms in the mathematical model. By using Taylor approximation, the nonlinear terms can be expressed as a linear model, therefore will the nonlinear resistance $R|i|i$ be linearized by a first-order Taylor Approximation.

The standard form of the Taylor approximation are determined as:

$$f(x) = f(a) + \frac{f'(a)}{1!} \cdot (x - a) + \frac{f''(a)}{2!} \cdot (x - a)^2 + \dots + \frac{f^n(a)}{n!} \cdot (x - a)^n \quad (2.30)$$

The first order Taylor approximation can be seen as:

$$f(x) = f(a) + f'(a) \cdot (x - a) \quad (2.31)$$

A linear approximation of $R|\bar{i}|\bar{i}$, can now be expressed by using Taylor approximation. Defining function $f(i)$ equal to our nonlinear term:

$$f(i) = R|i|i \quad (2.32)$$

Taking the derivative of the nonlinear term:

$$f'(i) = \frac{d}{di} f(i)$$

$$= 2R|i|$$

To simplify the nonlinear resistance, it is defined as:

$$f'(\bar{i}) = 2R|\bar{i}| \equiv r$$

Using Taylor approximation to reduce the terms, where: $i = \bar{i} + \hat{i}$:

$$\begin{aligned} f(i) &= f(\bar{i}) + f'(\bar{i}) \cdot (i - \bar{i}) \\ &= f(\bar{i}) + r \cdot (i - \bar{i}) \\ &= f(\bar{i}) + r \cdot \hat{i} \end{aligned}$$

Inserting our new term in our steady-state equation, by replacing $R|\bar{i}|\bar{i}$ with $f(\bar{i})$ and solving an steady state expression for input \bar{v}_a :

$$\bar{v}_a = f_1(\bar{i}_1) + f_3(\bar{i}_4) + f_4(\bar{i}_2) + f_9(\bar{i}_A) + c \quad [V] \quad (2.33)$$

The equation for the KVL with linear expressions:

$$i = \bar{i} + \hat{i} \quad [A] \quad (2.34)$$

$$V_a = \bar{v}_a + \hat{v}_a \quad [V] \quad (2.35)$$

Where:

\bar{i} is the value of the operating point. [A]

\hat{i} is the value of the incremental. [A]

\bar{v}_a is the value of the operating point. [V]

\hat{v}_a is the value of the incremental. [V]

By using the linear term from the Taylor approximation and inserting that into equation 2.28, and by substituting V_a with the operating point and the incremental value the following equation is given:

$$0 = -(v_a + \hat{v}_a) + f_1(\bar{i}_1) + r_1\hat{i}_1 + L_1 \frac{d(\hat{i}_1)}{dt} + f_3(\bar{i}_4) + r_3\hat{i}_4 + L_3 \frac{d(\hat{i}_4)}{dt} + f_4(\bar{i}_2) + r_4\hat{i}_2 + L_4 \frac{d(\hat{i}_2)}{dt} + f_9(\bar{i}_A) + r_9\hat{i}_A + L_9 \frac{d(\hat{i}_A)}{dt} + c \quad (2.36)$$

By substituting with the steady state equation for \bar{v}_a , found in equation 2.33, which follows step 4 by replacing all nonlinear terms with zero'th and first order terms of Taylor series, then the following equation is given:

$$0 = -(f_1(\bar{i}_1) + f_3(\bar{i}_4) + f_4(\bar{i}_2) + f_9(\bar{i}_A) + c + \hat{v}_a) + f_1(\bar{i}_1) + r_1\hat{i}_1 + L_1 \frac{d(\hat{i}_1)}{dt} + f_3(\bar{i}_4) + r_3\hat{i}_4 + L_3 \frac{d(\hat{i}_4)}{dt} + f_4(\bar{i}_2) + r_4\hat{i}_2 + L_4 \frac{d(\hat{i}_2)}{dt} + f_9(\bar{i}_A) + r_9\hat{i}_A + L_9 \frac{d(\hat{i}_A)}{dt} + c \quad (2.37)$$

Step 5 will be used to cancel the constant terms in the differential equations leaving only the linear terms. The linear approximation can then be defined as:

$$0 = -\hat{v}_a + r_1\hat{i}_1 + L_1 \frac{d(\hat{i}_1)}{dt} + r_3\hat{i}_4 + L_3 \frac{d(\hat{i}_4)}{dt} + r_4\hat{i}_2 + L_4 \frac{d(\hat{i}_2)}{dt} + r_9\hat{i}_A + L_9 \frac{d(\hat{i}_A)}{dt} \quad (2.38)$$

Where the input v_a can be solved as:

$$\hat{v}_a = r_1\hat{i}_1 + L_1 \frac{d(\hat{i}_1)}{dt} + r_3\hat{i}_4 + L_3 \frac{d(\hat{i}_4)}{dt} + r_4\hat{i}_2 + L_4 \frac{d(\hat{i}_2)}{dt} + r_9\hat{i}_A + L_9 \frac{d(\hat{i}_A)}{dt} \quad (2.39)$$

Laplace transform into frequency domain:

$$V_a(s) = I_1(s) \cdot (R_1 + sL_1) + I_4(s) \cdot (R_3 + sL_3) + I_2(s) \cdot (R_4 + sL_4) + I_A(s) \cdot (R_9 + sL_9) \quad (2.40)$$

By then proceeding the same way as above, it is possible to determine the Laplace transform equation for each loop. For the rest of the linear mesh loop equations, see appendix A.1.5.

This section established an electric equivalent of the distribution network and is being linearised using KVL and Taylor series, which lead to six linear transfer function for the system. To analysis this system from one input to a output, the system must be transformed into a multiple input multiple output system. But before the system can be evaluated the parameters for the system needs to be calculated. To calculate the parameters the flow in the operating point must be known, which leads to the next section about determining the flow in the operating point.

2.5 Determination of water flow in the operating point

In this section the water flow of the physical system will be calculated for the operating point.

To be able to calculate the parameters of the linearised model the flow, q must be known in the operating point for the distribution system. To find q , a measurement from the laboratory will be used, where the operating point for the two pumps is the differential pressure and is 0.377 bar for C_{18} and 0.366 bar for C_{25} . On figure 2.18, the water distribution network is shown.

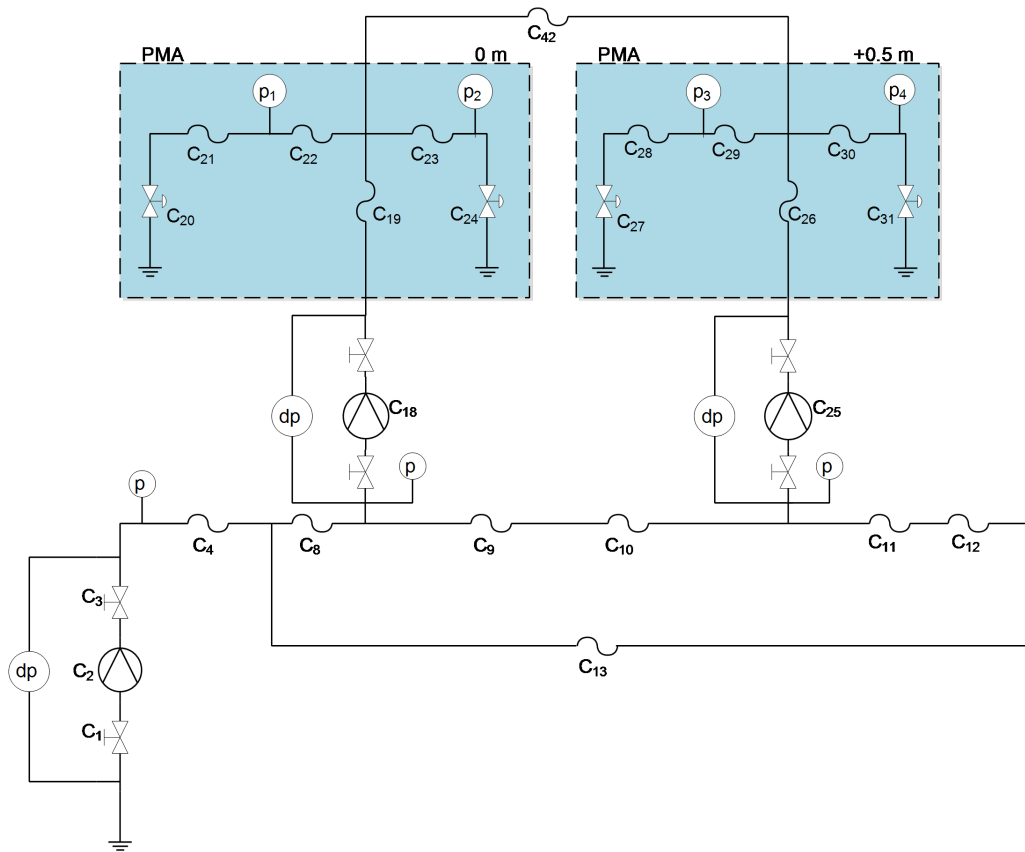


Figure 2.18: Diagram of the reduced distribution system.

To find the water flow in the system the pressure sensors at p_2 and p_4 are used to find

the pressure, see appendix A.3.3 or on figure 2.19. These measurements will be used to calculate the water flow backwards in the system.

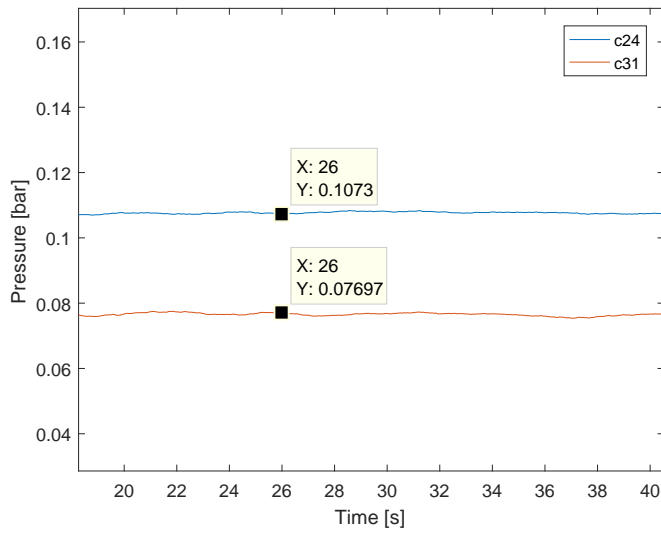


Figure 2.19: Filtered MATLAB plot with the running average pressure over time, with a window size of 80 points.

When the pressure is known equation 2.22 from section 2.3 for a valve can be used to find the water flow. The test is conducted for a fully-open valve which means that the constant K_{vs} is known from the datasheet. The equation for q is shown below:

$$q = k_{vs} \cdot \sqrt{\Delta p} \quad [\text{m}^3/\text{h}] \quad (2.41)$$

Where:

K_{vs} is the conductivity of a valve. $[\text{m}^3/\text{s}]$

Δp is the pressure across the valve. $[\text{Pa}]$

q is the water flow. $[\text{m}^3/\text{s}]$

The conductivity for a fully-open valve is 1 (refer to CD [Datasheet/Jumo_sensor]). To see the calculation refer to journal A.1.2. The results are shown below:

$$p_2 \rightarrow q_{p2} = 0.328 \frac{m^3}{hr} \quad p_4 \rightarrow q_{p4} = 0.276 \frac{m^3}{hr} \quad (2.42)$$

The water flow is now known for q_{p2} and q_{p4} in the network. Because the pressure drop across C_{23} and C_{24} is the same as the pressure drop across C_{20} , C_{21} and C_{22} the water flow through C_{20} , C_{21} and C_{22} is the same as the water flow through C_{23} and C_{24} . This also applies to the other PMA. To find the water flow through C_{42} the pressure drop across the pipe must be known. To do so, the model for a pipe, which is derived in section 2.3, with the addition of an extra part, which is the height difference. This can be described as $\Delta z \cdot g \cdot \rho$ where Δz is the difference in height, g is the gravitation constant and ρ is the density of the water. The model for the pipe can be seen below:

$$\frac{\rho \cdot l}{A} \cdot \frac{d}{dt}q = \Delta p - \left(k_f \frac{\rho \cdot 8}{\pi^2 \cdot D^4} + \frac{8 \cdot f \cdot \rho \cdot l}{\pi^2 \cdot D^5} \right) \cdot |q| \cdot q - \Delta z \cdot g \cdot \rho \quad [\text{Pa}] \quad (2.43)$$

This equation is used to calculate the pressure drop across C_{23} and C_{30} and the calculations can be seen in appendix A.1.2. When the pressure drop across C_{42} is known, the model for a pipe is used to find the water flow through C_{42} . The calculations can be seen in appendix A.1.2. The water flow through C_{42} is:

$$q_{42} = -0.045 \quad [\text{m}^3/\text{h}] \quad (2.44)$$

Because the flow is negative across C_{42} , which means that the flow goes from the upper PMA to lower PMA. This can be seen on figure 2.20 where the water flow in the upper part of the system also can be seen.

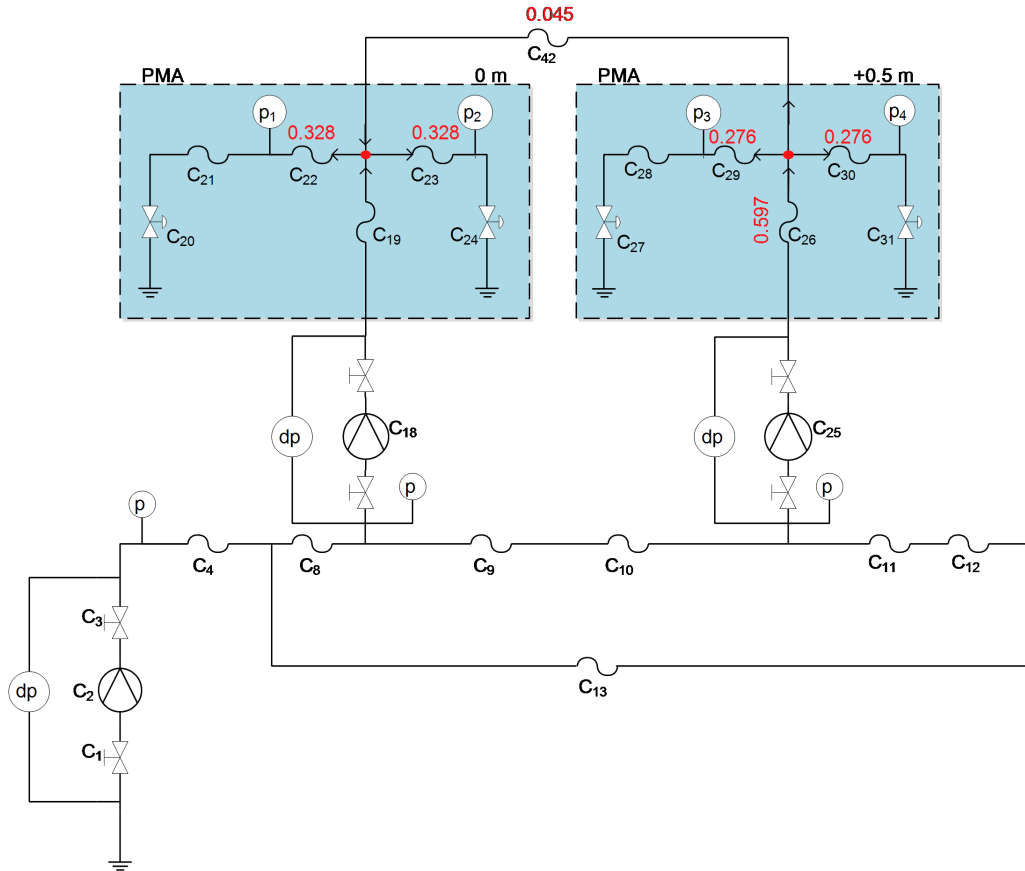


Figure 2.20: Figure of the system with water flow values in m^3/h and arrows that indicate flow direction.

To calculate the flow across C_{19} and C_{26} junction rule is used for the red dot on figure 2.20. Which result in a water flow for C_{19} at $0.611 \text{ m}^3/\text{h}$ and for C_{26} at $0.597 \text{ m}^3/\text{h}$.

To calculate the water flow in the entire distribution network the flow in the lower part needs to be found. It can be found by measuring the pressure from the sensors that are placed before each pump, that are pumping water into the PMA's. When the pressure is known for both points, the model for a pipe can be used to calculate the flow across C_9 and C_{10} . The pressure measurement at the pumps can be seen on figure 2.21 or in appendix A.3.3.

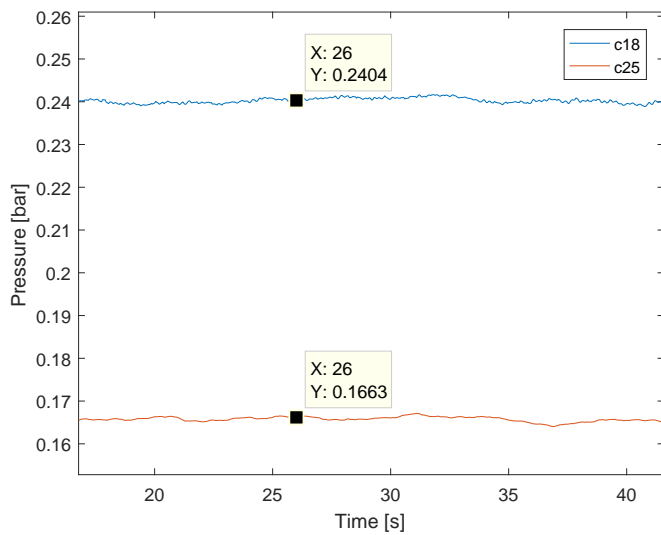


Figure 2.21: Filtered MATLAB plot with the running average pressure over time at the pumps C_{18} and C_{25} , were the window size is 80 points.

The model for the pipe can be used to find the water flow through C_9 and C_{10} , the calculation can be seen in appendix: A.1.2.

$$q_{9,10} = 0.777 \quad [\text{m}^3/\text{h}] \quad (2.45)$$

With the water flow known through C_9 and C_{10} the flow for the rest of the lower part can be calculated. In figure 2.22, the flow for the entire system can be seen:

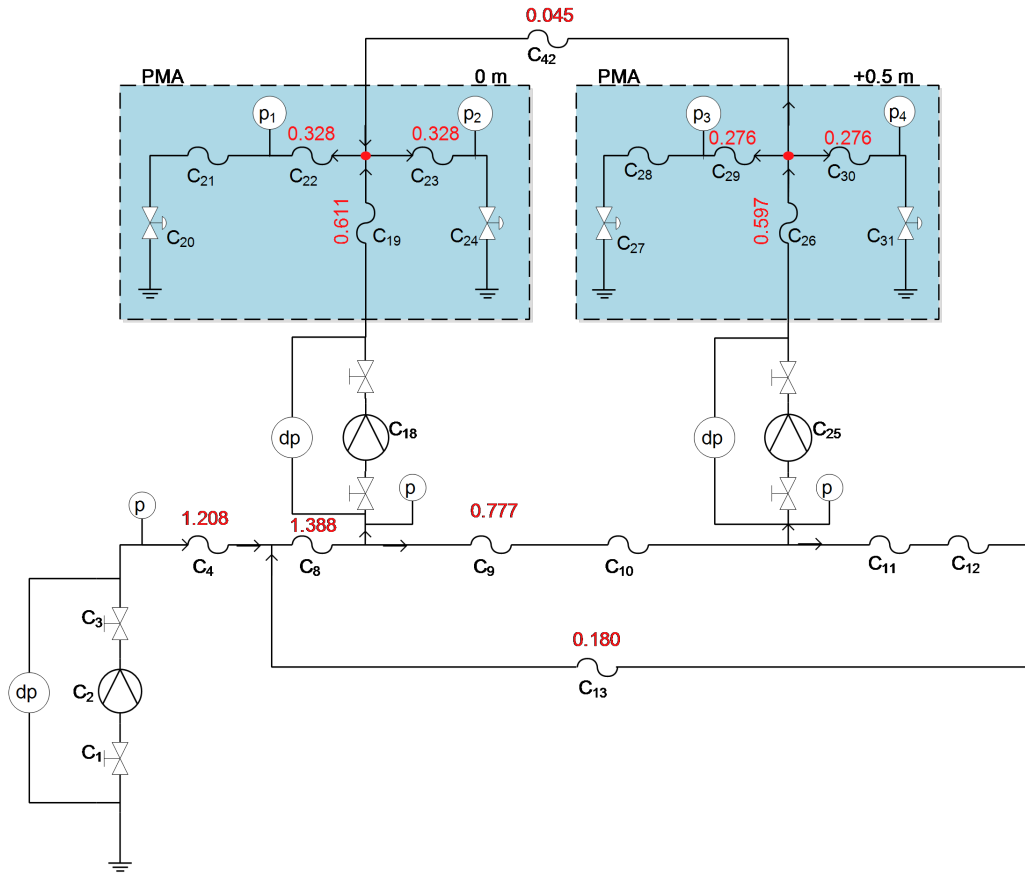


Figure 2.22: Figure of the system with flow values in m^3/h and arrows that indicate flow direction.

The water flow through C_8 is the sum of the junction after the pipe. It is a summation of the water flow that goes through the pump and the water flow through C_9 and C_{10} . Therefore the flow through C_8 is calculated to $1.388 \text{ m}^3/\text{h}$. The flow through C_{11}, C_{12} and C_{13} is calculated to $0.180 \text{ m}^3/\text{h}$ which is the flow through C_9 and C_{10} minus the flow that goes up through the pump C_{25} . Finally, the flow that comes into the system from C_2 is equal to the flow at the outputs ($q_{p1}, q_{p2}, q_{p3}, q_{p4}$), therefore the flow into the system is $1,208 \text{ m}^3/\text{h}$. Calculations can be seen in appendix A.1.2.

With the known water flows, the linearised model for the distribution system can be obtained by calculating the parameters for all the pipes and valves. These calculation will not be shown in the main report but can be seen in appendix A.1.1. With the parameters known for the system it is now possible to obtain a transfer function with the use of the concept multiple inputs and multiple outputs, which will be explained in the next section.

2.6 Multiple Input and Multiple Output

This section will introduce the concept of using multiple input and multiple output (MIMO) in a system. The method of obtaining the transfer function for the system will be explained.

If a system has more than one variable that can be manipulated and more than one input that can be controlled and the interaction between these can't reduce the model

further, it can be considered a MIMO system.

For a MIMO system that can be represented as a linear time invariant (LTI) model, it can be described with a transfer matrix function, where input and output are vectors rather than scalars.

$$\begin{pmatrix} Y_{1,1}(s) \\ Y_{2,1}(s) \\ \vdots \\ Y_{m,1}(s) \end{pmatrix} = \begin{pmatrix} G_{1,1}(s) & G_{1,2}(s) & \cdots & G_{1,n}(s) \\ G_{2,1}(s) & G_{2,2}(s) & \cdots & G_{2,n}(s) \\ \vdots & \vdots & \ddots & \vdots \\ G_{m,1}(s) & G_{m,2}(s) & \cdots & G_{m,n}(s) \end{pmatrix} \begin{pmatrix} U_{1,1}(s) \\ U_{2,1}(s) \\ \vdots \\ U_{m,1}(s) \end{pmatrix} \quad [.] \quad (2.46)$$

Where the matrix $G(s)$ contains the transfer function for the system, the vectors $U(s)$ and $Y(s)$ are the input and output.

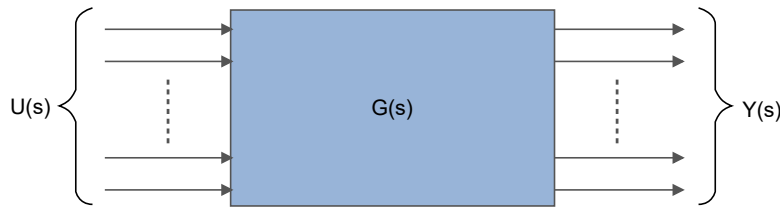


Figure 2.23: A figure of a MIMO system block

The electrical equivalent and linearization for the system was describe in the previous section 2.4 and two inputs $V_{a,b}(s)$ were defined. To find the voltages over two output, an expression for the currents of the system is needed, based on equation 2.47 it is possible to deduce the current.

$$M_E(s) \cdot i_c(s) = M_{v_{a,b}}(s) \quad [.] \quad (2.47)$$

Where:

$M_E(s)$ is a matrix containing the resistance and inductance of the linearised system. $[.]$

$M_{v_{a,b}}(s)$ is a matrix containing ones or zeros, corresponding to $v_{a,b}(s)$. $[.]$

$i_c(s)$ is a vector for the currents of the system. $[.]$

$v_{a,b}(s)$ are vectors for the voltages of the system. $[.]$

For more information on the calculation of the matrix refer to appendix A.1.6. As the size of several matrix extends the limitation of this report, they will be shown as elements instead and is found on the CD [Calculations/Matrix_[matrix name]].

By isolating the currents in equation 2.47, a new matrix is defined.

$$M_I(s) = M_E^{-1}(s) \cdot M_{v_{a,b}}(s) \quad [.] \quad (2.48)$$

With the expression for the currents it is possible to determine the matrix $G(s)$ for two output, by defining a matrix $M_y(s)$ for the selected output and multiply it with $M_I(s)$.

$$G(s) = M_{y_{a,b}}(s) \cdot M_E^{-1}(s) \cdot M_{v_{a,b}}(s) \quad [.] \quad (2.49)$$

Where:

$M_{y_{a,b}}(s)$ is a matrix containing ones or zeros, corresponding to $y_{a,b}(s)$. $[.]$

$y_{a,b}(s)$ are vectors for the output of the system. $[.]$

The concept is illustrated on figure 2.24, where the matrix $M_y(s)$ retain the wanted outputs and remove the others.

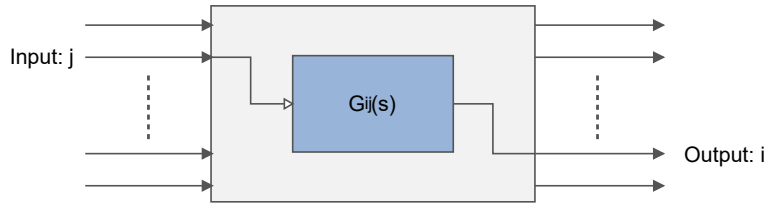


Figure 2.24: A figure of a MIMO system, where a input is channel to a specific output

There are four measurable points to chose between, two of which are dynamic. Any combination can then be selected and examined relatively easy by replacing the matrix. Since it is the voltages over the measure points that needs to be examined, it is the component included after this point that is inserted in the matrix corresponding to the current loop. Two possible matrix are shown, one without dynamic parts, seen in equation 2.50 and one with dynamic parts, seen in equation 2.51.

$$M_{y_{a,b}}(s) = \begin{bmatrix} 0 & R_{18} & 0 & 0 & 0 & 0 \\ 0 & 0 & 0 & R_{20} & 0 & 0 \end{bmatrix} \quad [\cdot] \quad (2.50)$$

$$M_{y_{2a,b}}(s) = \begin{bmatrix} (R_8 + L_8s + R_{17}) & 0 & 0 & 0 & 0 & 0 \\ 0 & 0 & (R_{11} + L_{11}s + R_{19}) & 0 & 0 & 0 \end{bmatrix} \quad [\cdot] \quad (2.51)$$

The matrix of $G(s)$ can then be expressed as.

$$G(s) = \begin{bmatrix} G_{11}(s) & G_{12}(s) \\ G_{21}(s) & G_{22}(s) \end{bmatrix} \quad [\cdot] \quad (2.52)$$

The transfer function for each element of $G(s)$, that is obtained by having selected the matrix $M_{y_{a,b}}$, can be seen below.

$$G_{11}(s) = \frac{0.130(s + 7.453)(s + 6.013)(s + 0.698)(s^2 + 6.367s + 10.680)}{(s + 7.205)(s + 6.068)(s + 5.760)(s + 2.524)(s + 1.716)(s + 0.657)} \quad (2.53)$$

$$G_{12}(s) = \frac{0.071(s + 8.353)(s + 7.453)(s + 5.980)(s + 2.113)(s + 0.676)}{(s + 7.205)(s + 6.068)(s + 5.760)(s + 2.524)(s + 1.716)(s + 0.657)} \quad (2.54)$$

$$G_{21}(s) = \frac{0.052(s + 10.090)(s + 7.145)(s + 6.205)(s + 2.635)(s + 0.697)}{(s + 7.205)(s + 6.068)(s + 5.760)(s + 2.524)(s + 1.716)(s + 0.657)} \quad (2.55)$$

$$G_{22}(s) = \frac{0.117(s + 7.199)(s + 6.205)(s + 4.724)(s + 2.305)(s + 0.677)}{(s + 7.205)(s + 6.068)(s + 5.760)(s + 2.524)(s + 1.716)(s + 0.657)} \quad (2.56)$$

The transfer function for each element of $G2(s)$ having selected $M_{y_{2a,b}}$, can be seen below.

$$G_{211}(s) = \frac{0.014(s + 12.120)(s + 6.903)(s + 6.013)(s + 0.698)(s^2 + 6.367s + 10.680)}{(s + 7.205)(s + 6.068)(s + 5.760)(s + 2.524)(s + 1.716)(s + 0.657)}$$

(2.57)

$$G2_{12}(s) = \frac{0.008(s + 12.120)(s + 8.353)(s + 6.903)(s + 5.980)(s + 2.113)(s + 0.676)}{(s + 7.205)(s + 6.068)(s + 5.760)(s + 2.524)(s + 1.716)(s + 0.657)} \quad (2.58)$$

$$G2_{21}(s) = \frac{0.007(s + 10.090)(s + 10.080)(s + 7.145)(s + 5.799)(s + 2.635)(s + 0.697)}{(s + 7.205)(s + 6.068)(s + 5.760)(s + 2.524)(s + 1.716)(s + 0.657)} \quad (2.59)$$

$$G2_{22}(s) = \frac{0.015(s + 10.080)(s + 7.199)(s + 5.799)(s + 4.724)(s + 2.305)(s + 0.677)}{(s + 7.205)(s + 6.068)(s + 5.76)(s + 2.524)(s + 1.716)(s + 0.657)} \quad (2.60)$$

Having found $G(s)$ and $G2(s)$, the system can now be described as a MIMO system (see 2.46), with two input $V_{a,b}(s)$ and two output $Y_{a,b}(s)$. With the transfer functions for both being such a high order, it has been chosen to approximate it to a lower order. Furthermore has it been chosen, to first focus on $G(s)$ and ensure it works, before continuing with $G2(s)$ as the required steps, should be similar to $G(s)$.

2.7 System approximation

In this section, the transfer functions of matrix $G(s)$, that was found in section 2.6, will be approximated to a lower order, using frequency response analysis.

Although a high order system can be controlled, it is computationally wise difficult. If the order of the system could be reduced without changing the properties of the system, the computation would become easier. Reduction is often possible as the contribution from a zero and a pole, placed relative close to each other, can be considered relative small. A water distribution network is typical relative slow, to avoid pressure surge, which can cause damage on the system, therefore is fast transition in the pressure undesirable. A first order approximation would therefore be preferable.

To approximate a first order system, the following steps are used:

1. Plot the frequency response of the transfer function.
2. Obtain the first corner frequency.
3. Plot the non-approximated transfer function and the approximated transfer function.
4. Calculate the gain from the difference in magnitude.
5. Insert the calculated gain in the approximated transfer function and repeat step 3.

6. Ajust the perameters if necessary.

Following step 1 through 2, the frequency response for element $G_{11}(s)$, which transfer function can be seen below or found in section 2.6.

$$G_{11}(s) = \frac{0.130(s + 7.453)(s + 6.013)(s + 0.698)(s^2 + 6.367s + 10.680)}{(s + 7.205)(s + 6.068)(s + 5.760)(s + 2.524)(s + 1.716)(s + 0.657)} \quad (2.61)$$

To obtain the corner frequency, the location where the magnitude drops by three dB is found. This can be seen in figure 2.25.

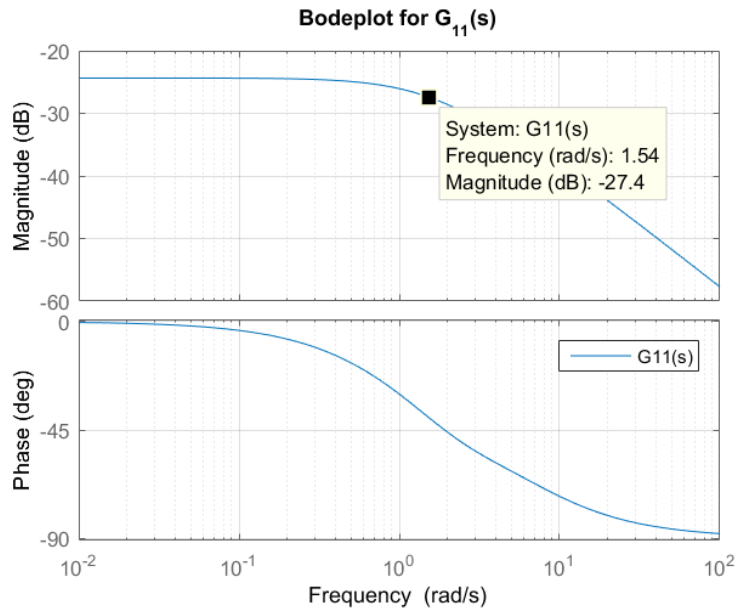


Figure 2.25: Bodeplot for $G_{11}(s)$

The corner frequency was found at 1.540 rad/s. The element $G_{11}(s)$ is then replaced with the approximated element $G_{a11}(s)$.

$$G_{a11}(s) = \frac{K}{s + 1.540} \quad (2.62)$$

Where:

The constant K is a gain.

[\cdot]

For step 3 and 4, a gain K is set to be equal to one, thereby giving the frequency response seen in figure 2.26.

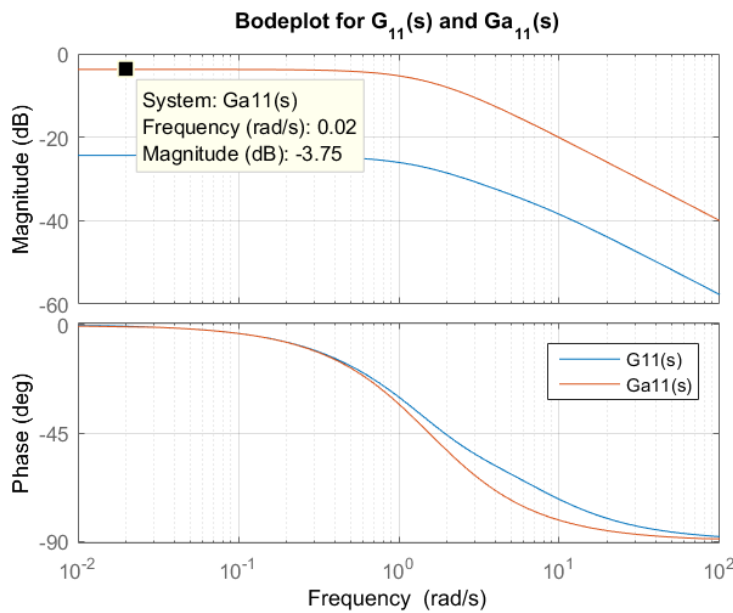


Figure 2.26: Bodeplot for $G_{11}(s)$ and $G_{a11}(s)$

To align the two plots, a new gain has to be calculated, this can be done using the following equation.

$$K = 10^{\frac{G_{11}dB - G_{a11}dB}{20dB}} \quad [.] \quad (2.63)$$

The magnitude for $G_{11}(s)$ is found to be -24.4 dB and for $G_{a11}(s)$ the magnitude is -3.75 dB, both at 0.02 rad/s, thereby is K equal to 0.093 .

Following step 5 both transfer functions are plotted in figure 2.27. The magnitude of G_{a11} align relatively close to $G_{11}(s)$, up to 2 rad/s, where the phase start to deviate at 0.7 rad/s. To improve this, it would require a higher order approximation, but the first order is considered sufficiently close.

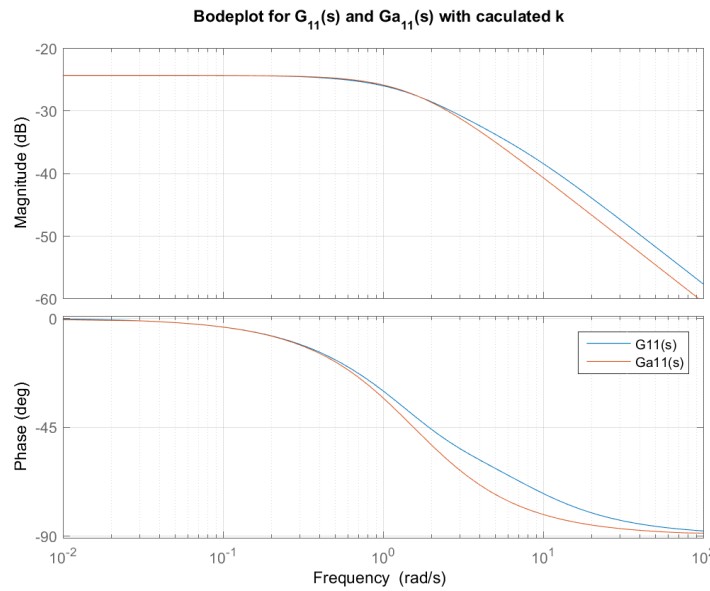


Figure 2.27: Bodeplot for $G_{11}(s)$ and $G_{a11}(s)$ with new gain K .

The remaining three approximations are found using the same method, therefore the steps are repeated for element $G_{22}(s)$, which transfer function was found in section 2.6, can be seen below.

$$G_{22}(s) = \frac{0.117(s + 7.199)(s + 6.205)(s + 4.724)(s + 2.305)(s + 0.677)}{(s + 7.205)(s + 6.068)(s + 5.760)(s + 2.524)(s + 1.716)(s + 0.657)} \quad (2.64)$$

A frequency response of $G_{22}(s)$, can be seen in figure 2.28, where the corner frequency was found at 1.820 rad/s.

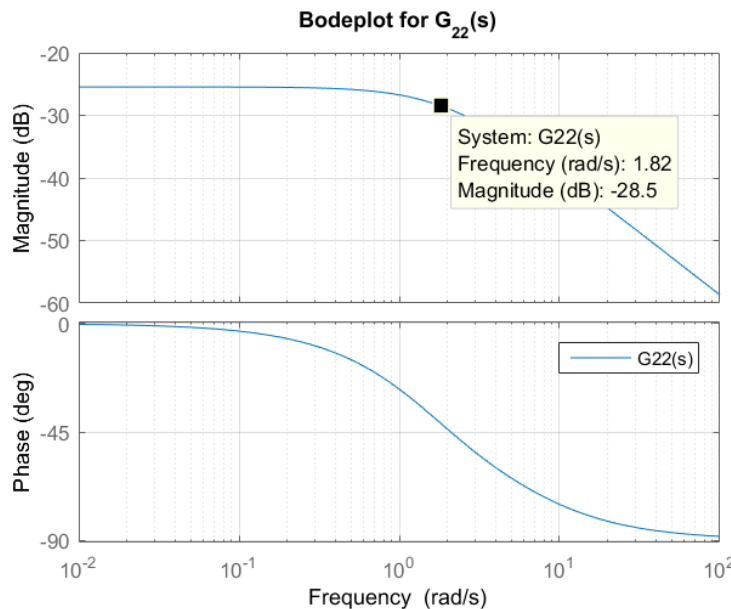


Figure 2.28: Bodeplot for $G_{22}(s)$

The element $G_{22}(s)$ is then replaced with the approximated element $Ga_{22}(s)$.

$$Ga_{22}(s) = \frac{K}{s + 1.820} \quad (2.65)$$

To align the two plots, a new gain has to be calculated. Setting K equal to one and plotting the two transfer functions, is giving the resulting frequency response, seen in figure 2.29.

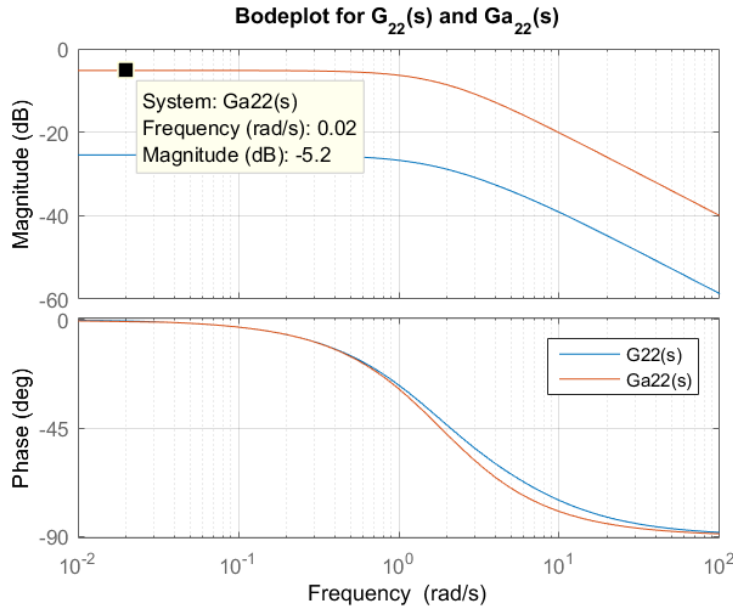


Figure 2.29: Bodeplot for $G_{22}(s)$ and $Ga_{22}(s)$

The magnitude for $G_{22}(s)$ is found to be -25.5 dB and for $Ga_{22}(s)$ the magnitude is -5.2 dB, both at 0.02 rad/s. To calculate the necessary gain for K , equation 2.63 is used, thereby is K equal to 0.097 . In figure 2.30 is the plotted transfer functions, the magnitude and phase of Ga_{22} align relatively close to $G_{22}(s)$, until they have reached 2 and 0.7 rad/s. As with element $Ga_{11}(s)$, a second order approximation would be needed to improve it.

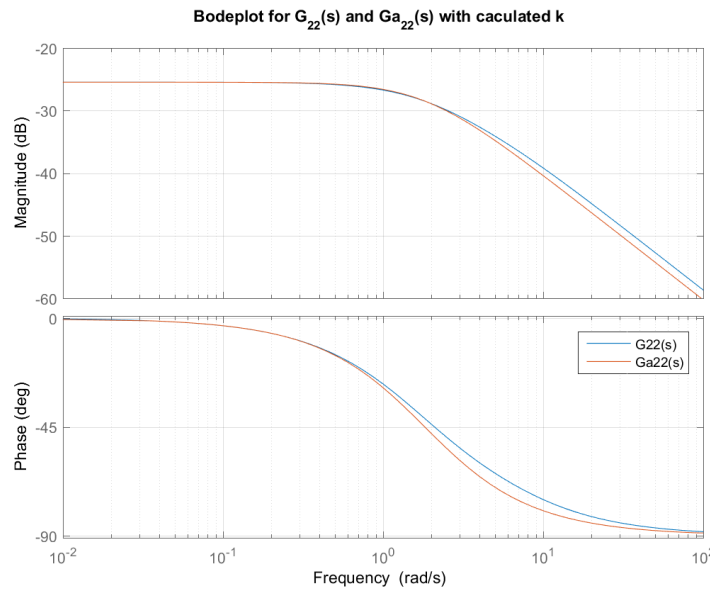


Figure 2.30: Bodeplot for $G_{22}(s)$ and $G_{a22}(s)$ with new gain K .

With both element $G_{11}(s)$ and $G_{22}(s)$ approximated, the next element is $G_{12}(s)$. The transfer function for $G_{12}(s)$, was found in section 2.6 and can be seen below.

$$G_{12}(s) = \frac{0.071(s + 8.353)(s + 7.453)(s + 5.980)(s + 2.113)(s + 0.676)}{(s + 7.205)(s + 6.068)(s + 5.760)(s + 2.524)(s + 1.716)(s + 0.657)} \quad (2.66)$$

A plot of the frequency response can be seen in figure 2.31, where the corner frequency was found at 1.750 rad/s.

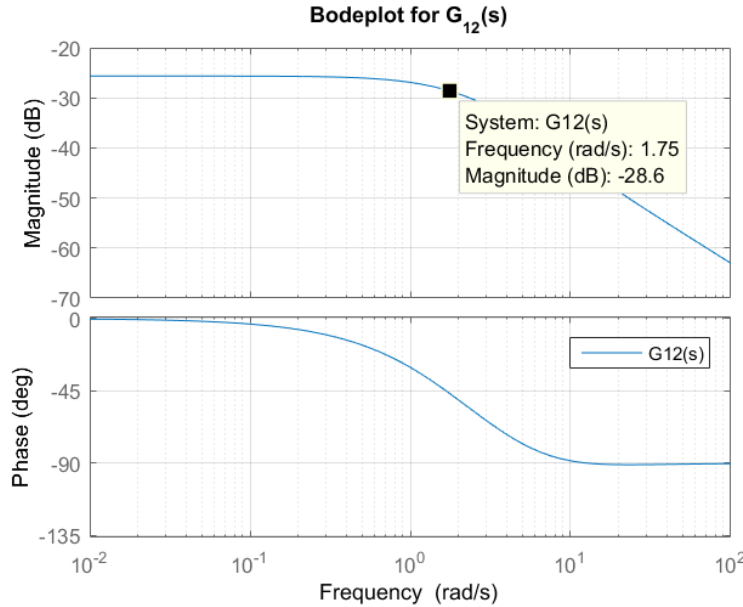


Figure 2.31: Bodeplot for $G_{12}(s)$

By replacing element $G_{12}(s)$ with the approximated element $Ga_{12}(s)$.

$$Ga_{12}(s) = \frac{K}{s + 1.750} \quad (2.67)$$

A plot of the two transfer functions, can be seen in figure 2.32, were K is set equal to one.

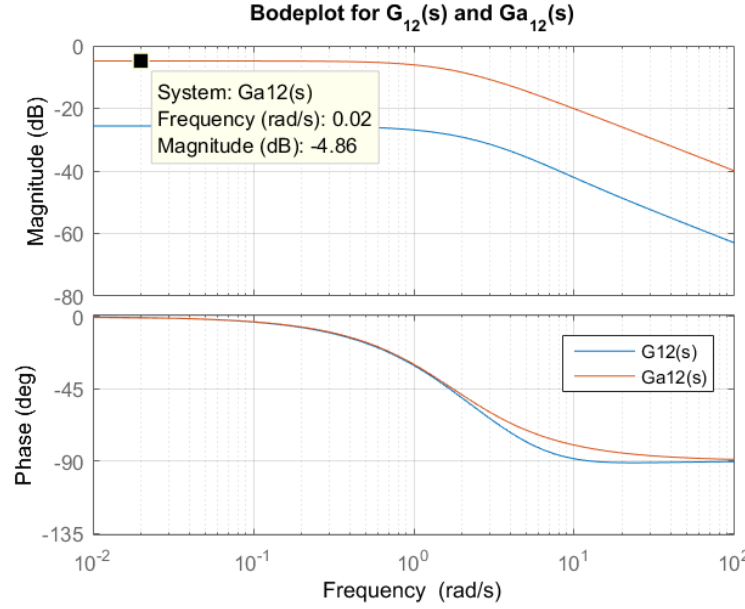


Figure 2.32: Bodeplot for $G_{12}(s)$ and $Ga_{12}(s)$

The gain K , is then calculated with a magnitude of -25.6 dB for $G_{12}(s)$ and -4.86 dB for $Ga_{12}(s)$ at 0.02 rad/s, with equation 2.63, to align the two transfer functions. The calculated gain K is then equal to 0.092 . The result can be seen in figure 2.33, where the magnitude and phase of Ga_{22} , align relatively close to $G_{22}(s)$, until they have reached 4 and 1 rad/s.

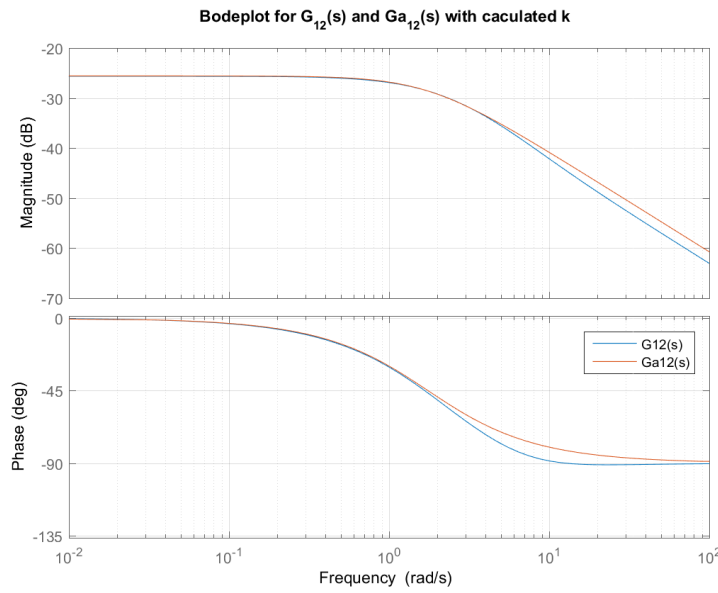


Figure 2.33: Bodeplot for $G_{12}(s)$ and $G_{a12}(s)$ with new gain K .

The remaining element is $G_{21}(s)$, for which the transfer function was found in section 2.6, is seen below.

$$G_{21}(s) = \frac{0.052(s + 10.090)(s + 7.145)(s + 6.205)(s + 2.635)(s + 0.697)}{(s + 7.205)(s + 6.068)(s + 5.760)(s + 2.524)(s + 1.716)(s + 0.657)} \quad (2.68)$$

A frequency response of the transfer function is seen on figure 2.34, where the corner frequency was found at 1.420 rad/s.

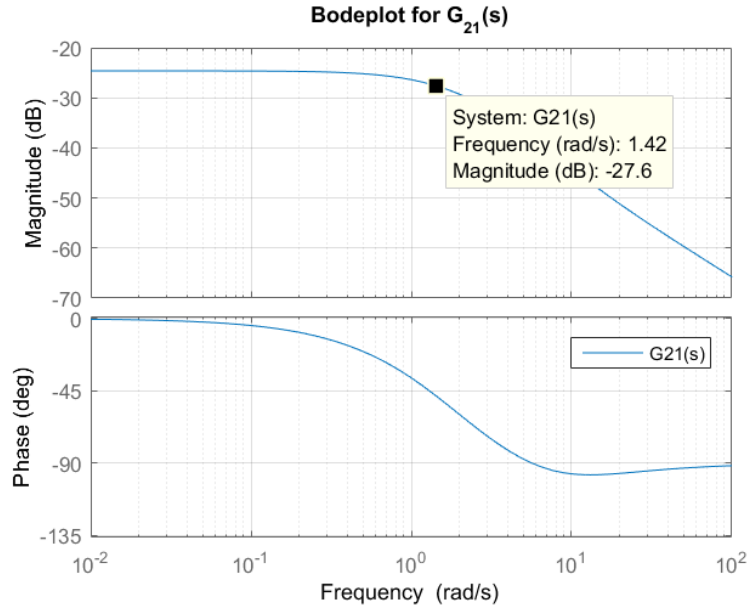


Figure 2.34: Bodeplot for $G_{21}(s)$

Replacing element $G_{21}(s)$ with the approximated $Ga_{21}(s)$ gives.

$$Ga_{21}(s) = \frac{K}{s + 1.420} \quad (2.69)$$

Then plotting both transfer function in figure 2.35, with K set equal to one. The gain K can then be calculated using equation 2.63 where the magnitude for $G_{21}(s)$ is found at -24.6 dB and at -3.05 dB for $Ga_{21}(s)$, both at 0.02 rad/s. K is then equal to 0.084 . The result is seen in figure 2.36.

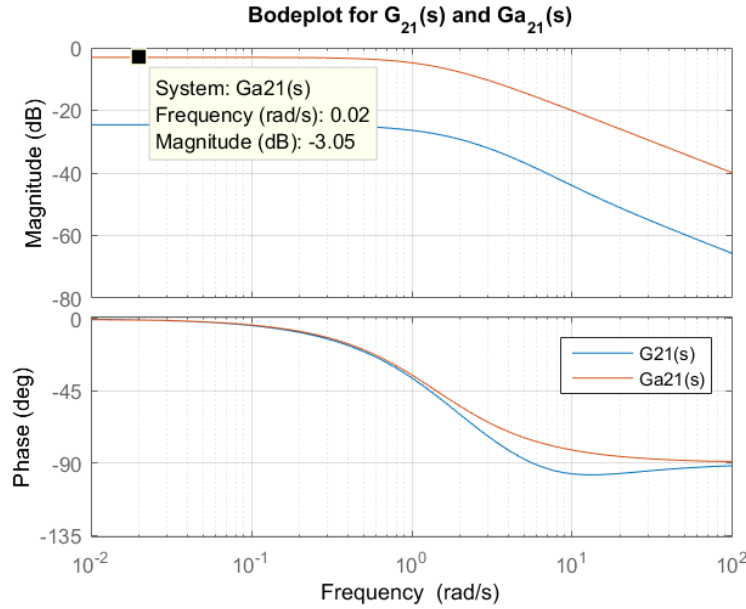


Figure 2.35: Bodeplot for $G_{21}(s)$ and $Ga_{21}(s)$

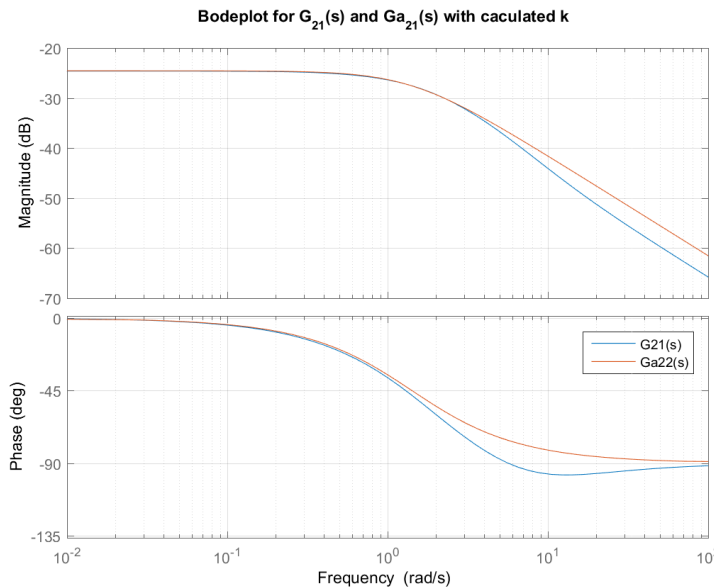


Figure 2.36: Bodeplot for $G_{21}(s)$ and $Ga_{21}(s)$ with new gain K .

As seen in figure 2.36, the magnitude and phase of G_{21} align relatively close to $G_{21}(s)$, but starts to deviate after reaching 2 and 0.7 rad/s. The deviation has been relative consistent for all element, except from element $G_{12}(s)$, which is better and the same applies for the magnitudes. As mentioned throughout this section, to improve the phase and magnitude for all elements, a second order approximation would be needed. This would require a zero in the left half plane to maintain the phase and a additional pole to force the magnitude down.

Thereby, the approximated matrix of $G(s)$ consisting of four first order approximations, giving a new matrix $G_a(s)$.

$$G_a(s) = \begin{bmatrix} \frac{0.093}{s+1.540} & \frac{0.092}{s+1.750} \\ \frac{0.084}{s+1.420} & \frac{0.097}{s+1.820} \end{bmatrix} \quad [.] \quad (2.70)$$

With the transfer functions reduced to four first order approximations, the physical system will be analysed in the next section.

2.8 Analysis of the physical system

This section contains an analysis of the physical system in the laboratory, to obtain the parameters for the system response and thereby calculate the transfer function for the matrix $G(s)$. It should be notice, that matrix $G(s)$ only refer to the physical system in this section. The water distribution network is shown on figure 2.37 and is used as reference together with table 2.6.

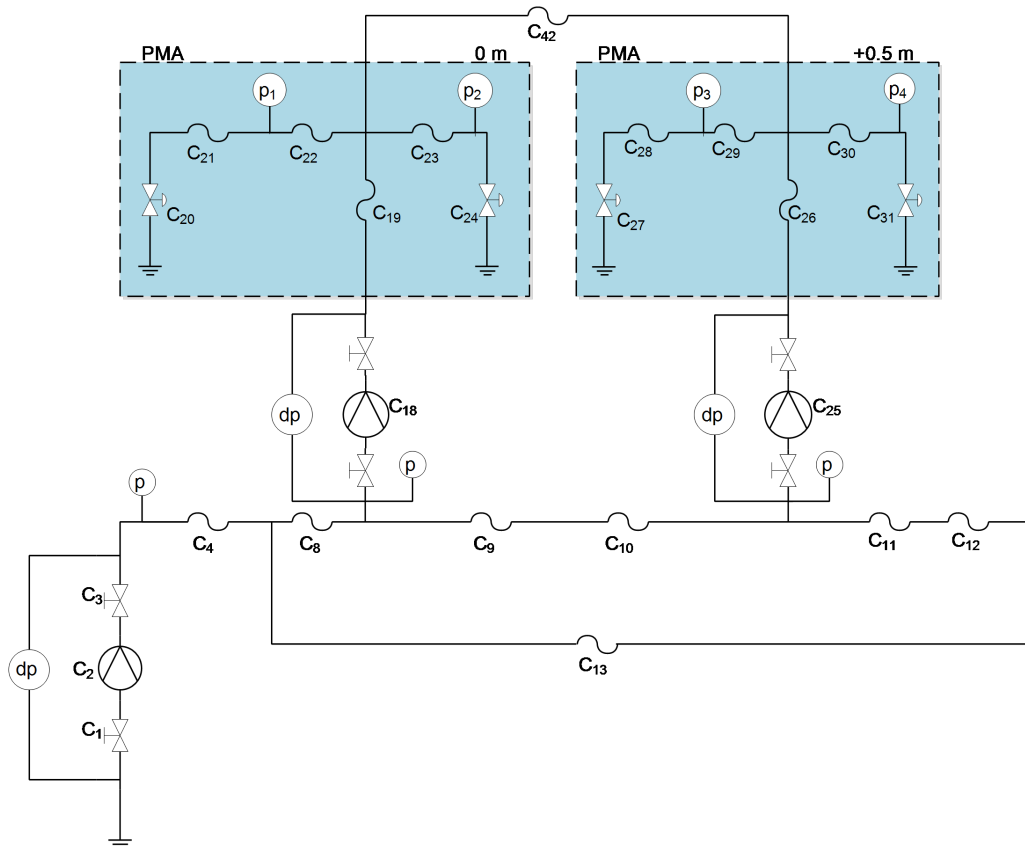


Figure 2.37: Diagram of the reduced distribution system.

	$C_{18} (V_a)$	$C_{25} (V_b)$
$C_{24} (P_2)$	$G_{11}(s)$	$G_{12}(s)$
$C_{31} (P_4)$	$G_{21}(s)$	$G_{22}(s)$

Table 2.6: Table of relation between element of $G(s)$, Input 1 (C_{18}), Input 2 (C_{25}), Output 1 (C_{24}) and Output 2 (C_{31}).

The system response for C_{18} and C_{25} were obtained from a measurement performed on the physical system (see appendix A.3.2), where the valves C_{20} , C_{24} , C_{27} and C_{31} are fully opened and a step starting from the operation point at 0.5 to 0.6 is applied to the pumps respectively to C_{18} and thereafter C_{25} . The goal of the analysis, is to find the transfer function between the inputs of C_{18} and C_{25} , to the output C_{24} and C_{31} . The output for the valves C_{24} and C_{31} , where the step is performed on C_{18} and C_{25} , is shown in figure 2.38, where a step is applied at P2, from the set point at 0.11 to 0.1165 bar and for P4 from the set point 0.08 to 0.08629 bar.

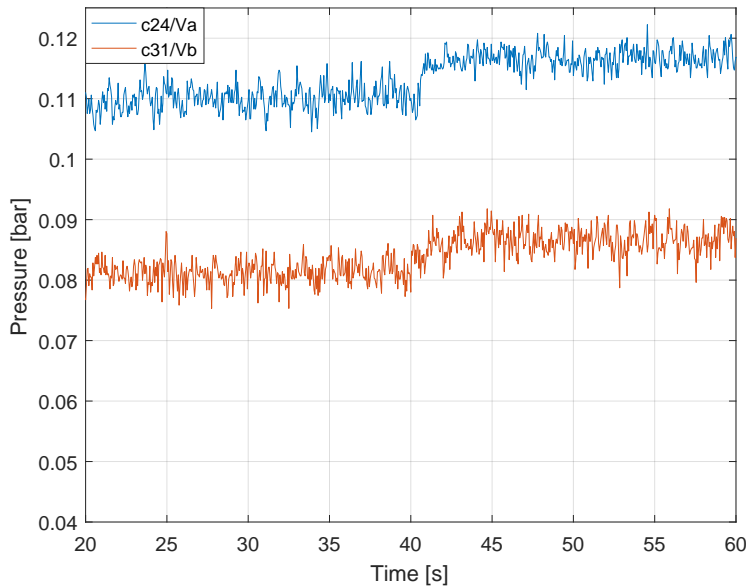


Figure 2.38: Step response for the outputs C_{24} and C_{31} , with a step on C_{18} (Va) and C_{25} (Vb).

The outputs in figure 2.38, corresponds to element $G_{11}(s)$ and $G_{22}(s)$ of the physical system. It can be seen, that both outputs have the characteristic of a first order system. In figure 2.39 the output from valve C_{31} and C_{24} is shown, where the step is respectively performed on C_{18} and C_{25} .

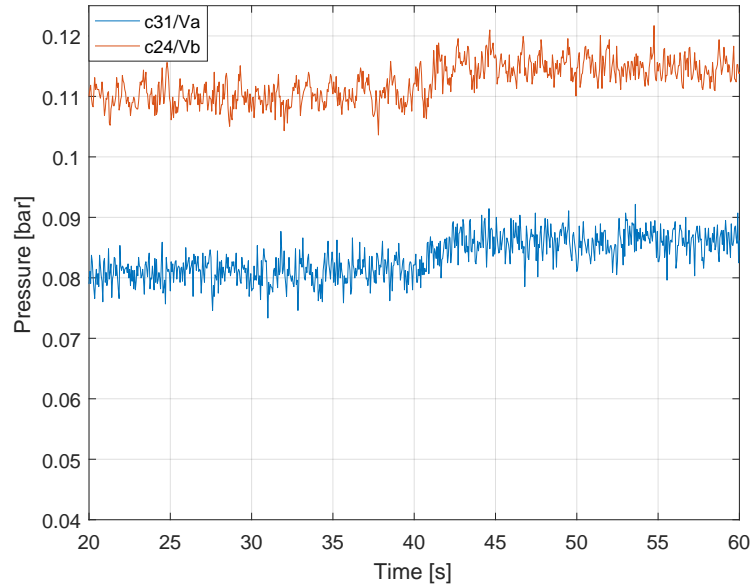


Figure 2.39: Step response for outputs C_{31} and C_{24} , with a step on C_{18} (V_a) and C_{25} (V_b).

The outputs in figure 2.39, corresponds to element $G_{12}(s)$ and $G_{21}(s)$ of the physical system. The characteristic of both outputs are a first order system and therefore can all four measurement be analysed as first orders. The analysis for G_{11} will be shown in the main report. To see the analysis for the remaining three first orders, refer to appendix A.3.2.

A first order transfer function is shown in equation 2.71:

$$G(s) = \frac{K}{\tau \cdot s + 1} \quad (2.71)$$

To find the gain K and the time constant τ , the system response is analysed. In figure 2.40, the step response and the moving average for G_{11} is shown.

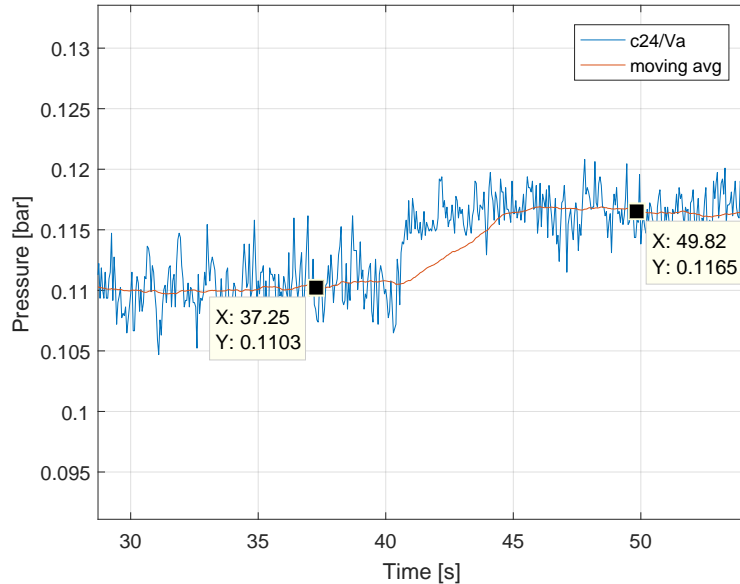


Figure 2.40: Step response and moving average for G_{11} (c_{24}/V_a), were a moving average is used with a window size of 80 points.

To find the time constant, the set point and steady state of the final parameter must be known. Therefore has a filter been used to find the moving average of the measured data. The moving average has a window size of 80 points because it gave the best approximation of the set point and steady state parameter. The set point of G_{11} is measured to be:

$$\text{Set point} = 0.1103 \quad [\text{bar}] \quad (2.72)$$

The steady state value of G_{11} , where a step from the set point is applied, is measured to be:

$$\text{Steady state value} = 0.1165 \quad [\text{bar}] \quad (2.73)$$

The increment of the step response can be found as:

$$\begin{aligned} \text{increment} &= \text{Steady state value} - \text{Set point} \\ &= 0.1165 - 0.1103 \\ &= 0.0062 \end{aligned} \quad [\text{bar}] \quad (2.74)$$

Calculating the point at 63 %:

$$\begin{aligned} &= 0.63 \cdot \text{increment} \\ &= 0.63 \cdot 0.0062 \\ &= 0.0039 \end{aligned} \quad [\cdot] \quad (2.75)$$

63 % from the starting value:

$$\begin{aligned} 63\% &= \text{Set point} + 0.0039 \\ &= 0.1142 \end{aligned} \quad [\cdot] \quad (2.76)$$

With the pressure known at 63 %, the time constant τ can be found by subtracting the time at 63 % from the time at the step start at 0 %. In figure 2.41 these points are plotted.

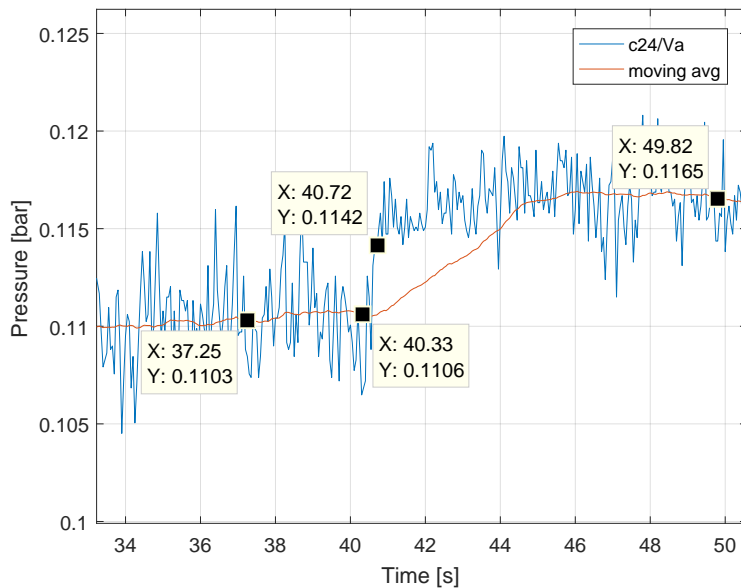


Figure 2.41: Step response and moving average for G_{11} (c_{24}/Va), were a moving average is used with a window size of 80 points.

τ is calculated in the following equation:

$$\tau = 40.72 - 40.33 \quad [\text{s}] \quad (2.77)$$

$$\tau = 0.39 \quad [\text{s}] \quad (2.78)$$

With τ known the remaining factor to be calculated is the gain K. The gain K is found by taking the increment of the output and divide it by the increment of the input step, on the pump. In figure 2.42, the step response for the pump C_{18} is shown.

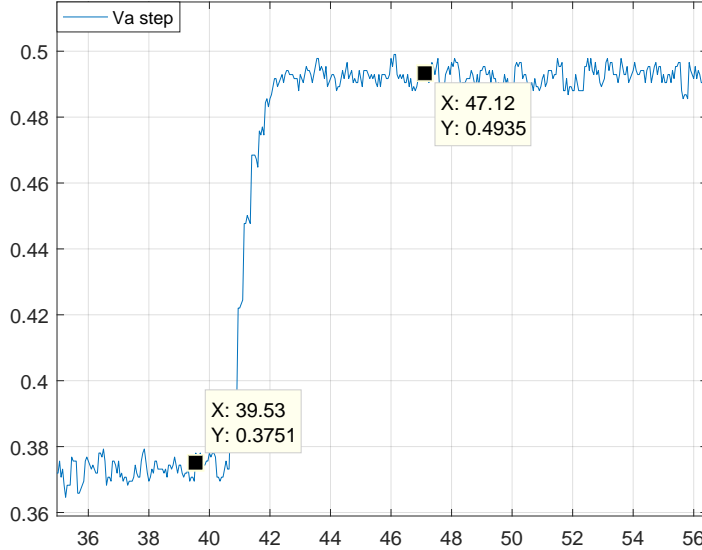


Figure 2.42: Step response for the pump C_{18} (Va).

The increment for the step response on the pump can be calculated as:

$$\begin{aligned} \text{Input increment} &= 0.4935 - 0.3751 & [\text{bar}] \quad (2.79) \\ &= 0.1184 & [\text{bar}] \end{aligned}$$

To find K the increment of the output is divide by increment of the input which is shown in the following equation:

$$\begin{aligned} K &= \frac{\text{Output increment}}{\text{Input increment}} & [.] \quad (2.80) \\ &= \frac{0.0062}{0.1184} \\ &= 0.0524 \end{aligned}$$

The first order transfer function for element G_{11} is now calculated and can be seen in the following equation:

$$G_{11} = \frac{0.0524}{0.39 \cdot s + 1} \quad (2.81)$$

The first order transfer functions for element G_{11} , G_{12} , G_{21} and G_{22} can be seen in the new matrix $G_b(s)$:

$$G_b(s) = \begin{bmatrix} \frac{0.0524}{0.39 \cdot s + 1} & \frac{0.03729}{0.24 \cdot s + 1} \\ \frac{0.04375}{0.35 \cdot s + 1} & \frac{0.0484}{0.37 \cdot s + 1} \end{bmatrix} \quad [\cdot] \quad (2.82)$$

The transfer functions and the set points for the physical system is known. The set point for P2 was found to be 0.11 bar and the set point for P4 was found to be 0.08 bar. In the next section these will be compared with the transfer functions from the approximated model $G_a(s)$ from section 2.7, to determine if the model correspond to the physical system.

2.9 Model verification

In this section, the approximated model $G_a(s)$ from section 2.7 will be compared with the physical model $G_b(s)$ from section 2.8, to determine if the model fits the physical system.

The model from section 2.7 can be seen on equation 2.83:

$$G_a(s) = \begin{bmatrix} \frac{0.093}{s+1.540} & \frac{0.092}{s+1.750} \\ \frac{0.084}{s+1.420} & \frac{0.097}{s+1.820} \end{bmatrix} \quad [\cdot] \quad (2.83)$$

The equation represent four first orders transfer functions. These transfer functions is calculated in mWC and therefore will they be converted into bar before compared with the physical model from section 2.8. Furthermore will the transfer function $G_a(s)$ be rearrange over to the standard first order transfer function form as seen on equation 2.84. To see the calculations refer to appendix A.1.7:

$$G(s) = \frac{K}{\tau \cdot s + 1} \quad (2.84)$$

$$G_a(s) = \begin{bmatrix} \frac{0.00604}{0.65 \cdot s + 1} & \frac{0.00526}{0.57 \cdot s + 1} \\ \frac{0.00591}{0.70 \cdot s + 1} & \frac{0.00533}{0.55 \cdot s + 1} \end{bmatrix} \quad [\cdot] \quad (2.85)$$

In equation 2.86 the transfer function for the physical model from section 2.8 can be seen:

$$G_b(s) = \begin{bmatrix} \frac{0.0524}{0.39 \cdot s + 1} & \frac{0.03729}{0.24 \cdot s + 1} \\ \frac{0.04375}{0.35 \cdot s + 1} & \frac{0.0484}{0.37 \cdot s + 1} \end{bmatrix} \quad [\cdot] \quad (2.86)$$

The equation represent four first order transfer functions. These transfer function 2.85 and 2.86 will be plotted element wise together in a bodeplot to determine if the model from system approximation 2.85 is similar to the physical model 2.86 which is derived from the physical system.

In figure 2.43 (a), a bodeplot of $G_{a11}(s)$ and $G_{b11}(s)$ is shown and in figure 2.43 (b), a bodeplot of $G_{a12}(s)$ and $G_{b12}(s)$ is shown.

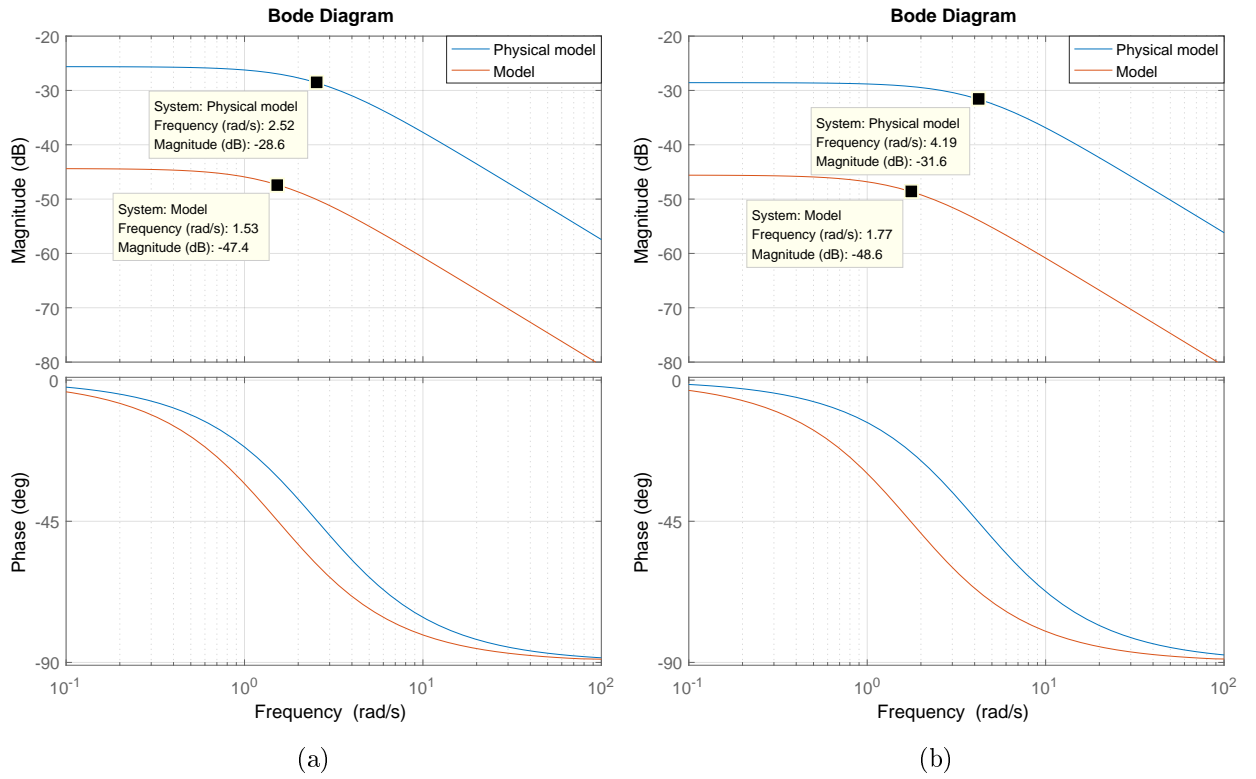


Figure 2.43: (a) Bodeplot of the physical model $G_{b11}(s)$ and the model $G_{a11}(s)$. (b) Bodeplot of the physical model $G_{b12}(s)$ and the model $G_{a12}(s)$.

From both figures, it can be concluded that the magnitude for the model does not correspond to the physical model. The physical model has approximately a factor 10 more in gain than the model. The phase is close to match, but as the bandwidth is smaller for the model than the physical model the phase will not fit.

In figure 2.44 (a), a bodeplot of $G_{a21}(s)$ and $G_{b21}(s)$ is shown and in figure 2.43 (b), a bodeplot of $G_{a22}(s)$ and $G_{b22}(s)$ is shown.

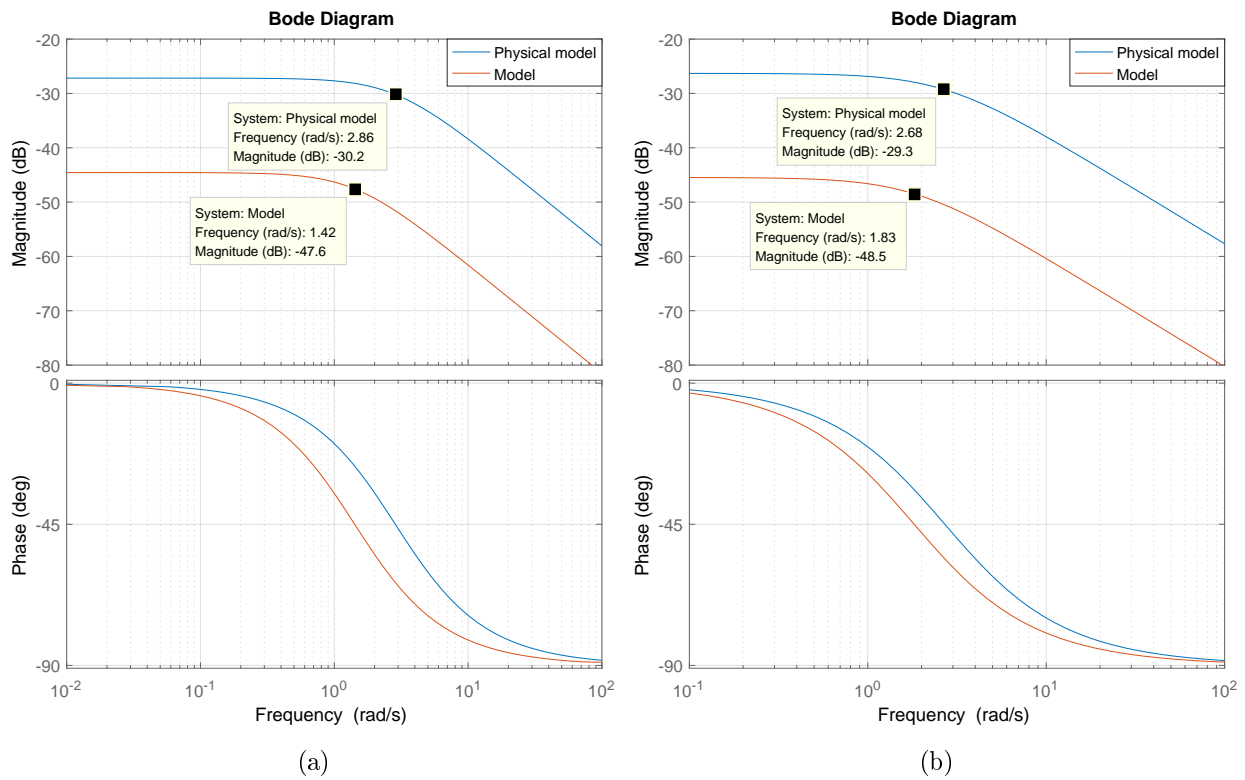


Figure 2.44: (a) Bodeplot of the physical model $Gb_{21}(s)$ and the model $Ga_{21}(s)$. (b) Bodeplot of the physical model $Gb_{22}(s)$ and the model $Ga_{22}(s)$.

The same conclusion can be drawn from figure 2.44 as stated with figure 2.43. The model does not correspond to the physical model and will therefore not be used in the system design and instead the physical model will be used to design the controller. The reason not to improve the model is that time is limited and it has been chosen to focus on making a controller for the system.

A possible reason for the models mismatch, could be the parameters calculated for the pipes, which did not include curves and bends and could be a factor to why the model does not correspond to the physical model.

Through this chapter, it can be concluded that a model for the pipes, valves and pumps was found based on an existent physical system which lead to an electric equivalent for the system. It is also concluded that in this chapter, the models and the electric equivalent have been derived, leading to six equations using KVL which have been linearised using the Taylor approximation. Furthermore, it can be concluded, that a MIMO system could be derived from the linearised equation and approximated to four first order transfer function. It was also possible to approximate four first order transfer function for the physical model. Finally, it could be concluded that the calculated model had similarities to the physical model, but could not be considered identical to it.

System requirement 3

This chapter will cover the requirements for the complete system, these are objectives for when system fulfill the problem statement. For each of the description there will be a individual test, to check if these requirements are met.

3.1 Requirement

In this section the requirements of the system will be defined, including a short description reasoning each requirement.

The focus of this project is to maintain a certain pressure at the critical points, when multiple PMA's are interconnected, which have been stated in the problem statement in section 1.3. As a notice, this means that all four valves will be fully opened when the tests are running, since the linearization includes them all.

As the pressure for end user must always be high enough to perform everyday tasks effectively, a requirement for the controllers is to maintain constant pressure at the critical points P2 and P4.

1. Regulate the output pressure to a constant set point for P2 and P4.
 - Set point for P2 equal to 0.1103 bar and set point for P4 equal to 0.08 bar these set point are found in section 2.8.

The system must not have any pressure surge because it would be undesirable for the system and the end user. It could potential cause a valve or a pipeline to be damaged as mentioned in 1.2. A way to eliminate pressure surge from the system is to make it very slow. But not to the degree that it is notable at the end user. Therefore it is chosen that the rise time for the controller should not be slower than 60 seconds to ensure that the end user is not affected.

2. Rise time should not be slower than 60 seconds.

The steady state error of the output must not deviate more than $\pm 5\%$. Which means that it must not be lower then -5 % the reference value or 5 % higher than the reference value.

3. Steady state error of the set points must deviate with more than $\pm 5\%$ for the outputs P2 and P4.

As oscillations in pressure may concern the end-user, the system must not have any overshoot.

4. Overshoot must not be higher than 0 % at the outputs P2 and P4.

The outputs must remain stable at the set points and therefore not oscillate.

5. The system response for output P2 and P4 must not oscillate but remain stable, which also refer to requirement 1 and 3.
6. The decoupling should compensate for the interconnection between the two PMA's.

3.2 Test specification

In this section, a description on how the tests will be performed, so the requirements in section 3.1 can be considered fulfilled. A single test can cover one or more requirement.

Test for system requirements

The purpose of this test is to examine whether the closed-loop system satisfy the requirements. This test will include the following requirements:

1. Regulate the output pressure to a constant set point for P2 and P4.
 - Set point for P2 equal to 0.1103 bar and set point for P4 equal to 0.08 bar these set point are found in section 2.8.
2. Rise time should not be slower than 60 seconds.
3. Steady state error of the set points must deviate with more than $\pm 5\%$ for the outputs P2 and P4.
4. Overshoot must not be higher than 0 % at the outputs P2 and P4.
5. The system response for output P2 and P4 must not oscillate but remain stable, which also refer to requirement 1 and 3.
6. The decoupling should compensate for the interconnection between the two PMA's.

By using the water distribution network at the Dept. of Electronic Systems, Section for Automation and Control (AAU no. 100911) the controller will be implemented in the system. A test will be conducted on the system where the system have to perform within the limits of the requirements.

The first test will be made where the desired reference is hold as constant, to verify that the control system can maintain the desired pressure at the outputs.

The second test will be made from the set point where a step is applied as reference to the hydraulic controller. To verify that the requirements are met the data will be logged and analyzed to see if the reference values from the requirements are satisfied.

If the controller manages to perform this test within the the limits defined in the requirements, this test will be deemed successful.

System design 4

This chapter will be a successor of the System analysis in Chapter 2, where cascade control will be explained and the control system will be analysed and designed to satisfy the system requirements found in section 3.1.

4.1 Cascade control

In this section, the concept and choice of using cascade control is explained. The functionality of each block is described and a procedure to design a cascade controller will be listed.

The functional block diagram for one input/Output of the system, implemented as a cascade control, can be seen in figure 4.1:

In figure 4.1 the secondary and primary loop of the cascade controller can be seen.

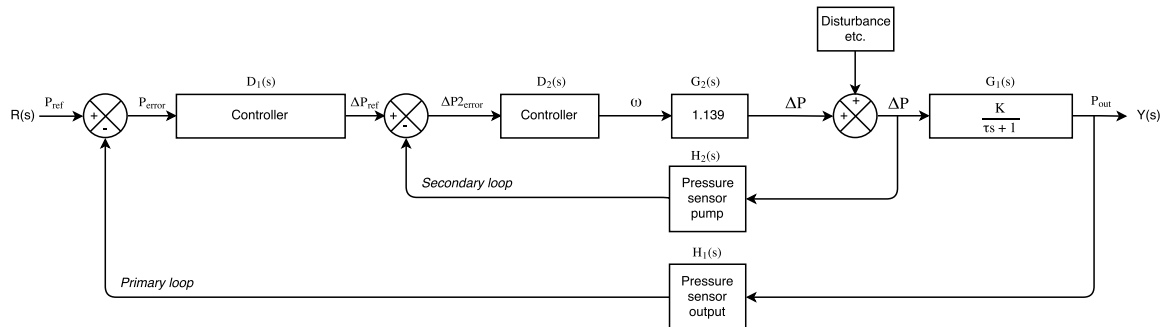


Figure 4.1: Block diagram of the cascade controller with transfer functions for the plants.

It has been chosen to design the control system as a cascade controller as the distribution system has multiple sensors and two variables to control. The reason for choosing a cascade controller, is because that the hydraulic system expect a pressure as input, but the pump takes a velocity. A cascade control adds an additional controller, which can convert velocity into pressure. This is beneficial because then the pump can then be ignored in regard to controlling the primary loop under certain conditions. Furthermore a cascade controller corrects disturbance and gain variation in the secondary loop, before it can influence primary loop [Michael A. Johnson, 2005].

For a cascade controller the secondary loop is designed first and thereafter the primary loop is designed. The secondary loop should be designed to be as fast as possible or atleast 3-5 times faster than the primary loop to avoid problem with instability. [VanDoren, 2014].

The functional block diagram consists of the primary and secondary loop. The secondary loop represents a controller $D_2(s)$ and the pump $G_2(s)$, which is a gain found in the model for the pump in section 2.3. Furthermore the differential sensor for the pump is placed in the secondary loop. The primary loop represent the hydraulic model $G_1(s)$, which is a first order transfer function analyzed and derived in section 2.8. Furthermore the controller $D_1(s)$ is placed in the primary loop as well as the pressure sensor at the output.

As it is the pressure at the critical point $Y_s(s)$ that need to be controlled, the controller $D_1(s)$ take a reference P_{ref} minus the measured P_{out} giving P_{error} in the primary loop. To correct the pressure ΔP , the controller for the pump $D_2(s)$ will either have to increase or decrease the pressure across the pump, which is done by controlling the velocity ω . Therefore a controller $D_2(s)$ is added, to take the correction pressure ΔP_{ref} as a reference, minus the measured ΔP giving ΔP_{2error} in the secondary loop. Any disturbance in secondary loop will be corrected, before it affect the primary loop, if the loop is sufficiently faster, compared to the primary loop.

The system design will be performed in the following order, with respect to the design of a cascade control.

First: the secondary loop must be designed, to be atleast 3-5 times faster then the primary loop, that must accommodate for the requirement of the system.

Second: An analysis of whether decoupling is needed. If it is needed, a decoupler must be implemented, before the system can be considered as two single input single outputs (SISO) loop for the hydraulic model.

Third: the primary loop can be designed and a test of the functionality and stability, of the system can be performed. The fulfilment of the requirement can then be verified.

With a control design chosen and a design procedure found, the next section look into the design of controller for the secondary loops.

4.2 Design of pump controller

In this section, the controller in the secondary loop for the cascade control, will be designed in accordance with the design procedure in section 4.1.

The controller for the pump, is in the secondary loop, in the functional block diagram (see figure 4.2). The use of the controller, has the purpose to transform the angular velocity, ω , to a unit of pressure, as the hydraulic system is expecting a input of pressure. The conversion have to be done as fast as possible, but in consideration of stability. Therefore, a controller will be designed for the pump to deliver a certain pressure, controlled by the pump.

As this section only will focus on the secondary loop, as marked with the blue box in figure 4.2, the primary loop will in this section temporary be removed for the functional block diagram.

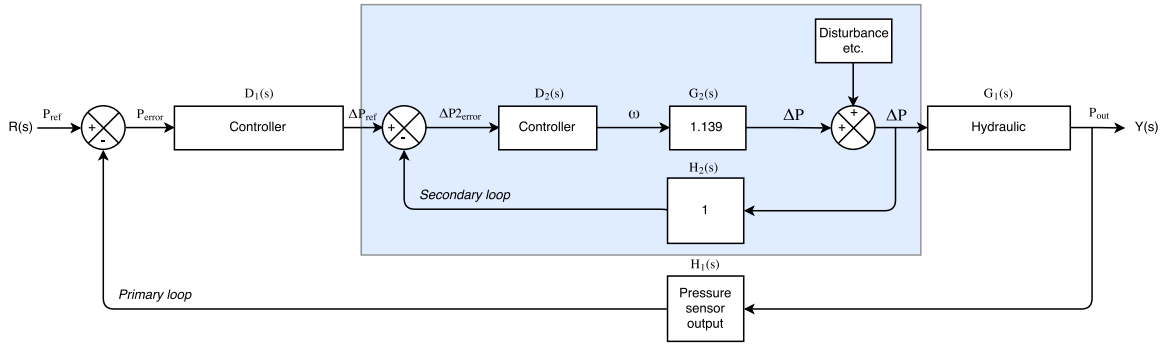


Figure 4.2: Functional block diagram for the pump (blue area).

Where the pump was determined in section 2.3 (equation 2.26), to be a gain at $G_2(s) = 1.139$. The transfer function for the pressure sensor of the pump is determined to be $H_2(s) = 1$, because of the system being much slower than the sampling time of the sensor [Gene F. Franklin, 1997].

Since the pump only consist of a gain, the response will produce steady state error. Therefore by adding an integral controller the steady state error will be eliminated. On figure 4.3, a gain, K multiplied on a integral have been added as controller for the pump.

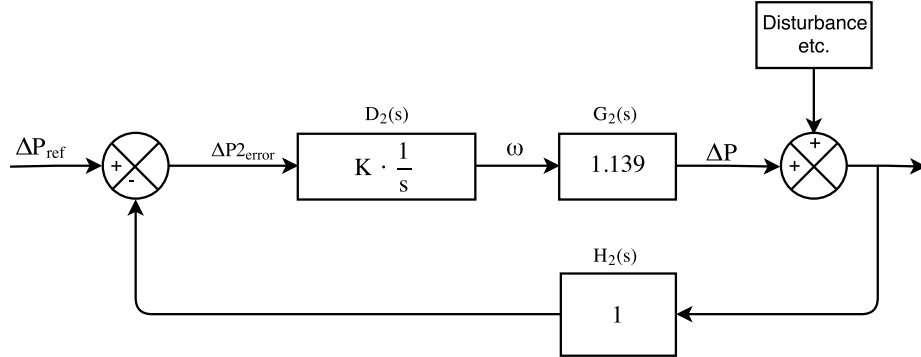


Figure 4.3: Functional block diagram for the pump with Integral control.

The open loop of the system is derived as:

$$OL(s) = D_2(s)G_2(s) \quad (4.1)$$

$$= \frac{K}{s} \cdot 1.139 \quad (4.2)$$

The closed loop of the system is derived as:

$$\begin{aligned}
 CL(s) &= \frac{D_2(s) \cdot G_2(s)}{1 + D_2(s) \cdot G_2(s)} \\
 &= \frac{K \cdot \frac{1}{s} \cdot 1.139}{1 + K \cdot \frac{1}{s} \cdot 1.139} \\
 &= \frac{K \cdot 1.139}{s + K \cdot 1.139}
 \end{aligned} \tag{4.3}$$

Where:

$D_2(s)$ is the controller in the secondary loop.

$G_2(s)$ is the plant in the secondary loop.

$H_2(s)$ is the sensor in the secondary loop.

The closed loop is a first order system, therefore first order analysis can be used, the standard form of a first order system are shown in equation 4.4.

$$C(s) = \frac{1}{\tau s + 1} \tag{4.4}$$

Where:

τ is the time constant. [s]

In equation 4.3, the time constant can be derive from the pole location $\frac{1}{\tau} = K \cdot 1.139$, solving for the time constant $\tau = \frac{1}{K \cdot 1.139}$, it is now clear how to determine the time constant and then the gain K and therefore find the new pole location for the closed loop transfer function of the pump controller.

The rise time can be calculated from the time constant:

$$t_r = \tau \cdot (\ln(0.9) - \ln(0.1)) \tag{4.5}$$

By knowing the rise time, the time constant τ can be solved.

$$\tau = \left(\frac{1}{\ln(0.9) - \ln(0.1)} \right) \cdot t_r \tag{4.6}$$

The parameter K is found from the time constant τ , where the rise time have been chosen from the perspective, of having manageable numbers as seen in table 4.1 and also by having a reasonably response time.

$$K = \frac{1}{\tau \cdot 1.139} \tag{4.7}$$

Different gains of K have been calculated from equation 4.7, from a various of rise times, which defines the time constant τ used in equation 4.7. The various of gains K is analyzed to find the best fit according to response time for the pump.

K	t_r [s]	$\min t_r$ [s]
1	1.9	5.7
0.772	2.5	7.5
0.643	3	9
0.551	3.5	10.5
0.482	4	12
0.429	4.5	13.5
0.386	5	15

Table 4.1: Table of parameter K , where t_r is the calculated rise time for the secondary loop and $\min t_r$ is the minimum rise time for the primary loop, which is calculated to be 3 times slower than the secondary loop.

The list of different gains in table 4.1, is observed in the physical system by individually making a step response with the gains of K , obtained in test journal A.3.5. The step is performed from ≈ 0.3788 to 0.4961 bar. The step responses are merged into one graph, see figure 4.4, to compare and to analyze the step response from each gain of K , all step responses start at the time of 40 seconds.

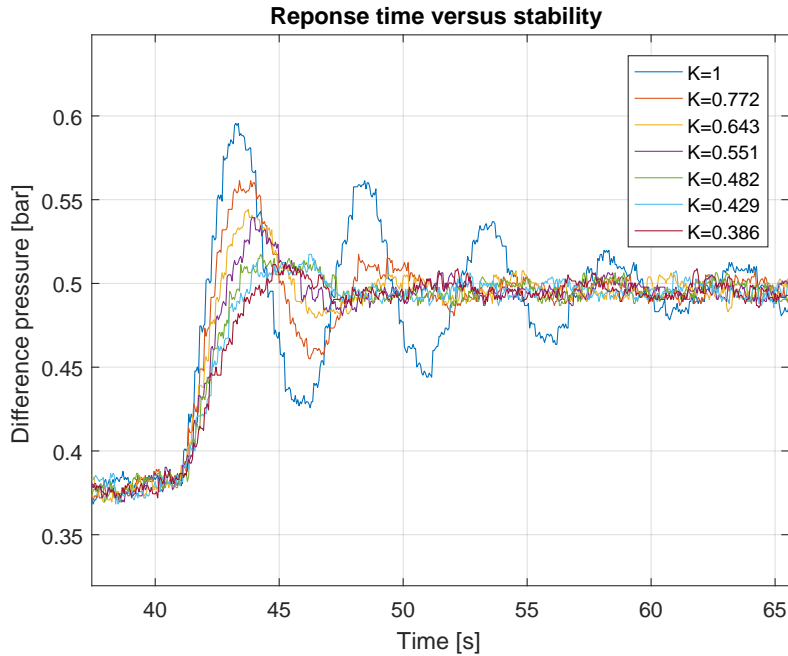


Figure 4.4: Response time for several gains of K , where a greater gain K give faster response time, but also longer settling time and larger overshoot, were the steps are applied at 40 seconds.

On figure 4.4, it can be observed that there is an overshoot when performing a step at the reference on the secondary loop. As for a first order system, there should not occur an overshoot, therefore it is assumed that the overshoot could come from delay in the pump. This would also correspond to why the step does not start at 40 seconds.

The observations stopped at a calculated rise time at 5 seconds, where the overshoot of the curve characteristic seemed sufficiently reduced. In figure 4.4 several graphs are plotted for the gain K , where a higher K gives better response time, but longer settling time and larger overshoot. Having a faster response time is desirable, but could come at the cost of

overshoot, which is undesirable.

The longer settling time and overshoot, could give stability issues as it might propagates into the primary loop. Making the two loops compete against each other and therefore the secondary loop can have trouble getting back from the fluctuations, which could make the closed loop system unstable. From the perspective of stability a high settling time and overshoot should be avoided. As the settling time and overshoot for K equal to 1, 0.772 and 0.643 is approximately 25, 15 and 10 seconds, are these opted out.

Further is it chosen to use a gain with little overshoot, where the rise time at 4.5 seconds is not the fastest nor the slowest of the chosen range of gain K , the gain chosen is K equal to 0.429.

The choice of the gain constant $K = 0.429$, seem to be a good fit for the pump, although the less overshoot also have a cost as it increased the rise time.

The closed loop for the secondary controller with the new gain $K = 0.429$:

$$\begin{aligned} CL(s) &= \frac{K \cdot \frac{1}{s} \cdot 1.139}{1 + K \cdot \frac{1}{s} \cdot 1.139} \\ &= \frac{0.489}{s + 0.489} \end{aligned} \tag{4.8}$$

From the closed loop transfer function in equation 4.8, it can be seen that there are no poles in the right half plane, but only the pole located in $p = -0.489$. Therefore the system is stable.

Verification of the pump controller

The pump controller is calculated by theory and is going to be tested by the physical water system in the laboratory, to verify if the designed controller also fit the physical system. Therefore a test is performed on both pumps, by measuring the difference pressure across the pump, applying a step as reference, starting from the operation point. The calculations for the rise time of V_a will be shown in the section and the results for V_b will be shown. The test journal with the steps done in the laboratory can be seen in journal A.3.5.

On figure 4.5, a step as reference is applied on pump V_a , from the operation point at the difference pressure ΔP equal 0.3788 to 0.4961 bar, which corresponds to the angular velocity $\omega = 0.5$ to $\omega = 0.6$ as input for the pump.

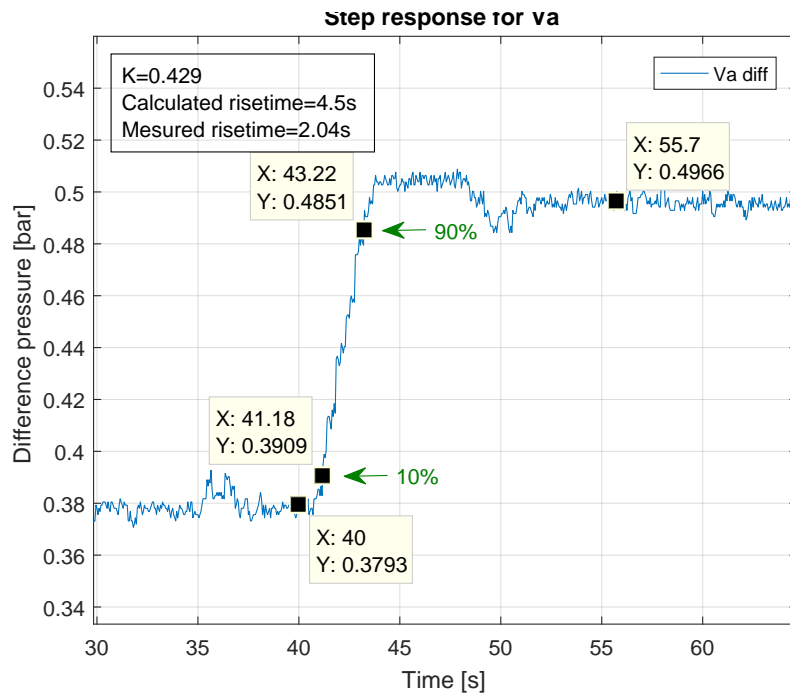


Figure 4.5: Step response for the differential pressure across V_a with the measured rise time.

On figure 4.6, a step as reference is applied on pump V_b , from the operation point at the difference pressure ΔP equal 0.3663 to 0.4802 bar, which corresponds to the angular velocity $\omega = 0.5$ to $\omega = 0.6$ as input for the pump.

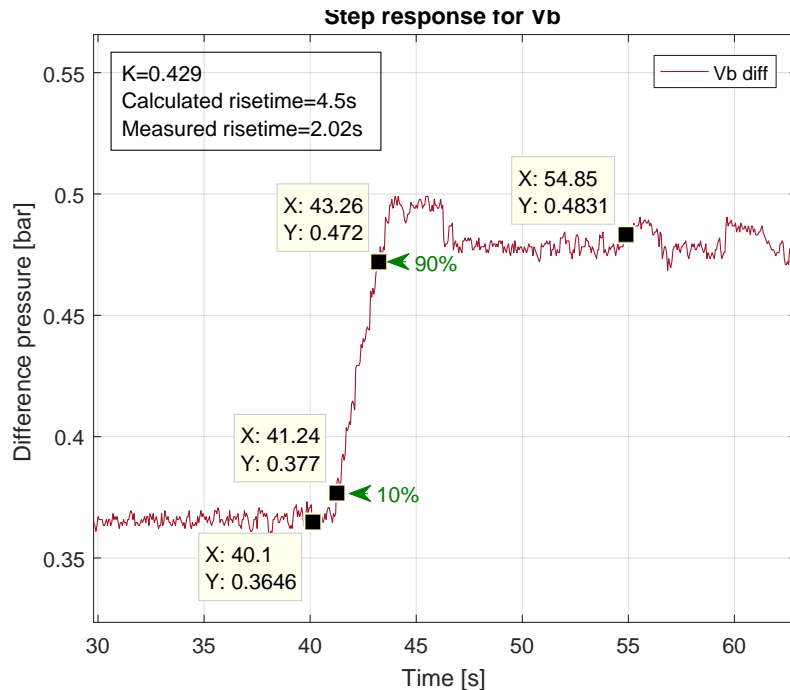


Figure 4.6: Step response for the differential pressure across V_b with the measured rise time.

As seen on figure 4.5 and figure 4.6, the measured rise time is approximately 2 seconds,

which is approximately 2.5 seconds less than the expected rise time that was calculated. Where the response is seen as a first order system, the overshoot seen in both figures is assumed as pump delay, hence is not part of the linear pump model derived in section 2.3, which is derived as a gain.

The measured rise time of the step responses is faster than expected and the gain value of $K = 0.429$ is going to be used in the integral controller for the pump. There is no poles in the right half plane, but only the pole located in $p \approx -0.489$, see equation 4.8. Therefore the system is verified to be stable.

The secondary loop is now inserted into the full cascade functional block diagram as seen in 4.7.

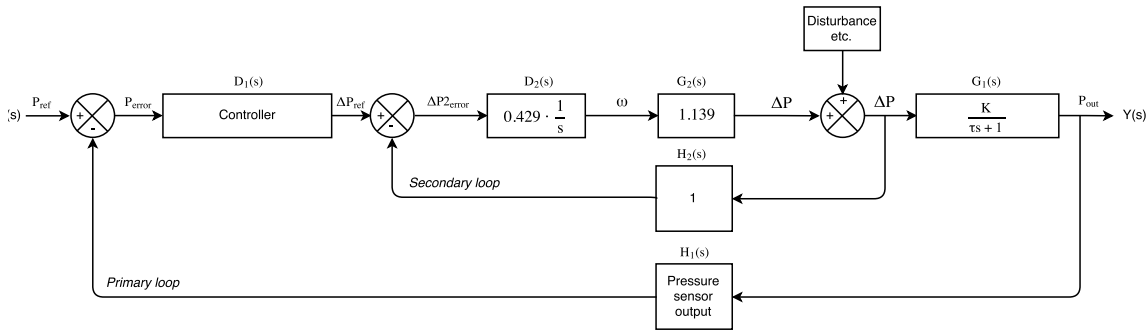


Figure 4.7: Functional block diagram of the cascade controller, with inserted values in the secondary loop.

According to the cascade system, the design requirement for the primary loop should be met, with a rise time at least three times slower than the secondary loop. Because of an error in earlier measurement the the hydraulic controller have been designed to 16.5 seconds, there have not been enough time to design a new controller. The cause of changes could have been in a faster controller for the hydraulic system.

A controller requirement for the hydraulic controller can therefore be made:

$$\begin{aligned} tr_{primary_loop} &\geq 3 \cdot tr_{secondary_loop} & [s] \quad (4.9) \\ &\geq 3 \cdot 5.5s \\ &\geq 16.5s \end{aligned}$$

The hydraulic controller should at least have a rise time of 16.5 seconds.

A controller for the pumps has been designed, thereby is the secondary loops done. This leads to the next step of the design procedure, the analysis of whether decoupling i needed.

4.3 Decoupling

In this section, an analysis of the necessity to decouple the hydraulic model , from a TITO to a SISO system, will be examined. The analysis will be based on decoupling theory and the calculations can be found in appendix A.2.1. The results of the calculations, can be found at the end of this section.

The decoupler will address the interactions between the two loops which are dependent of each other, but where the impact can be reduced [Karl J. Åstrøm, 2005]. The interactions in the system needs to be defined first. The system in this project is introduced as a two inputs two outputs (TITO) system, as illustrated in figure 4.8 [Knudsen,].

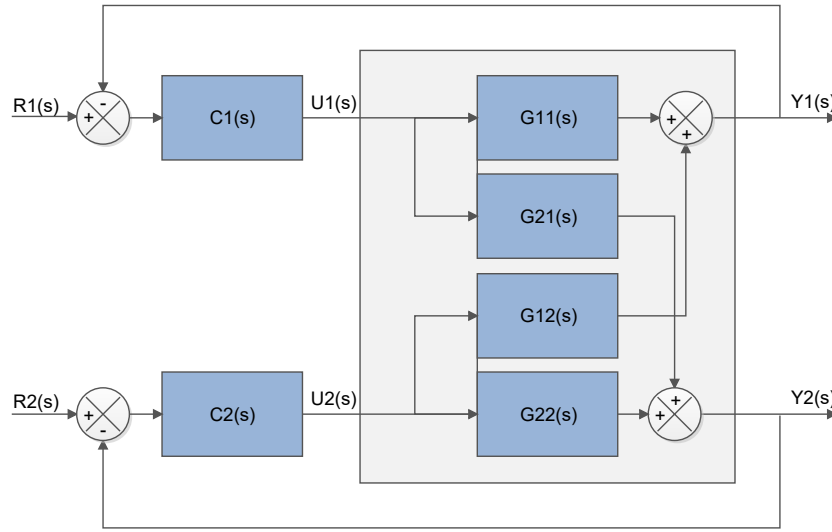


Figure 4.8: The interactions in a non-decoupled TITO system. It is assumed that the secondary loops pump controller from section 4.2 is sufficiently fast, so they can be ignored.

Where:

$R_1(s)$ and $R_2(s)$ are the two reference signals.

$C_1(s)$ and $C_2(s)$ are the two primary loop PI controller blocks.

$U_1(s)$ and $U_2(s)$ are the output signals of the controllers.

$G_{ij}(s)$ is the process in the system.

$Y_1(s)$ and $Y_2(s)$ are the two outputs of the system.

From figure 4.8, the process of the system can be represented by the following equations:

$$Y_1(s) = G_{11}(s)U_1(s) + G_{12}(s)U_2(s) \quad (4.10)$$

$$Y_2(s) = G_{21}(s)U_1(s) + G_{22}(s)U_2(s) \quad (4.11)$$

Where $G_{ij}(s)$ is the transfer function from the j^{th} input to the i^{th} output as introduced in section 2.6 figure 2.24.

Using Bristol's Relative Gain Array (RGA), which is a method to investigate how the static gain of one loop, is influenced by the gain of other loop in the system. Thereby, it is possible to see the impact of the interactions [Karl J. Åstrøm, 2005].

Assuming that the second loop is in perfect control and therefore setting the output of the second loop in equation 4.10 equal to zero.

$$Y_1(s) = G_{11}(s)U_1(s) + G_{12}(s)U_2(s) \quad (4.12)$$

$$0 = G_{21}(s)U_1(s) + G_{22}(s)U_2(s) \quad (4.13)$$

By solving U_2 from equation 4.13, and eliminating it in equation 4.12. The equation for

the first output can be derived:

$$Y_1(s) = \frac{G_{11}(s)G_{22}(s) - G_{12}(s)G_{21}(s)}{G_{22}(s)} \cdot U_1(s) \quad (4.14)$$

Now Bristol's interaction index λ for the TITO system, which refer to the static condition, can be derived:

$$\lambda = \frac{\text{static gains of loop 1 for open loop in loop 2}}{\text{static gains of loop 1 for closed loop in loop 2}} \quad (4.15)$$

The Bristol's interaction index λ can then be expressed as:

$$\begin{aligned} \lambda &= \frac{G_{11}(0)}{\frac{G_{11}(0)G_{22}(0) - G_{12}(0)G_{21}(0)}{G_{22}(0)}} \\ &= \frac{G_{11}(0)G_{22}(0)}{G_{11}(0)G_{22}(0) - G_{12}(0)G_{21}(0)} \end{aligned} \quad (4.16)$$

If $G_{12}(0) \cdot G_{21}(0) = 0$ in the denominator of equation 4.16, then is $\lambda = 1$, which means that there is no interaction between the loops. Small or negative numbers of λ indicates that there is interaction between the loops.

A difference method to obtained Bristol's Relative Gain Array is using matrices and component-wise multiplication:

$$R_{ij} = G_{ij}(0)G_{ij}^{-T}(0) \quad (4.17)$$

Where:

$G(0)$ is the static gain of the hydraulic model. $[::]$
 $G^{-T}(0)$ is the inverse transpose of the static gain for the hydraulic model. $[::]$

The relative gain array in a TITO system can be defined as:

$$R = \begin{pmatrix} \lambda & 1 - \lambda \\ 1 - \lambda & \lambda \end{pmatrix} \quad (4.18)$$

To figure out which input, $U_1(s)$ or $U_2(s)$, that should control either output $Y_1(s)$ or Y_2 , a pairing of signals needs to be considered.

For the interaction index λ :

- $\lambda = 1$ or $\lambda = 0$ there is no interaction between the loops.
- $\lambda < 0.5$ the loops needs to be swapped.
- Gain outside of $0.67 < \lambda < 1.5$, decoupling can improve the control significantly.

Its recommended by Bristol's RGA that the pairing should be designed, so the relative gain is positive and as close to 1 as possible, so interaction between the loops are minimized [Karl J. Åström, 2005].

To establish whether a decoupler is necessary, finding the dynamic coupling factor Q , would be needed, and can be obtained by three open loop transfer function from figure 4.8 [Knudsen,].

$$S_1(s) = -C_1(s)G_{11}(s) \quad (4.19)$$

$$S_2(s) = -C_2(s)G_{22}(s) \quad (4.20)$$

$$S_3(s) = C_1(s)G_{21}(s)C_2(s)G_{12}(s) = S_1(s) \cdot S_2(s) \cdot Q(s) \quad (4.21)$$

Where:

$S_1(s)$ is the open loop from $R_1(s)$ to $Y_1(s)$.

S_2 is the open loop from $R_2(s)$ to $Y_2(s)$.

$S_3(s)$ is the open loop from $R_1(s)$ to $Y_2(s)$ and from $R_2(s)$ to $Y_1(s)$.

The interesting part is the last loop, $S_3(s)$ because it describes the interaction between the two inputs and outputs. Therefore the dynamic coupling factor $Q(s)$ can be derived from equation 4.21:

$$Q(s) = \frac{G_{12}(s)G_{21}(s)}{G_{11}(s)G_{22}(s)} \quad (4.22)$$

For $|Q(s)| \ll 1$, at a defined frequency range, the interaction in the system can be approximated to be zero and the system can be described as two SISO systems, without the need for a decoupler.

If this is not the case, applying a decoupler which can be described as transfer functions F_{ij} is added to G_{ij} , which counteract the interaction between the loops, as seen in figure 4.9 [Knudsen,].

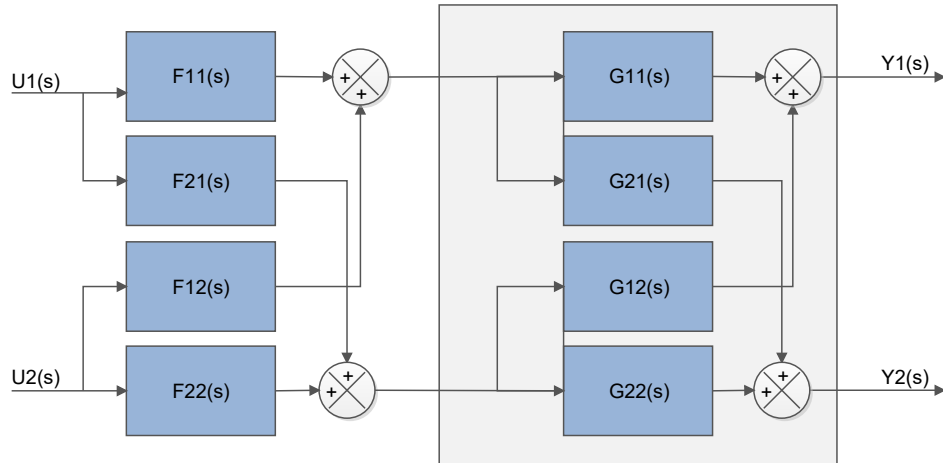


Figure 4.9: Figure of the decoupler and the TITO system. The two PI controller are not included in this figure.

By finding the relation between each cross-input and cross-output of $G(s)$, it is possible to find the counteracting transfer functions. From figure 4.9, the relation between each cross-input and cross-output and be derived as:

$$\frac{Y_2(s)}{U_1(s)} = F_{21}(s)G_{22}(s) + F_{11}(s)G_{21}(s) = 0 \quad (4.23)$$

$$\frac{Y_1(s)}{U_2(s)} = F_{12}(s)G_{11}(s) + F_{22}(s)G_{12}(s) = 0 \quad (4.24)$$

From equation 4.23, $F_{21}(s)$ can be derived as:

$$F_{21}(s) = -F_{11}(s) \frac{G_{21}(s)}{G_{22}(s)} \quad (4.25)$$

From equation 4.24, $F_{12}(s)$ can be derived as:

$$F_{12}(s) = -F_{22}(s) \frac{G_{12}(s)}{G_{11}(s)} \quad (4.26)$$

Having derived $F_{21}(s)$ and $F_{12}(s)$ from the relation between each cross-input and cross-output of $G(s)$, they can be substituted in the decoupler as seen in figure 4.10 [Knudsen,].

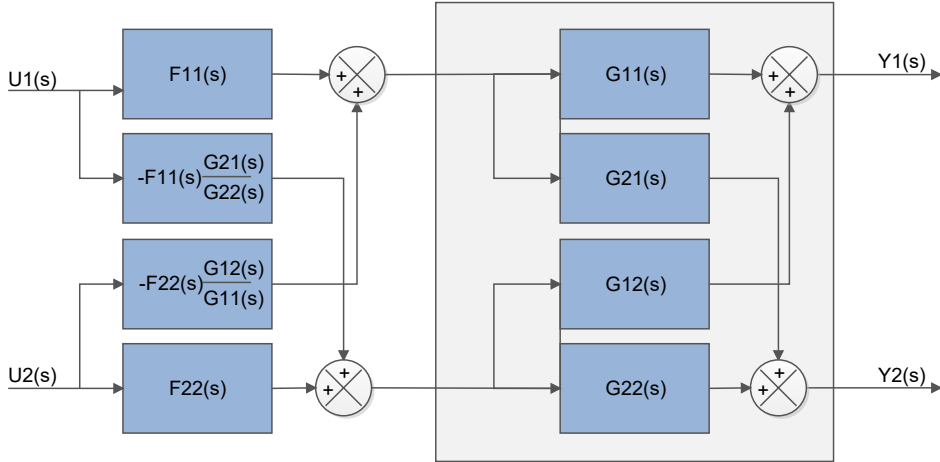


Figure 4.10: A figure of the substituted transfer functions in the decoupler. The two PI controller are not included in this figure.

Thereby the decoupler have been implemented and the system can be approximated as two SISO's. To replace it with the dynamic coupling factor, $F_{21}(s)$ and $F_{12}(s)$ is also substituted in equation 4.23 and equation 4.24:

From input $U_1(s)$ to output $Y_2(s)$:

$$\frac{Y_2(s)}{U_1(s)} = -F_{11}(s) \frac{G_{21}(s)}{G_{22}(s)} G_{22}(s) + F_{11}(s) G_{21}(s) = 0 \quad (4.27)$$

From input $U_2(s)$ to output $Y_1(s)$:

$$\frac{Y_1(s)}{U_2(s)} = -F_{22}(s) \frac{G_{12}(s)}{G_{11}(s)} G_{11}(s) + F_{22}(s) G_{12}(s) = 0 \quad (4.28)$$

The two SISO systems can now be determined with the dynamic coupling factor $Q(s)$:

SISO from input $U_1(s)$ to output $Y_1(s)$:

$$\begin{aligned} \frac{Y_1(s)}{U_1(s)} &= -F_{11}(s) \frac{G_{21}(s)}{G_{22}(s)} G_{12}(s) + F_{11}(s) G_{11}(s) \\ &= \left(1 - \frac{G_{12}(s) G_{21}(s)}{G_{11}(s) G_{22}(s)}\right) F_{11}(s) G_{11}(s) \\ &= (1 - Q(s)) F_{11}(s) G_{11}(s) \end{aligned} \quad (4.29)$$

SISO from input $U_2(s)$ to output $Y_2(s)$:

$$\begin{aligned} \frac{Y_2(s)}{U_2(s)} &= -F_{22}(s) \frac{G_{12}(s)}{G_{11}(s)} G_{21}(s) + F_{22}(s) G_{22}(s) \\ &= \left(1 - \frac{G_{12}(s)G_{21}(s)}{G_{11}(s)G_{22}(s)}\right) F_{22}(s) G_{22}(s) \\ &= (1 - Q(s)) F_{22}(s) G_{22}(s) \end{aligned} \quad (4.30)$$

These two SISO can then be represented as shown on figure 4.11. For $|Q(s)| \ll 1$, at a defined frequencies ranges, the interaction between the loops can be ignored. If $|Q(s)|$ is relative small it can be considered as a small gain multiplied on the process.

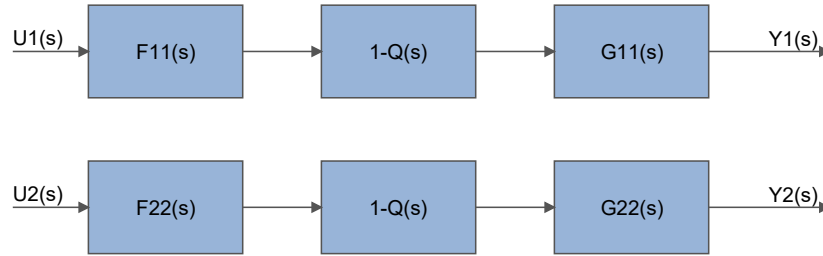


Figure 4.11: The two SISOs of the decoupled system, with $F_{11}(s)$ and $F_{22}(s)$ remaining

If $F_{11}(s)$ and $F_{22}(s)$ is chosen to be equal to one, the calculations of $F_{21}(s)$ and $F_{12}(s)$ become relative simple. The decoupled system can then be reduced, as seen on figure 4.12.

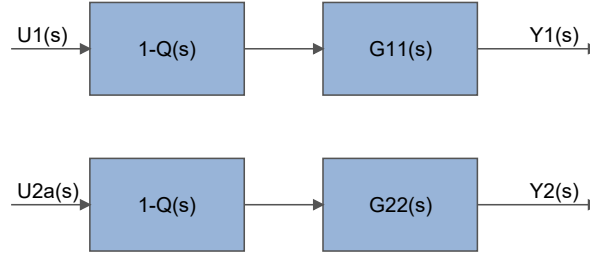


Figure 4.12: The two SISOs of the decoupled system

The calculations of Bristols relative gain array, the dynamic coupling factor and the two SISO's was performed in appendix A.2.1. The results from these calculation will now be listed.

The calculations of the relative gain array, for the TITO system gave the following result:

$$R = \begin{pmatrix} 2.808 & -1.808 \\ -1.808 & 2.808 \end{pmatrix} \quad [\cdot] \quad (4.31)$$

Where the interaction index $\lambda = 2.808$, so it can be determined, there is interaction between the loop and a decoupling of the system could therefore improve the control. Furthermore, as the interaction index is greater than 0.5 the loops does not need to be swapped.

Although the interaction index, indicate that a decoupler could improve a system, it is the decoupling factor that indicate the necessity for it. Based on figure 4.13, it was found that the smallest dynamic coupling factor for $|Q(0.2)| = 0.645$, which can't be considered $|Q(s)| \ll 1$. Therefore is it necessary to implement a decoupler in the system before it can be described as two SISO's.

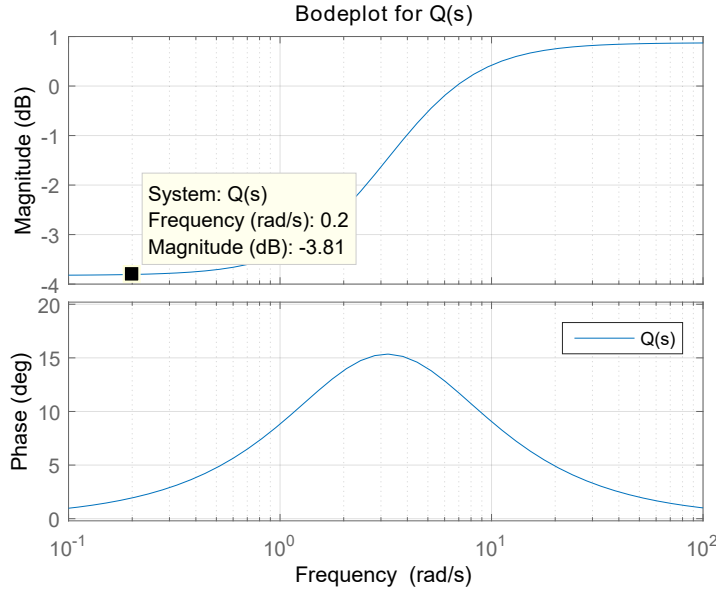


Figure 4.13: Frequency response for the dynamic coupling factor $Q(s)$.

For the decoupler, $F_{11}(s)$ and $F_{22}(s)$ is chosen to be equal to one. The calculations for the $F_{12}(s)$ and $F_{21}(s)$ transfer function, then gave the following results:

$$\begin{aligned} F_{12}(s) &= -F_{22}(s) \frac{G_{12}(s)}{G_{11}(s)} & (4.32) \\ &= \frac{-1.158(s + 2.564)}{(s + 4.167)} \end{aligned}$$

The decoupler, $F_{21}(s)$ can be derived as:

$$\begin{aligned} F_{21}(s) &= -F_{11}(s) \frac{G_{21}(s)}{G_{22}(s)} & (4.33) \\ &= \frac{-0.956(s + 2.703)}{(s + 2.857)} \end{aligned}$$

To verify that the decoupler have the desired effect the calculation of the dynamic decoupling factor for the decoupled system resulted in figure 4.14. Where is was found that the highest dynamic decoupling factor for $|Q_d(0.2)| = 0.003$, which can be considered $|Q_d(s)| \ll 1$. Therefore, two SISO loops can be established.

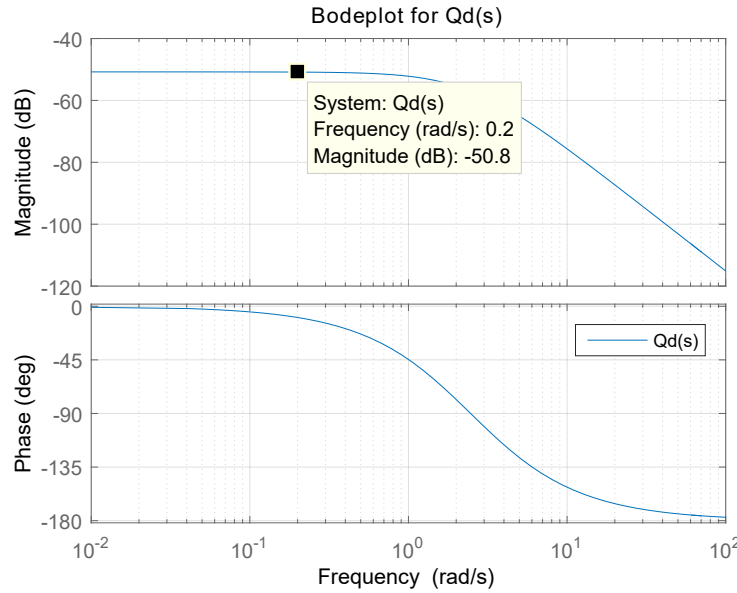


Figure 4.14: Frequency response for the decoupled dynamic coupling factor $Q_d(s)$.

The first SISO loop from input $U_1(s)$ to output $Y_1(s)$, where $Q(s)$ is ignored and $F_{11}(s)$ is equal to one:

$$\begin{aligned} \frac{U_1(s)}{Y_1(s)} &= (1 - Q(s))F_{11}(s)G_{11}(s) \\ &= \frac{0.054}{0.39s + 1} \end{aligned} \quad (4.34)$$

The second SISO from input $U_2(s)$ to output $Y_2(s)$, where $Q(s)$ is ignored and $F_{22}(s)$ is equal to one:

$$\begin{aligned} \frac{U_2(s)}{Y_2(s)} &= (1 - Q(s))F_{22}(s)G_{22}(s) \\ &= \frac{0.049}{0.37s + 1} \end{aligned} \quad (4.35)$$

Thereby can ordinary SISO rules be used to design the controllers for the two systems.

In this section it was determined that there is interaction between the two input and two output and it were sufficiently large, so decoupling was considered. Finding the dynamic decoupling factor confirmed, that the system needed to be decoupled and two transfer function describing the decoupler were found. A verification of the decoupler confirmed the theory and two SISO loops was established.

4.4 Design of hydraulic controller

In this section the primary controller shown in functional block diagram (see figure 4.15) will be designed. The purpose of the hydraulic controller is to control the output pressure at the valves. The primary controller needs to be 3-5 times slower than the secondary

controller designed in section 4.2 and shown in equation 4.9. This section will use the SISO's found in section 4.3 and the controller will be design after these transfer functions.

In figure 4.15 the functional block diagram is shown.

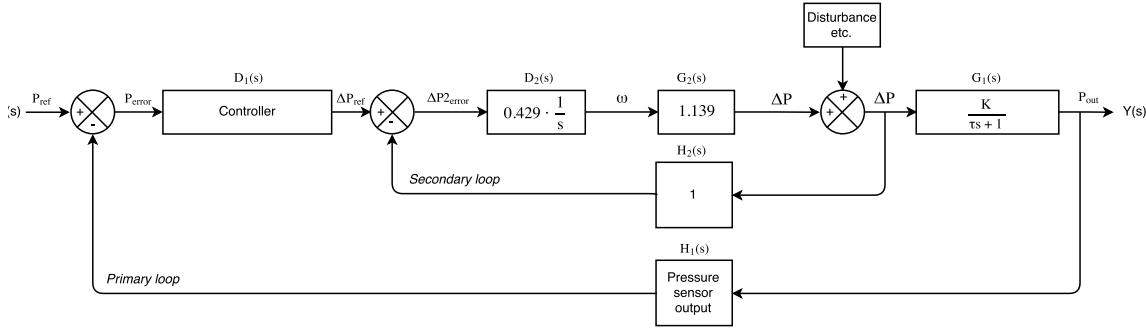


Figure 4.15: Functional block diagram of the cascade controller, with inserted values in the secondary loop.

In this section the controller $D_1(s)$ will be designed. $D_1(s)$ will be referred to as D_{11} and the plant $G_1(s)$ will be referred to as $G_{11}(s)$. The reason for this, is there will be designed two controllers in this section $D_{11}(s)$ and $D_{22}(s)$ respectively to $G_{11}(s)$ and $G_{22}(s)$ which are found in section 4.3. The transfer function for the pressure sensor $H_1(s)$ is determined to be equal to 1, because the time of the sensor do not have any influence of the system.

From section 4.3 equation 4.34 the following transfer function was calculated:

$$\frac{U_1(s)}{Y_1(s)} = (1 - Q(s))F_{11}(s)G_{11}(s) \quad (4.36)$$

$$= \frac{0.054}{0.39s + 1}$$

This transfer function will be referred to as $G_{11}(s)$. On figure 4.16 the root locus for $G_{11}(s)$ is shown.

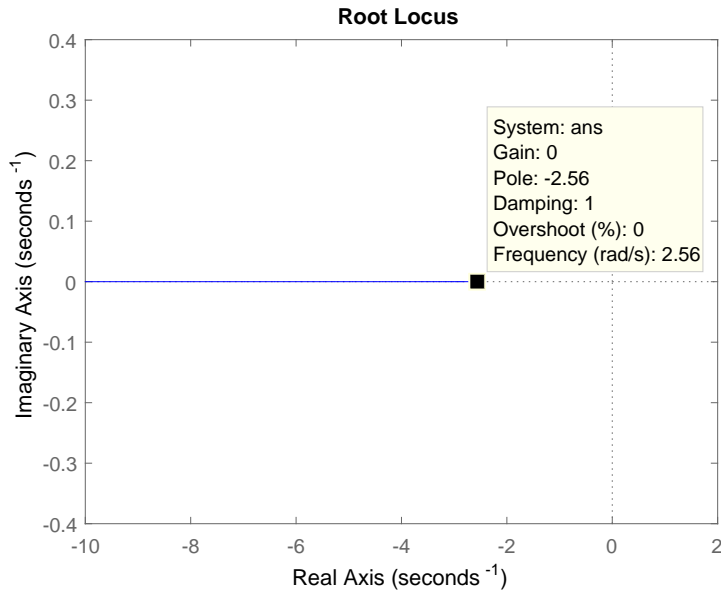


Figure 4.16: Root locus of $G_{11}(s)$.

In the figure the pole can be read to be at -2.56. A PI controller will be designed, where the proportional term is used to cancel out the pole in equation 4.36 and the integral term to eliminate the steady state error.

The open loop (OL) transfer functions with the PI controller is as followed:

$$\begin{aligned} OL(s) &= D_{11}(s)G_{11}(s) \\ &= \left(K_P + \frac{K_i}{s} \right) \cdot \frac{0.054}{0.39s + 1} \end{aligned} \quad (4.37)$$

By multiplying K_i outside the parenthesis the following OL transfer function is given:

$$OL(s) = K_i \cdot \left(\frac{K_P}{K_i} + \frac{1}{s} \right) \cdot \frac{0.054}{0.39s + 1} \quad (4.38)$$

Taking the ratio between K_P/K_i equal to 0.39 then the following OL is given.

$$OL(s) = K_i \cdot \left(0.39 + \frac{1}{s} \right) \cdot \frac{0.054}{0.39s + 1} \quad (4.39)$$

In figure 4.17 the root locus can be seen for the OL transfer function 4.39.

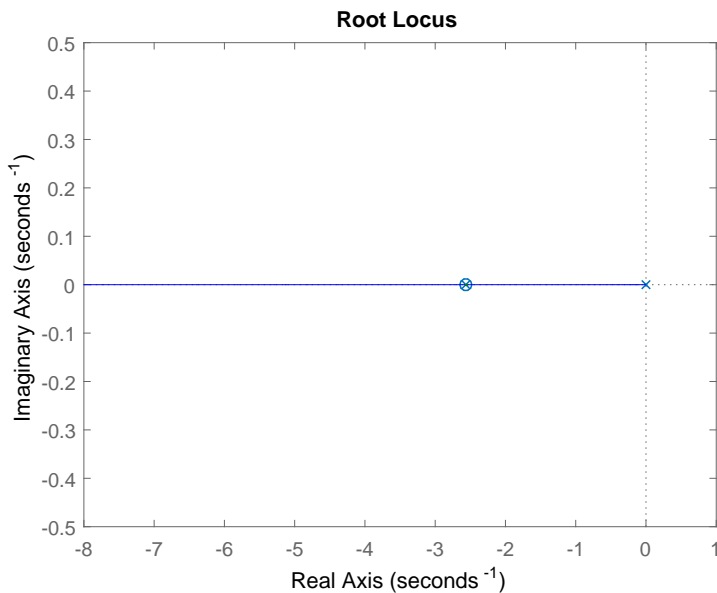


Figure 4.17: Root locus of OL transfer function 4.39.

It can be seen that the zero is placed at the same location as the pole. These will cancel each other and left will be the pole in zero. By reducing equation 4.39 the following OL transfer function is given.

$$OL(s) = \frac{0.054 \cdot Ki}{s} \quad (4.40)$$

By increasing Ki in equation 4.40 the pole in the origin will move to the left on figure 4.17 which can be seen from the CL transfer function in equation 4.41.

$$\begin{aligned} CL(s) &= \frac{OL(s)}{1 + OL(s)} \\ &= \frac{\frac{0.054 \cdot Ki}{s}}{1 + \frac{0.054 \cdot Ki}{s}} \\ &= \frac{0.054 \cdot Ki}{s + 0.054 \cdot Ki} \end{aligned} \quad (4.41)$$

To find the gain, Ki that will fulfilled the cascade requirement of 3-5 times slower than the secondary loop the time constant τ for a rise time of 16.5 seconds needs to be found. When τ is known the pole location can be found by taking $1/\tau$ and by using root locus on the OL transfer function the gain can be found.

Determining the time constant τ for a risetime of 16.5 seconds.

$$\begin{aligned} \tau &= \left(\frac{1}{\ln(0.9) - \ln(0.1)} \right) \cdot t_r \\ &= \left(\frac{1}{\ln(0.9) - \ln(0.1)} \right) \cdot 16.5s \\ &= 7.509s \end{aligned} \quad (4.42)$$

Now the location of the pole can be found:

$$p = -\frac{1}{\tau} \quad (4.43)$$

$$= -\frac{1}{7.509}$$

$$= -0.133$$

With the OL known root locus will be used to find the gain that will place the pole at -0.133 to get a rise time of 16.5. In figure 4.18 the root locus of the OL transfer function for equation 4.40 shown.

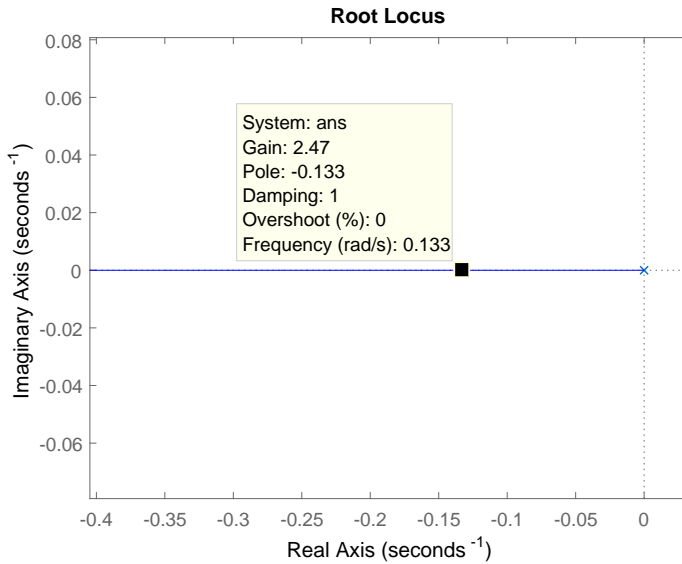


Figure 4.18: Root locus for OL transfer function 4.40.

On the figure the gain can be read to be 2.47. With the gain known it will be multiplied on the OL transfer function to find the new OL transfer function for the hydraulic model with a rise time of 16.5 s. From equation 4.44 the new OL transfer function is known.

$$\begin{aligned} OL(s) &= \frac{0.054 \cdot Ki}{s} \quad (4.44) \\ &= \frac{0.054 \cdot 2.47}{s} \\ &= \frac{0.133}{s} \end{aligned}$$

From the closed loop transfer function it can be seen that the pole is placed at -0.133 as shown in equation 4.45.

$$CL(s) = \frac{0.054 \cdot Ki}{s + 0.054 \cdot Ki} \quad (4.45)$$

$$= \frac{0.133}{s + 0.133}$$

To verify that desired rise time is archived a step will be performed on this transfer function. In figure 4.19 a step is performed on the CL(s) transfer function from equation 4.45.

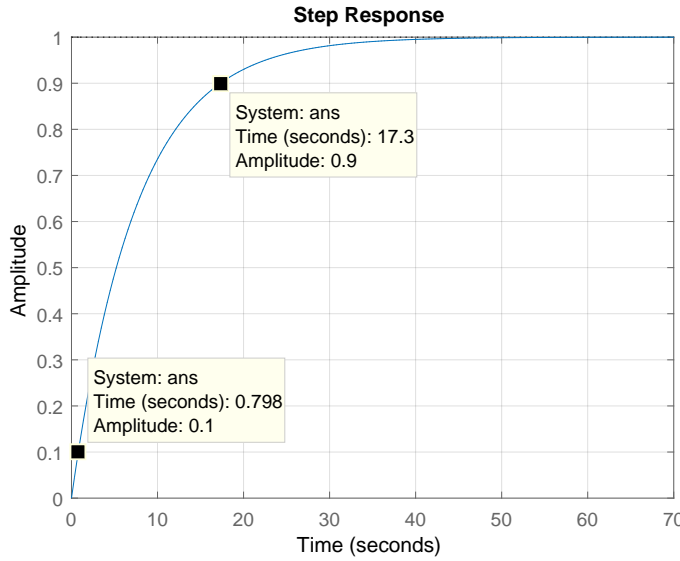


Figure 4.19: Step response for CL(s) transfer function 4.45.

On the figure the 10% and 90% of the response is found, the rise time can then be calculated.

$$\begin{aligned} tr &= \text{time}_{90\%} - \text{time}_{10\%} \\ &= 17.3 - 0.798 \\ &= 16.5020 \approx 16.5 \end{aligned} \quad (4.46)$$

From the root locus it can be analysed that the pole is located at the calculated position -0.133 and the system is stable because the pole is located at the real axis. It can also be analysed that the system have zero overshoot because the pole is placed on the real axis and therefore the damping factor is equal to 1, which also can be read from the root locus, this is expected as the system is of first order. Hence the controller $D_{11}(s)$ for $G_{11}(s)$ is deemed successful and will be tested on the distribution network in the laboratory to verified it.

$$D_{11}(s) = \left(0.39 + \frac{2.47}{s} \right) \quad (4.47)$$

In figure 4.20 the hydraulic controller $D_{11}(s)$ is implemented and the plant $G_{11}(s)$ is also included in the functional block diagram.

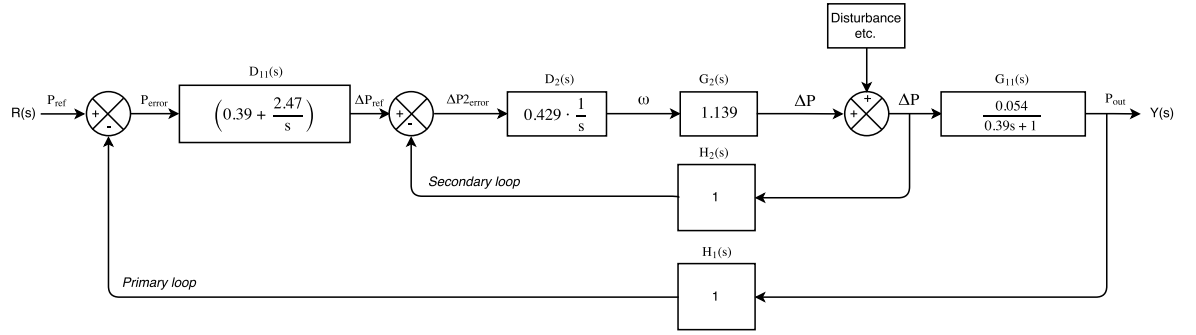


Figure 4.20: Functional block diagram of the cascade controller, with inserted values for $D_{11}(s)$ in the primary and secondary loop.

From section 4.3 equation 4.35 the following transfer function was calculated:

$$\frac{U_2(s)}{Y_2(s)} = (1 - Q(s))F_{22}(s)G_{22}(s) \quad (4.48)$$

$$= \frac{0.049}{0.37s + 1}$$

The same approach was used to designed the controller $D_{22}(s)$, and therefore only the result will be shown. The calculations can be found in appendix A.2.2. The calculations resulted in the following hydraulic controller for $G_{22}(s)$

$$D_{22}(s) = \left(0.37 + \frac{2.74}{s} \right) \quad (4.49)$$

In figure 4.21 the hydraulic controller $D_{22}(s)$ is implemented and the plant $G_{22}(s)$ is also included in the functional block diagram.

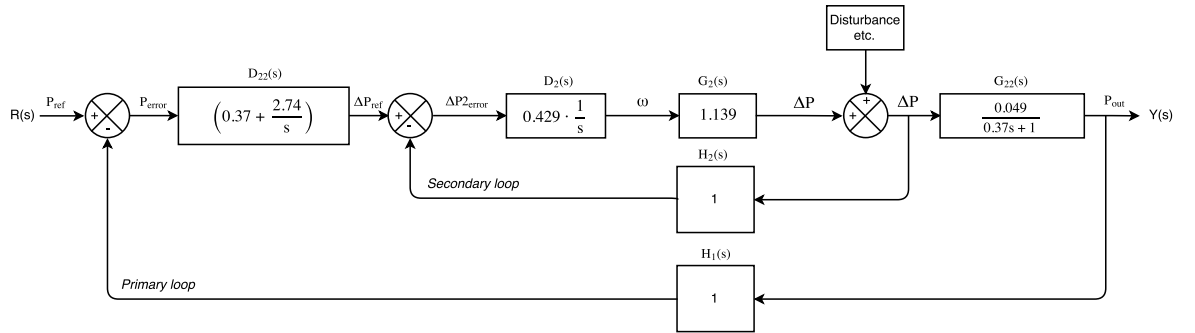


Figure 4.21: Functional block diagram of the cascade controller, with inserted values for $D_{22}(s)$ in the primary and secondary loop.

The reason that K_P is equal to 0.39 is that the close loop transfer function will result in a first order system and this is desirable because then the system have no overshoot. This is with the assumption that the pole is located in 2.564 this could prove to be wrong because the transfer function for the physical system is measured and read and there could be deviations. This is also the case for the second controller $D_{22}(s)$.

These controllers $D_{11}(s)$ and $D_{22}(s)$ will be used in the accepttest to verify the requirements from section 3.1. The controllers for the hydraulic model has been designed and the primary loops is complete, thereby is the cascade control design finished.

Through this chapter, it can be concluded that a cascade control could be used as a control design for this system. It can be concluded that two controller was designed for the secondary loop and an analysis of decoupling lead to the implementation of a decoupler. Which made it possible to establish two SISO loop for the system. Furthermore it can be concluded that two controller for the primary loop was designed.

Implementation 5

In this chapter, the implementation of the final product will be illustrated, where implementation of the important parts of the designed control system will be explained and how it is implemented into Simulink Real Time workshop.

On figure 5.1, is a block diagram of the control system, set up as a cascade controller. Starting from the right of figure 5.1, is the water system. The water system was analysed throughout Chapter 2, where four first order transfer function was derived. To the left of the water system is two integral controllers, that were designed in section 4.2. They are implemented in the secondary loops of the cascade controller to convert the velocity to pressure. To the left of the integral controllers, is the decoupler (F11-F22), that was implemented in the primary loop of the cascade controller, after an analysis in section 4.3. The analysis required the four transfer function from the water system, which is illustrated by the four transfer function (G11-G22). The implementation of a decoupler made it possible to describe the system as two SISO loops. To the left of the decoupler, is two PI controllers, that were designed in section 4.4. They are implemented in the primary loops of the cascade controller to regulate the pressure at the critical points.

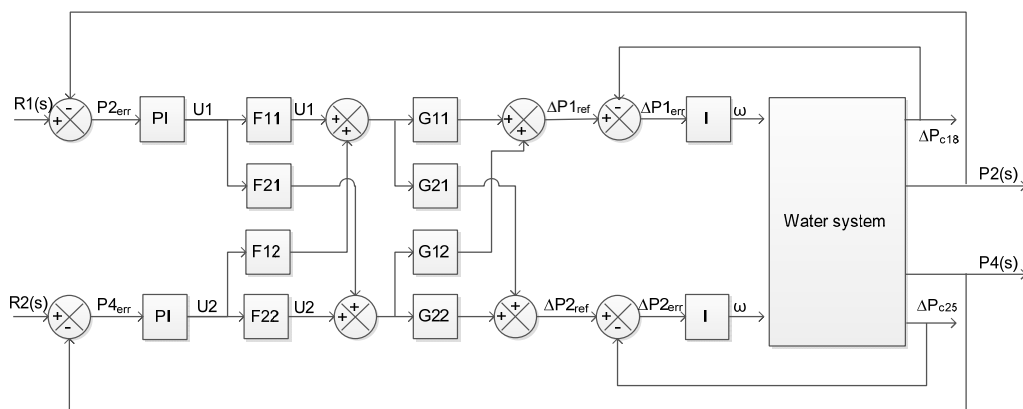


Figure 5.1: Block diagram over the fully implemented system. The four transfer function (G11-G22) is used for illustration purpose.

On figure 5.2, is a simplified version of figure 5.1. This is with the actual implementation of the decoupler. The decoupler takes a signal from one SISO loop and inverse it, the signal is then added to the other SISO loop. This is compensating for the interconnection G21 and G12 seen in figure 5.1.

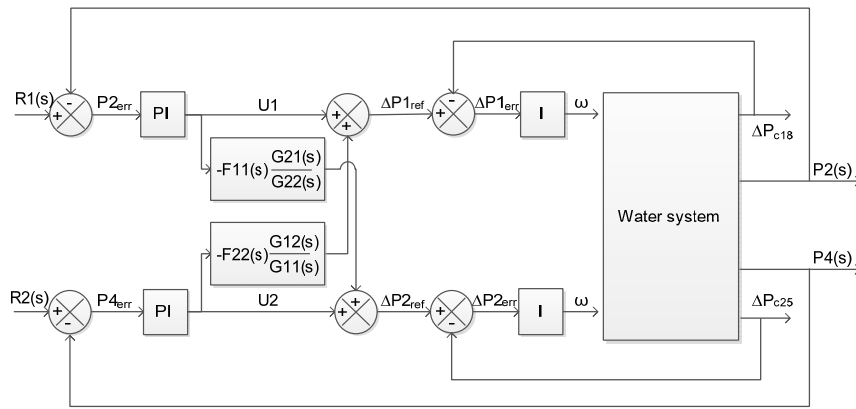


Figure 5.2: Block diagram over the fully implemented system, with the actual decoupler implemented.

The Simulink Real Time workshop implementation of the full system can be seen in figure 5.3. The cascade controller is implemented in discrete time, with a sampling time of 20 Hz. For this purpose a function in MATLAB was used.

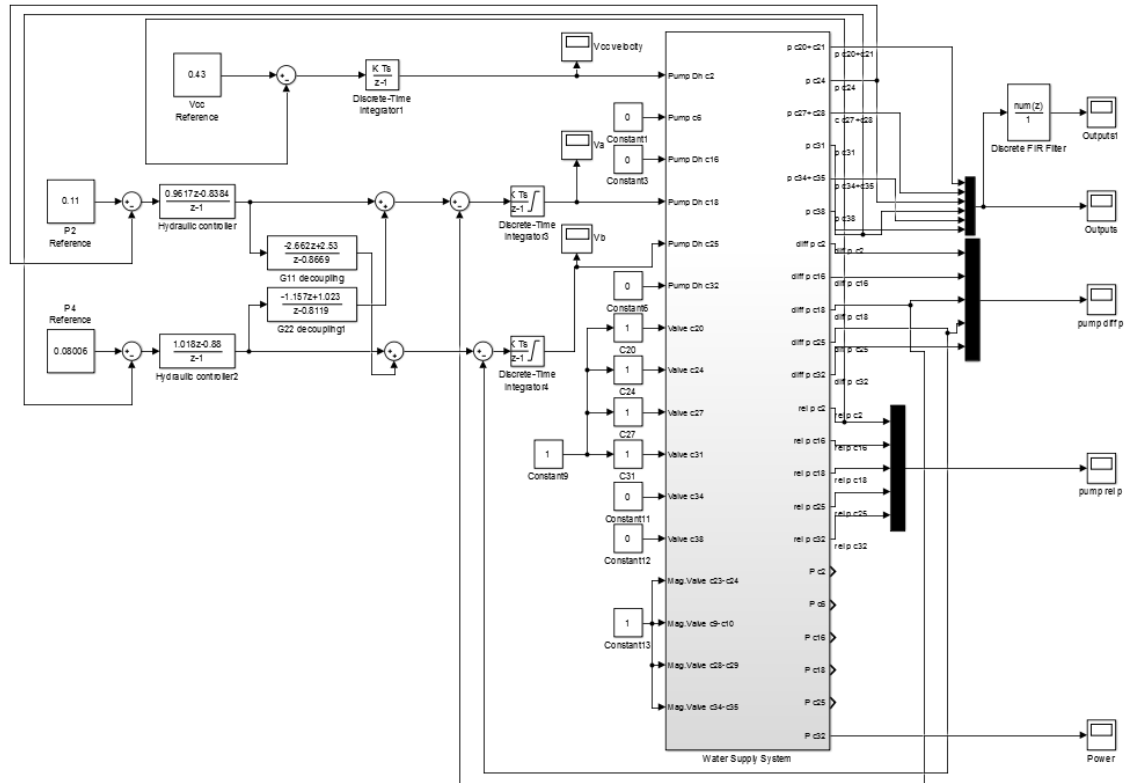


Figure 5.3: Simulink Real Time workshop implementation of the control system

Accepttest 6

In this chapter the requirements stated in section 3.1 will be tested on the physical system.

6.1 Test of steady state error

In this section the P2 and P4 outputs will be measured to check if the outputs is in between the steady state requirement limits and also if the designed control system can keep a certain pressure for the output. Therefore two requirements are being tested in this section, the test setup can be seen in the test of steady state error journal in appendix A.3.6.

The requirement introduced in System requirement, section 3.1, requirement no. one was set to be:

1. *Regulate the output pressure to a constant set point for P2 and P4.*
 - *Set point for P2 equal to 0.1103 bar and set point for P4 equal to 0.08 bar these set point are found in section 2.8.*

The requirement introduced in System requirement, section 3.1, requirement no. three was set to be:

3. *Steady state error of the set points must deviate with more than $\pm 5\%$ for the outputs P2 and P4.*

The requirement introduced in System requirement, section 3.1, requirement no. five was set to be:

5. *The system response for output P2 and P4 must not oscillate but remain stable, which also refer to requirement 1 and 3.*

The reference for the output at P2 is 0.1103 bar and must be in between the steady state limit of $\pm 5\%$, which is a range between 0.1158 to 0.1048 bar. On figure 6.1, the measured output pressure for P2 is presented, where the red dashed lines indicate the limits of a steady state error of $\pm 5\%$. As seen at the figure, the output pressure passed the steady state test, by only having a few spikes crossing the limits, which is assumed to be noise at the pressure sensors.

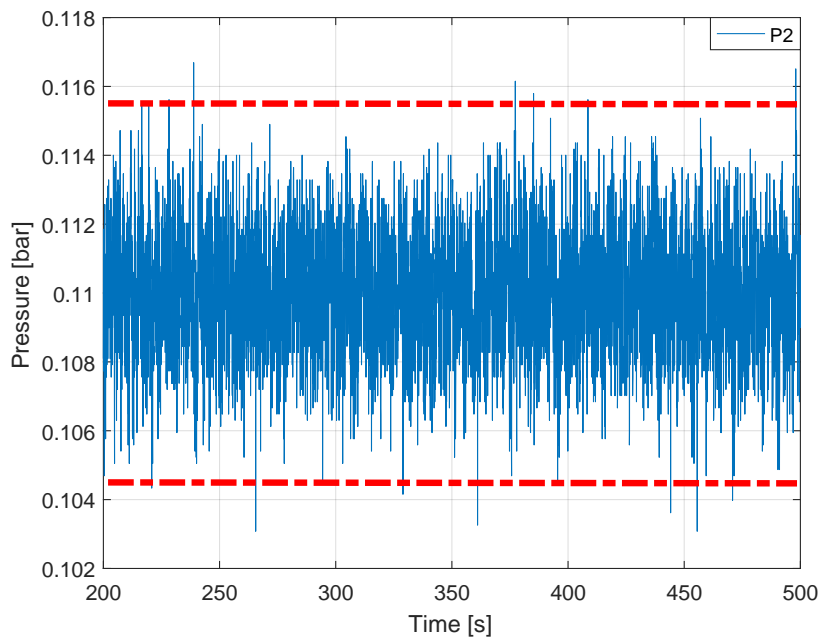


Figure 6.1: Pressure at the output P2, where the red dashed lines indicate the limits.

A way to reduce this noise is to use a FIR filter as seen on figure 6.2. The pressure at the output P2 is measured connected to a FIR filter, which is taking the mean value of seven samples, the filter was introduced to the output to make a noise reduction. As seen in the figure 6.2, the output pressure for P2 is not deviating as much as the plot without the FIR.

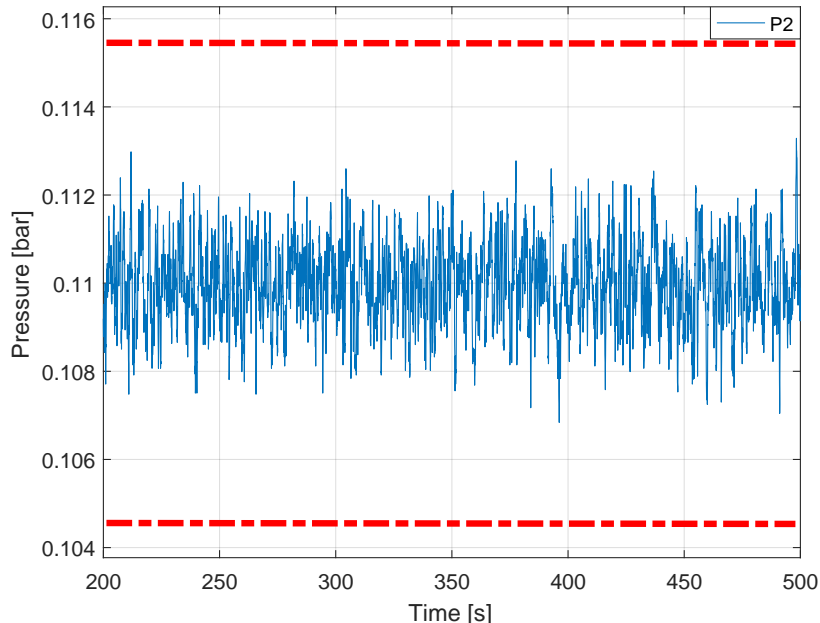


Figure 6.2: Pressure at the output P2 with FIR filter, where the red dashed lines indicate the limits.

The reference for the output at P4 is 0.08 bar and must be in between the steady state limits of $\pm 5\%$, which is a range between 0.084 to 0.074 bar. On figure 6.3, the measured

output pressure for P4 is presented, where the red dashed lines indicate the limits of a steady state error of $\pm 5\%$. As seen at figure 6.3, the output pressure passed the steady state test, although the measurement having a few more spikes crossing the limits than the output P2. The spikes is as before, assumed to be noise at the pressure sensors.

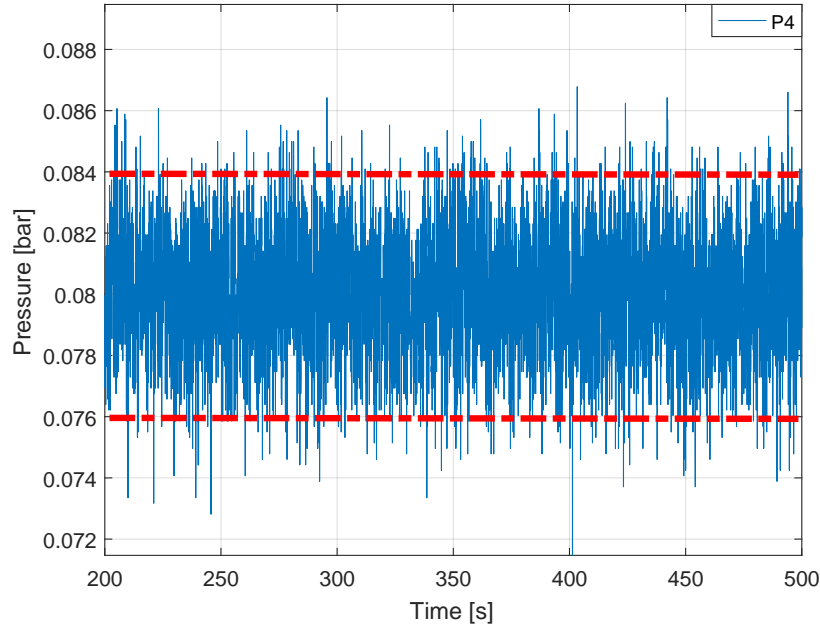


Figure 6.3: Pressure at the output P4, where the red dashed lines indicate the limits.

On figure 6.4, the pressure at the output P4 is measured with a connected FIR filter to reduce this noise.

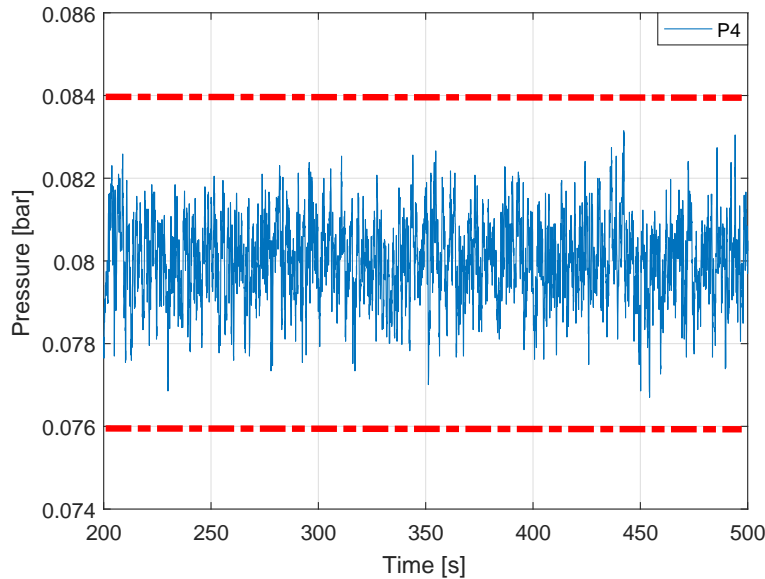


Figure 6.4: Pressure at the output P4 with FIR filter, where the red dashed lines indicate the limits.

Both steady state test at the outputs P2 and P4 passed the test, even though there was some spikes crossing the limits set as requirements. Implementing the FIR filter illustrated a less disturbed output signal, where the spikes was reduced to under the limits. As this test also illustrates that the system can control a pressure at the operation area for the output, this requirement is also fulfilled. The stability requirement set for the system response for output P2 and P4 also passed the test as both of the output signals remained stable doing the test.

6.2 System response

In this section the parameters for the system response for output P2 and P4, will be evaluated to see if the rise time, overshoot and stability meet the requirements. The test setup can be seen in System response in appendix 6.2. Furthermore the decoupling will be evaluated regarding to requirement 6.

The requirement introduced in System requirement, section 3.1, requirement no. two was set to be:

2. *Rise time should not be slower than 60 seconds.*

The requirement introduced in System requirement, section 3.1, requirement no. four was set to be:

4. *Overshoot must not be higher than 0 % at the outputs P2 and P4.*

The step for output P2 is shown in figure 6.5, the step is applied from the reference from 0.1103 to 0.1163 bar. The red dashed lines indicate the 5% steady state error limit for the desired pressure, which is 0.1165 bar. The green line indicate the desired pressure as the system response should reach.

The rise time for the output P2 is measured on the physical system to be approx 45.263 seconds, although in theory the rise time was calculated to be 16.5 seconds, see equation 4.46 in section 4.4. It can be concluded from figure 6.5, that there is no overshoot at the output P2.

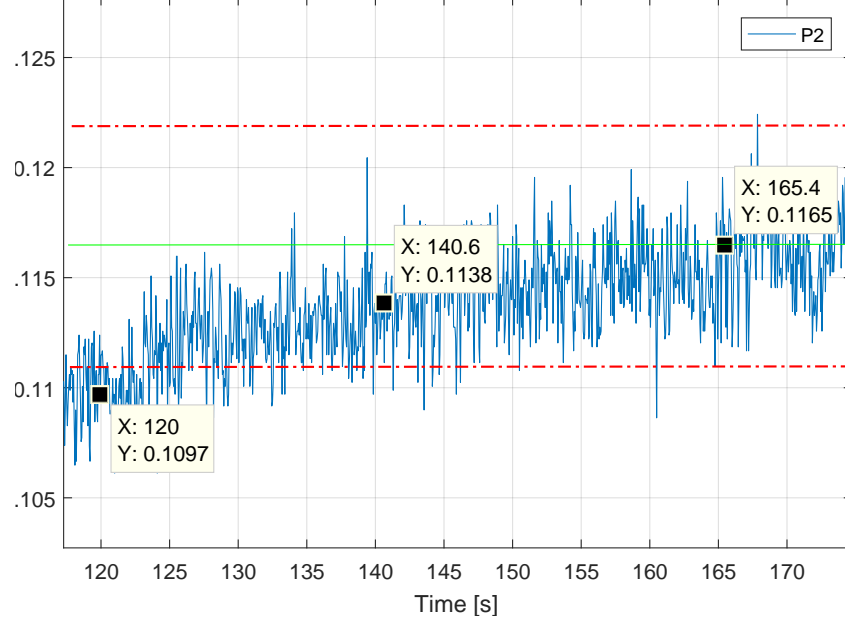


Figure 6.5: Pressure at the output P2, while performing a step, the red dashed lines indicate the steady state limits.

The step for output P4 is shown in figure 6.6, the step is applied from the reference from 0.08 to 0.0863. The red dashed lines indicate the 5% steady state error limit for the desired pressure, which is 0.08629 bar. The green line indicate the desired pressure as the system

response should reach.

The rise time for the output P4 is measured on the physical system to be approx 45.263 seconds, although in theory the rise time was calculated to be 16.5 seconds, see equation 4.46 in section 4.4. It can be concluded from figure 6.6, that there is no overshoot at the output P4.

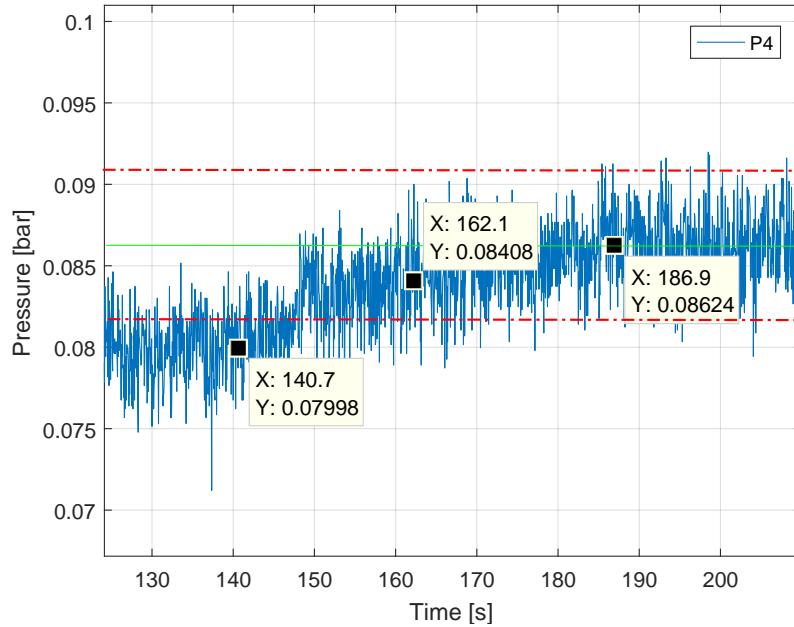


Figure 6.6: Pressure at the output P4, while performing a step, the red dashed lines indicate the steady state limits.

Although the rise time for output P2 and P4 is slower than expected, they are for this system still sufficient to maintain the pressure when a step is applied. A reason to why the response does not have the calculated rise time, could be that the decoupling factor $Q(s)$ in section 4.3 that was assumed to be very small and therefore it was not taking into the calculations when calculating the controller for the hydraulic model. By ignoring this factor some dynamics have been removed and this could be the reason why the response does not correspond with the calculations. Both the rise time for P2 at approx 45 seconds and the rise time for P4 at approx 48 seconds meet the requirement no. two, in System requirement 3.1. According to the requirement no. four in System requirement 3.1, it can be seen in figure 6.5 and in figure 6.6 that the requirement is met by not having overshoot.

The requirement introduced in System requirement, section 3.1, requirement no. six was set to be:

6. The decoupling should compensate for the interconnection between the two PMA's.

In figure 6.7, the functionality of the decoupling can be seen, where the data is from a test, that can be found in appendix A.3.7.

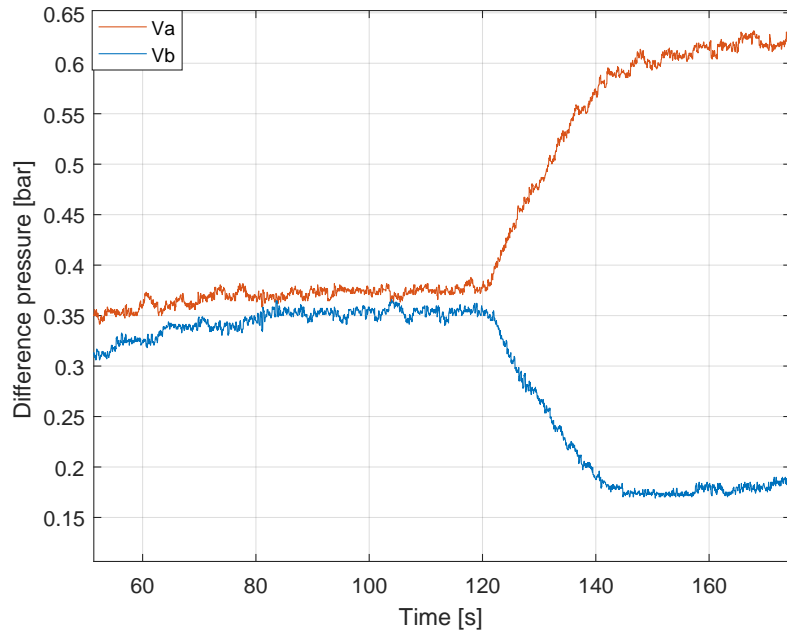


Figure 6.7: Shows the decoupling, when a step is applied from 0.1103 to 0.1165 bar to the reference value P2.

It can be seen that when a step is performed on the output P2, that the difference pressure at V_a increases, while the difference pressure at V_b decreases to compensate for this increment on V_a. In figure 6.8 is the output for when the step is applied to the output P2 can be seen.

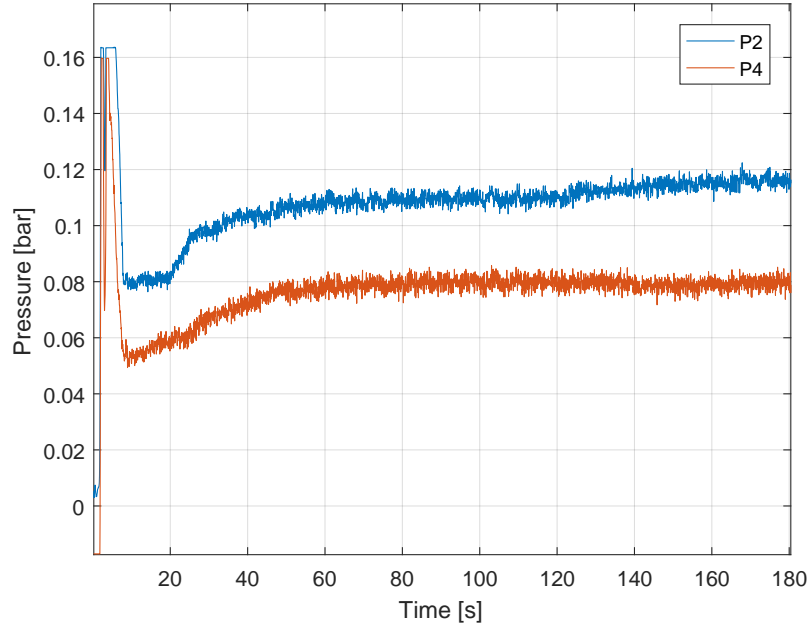


Figure 6.8: Pressure at the output P2 and P4, where a step is performed at P2, while P4 is regulated to be steady.

It can be seen that when P2 is increasing, P4 remain at the reference value. Which indicate that the decoupling works.

In figure 6.9 the decoupling is shown, when a step is applied to the reference value P4.

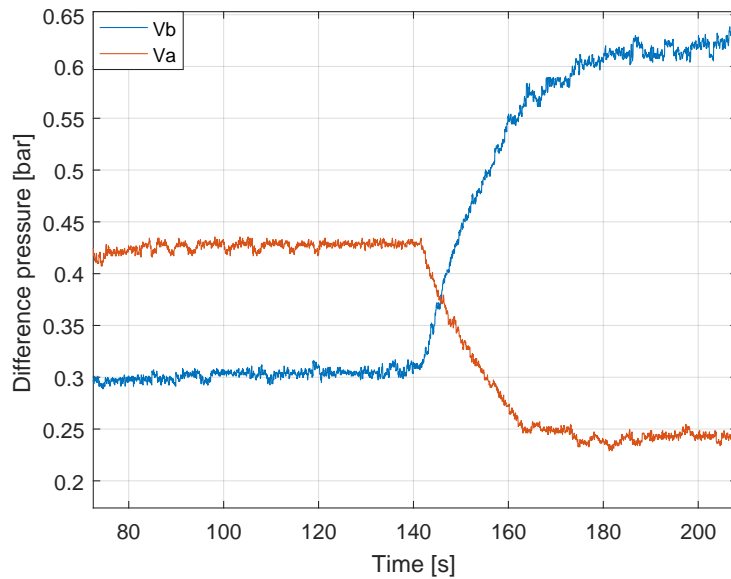


Figure 6.9: Shows the decoupling, when a step is applied from 0.08 to 0.08629 bar to the reference value P4.

The same observation can be seen from figure 6.9, when a step is applied to P4, Vb is increasing while Va is decreasing to compensated. Figure 6.10 shows the output at P2 and P4.

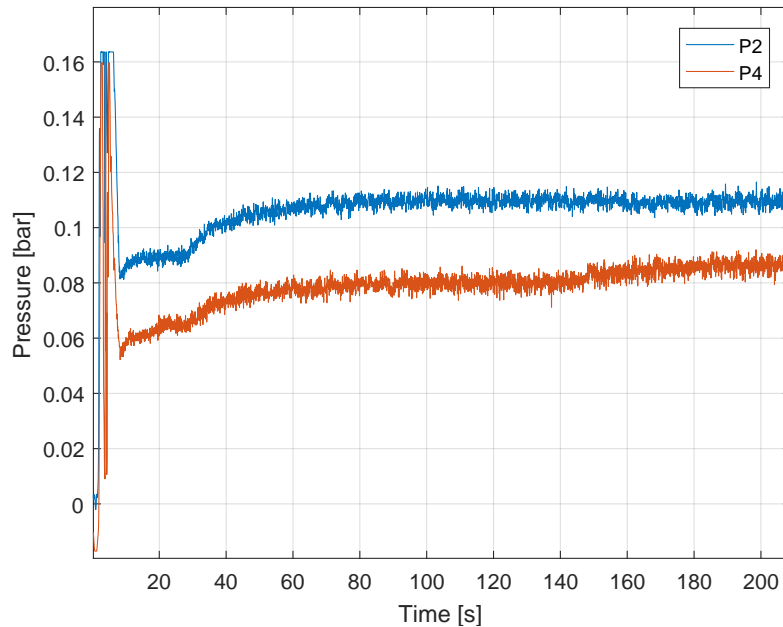


Figure 6.10: Pressure at the output P2 and P4, where a step is performed at P4, while P2 is regulated to be steady.

From the figure 6.10, it can be seen that when the output P4 is increasing, the output at

P2 remains at the reference value, which indicates that the decoupling works.

From the observation it can be concluded that the decoupling works, because it is able to keep its reference value when a step is applied to the other PMA.

Conclusion

7

In this chapter the final conclusions for the report is performed, which will conclude on the result obtained in this report.

Controllers have been designed with the goal of controlling certain outputs for a water distribution system, which is based on the problem statement from section 1.3

How can multiple pressure management areas be regulated when these are interconnected and still maintaining a certain water pressure at the critical point?

Through the System analysis chapter 2, the physical water system at Aalborg University in The Department of Electronic Systems, Section for Automation and Control have been analyzed to find a hydraulic and a pump model. Through calculations it have concluded that these models did not fit and therefore other methods have been used to find a model that corresponded to the physical system. One of the methods was calculating a linear slope for the pump instead of using the linear pump model derived in section 2.3. Another method was analyzing the system response to obtain the transfer functions for the system, instead of using the transfer functions found in System approximation section 2.7. These two methods mentioned above was used to design the controllers.

To achieve the requirements from chapter 3 a cascade controller have been designed to regulate the water pressure at the critical points. The cascade controller was design and tested in the laboratory. The tested showed that the system did not behave as expected. The system was much slower than expected but did still satisfy the requirements. The reason for this error in rise time, could be that the dynamic factor $Q(s)$ was left out of the calculations because it considered very small. This have found to be an error and because of time limits it have not been corrected in this report. Furthermore is the pump controller faster than expected in previous calculations and because of time limits it has not be possible to recalculate, with the new parameter. This could lead to a faster rise time for the hydraulic controller, which would make the system potentially much faster than it is now.

From the chapter 6 it have been concluded that the decoupling works, because it is able to counter act a change in the other PMA. Furthermore is the system able to keep a certain reference value at the output within a steady state error of $\pm 5\%$. The system is stable and have no overshoot at the output. The rise time is within the requirement even though is it much slower than calculated.

It can be concluded that the control system is able to regulate the pressure at the critical points within the operating areas. The system is just not as fast as desired, which is allowing for continued extension on the project to make the response faster with the improvement of the dynamic decoupling factor.

Optimization 8

This chapter will describe the optimization that could be implemented on the physical system.

Several improvements can be made for the system. Such as include more parameters for the pipes that includes bends and angles. Implementation of a flow measurement device that will make calculation for pressure across the pipes more accurate.

Another improvement could be the calculated model because it does not fit the physical system. A improvement would be recalculating it and make it match to the physical system and design the controller after this model.

The pump model could be improved, as it is for now, the flow q , is seen as a constant that does not vary. But this is not the case because when the pressure changes the flow also changes. Therefore a new Taylor approximation would have to be made which takes the derivative with the respect to ω and q .

The main pump is also considered as a constant which is a mistake because it also varies. The project design a controller to compensate for this variation this controller was made slow. A improvement would be to tune this controller by making a model for the main pump the same way that a model for the pumps C_{18} and C_{25} are calculated.

Perspective 9

In this chapter a perspective on the final product and examine what a final product would look like if time and resources would not have been a limiting factor.

The physical system is a down scaled system which means that it needs to be tested in a bigger environment before any conclusion can be draw about working in a real life scenario. The physical system needs to be tested up against a daily water usage to see if it is still able to keep a certain water pressure at the critical point. As mentioned the physical system is a down scaled system, therefore in a real system the pipes, valves and pumps are on a much bigger scale and therefore the calculations in this report would need to be recalculated to fit to a urban environment.

If the final product verified all requirements and if it was implemented in a urbane environment it could potentially help reducing water leaks in a these environments, by reducing the water pressure from the main supply to the pressure management area. And in the theory resulting in reduce energy used on the water treatment. Furthermore it could potentially reduce the risk to infrastructure such as roads and buildings by reducing these leaks with pressure management.

Discussion 10

In this chapter it will be discussed on the choices that have been made in this project whether it has been the right choice or if there were other opportunities.

It was found that the use of the dynamic decoupling factor in this report, was performed incorrectly. The factor Q_s , was found at a frequency and made the statement that a decoupler was needed, which is correct. Having implemented the decoupler, the recalculated factor Q , confirmed that the decoupler worked, which is also correct. From this point, Q was considered to be zero, as it was much smaller than one, this is incorrect. The transfer function $Q(s)$, has to be included in the two SISO loops and used in the design of the controllers, in the primary loops. This would have made the open loop, a third order transfer function for each SISO, giving a different result than this report currently present. The mistake was realized too late to be rectified, in time for the submission deadline.

Bibliography

- [Council, 2009] Council, N. R. D. (2009). Water efficiency saves energy:. Last visited on 2016-22-05, <https://www.nrdc.org/water/files/energywater.pdf>.
- [Feldman, 2009] Feldman, M. (2009). Aspects of energy efficiency in water supply systems. Last visited on 2016-22-05, http://www.miya-water.com/user_files/Data_and_Research/miyas_experts_articles/08_Other%20aspects%20of%20NRW/01_Aspects%20of%20Energy%20Efficiency%20In%20Water%20Supply%20Systems.pdf.
- [Fuchs, 2012] Fuchs, J. (2012). Valves – manual valves – ball, rotary and piston valves. Last visited on 2016-22-05, <http://www.ctgclean.com/tech-blog/2012/03/valves-manual-valves-ball-rotary-and-piston-valves/>.
- [Gene F. Franklin, 2015] Gene F. Franklin, J. David Powell, A. E.-N. (2015). Feedback control of dynamic systems. ISBN-13: 978-1-29-206890-9, Publisher: Pearson.
- [Gene F. Franklin, 1997] Gene F. Franklin, J. David Powell, M. L. W. (1997). Digital control of dynamic systems. ISBN-13: 978-0201820546, Publisher: Addison-Wesley.
- [GIZ, 2011] GIZ (2011). Guidelines for water loss reduction. Last visited on 2016-22-05, <https://www.giz.de/fachexpertise/downloads/giz2011-en-guideline-water-loss-reduction.pdf>.
- [Grundfos, 2015] Grundfos (2015). kvs value. Last visited on 2016-22-05, <http://www.grundfos.com/service-support/encyclopedia-search/kvs-value.html>.
- [H.E. Burroughs,] H.E. Burroughs, S. J. H. Managing indoor air quality. ISBN-13: 978-1439870143, Publisher:.
- [Kallesøe, 2005] Kallesøe, C. S. (2005). Fault detection and isolation in centrifugal pumps. ISBN-10: 87-90664-22-1.
- [Karl J. Åstrøm, 2005] Karl J. Åstrøm, T. H. (2005). Advanced pid control. ISBN-13: 978-1556179426, Publisher: ISA.
- [Knudsen,] Knudsen, M. Decoupling notat 2. Apartment of Processcontrol, Inst. of Electronic Systems, AAU, MIMOreg-MK.pdf.
- [Maninder Pal and Flint, 2010] Maninder Pal, N. D. and Flint, J. (2010). Detecting & locating leaks in water distribution polyethylene pipes. Last visited on 2016-22-05, http://www.iaeng.org/publication/WCE2010/WCE2010_pp889-894.pdf.
- [Michael A. Johnson, 2005] Michael A. Johnson, M. H. M. (2005). Pid control: New identification and design methods. ISBN-13: 9781852337025, Publisher: Springer.
- [Modelling and Control, 2015] Modelling, C. and Control (2015). Linearization. Last visited on 2016-22-05, notelinearization.pdf.
- [Pedersen, 2010] Pedersen, L. (2010). Fysik 112 - førstehjælp til formler. ISBN-13: 9788757127270, Publisher: Nyt Teknisk Forlag.

- [Prabhata K. Swamee, 2008] Prabhata K. Swamee, A. K. S. (2008). Design of water supply pipe networks. ISBN-13:9780470225042, Publisher: John Wiley and Sons.
- [Toolbox,] Toolbox, E. Laminar, transitional or turbulent flowl. Last visited on 2016-24-05, http://www.engineeringtoolbox.com/laminar-transitional-turbulent-flow-d_577.html.
- [VanDoren, 2014] VanDoren, V. (2014). Fundamentals of cascade control. Last visited on 2016-24-05, <http://www.controleng.com/single-article/fundamentals-of-cascade-control/bcedad6518aec409f583ba6bc9b72854.html>.
- [Water, 2016] Water, A. (2016). The importance of water and your health. Last visited on 2016-22-05, <http://www.freerdrinkingwater.com/water-education/water-health.htm>.
- [Wavin, 2012] Wavin (2012). Trykteknisk håndbogfor wavin pe-/upvc trykrØrssystemer. Last visited on 2016-21-03, <http://docplayer.dk/3271301-Juli-2012-trykteknisk-haandbog-for-wavin-pe-upvc-trykroersystemer-solutions-for-e.html>.
- [Wavin, 2015] Wavin (2015). Tigris k1 commercial press-fit plumbing. Last visited on 2016-21-03, [Wavin_technical_specification_guide.pdf](#).
- [Wegelin, 2009] Wegelin, R. M. . W. (2009). Implementation of pressure management in municipal water supply system. Last visited on 2016-22-05, http://www.miya-water.com/user_files/Data_and_Research/miyas_experts_articles/3_DMAs_Pressure_management/03_Implementation%20of%20pressure%20management%20in%20municipal%20water%20supply%20systems.pdf.
- [Wermac, 2016] Wermac (2016). Introduction to pumps - centrifugal pump. Last visited on 2016-21-03, http://www.wermac.org/equipment/pumps_centrifugal.html.

Appendix A

A.1 System analysis

This appendix contain the calculations done throughout Chapter 2. The purpose is to elaborate further on the calculations or found parameters, used in the different sections.

A.1.1 Calculation of the pipes

This appendix will cover the calculation to find the parameters for the pipes. Only one pipe will be explained in detail, the rest of the calculations can be found on CD [calculations/pipe and valve calculations]

In figure A.1 the electric equivalent is shown, which illustrates the placement of the pipes which are split into a resistor part and an inductor part.

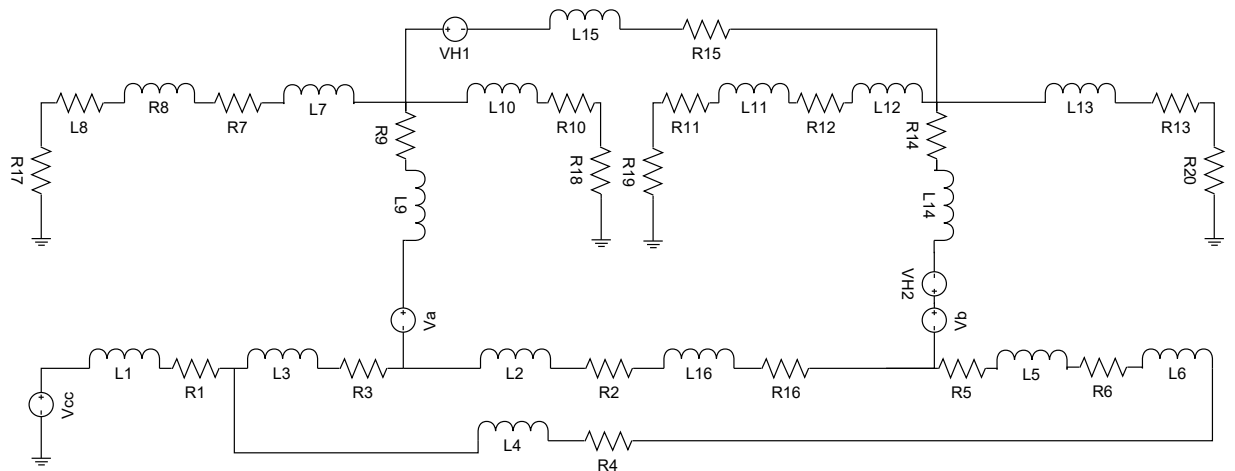


Figure A.1: Electric equivalent for the water supply system.

In the table A.1, the difference in types of pipes, which indicates type, length, diameter and roughness height is described. This will be used to calculated the different parameters for the pipes.

Pipe number	Type	Length [m]	Diameter [mm]	ϵ [mm]
R1/L1	PEM	5	20	0.01
R2/L2 & R3/L3 & R4/L4 & R5/L5 & R6/L6 & R16/L16	PEM	10	20	0.01
R10/L10 & R13/L13 & R15/L15	PEX	2	10	0.007
R7/L7 & R8/L8 & R11/L11 & R12/L12	PEX	1	10	0.007
R14/L14	PEX	3	10	0.007
R9/L9	PEX	2	10	0.007

Table A.1: Table of the different types of pipes. Type, length and diameter.

In the following example the parameters for R1 and L1 will be calculated.

Before the k_v and the inertia can be calculated, some parameters must be known as Reynolds number R, the kinematic viscosity of fluid v_f and the friction factor f. The kinematic viscosity can be found as equation A.1 shows:

$$v_f = 1.792 \cdot 10^{-6} \left(1 + \left(\frac{T}{25} \right)^{1.165} \right)^{-1} \quad [\text{m}^2/\text{s}] \quad (\text{A.1})$$

Where:

T is the temperature of the water. $[\text{ }^\circ\text{C}]$

$$v_f = 1.792 \cdot 10^{-6} \left(1 + \left(\frac{20}{25} \right)^{1.165} \right)^{-1} \quad [\text{m}^2/\text{s}] \quad (\text{A.2})$$

The temperature is considered to be $20 \text{ }^\circ\text{C}$, which is the most common ambient temperature [H.E. Burroughs,].

$$v_f = 1.012 \cdot 10^{-6} \quad [\text{m}^2/\text{s}] \quad (\text{A.3})$$

Reynolds number can be found as shown in equation A.4:

$$\mathbf{R} = \frac{4 \cdot q}{\pi \cdot v_f \cdot D} \quad [\cdot] \quad (\text{A.4})$$

Where:

q is the flow through the pipe. $[\text{m}^3/\text{s}]$

D is the diameter of the pipe. $[\text{m}]$

From section 2.5 the flow is known through every pipe in the system therefore Reynolds number can be calculated as:

$$\mathbf{R} = \frac{4 \cdot 3.356 \cdot 10^{-4}}{\pi \cdot 1.012 \cdot 10^{-6} \cdot 0.02} \quad [\cdot] \quad (\text{A.5})$$

$$\mathbf{R} = 2.097 \cdot 10^4 \quad [\cdot] \quad (\text{A.6})$$

Because the Reynold's is larger then 4000 it is turbulent flow. [Toolbox,]
The friction factor can be found as shown in equation A.7

$$f = 1.325 \left(\ln \left(\frac{\epsilon}{3.7 \cdot D} + \frac{5.74}{\mathbf{R}^{0.9}} \right) \right)^{-2} \quad [\cdot] \quad (\text{A.7})$$

$$f = 1.325 \left(\ln \left(\frac{5 \cdot 10^{-5}}{3.7 \cdot 0.02} + \frac{5.74}{(2.097 \cdot 10^4)^{0.9}} \right) \right)^{-2} \quad [\cdot] \quad (\text{A.8})$$

$$f = 0.031 \approx 0.03 \quad [\cdot] \quad (\text{A.9})$$

It has been chosen to use 0.03 as the friction constant for all the pipes.

The k_v factor from equation 2.20 can now be calculated as shown in equation A.10

$$k_v = \left(k_f \cdot \frac{\rho \cdot 8}{\pi^2 \cdot D^4} + f \cdot \frac{8 \cdot \rho \cdot l}{\pi^2 \cdot D^5} \right) \quad [(\text{Pa} \cdot \text{s}^2)/\text{m}^6] \quad (\text{A.10})$$

Where:

ρ is the density of the water. $[\text{kg}/\text{m}^3]$
 k_f is the form-loss coefficient. $[\cdot]$

k_f has the value of 1.8 according to [Prabhata K. Swamee, 2008] for a service connection.

$$k_v = \left(1.8 \cdot \frac{1000 \cdot 8}{\pi^2 \cdot 0.02^4} + 0.031 \cdot \frac{8 \cdot 1000 \cdot 5}{\pi^2 \cdot 0.02^5} \right) \quad [(\text{Pa} \cdot \text{s}^2)/\text{m}^6] \quad (\text{A.11})$$

$$k_v = 4.711 \cdot 10^{10} \quad [(\text{Pa} \cdot \text{s}^2)/\text{m}^6] \quad (\text{A.12})$$

The inertia from equation 2.20 can be calculated as shown on equation A.13

$$J = \frac{\rho \cdot l}{A} \quad [(\text{Pa} \cdot \text{s}^2)/\text{m}^3] \quad (\text{A.13})$$

Where:

A is the area of a pipe. $[\text{m}^2]$

$$J = 1.592 \cdot 10^7 \quad [(\text{Pa} \cdot \text{s}^2)/\text{m}^3] \quad (\text{A.14})$$

The pressure drop for R1/L1 can be calculated with the flows known from section 2.5 as equation A.15 shows:

$$\Delta p = J \cdot \frac{d}{dt} q + k_v \cdot |q| \cdot q \quad [\text{Pa}] \quad (\text{A.15})$$

$$\Delta p = 1.592 \cdot 10^7 \cdot \frac{d}{dt} (3.356 \cdot 10^{-4}) + 4.711 \cdot 10^{10} \cdot |3.356 \cdot 10^{-4}| \cdot 3.356 \cdot 10^{-4} [\text{Pa}] \quad (\text{A.16})$$

The results for pressure will be calculated in meter water column and not in pascal, because if the parameter was in pascal the result would be very small, therefore it is converted from Pa to mWc.

$$\Delta p = 1.086 \quad [\text{mWc}] \quad (\text{A.17})$$

In the table A.2 the result for rest of the pipes are shown.

Pipe number	$q [m^3/s]$	$J \cdot \frac{d}{dt} q [\text{mWc}]$	$\Delta k_v \cdot q \cdot q [\text{mWc}]$	$\Delta p [\text{mWc}]$
R1/L1	$3.356 \cdot 10^{-4}$	0.541	0.545	1.086
R3/L3	$3.856 \cdot 10^{-4}$	1.29	1.252	2.542
R2/L2 & R16/L16	$2.158 \cdot 10^{-4}$	0.404	0.7	1.104
R4/L4 & R5/L5 & R6/L6	$5 \cdot 10^{-5}$	0.022	0.162	0.184
R10/L10	$9.111 \cdot 10^{-5}$	0.535	0.237	0.772
R13/L13	$7.667 \cdot 10^{-5}$	0.379	0.199	0.578
R15/L15	$1.25 \cdot 10^{-5}$	0.01007	0.032	0.0421
R7/L7 & R8/L8	$9.111 \cdot 10^{-5}$	0.329	0.118	0.447
R11/L11 & R12/L12	$7.667 \cdot 10^{-5}$	0.233	0.1	0.333
R14/L14	$1.658 \cdot 10^{-4}$	2.455	0.646	3.101
R9/L9	$1.697 \cdot 10^{-4}$	1.719	0.441	2.16

Table A.2: The pressure difference over the pipes.

To see the calculation for the rest of the pipes refer to CD [calculations/pipe and valve calculations].

A.1.2 Calculation of the water flow

This appendix will cover the calculations for the flow in the distribution system.

To find the flow in the PMA's the pressure sensor p_2 and p_4 are used.

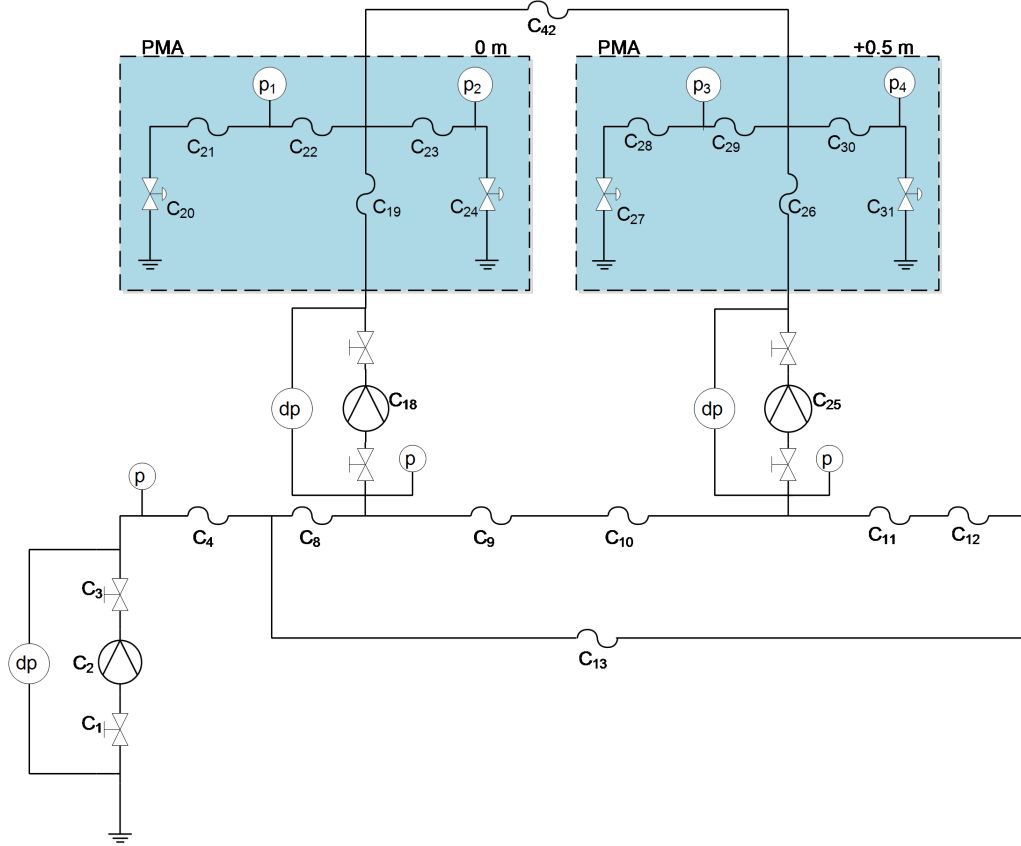


Figure A.2: Diagram of the distribution system.

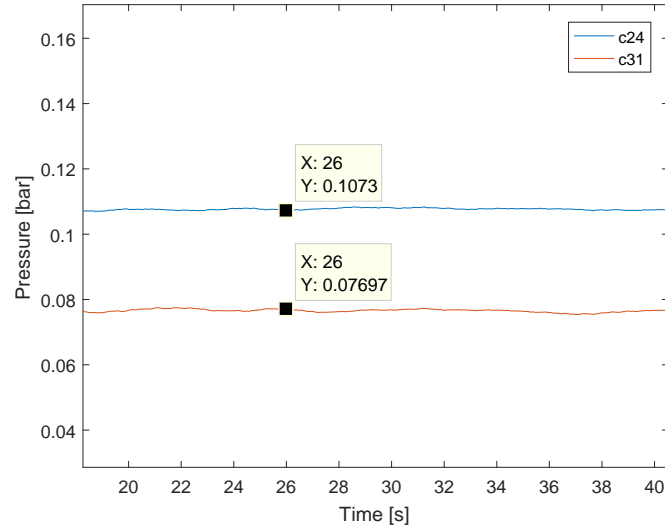


Figure A.3: Filtered MATLAB plot with the running average pressure over time.

The pressure is known from journal A.3.3 and can be seen on figure A.3. The pressure

across valve $C_{24} = 0.1077$ bar and $C_{31} = 0.0764$ bar. When the pressure is known the equation for a valve can be used from section 2.3.

$$q = k_{vs} \cdot \sqrt{\Delta p} \quad [\text{m}^3/\text{h}] \quad (\text{A.18})$$

Where:

K_{vs} is the conductivity of a valve. $[\text{m}^3/\text{s}]$

Δp is the pressure across the valve. $[\text{Pa}]$

q is the water flow. $[\text{m}^3/\text{s}]$

K_{vs} is equal to 1 according to the datasheet when the valves are fully-open (refer to CD [Datasheet/Jumo_sensor]).

$$q_{24} = 1 \cdot \sqrt{0.1077} = 0.328 \quad [\text{m}^3/\text{h}] \quad (\text{A.19})$$

$$q_{31} = 1 \cdot \sqrt{0.0764} = 0.276 \quad [\text{m}^3/\text{h}] \quad (\text{A.20})$$

When the water flow is known the pressure loss across C_{23} and C_{30} can be calculated with the equation for the model of the pipe, which have been found in section 2.3. This will be used to find the water flow across C_{42} .

$$\frac{\rho \cdot l}{A} \cdot \frac{d}{dt} q = \Delta p - \left(k_f \frac{\rho \cdot 8}{\pi^2 \cdot D^4} + \frac{8 \cdot f \cdot \rho \cdot l}{\pi^2 \cdot D^5} \right) \cdot |q| \cdot q \quad [\text{Pa}] \quad (\text{A.21})$$

Where:

ρ is the density of the water. $[\text{kg}/\text{m}^3]$

l is the length of the pipe. $[\text{m}]$

A is the area of a circle. $[\text{m}^2]$

q is the flow. $[\text{m}^3/\text{h}]$

Δp is the pressure difference. $[\text{Pa}]$

k_f is the form-loss coefficient. $[.]$

D is the diameter of the pipe. $[\text{m}]$

f is the friction factor. $[.]$

This equation is solved for the pressure difference:

$$\Delta p = \frac{\rho \cdot l}{A} \cdot \frac{d}{dt} q + \left(k_f \frac{\rho \cdot 8}{\pi^2 \cdot D^4} + \frac{8 \cdot f \cdot \rho \cdot l}{\pi^2 \cdot D^5} \right) \cdot |q| \cdot q \quad [\text{Pa}] \quad (\text{A.22})$$

The pressure difference for C_{23} is equal to:

$$\begin{aligned} \Delta p_{23} &= \frac{1000 \cdot 2}{7.854 \cdot 10^{-5}} \frac{d}{dt} 0.328 + \left(1.8 \frac{1000 \cdot 8}{\pi^2 \cdot 0.01^4} + \frac{8 \cdot 0.03 \cdot 10002}{\pi^2 \cdot 0.01^5} \right) \\ &\quad \cdot |0.328| \cdot 0.328 [\text{Pa}] \end{aligned} \quad (\text{A.23})$$

$$\Delta p_{23} = 7717.5 \quad [\text{Pa}] \quad (\text{A.24})$$

Convert this value into bar instead of Pa, because the pressure sensors on the systems measures in bar and the graphs are in bar. $p_{23} = 0.077$ bar. Same calculation have been made for C_{30} just with the right flow value(0.276), this result in a pressure difference of $C_{30} = 0.059$ bar.

With the pressure loss across C_{23} and C_{30} known the flow across C_{42} can be calculated. To do so the pressure across C_{42} must be known. This can be found with the use of the pressure sensors. The pressure at p_2 is equal to 0.1077and the pressure loss across C_{23} is equal to 0.077 bar. To find the pressure before C_{42} is the summation of these values. The same goes p_4 and C_{30} . The pressure between C_{23} and C_{42} is 0.185 bar and the pressure between C_{30} and C_{42} is 0.135 bar. With the pressure difference across C_{42} known the water flow across it can be calculated with the use of the model for a pipe.

$$\Delta p = \frac{\rho \cdot l}{A} \cdot \frac{d}{dt} q + \left(k_f \frac{\rho \cdot 8}{\pi^2 \cdot D^4} + \frac{8 \cdot f \cdot \rho \cdot l}{\pi^2 \cdot D^5} \right) \cdot |q| \cdot q + \Delta z \cdot g \cdot \rho \quad [\text{Pa}] \quad (\text{A.25})$$

Where:

Δz is the hight difference from input to output of the pipe. [m]
 g is the Gravity of Earth. [m/s²]

Because there is a level difference in C_{42} the height needs to be included in the model for the pipe. This equation needs to be solved for q:

$$q = \frac{\pi \cdot \sqrt{8} \cdot D^{5/2} \cdot \sqrt{g \cdot \Delta z \cdot \rho - \Delta p}}{8 \cdot \sqrt{f \cdot l \cdot \rho + D \cdot \rho \cdot k_f}} \quad [\text{m}^3/\text{h}] \quad (\text{A.26})$$

The friction factor has been chosen to be 0.03, which is deemed to be a fine approximation for the system. k_f has the value of 1.8 according to [Prabhata K. Swamee, 2008] for a service connection.

$$q = \frac{\pi \cdot \sqrt{8} \cdot 0.01^{5/2} \cdot \sqrt{9.807 \cdot 0.5 \cdot 1000 - (0.185 - 0.135)}}{8 \cdot \sqrt{0.03 \cdot 2 \cdot 1000 + 0.01 \cdot 1000 \cdot 1.8}} = -0.045 \quad [\text{m}^3/\text{h}] \quad (\text{A.27})$$

To calculate the flow across C_{19} and C_{26} junction rule is used.

$$q_{19} = 0.328 + 0.328 - 0.045 = 0.611 \quad [\text{m}^3/\text{h}] \quad (\text{A.28})$$

$$q_{26} = 0.276 + 0.276 + 0.045 = 0.597 \quad [\text{m}^3/\text{h}] \quad (\text{A.29})$$

Which result in a water flow for C_{19} at $0.611 \text{ m}^3/\text{h}$ and for C_{26} at $0.597 \text{ m}^3/\text{h}$.

To calculate the water flow across C_9 and C_{10} the pressure must be known. This can be found by using the measurement from the laboratory A.3.3, which can be seen on figure A.4.

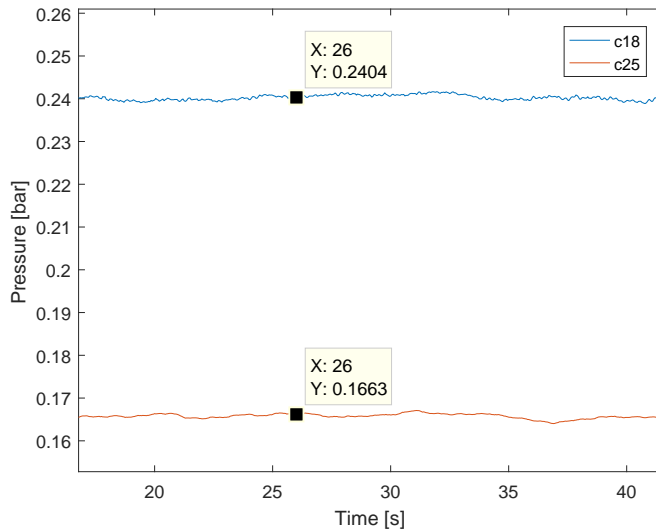


Figure A.4: Filtered MATLAB plot with the running average pressure over time at the pumps C_{18} and C_{25} .

With the pressure known the water flow can be calculated with use of equation A.26 without the height difference:

$$q = \frac{\pi \cdot \sqrt{8} \cdot D^{5/2} \cdot \sqrt{\Delta p}}{8 \cdot \sqrt{f \cdot l \cdot \rho + D \cdot \rho \cdot k_f}} \quad [\text{m}^3/\text{h}] \quad (\text{A.30})$$

$$q_{9,10} = \frac{\pi \cdot \sqrt{8} \cdot 0.02^{5/2} \cdot \sqrt{(0.2404 - 0.1663)}}{8 \cdot \sqrt{0.03 \cdot 20 \cdot 1000 + 0.02 \cdot 1000 \cdot 1.8}} = 0.777 \quad [\text{m}^3/\text{h}] \quad (\text{A.31})$$

With the water flow across C_9 and C_{10} known the water flow for the rest of the system can be calculated. To calculate the water flow across C_8 the junction rule is used on the junction after C_8 . It is a summation of the water flow going up through the pump, which is $0.611 \text{ m}^3/\text{h}$ and the water flow across C_9 and C_{10} , which is $0.777 \text{ m}^3/\text{h}$.

$$q_8 = 0.777 + 0.611 = 1.388 \quad [\text{m}^3/\text{h}] \quad (\text{A.32})$$

To calculate the junction after C_{10} the water flow across C_{11}, C_{12} and C_{13} is unknown. It can be calculated by subtracting the water flow up through the pump and the water flow across C_9 and C_{10} .

$$q_{11,12,13} = 0.777 - 0.597 = 0.180 \quad [\text{m}^3/\text{h}] \quad (\text{A.33})$$

The water flow across C_4 is equal to the flow at the outputs.

$$q_4 = 0.328 + 0.328 + 0.276 + 0.276 = 1.208 \quad [\text{m}^3/\text{h}] \quad (\text{A.34})$$

A.1.3 Linear model of the centrifugal pump

The purpose of this appendix is to derive the linear model for the pump in section 2.1 from the expression 2.24, which is also seen in equation A.35. Unless otherwise stated measurement data refers to appendix A.3.4.

$$\Delta P = -a_{n2} \cdot q^2 + a_{n1} \cdot q \cdot \omega + a_{n0} \cdot \omega^2 \quad (\text{A.35})$$

Because q is changing slowly compared to the dynamics of the pump, q is considered as a constant.

The standard first order Taylor approximation:

$$f(\omega) = f(\bar{\omega}) + f'(\bar{\omega}) \cdot (\omega - \bar{\omega}) \quad (\text{A.36})$$

Taking the derivative for the second term, with respect to ω :

$$f_1(\bar{\omega}) = a_{n1} \cdot \bar{q} \cdot \bar{\omega} \quad (\text{A.37})$$

$$f'_1(\bar{\omega}) = a_{n1} \cdot \bar{q} \quad (\text{A.38})$$

$$\equiv AN1 \quad (\text{A.39})$$

Taking the derivative for the third term, with respect to ω :

$$f_2(\bar{\omega}) = a_{n0} \cdot \bar{\omega}^2 \quad (\text{A.40})$$

$$f'_2(\bar{\omega}) = 2a_{n0} \cdot \bar{\omega} \quad (\text{A.41})$$

$$\equiv AN0 \quad (\text{A.42})$$

Taylor approximation on the secound term, where $\omega = \bar{\omega} + \hat{\omega}$:

$$f_1(\omega) = f_1(\bar{\omega}) + f'_1(\bar{\omega}) \cdot (\omega - \bar{\omega}) \quad (\text{A.43})$$

$$f_1(\omega) = f_1(\bar{\omega}) + AN1 \cdot (\omega - \bar{\omega}) \quad (\text{A.44})$$

$$f_1(\omega) = f_1(\bar{\omega}) + AN1 \cdot \hat{\omega} \quad (\text{A.45})$$

Taylor approximation on the third term, where $\omega = \bar{\omega} + \hat{\omega}$:

$$f_2(\omega) = f_2(\bar{\omega}) + f'_2(\bar{\omega}) \cdot (\omega - \bar{\omega}) \quad (\text{A.46})$$

$$f_2(\omega) = f_2(\bar{\omega}) + AN0 \cdot (\omega - \bar{\omega}) \quad (\text{A.47})$$

$$f_2(\omega) = f_2(\bar{\omega}) + AN0 \cdot \hat{\omega} \quad (\text{A.48})$$

Rewriting $\Delta\bar{P}$ from the expressions found in equation A.37 and A.40.

$$\Delta\bar{P} = f_1(\bar{\omega}) + f_2(\bar{\omega}) + c \quad (\text{A.49})$$

Substituting $\Delta\bar{P}$ and replacing with the Taylor terms in equation A.35:

$$0 = -(\Delta\bar{P} + \Delta\hat{P}) + f_1(\bar{\omega}) + AN1 \cdot \hat{\omega} + f_2(\bar{\omega}) + AN0 \cdot \hat{\omega} + c \quad (\text{A.50})$$

$$0 = -(f_1(\bar{\omega}) + f_2(\bar{\omega}) + c + \Delta\hat{P}) + f_1(\bar{\omega}) + AN1 \cdot \hat{\omega} + f_2(\bar{\omega}) + AN0 \cdot \hat{\omega} + c \quad (\text{A.51})$$

$$0 = -\Delta\hat{P} + AN1 \cdot \hat{\omega} + AN0 \cdot \hat{\omega} \quad (\text{A.52})$$

Laplace transformation:

$$0 = -\Delta P(s) + AN1 \cdot \omega(s) + AN0 \cdot \omega(s) \quad (\text{A.53})$$

The transfer function for the pump:

$$C(s) = \frac{Out(s)}{In(s)} = \frac{\Delta P(s)}{\omega(s)} = AN1 + AN0 \quad (A.54)$$

The head parameters of the UPM2 25-60 180 centrifugal pump is given by Grundfos:

$$q \cdot q : a_{n0} = 0.6921 \quad (A.55)$$

$$q \cdot \omega : a_{n1} = -0.0177 \quad (A.56)$$

$$\omega \cdot \omega : a_{n2} = 0.0179 \quad (A.57)$$

With these parameters the linear model of pump, C_{18} and C_{25} can be calculated:

The linear model can be used to determine the slope at a certain pressure and angular velocity.

The linear equation with two variables is being used:

$$y = ax + b \quad (A.58)$$

Where:

y is the increasing value on the y-axis

x is the increasing value on the x-axis

a is the slope of the equation

b is the datum of the equation

The operation point at pump C_{18} is where the water flow is $q = 0.611 \frac{m^3}{h}$ and the difference pressure across the pump is $\Delta P = 0.377$ bar, with an angular velocity of 0.5. The slope of the system can then be obtained by inserting the parameters at the operation point into the linear model.

$$C_{18}(s) = \frac{Out(s)}{In(s)} = \frac{\Delta P(s)}{\omega(s)} = AN1 + AN0 \quad (A.59)$$

$$= a_{n1} \cdot \bar{q} + 2a_{n0} \cdot \bar{\omega} \quad (A.60)$$

$$= -0.0177 \cdot 0.611 + 2 \cdot 0.6921 \cdot 0.5 \quad (A.61)$$

$$= 0.681 \quad (A.62)$$

Where:

q is the water flow at the operation point. $[\frac{m^3}{h}]$

ω is the angular velocity of the centrifugal pump, scaled down to an interval between 0 and 1 $[rad/s]$

The linear model of the pump C_{18} results in a slope of 0.681. The increasing pressure value can be obtained by equation A.58, where $b = 0$.

$$y = ax + b \quad (A.63)$$

$$\Delta \hat{P} = (AN1 + AN0) \cdot \hat{\omega} \quad (A.64)$$

$$= 0.681 \cdot \hat{\omega} \quad (A.65)$$

Where:

$\Delta\hat{P}$ is the changes in the difference pressure

$\hat{\omega}$ is the changes in the angular velocity

At the operation point of pump C_{25} , the water flow is $q = 0.597 \frac{m^3}{h}$ and the difference pressure across the pump is $\Delta P = 0.366$ bar.

$$C_{25}(s) = \frac{Out(s)}{In(s)} = \frac{\Delta P(s)}{\omega(s)} = AN1 + AN0 \quad (A.66)$$

$$= a_{n1} \cdot \bar{q} + 2a_{n0} \cdot \bar{\omega} = -0.0177 \cdot 0.597 + 2 \cdot 0.6921 \cdot 0.5 \quad (A.67)$$

$$= 0.682 \quad (A.68)$$

The linear model of the pump C_{25} results in a slope of 0.682, which is almost equal to the slope found for pump C_{18} , that is because the water flow, q is not dominating in the linear model and is not doing much changes to the linear model.

The increasing pressure value can be obtained by equation A.58, where $b = 0$.

$$y = ax + b \quad (A.69)$$

$$\Delta\hat{P} = (AN1 + AN0) \cdot \hat{\omega} \quad (A.70)$$

$$= 0.682 \cdot \hat{\omega} \quad (A.71)$$

The linear model of the pumps are shown on figure A.5, where the blue line represent the physical measurements of the pumps in the laboratory and the red line represents the linear pump model. Because the datum are included in the physical measurements the operation point is added to the linear model, $b = 0.3849$

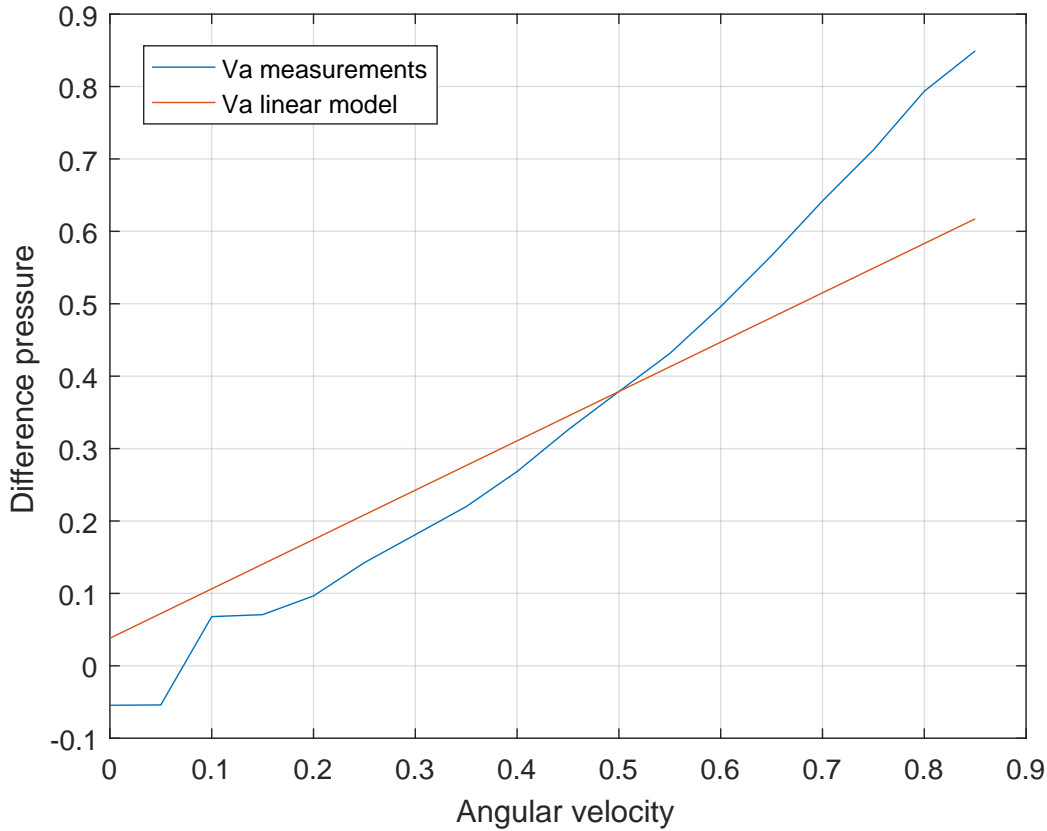


Figure A.5: Physical measurements versus the linear pump model.

The variations of the results could be caused by the linear approximation of the pump model with respect to the input velocity ω , where the water flow q is assumed constant in the linear model. This could be changed by a linear model with both ω and q as input and ΔP as output. fortunate the water system do not have water flow sensors, which are causing in a limitation in a SISO with ω and ΔP .

Calculation of slope

Because of the big deviations between the linear model and the physical measurement (refer to appendix A.3.4), a calculation of a linear slope from the measurements is made. From observations of the running system in the laboratory, the angular velocity is quite steady and do not vary much. On figure A.6, the angular velocity is therefore been chosen to vary $\dot{\omega} \pm 0.1$, where it is crossing the x-axis in the operation point $\omega = 0.5$ and a variation chosen $\omega = 0.4$ and $\omega = 0.6$.

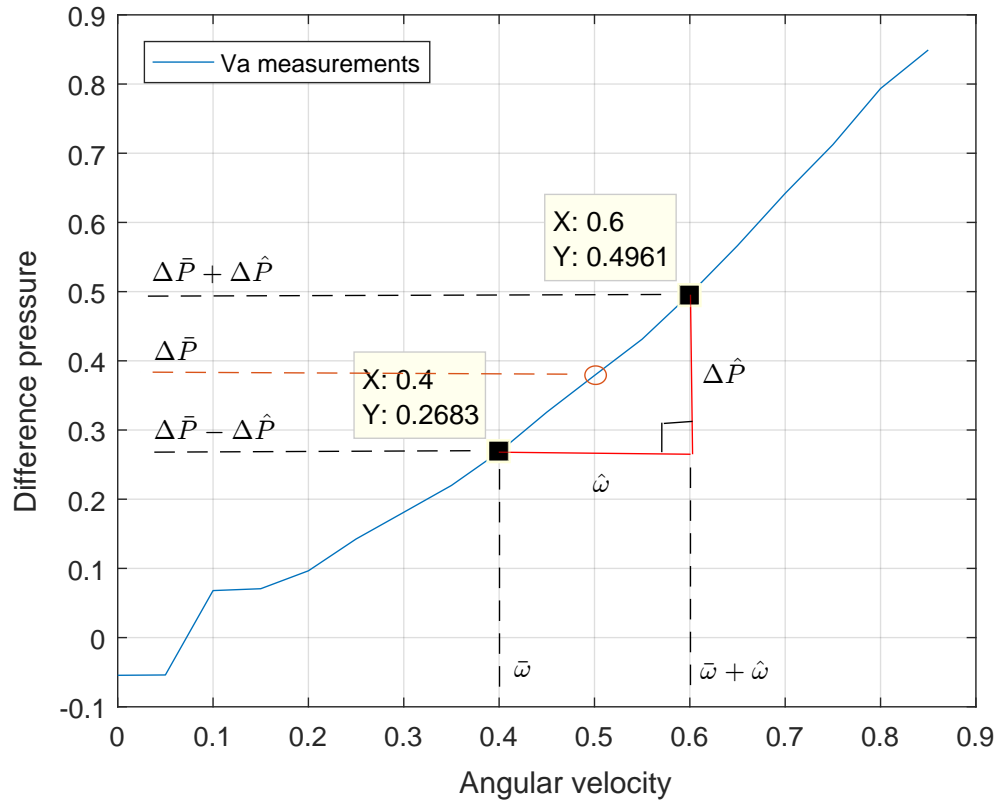


Figure A.6: Physical measurements, where two points have been chosen.

The slope can therefore be calculated from the two chosen points, to linearize around the operation point.

$$a = \frac{\Delta P_2 - \Delta P_1}{\omega_2 - \omega_1} = \frac{0.4961 - 0.2683}{0.6 - 0.4} = 1.139 \quad (\text{A.72})$$

The calculated slope versus the linear pump model against the physical measurements are shown on figure A.7.

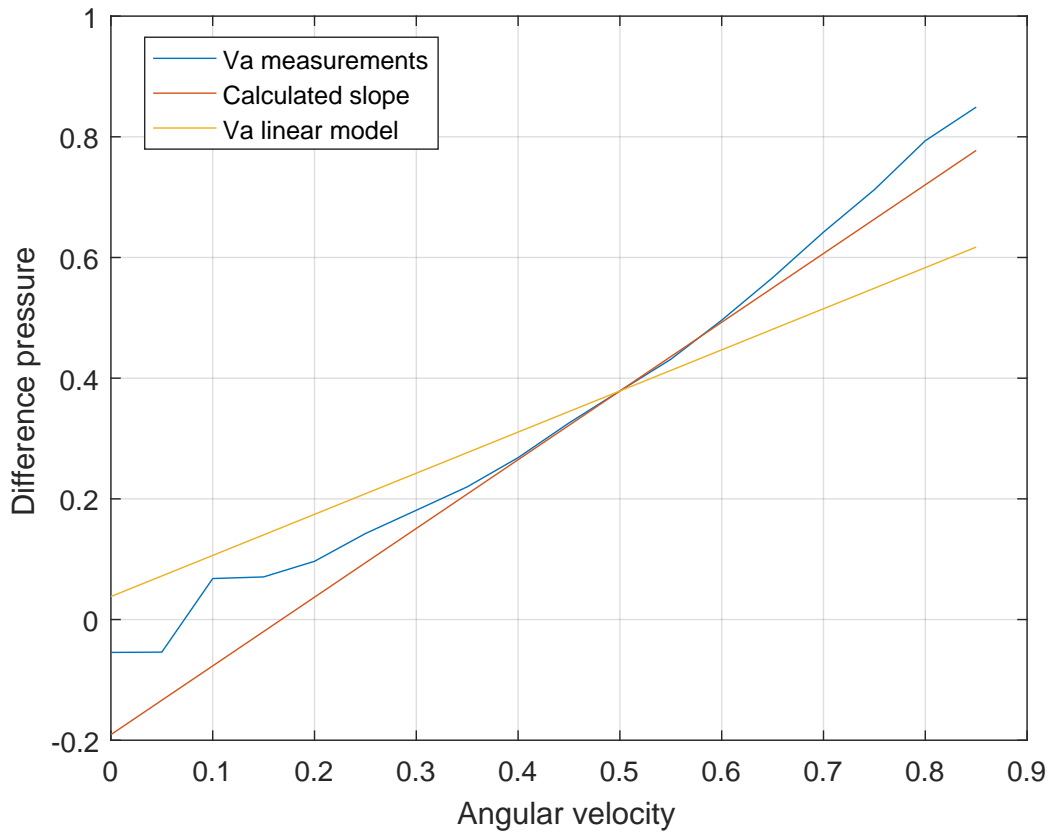


Figure A.7: Physical measurements against the linear model and calculated slope.

It can be concluded that the new calculated slope is a much better fit for the pump according to the errors for y_1 and y_2 in table A.3.

Table for pump V_A :

ω	$\Delta P: y_1$	$\Delta P: y_2$	Measurements	Error: y_1	Error: y_2
0	0.0381	-0.1907	-0.0545	-0.0926	0.1362
0,05	0.0722	-0.1338	-0.0540	-0.1262	0.0797
0,1	0.1063	-0.0768	0.0679	-0.0383	0.1447
0,15	0.1403	-0.0199	0.0706	-0.0697	0.0905
0,2	0.1744	0.0371	0.0965	-0.0779	0.0594
0,25	0.2085	0.0940	0.1425	-0.0660	0.0485
0,3	0.2425	0.1510	0.1811	-0.0614	0.0301
0,35	0.2766	0.2080	0.2199	-0.0567	0.0119
0,4	0.3107	0.2649	0.2683	-0.0424	0.0034
0,45	0.3447	0.3218	0.3258	-0.0189	0.0040
0,5	0.3788	0.3788	0.3788	0	0
0,55	0.4129	0.4358	0.4313	0.0184	-0.0044
0,6	0.4469	0.4927	0.4961	0.0492	0.0034
0,65	0.4810	0.5497	0.5665	0.0855	0.0169
0,7	0.5151	0.6066	0.6420	0.1269	0.0354
0,75	0.5491	0.6636	0.7124	0.1633	0.0488
0,8	0.5832	0.7205	0.7935	0.2103	0.0730
0,85	0.6173	0.7775	0.8492	0.2319	0.0717

Table A.3: Difference between different slopes versus the measurement

Where:

y_1 is the pressure with the linear model [bar]

y_2 is the pressure with the calculated slope [bar]

The pumps should be equal, but to identify, the same test have been done for pump V_B . First calculating the slope for pump V_B , from the measurements:

$$a = \frac{\Delta P_2 - \Delta P_1}{\omega_2 - \omega_1} = \frac{0.4802 - 0.2615}{0.6 - 0.4} = 1.0935 \quad (\text{A.73})$$

Table for pump V_B :

ω	$\Delta P: y_1$	$\Delta P: y_2$	Measurements	Error: y_1	Error: y_2
0	0.0256	-0.1805	-0.0499	-0.0755	0.1306
0,05	0.0597	-0.1258	-0.0481	-0.1078	0.0776
0,1	0.0938	-0.0711	0.0753	-0.0185	0.1464
0,15	0.1278	-0.0164	0.0755	-0.0523	0.0919
0,2	0.1619	0.0382	0.1017	-0.0602	0.0635
0,25	0.1960	0.0929	0.1327	-0.0633	0.0398
0,3	0.2300	0.1476	0.1760	-0.0540	0.0284
0,35	0.2641	0.2023	0.2148	-0.0493	0.0125
0,4	0.2982	0.2570	0.2615	-0.0367	0.0045
0,45	0.3322	0.3116	0.3167	-0.0155	0.0051
0,5	0.3663	0.3663	0.3663	0	0
0,55	0.4004	0.4210	0.4238	0.0234	0.0028
0,6	0.4344	0.4757	0.4802	0.0458	0.0045
0,65	0.4685	0.5303	0.5491	0.0806	0.0188
0,7	0.5026	0.5850	0.6212	0.1186	0.0362
0,75	0.5366	0.6397	0.6865	0.1499	0.0468
0,8	0.5707	0.6944	0.7681	0.1974	0.0737
0,85	0.6048	0.7490	0.8438	0.2390	0.0948

Table A.4: Difference between different slopes versus the measurement

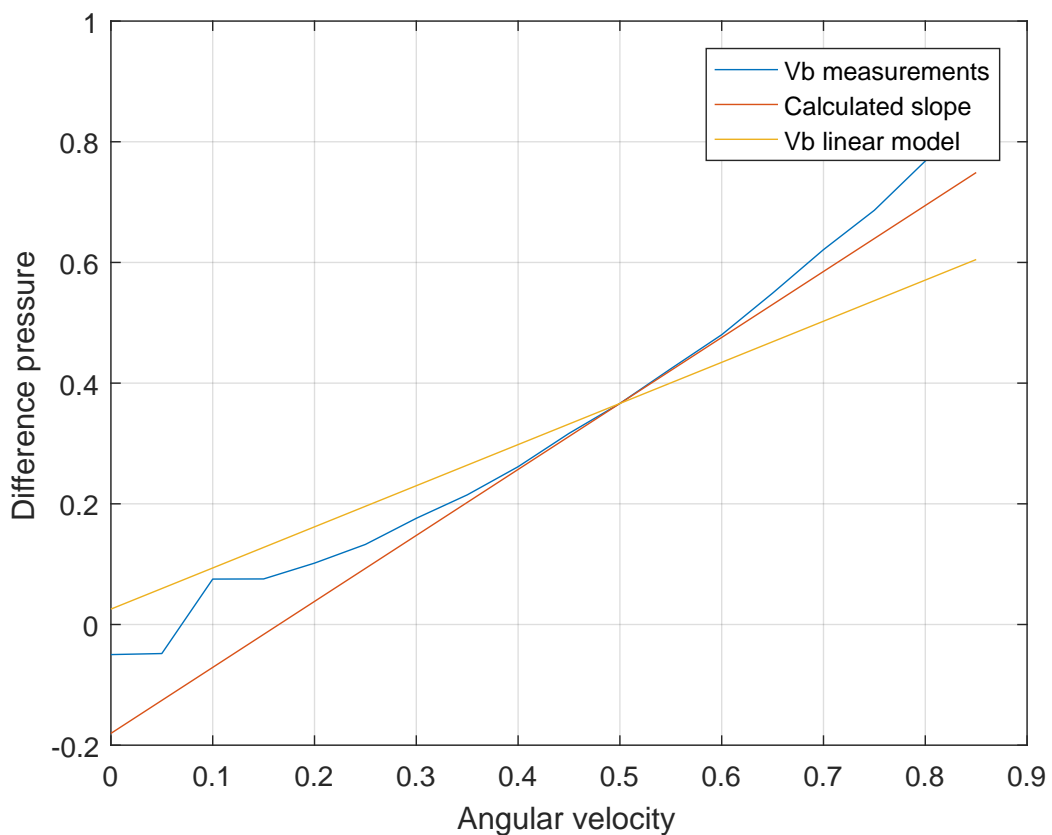


Figure A.8: Physical measurements against the linear model and calculated slope.

Because the two slope are almost equally, it is concluded that the deviation of the two slopes is measurement errors. The gain for both pumps are chosen to be 1.139.

A.1.4 KVL equations

The remaining mesh loops from section 2.4 can be found in this appendix.

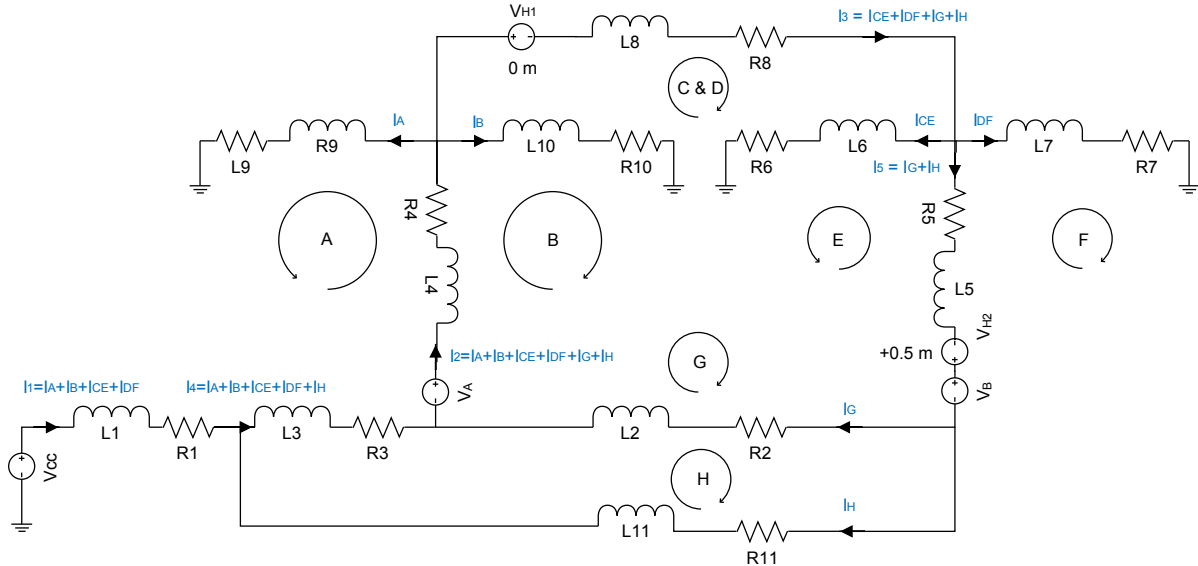


Figure A.9: reduced equivalent for the water supply system.

Where:

V_{CC} is the main pump (Pump 1).	[V]
V_A is the pump to network 1 (Pump 4).	[V]
V_{H1} present the height of network 1.	[V]
V_B is the pump to network 2 (Pump 5).	[V]
V_{H2} present the height of network 2.	[V]

For simplification the currents are determined as:

$$\begin{aligned} I_1 &= I_a + I_b + I_{CE} + I_{DF} & [A] \\ I_2 &= I_a + I_b + I_{CE} + I_{DF} + I_g + I_h & [A] \\ I_3 &= I_{CE} + I_{DF} + I_g + I_h & [A] \\ I_4 &= I_a + I_b + I_{CE} + I_{DF} + I_h & [A] \\ I_5 &= I_g + I_h & [A] \end{aligned}$$

Loop B:

$$\begin{aligned} -V_{cc} + R_1 \cdot i_1 + L_1 \frac{d(i_1)}{dt} + R_3 \cdot i_4 + L_3 \frac{d(i_4)}{dt} - V_a + L_4 \frac{d(i_2)}{dt} + R_4 \cdot i_2 + R_{10} \cdot I_B \\ + L_{10} \frac{d(i_B)}{dt} = 0 \end{aligned} \quad (\text{A.74})$$

Loop C to E:

$$\begin{aligned} -V_{cc} + R_1 \cdot i_1 + L_1 \frac{d(i_1)}{dt} + R_3 \cdot i_4 + L_3 \frac{d(i_4)}{dt} - V_a + L_4 \frac{d(i_2)}{dt} + R_4 \cdot i_2 + R_8 \cdot i_3 + V_{H1} \\ + L_8 \frac{d(i_3)}{dt} + R_6 \cdot I_{CE} + L_6 \frac{d(I_{CE})}{dt} = 0 \end{aligned}$$

(A.75)

Loop D to F:

$$\begin{aligned}
 -V_{cc} + R_1 \cdot i_1 + L_1 \frac{d(i_1)}{dt} + R_3 \cdot i_4 + L_3 \frac{d(i_4)}{dt} - V_a + L_4 \frac{d(i_2)}{dt} + R_4 \cdot i_2 + V_{H1} + R_8 \cdot i_3 \\
 + L_8 \frac{d(i_3)}{dt} + R_7 \cdot i_{DF} + L_7 \frac{di_{DF}}{dt} = 0
 \end{aligned} \tag{A.76}$$

Loop G:

$$\begin{aligned}
 -V_a + L_4 \frac{d(i_2)}{dt} + R_4 \cdot i_2 + V_{H1} + R_8 \cdot i_3 + L_8 \frac{d(i_3)}{dt} + R_5 \cdot i_5 + L_5 \frac{d(i_5)}{dt} - V_{H2} + V_b + R_2 \cdot I_G \\
 + L_2 \frac{di_G}{dt} = 0
 \end{aligned} \tag{A.77}$$

Loop H:

$$\begin{aligned}
 R_3 \cdot i_4 + L_3 \frac{d(i_4)}{dt} - V_a + R_4 \cdot i_2 + L_4 \frac{d(i_2)}{dt} - V_{H1} + R_8 \cdot i_3 + L_8 \frac{d(i_3)}{dt} + R_5 \cdot i_5 + L_5 \frac{d(i_5)}{dt} \\
 - V_{H2} + V_b + R_{11} \cdot i_H + L_{11} \frac{d(i_H)}{dt} = 0
 \end{aligned} \tag{A.78}$$

A.1.5 Linearization

The remaining linearised and Laplace transformed loops from section 2.4 can be found in this appendix.

Loop B:

After using the Taylor approximation, the following linear equation is obtained:

$$\hat{v}_a = r_1 \hat{i}_1 + L_1 \frac{d(\hat{i}_1)}{dt} + r_3 \hat{i}_4 + L_3 \frac{d(\hat{i}_4)}{dt} + r_4 \hat{i}_2 + L_4 \frac{d(\hat{i}_2)}{dt} + r_{10} \hat{i}_B + L_{10} \frac{d(\hat{i}_B)}{dt} \quad (\text{A.79})$$

By then using the Laplace transform into frequency domain, the following equation results:

$$V_a(s) = I_1(s) \cdot (R_1 + sL_1) + I_4(s) \cdot (R_3 + sL_3) + I_2(s) \cdot (R_4 + sL_4) + I_B(s) \cdot (R_{10} + sL_{10}) \quad (\text{A.80})$$

Loop C to E:

After using the Taylor approximation, the following linear equation is obtained:

$$\begin{aligned} \hat{v}_a = r_1 \hat{i}_1 + L_1 \frac{d(\hat{i}_1)}{dt} + r_3 \hat{i}_4 + L_3 \frac{d(\hat{i}_4)}{dt} + r_4 \hat{i}_2 + L_4 \frac{d(\hat{i}_2)}{dt} + r_8 \hat{i}_3 + L_8 \frac{d(\hat{i}_3)}{dt} + r_6 \hat{i}_{CE} \\ + L_6 \frac{d(\hat{i}_{CE})}{dt} \end{aligned} \quad (\text{A.81})$$

By then using the Laplace transform into frequency domain, the following equation results:

$$\begin{aligned} V_a(s) = I_1(s) \cdot (R_1 + sL_1) + I_4(s) \cdot (R_3 + sL_3) + I_2(s) \cdot (R_4 + sL_4) + I_3(s) \cdot (R_8 + sL_8) \\ + I_{CE}(s) \cdot (R_6 + sL_6) \end{aligned} \quad (\text{A.82})$$

Loop D to F:

After using the Taylor approximation, the following linear equation is obtained:

$$\begin{aligned} \hat{v}_a = r_1 \hat{i}_1 + L_1 \frac{d(\hat{i}_1)}{dt} + r_3 \hat{i}_4 + L_3 \frac{d(\hat{i}_4)}{dt} + r_4 \hat{i}_2 + L_4 \frac{d(\hat{i}_2)}{dt} + r_8 \hat{i}_3 + L_8 \frac{d(\hat{i}_3)}{dt} + r_7 \hat{i}_{DF} \\ + L_7 \frac{d(\hat{i}_{DF})}{dt} \end{aligned} \quad (\text{A.83})$$

By then using the Laplace transform into frequency domain, the following equation results:

$$\begin{aligned} V_a(s) = I_1(s) \cdot (R_1 + sL_1) + I_4(s) \cdot (R_3 + sL_3) + I_2(s) \cdot (R_4 + sL_4) + I_3(s) \cdot (R_8 + sL_8) \\ + I_{DF}(s) \cdot (R_7 + sL_7) \end{aligned} \quad (\text{A.84})$$

Loop G:

After using the Taylor approximation and substituting with V_a from equation A.83, the following linear equation is obtained:

$$\hat{v}_b = r_1 \hat{i}_1 + L_1 \frac{d(\hat{i}_1)}{dt} + r_3 \hat{i}_4 + L_3 \frac{d(\hat{i}_4)}{dt} + r_7 \hat{i}_{DF} + L_7 \frac{d(\hat{i}_{DF})}{dt} - r_5 \hat{i}_5 - L_5 \frac{d(\hat{i}_5)}{dt} - r_2 \hat{i}_G - L_2 \frac{d(\hat{i}_G)}{dt} \quad (\text{A.85})$$

By then using the Laplace transform into frequency domain, the following equation results:

$$\begin{aligned} V_b(s) = & I_1(s) \cdot (R_1 + sL_1) + I_4(s) \cdot (R_3 + sL_3) + I_{DF}(s) \cdot (R_7 + sL_7) - I_5(s) \cdot (R_5 + sL_5) \\ & - I_G(s) \cdot (R_2 + sL_2) \end{aligned} \quad (\text{A.86})$$

Loop H:

After using the Taylor approximation and substituting with V_a from equation A.83, the following linear equation is obtained:

$$\hat{v}_b = r_1 \hat{i}_1 + L_1 \frac{d(\hat{i}_1)}{dt} + r_7 \hat{i}_{DF} + L_7 \frac{d(\hat{i}_{DF})}{dt} - r_5 \hat{i}_5 - L_5 \frac{d(\hat{i}_5)}{dt} - r_{11} \hat{i}_H - L_{11} \frac{d(\hat{i}_H)}{dt} \quad (\text{A.87})$$

By then using the Laplace transform into frequency domain, the following equation results:

$$V_b(s) = I_1(s) \cdot (R_1 + sL_1) + I_{DF}(s) \cdot (R_7 + sL_7) - I_5(s) \cdot (R_5 + sL_5) - I_H(s) \cdot (R_{11} + sL_{11}) \quad (\text{A.88})$$

A.1.6 Multivariable equations

The purpose of this appendix is to describe the calculation for the equations used in section 2.6. As the size for several of the matrix described in this appendix is to large to fit within the margin of the paper, illustration or reference to the CD is used throughout this section. The equation is generally performed using MATLAB, where the script can be found on the CD [MATLAB/Matrix] unless otherwise stated.

On figure A.10 is the electric equivalent use for reference in this section.

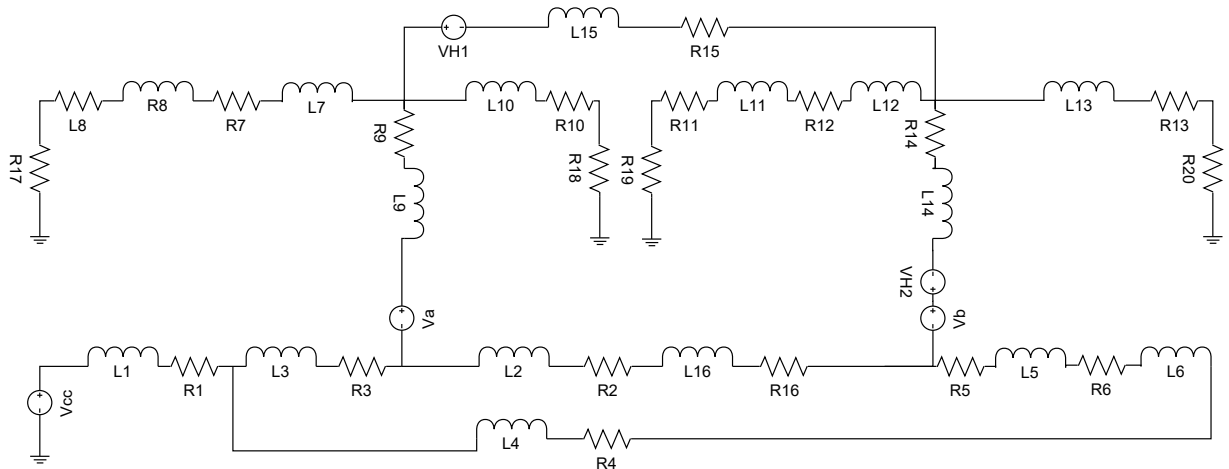


Figure A.10: Electric equivalent for the water supply system.

The first step is established and validated that the matrix $M_E(s)$ multiplied by the currents, are equal to $M_V(s)$ multiplied by the voltages. An illustration of equation A.89 can be seen in equation A.90.

$$M_E(s) \cdot i_c(s) = M_V(s) \cdot v_{a,b}(s) \quad (\text{A.89})$$

The $M_E(s)$ is a square matrix with 36 elements with multiple resistances and inductances per currents, it is therefore not feasible to include it in this paper, though all elements can be seen on the CD [Calculations/Matrix_ME].

$$\begin{bmatrix} E_{1,1}(s) & E_{1,2}(s) & \cdots & E_{1,6}(s) \\ E_{2,1}(s) & E_{2,2}(s) & \cdots & E_{2,6}(s) \\ \vdots & \vdots & \ddots & \vdots \\ E_{6,1}(s) & E_{6,2}(s) & \cdots & E_{6,6}(s) \end{bmatrix} \begin{pmatrix} I_A \\ I_B \\ I_{CE} \\ I_{DF} \\ I_G \\ I_H \end{pmatrix} = \begin{bmatrix} 1 & 0 \\ 1 & 0 \\ 1 & 0 \\ 1 & 0 \\ 0 & 1 \\ 0 & 1 \end{bmatrix} \begin{pmatrix} v_a \\ v_b \end{pmatrix} \quad (\text{A.90})$$

Where:

$E_{m,n}(s)$ is elements of the matrix $M_E(s)$ for the resistance and inductance.

[.]

The second step is to find the matrix $M_I(s)$, which is for the current. This is found by calculating.

$$M_I(s) = M_E^{-1}(s) \cdot M_{v_{a,b}}(s) \quad (\text{A.91})$$

Although the matrix consists of less elements than $M_E(s)$, it is still not feasible to include it because of the size of the equation, but each element can be seen on the CD

[Calculations/Matrix_MI]. The matrix becomes a strictly proper polynomial with 5. order in the numerator and 6. order in the denominator. To obtain the zeros and poles of the matrix it is possible to use the function "zpk" in Matlab. The function create a zero-pole-gain model were z, p are vectors and k is a scalar for each element.

$$Ic_{m,n} = k \frac{(s - z(1))(s - z(2))\dots(s - z(i))}{(s - z(1))(s - z(2))\dots(s - z(j))} \quad (\text{A.92})$$

An illustration of matrix M_I can be seen in equation A.93.

$$M_I(s) = \begin{bmatrix} Ic_{1,1}(s) & Ic_{1,2}(s) \\ Ic_{2,1}(s) & Ic_{2,2}(s) \\ \vdots & \vdots \\ Ic_{6,1}(s) & Ic_{6,2}(s) \end{bmatrix} \quad (\text{A.93})$$

Where:

$Ic_{m,n}(s)$ is elements of the matrix $M_I(s)$ for the zero-pole-gain model. $[\cdot]$

The third step is to find the matrix $G(s)$ containing the transfer functions for the system which multiplied with the input gives the output. As the currents for the system is defined, the wanted output yet remain to be selected, to achieve the wanted output a matrix $M_Y(s)$ containing only the components at the measurable points is defined. Two possible matrix is referring to figure A.10.

$$M_Y(s) = \begin{bmatrix} 0 & R_{18} & 0 & 0 & 0 & 0 \\ 0 & 0 & 0 & R_{20} & 0 & 0 \end{bmatrix} \quad (\text{A.94})$$

and

$$M_{Y2}(s) = \begin{bmatrix} (R_8 + L_8s + R_{17}) & 0 & 0 & 0 & 0 & 0 \\ 0 & 0 & (R_{11} + L_{11}s + R_{19}) & 0 & 0 & 0 \end{bmatrix} \quad (\text{A.95})$$

The matrix $G(s)$ and $G_2(s)$ can then be calculated by.

$$G(s) = M_{y_{a,b}}(s) \cdot M_E^{-1}(s) \cdot M_{v_{a,b}}(s) \quad (\text{A.96})$$

Each element of the matrix $G(s)$ and $G_2(s)$, can be seen here and in section 2.6. The matrix $G(s)$ is a strictly proper polynomial with 5. order in the numerator and 6. order in the denominator. The matrix $G_2(s)$ is an proper polynomial with 6. order in both the numerator and denominator. Obtaining the zeros and poles are done using the function "zpk" in MATLAB. An illustration of matrix $G(s)$ can be seen in equation A.97.

$$G(s) = \begin{bmatrix} G_{11}(s) & G_{12}(s) \\ G_{21}(s) & G_{22}(s) \end{bmatrix} \quad (\text{A.97})$$

The elements of $G(s)$ is:

$$G_{11}(s) = \frac{0.130(s + 7.453)(s + 6.013)(s + 0.698)(s^2 + 6.367s + 10.680)}{(s + 7.205)(s + 6.068)(s + 5.760)(s + 2.524)(s + 1.716)(s + 0.657)} \quad (\text{A.98})$$

$$G_{12}(s) = \frac{0.071(s + 8.353)(s + 7.453)(s + 5.980)(s + 2.113)(s + 0.676)}{(s + 7.205)(s + 6.068)(s + 5.760)(s + 2.524)(s + 1.716)(s + 0.657)} \quad (\text{A.99})$$

$$G_{21}(s) = \frac{0.052(s + 10.090)(s + 7.145)(s + 6.205)(s + 2.635)(s + 0.697)}{(s + 7.205)(s + 6.068)(s + 5.760)(s + 2.524)(s + 1.716)(s + 0.657)} \quad (\text{A.100})$$

$$G_{22}(s) = \frac{0.117(s + 7.199)(s + 6.205)(s + 4.724)(s + 2.305)(s + 0.677)}{(s + 7.205)(s + 6.068)(s + 5.760)(s + 2.524)(s + 1.716)(s + 0.657)} \quad (\text{A.101})$$

The elements of $G_2(s)$ is:

$$G_{211}(s) = \frac{0.014(s + 12.120)(s + 6.903)(s + 6.013)(s + 0.698)(s^2 + 6.367s + 10.680)}{(s + 7.205)(s + 6.068)(s + 5.760)(s + 2.524)(s + 1.716)(s + 0.657)} \quad (\text{A.102})$$

$$G_{212}(s) = \frac{0.008(s + 12.120)(s + 8.353)(s + 6.903)(s + 5.980)(s + 2.113)(s + 0.676)}{(s + 7.205)(s + 6.068)(s + 5.760)(s + 2.524)(s + 1.716)(s + 0.657)} \quad (\text{A.103})$$

$$G_{221}(s) = \frac{0.007(s + 10.090)(s + 10.080)(s + 7.145)(s + 5.799)(s + 2.635)(s + 0.697)}{(s + 7.205)(s + 6.068)(s + 5.760)(s + 2.524)(s + 1.716)(s + 0.657)} \quad (\text{A.104})$$

$$G_{222}(s) = \frac{0.015(s + 10.080)(s + 7.199)(s + 5.799)(s + 4.724)(s + 2.305)(s + 0.677)}{(s + 7.205)(s + 6.068)(s + 5.76)(s + 2.524)(s + 1.716)(s + 0.657)} \quad (\text{A.105})$$

A.1.7 Rearrange of first order transfer function

In this section the transfer function from section 2.7 will be converted to a first order transfer function.

The first order transfer function from section 2.7.

$$Ga(s) = \begin{bmatrix} \frac{0.093}{s+1.540} & \frac{0.092}{s+1.750} \\ \frac{0.084}{s+1.420} & \frac{0.097}{s+1.820} \end{bmatrix} \quad (\text{A.106})$$

This transfer function will be rearrange to fit the following equation, furthermore the gain in each element of matrix A.106 will be divide with 10 to convert from mWC to bar.

$$G(s) = \frac{K}{\tau \cdot s + 1} \quad (\text{A.107})$$

Calculation for $G_{11}(s)$:

τ will be found as:

$$\frac{1}{\tau} = 1.540 \quad (\text{A.108})$$

$$\tau = \frac{1}{1.540} \quad (\text{A.109})$$

$$= 0.65 \quad (\text{A.110})$$

Now the gain K can be calculated as:

$$\frac{K}{\tau} = 0.0093 \quad (\text{A.111})$$

$$K = 0.0093 \cdot \tau \quad (\text{A.112})$$

$$= 0.00604 \quad (\text{A.113})$$

$$G_{11}(s) = \frac{0.00604}{0.65 \cdot s + 1} \quad (\text{A.114})$$

Calculation for $G_{12}(s)$: τ will be found as:

$$\frac{1}{\tau} = 1.750 \quad (\text{A.115})$$

$$\tau = \frac{1}{1.750} \quad (\text{A.116})$$

$$= 0.57 \quad (\text{A.117})$$

Now the gain K can be calculated as:

$$\frac{K}{\tau} = 0.0092 \quad (\text{A.118})$$

$$K = 0.0092 \cdot \tau \quad (\text{A.119})$$

$$= 0.00526 \quad (\text{A.120})$$

$$G_{11}(s) = \frac{0.00526}{0.57 \cdot s + 1} \quad (\text{A.121})$$

Calculation for $G_{21}(s)$: τ will be found as:

$$\frac{1}{\tau} = 1.420 \quad (\text{A.122})$$

$$\tau = \frac{1}{1.420} \quad (\text{A.123})$$

$$= 0.70 \quad (\text{A.124})$$

Now the gain K can be calculated as:

$$\frac{K}{\tau} = 0.0084 \quad (\text{A.125})$$

$$K = 0.0084 \cdot \tau \quad (\text{A.126})$$

$$= 0.00591 \quad (\text{A.127})$$

$$G_{11}(s) = \frac{0.00591}{0.70 \cdot s + 1} \quad (\text{A.128})$$

Calculation for $G_{22}(s)$: τ will be found as:

$$\frac{1}{\tau} = 1.820 \quad (\text{A.129})$$

$$\tau = \frac{1}{1.820} \quad (\text{A.130})$$

$$= 0.55 \quad (\text{A.131})$$

Now the gain K can be calculated as:

$$\frac{K}{\tau} = 0.0097 \quad (\text{A.132})$$

$$K = 0.0097 \cdot \tau \quad (\text{A.133})$$

$$= 0.00532 \quad (\text{A.134})$$

$$G_{11}(s) = \frac{0.00532}{0.55 \cdot s + 1} \quad (\text{A.135})$$

The new $Ga(s)$ matrix calculated in bar:

$$Ga(s) = \begin{bmatrix} \frac{0.00604}{0.65 \cdot s + 1} & \frac{0.00526}{0.57 \cdot s + 1} \\ \frac{0.00591}{0.70 \cdot s + 1} & \frac{0.00533}{0.55 \cdot s + 1} \end{bmatrix} \quad (\text{A.136})$$

A.2 System design

This appendix contain the calculations done throughout Chapter 4. The purpose is to elaborate further on the calculations or found parameters, used in the different sections.

A.2.1 Decoupling of the TITO system

In this appendix the calculation of Bristols relative gain array, the dynamic coupling factor, the decoupler and the two SISO, is performed. The calculation is use in section 4.3 and is based on the theory form this section and uses the same sources.

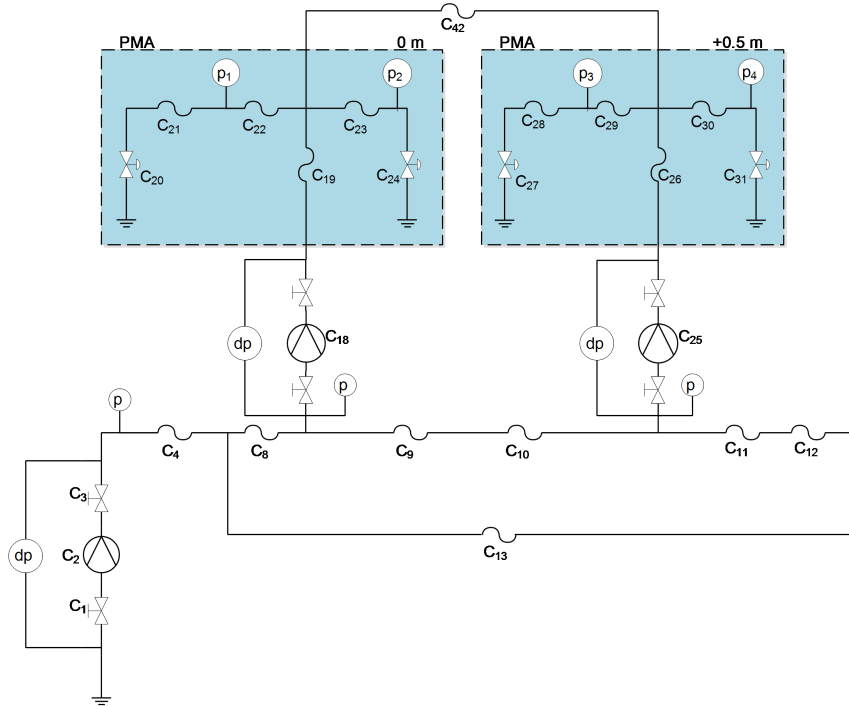


Figure A.11: The reduced distribution system.

Calculations for P2 and P4

By calculation Bristols relative gain array, the interaction index λ can be obtained [Karl J. Åström, 2005].

Bristols relative gain array can be calculated by doing a component-wise multiplication of the matrices:

$$R_{ij} = G_{ij}(0)G_{ij}^{-T}(0) \quad (\text{A.137})$$

Where:

$G(0)$ is the static gain of the hydraulic model. $[.]$

$G^{-T}(0)$ is the inverse transpose, of the static gain for the hydraulic model. $[.]$

The static gain of the system $G(s)$ are calculated to be:

$$G(0) = \begin{pmatrix} 0.053 & 0.038 \\ 0.044 & 0.049 \end{pmatrix} \quad (\text{A.138})$$

The inverse transpose, of the static gain for the hydraulic model $G(s)$, is calculated to be:

$$G^{-T}(0) = \begin{pmatrix} 53.618 & -48.471 \\ -41.318 & 58.015 \end{pmatrix} \quad (\text{A.139})$$

The relative gain array can then be calculated to be:

$$R_{ij} = G_{ij}(0)G_{ij}^{-T}(0) \quad (\text{A.140})$$

$$= \begin{pmatrix} 0.053 & 0.038 \\ 0.044 & 0.049 \end{pmatrix} \cdot \begin{pmatrix} 53.618 & -48.471 \\ -41.318 & 58.015 \end{pmatrix}$$

$$= \begin{pmatrix} 2.808 & -1.808 \\ -1.808 & 2.808 \end{pmatrix}$$

The relative gain array contain the interaction index λ as follows:

$$R = \begin{pmatrix} \lambda & 1-\lambda \\ 1-\lambda & \lambda \end{pmatrix} \quad (\text{A.141})$$

Where it can be observed that the interaction index $\lambda = 2.808$, which means there is interaction between the loops and a decoupling of the system could therefore improve the control. Furthermore, as the interaction index is greater than 0.5 the loops does not need to be swapped.

By calculating the dynamic coupling factor, the necessity for a decoupler can be determined.

The dynamic coupling factor can be defined as:

$$\begin{aligned} Q(s) &= \frac{G_{21}(s)G_{12}(s)}{G_{11}(s)G_{22}(s)} \\ &= \frac{1.106(s+2.703)(s+2.564)}{(s+4.167)(s+2.857)} \end{aligned} \quad (\text{A.142})$$

By plotting $Q(s)$ frequency response, is it possible to determine the coupling factor for all frequencies, as seen in figure A.12.

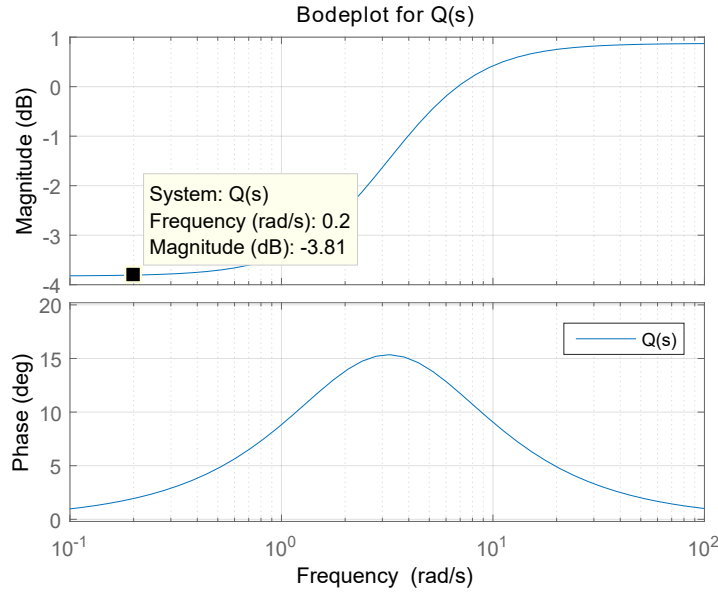


Figure A.12: Frequency response for the dynamic coupling factor $Q(s)$.

In figure A.12, it can be determined, that frequencies from 0.2 rad/s and down have a magnitude of -3.81 dB, which is the lowest the coupling factor can become. The coupling factor at the lowest magnitude can be calculated from the following equation:

$$|Q(0.2)| = 10^{\frac{-3.81 \text{ dB}}{20 \text{ dB}}} \quad (\text{A.143})$$

The coupling factor is then $|Q(0.2)| = 0.645$, this can't be considered $|Q(s)| \ll 1$ and therefore is a decoupler necessary, before the system can be described as two SISO's.

For the decoupler, $F_{11}(s)$ and $F_{22}(s)$ is chosen to be equal to one. $F_{12}(s)$ can then be derived as:

$$\begin{aligned} F_{12}(s) &= -F_{22}(s) \frac{G_{12}(s)}{G_{11}(s)} \\ &= \frac{-1.158(s + 2.564)}{(s + 4.167)} \end{aligned} \quad (\text{A.144})$$

The decoupler, $F_{21}(s)$ can be derived as:

$$\begin{aligned} F_{21}(s) &= -F_{11}(s) \frac{G_{21}(s)}{G_{22}(s)} \\ &= \frac{-0.956(s + 2.703)}{(s + 2.857)} \end{aligned} \quad (\text{A.145})$$

To establish whether decoupler have reduced the interaction, a new analysis of the decoupled dynamic coupling factor $Q_d(s)$ is performed. By rearranging the three open loop transfer function [Knudsen,]:

$$N_1(s) = F_{12}(s) + G_{11}(s) \quad (\text{A.146})$$

$$N_2(s) = F_{21}(s) + G_{22}(s) \quad (\text{A.147})$$

$$N_3(s) = G_{21}(s)G_{12}(s) = N_1(s) \cdot N_2(s) \cdot Q_d(s) \quad (\text{A.148})$$

The decoupled, dynamic coupling factor can then be defined as:

$$Q_d(s) = \frac{G_{21}(s)G_{12}(s)}{(F_{12}(s) + G_{11}(s))(F_{21}(s) + G_{22}(s))} \quad (\text{A.149})$$

$$Q_d(s) = \frac{0.018(s + 4.167)(s + 2.857)(s + 2.703)(s + 2.564)}{(s + 4.167)(s + 2.941)(s + 2.857)(s + 2.795)(s + 2.474)(s + 2.071)}$$

By plotting $Q_d(s)$ frequency response, it is possible to determine the decoupled coupling factor for all frequencies as seen in figure A.13.

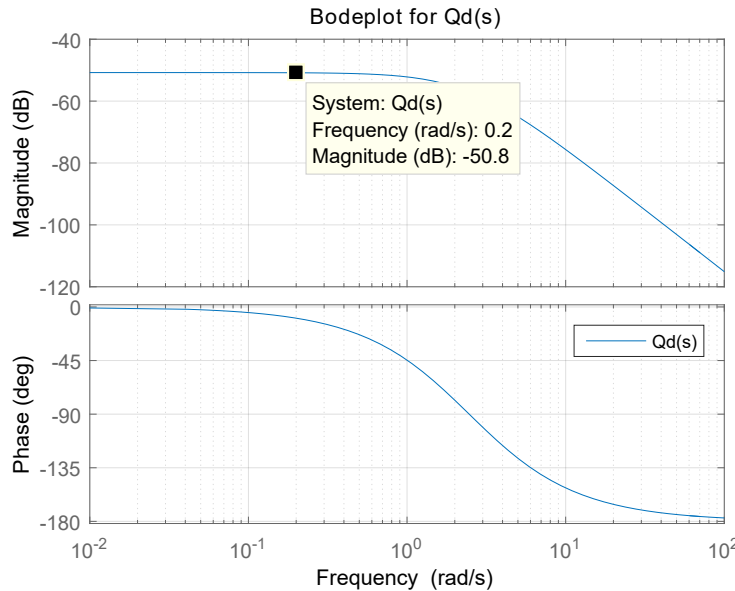


Figure A.13: Frequency response for the decoupled dynamic coupling factor $Q_d(s)$.

From figure A.13 it can be determine that frequencies from 0.3 rad/s and down have a magnitude of -50.8 dB, which is the highest the decoupled coupling factor can become. The coupling factor at the highest magnitude can be calculated from the following equation:

$$|Q_d(0.2)| = 10^{\frac{-50.8dB}{20dB}} \quad (\text{A.150})$$

The coupling factor is then $|Q_d(0.2)| = 0.003$, which can be considered $|Q_d(s)| \ll 1$. This means, two SISO loops can be established.

The two SISO's, were $Q(s) \approx 0$, $F_{11}(s)$ and $F_{22}(s)$ is equal to 1, are defined as: SISO from input U_1 to output Y_1 :

$$\frac{U_1(s)}{Y_1(s)} = (1 - Q(s))F_{11}(s)G_{11}(s) \quad (\text{A.151})$$

$$= \frac{0.054}{0.39s + 1}$$

SISO from input U_2 to output Y_2 :

$$\begin{aligned}\frac{U_2(s)}{Y_2(s)} &= (1 - Q(s))F_{22}(s)G_{22}(s) \\ &= \frac{0.049}{0.37s + 1}\end{aligned}\tag{A.152}$$

A.2.2 Hydraulic controller

In this appendix the controller $D_{22}(s)$ for $G_{22}(s)$ will be calculated.

In equation A.153 $G_{22}(s)$ can be seen.

$$\frac{U_2(s)}{Y_2(s)} = (1 - Q(s))F_{22}(s)G_{22}(s) \quad (\text{A.153})$$

$$= \frac{0.049}{0.37s + 1}$$

A PI controller will be designed as well for this transfer function. The purpose is to cancel the pole in 0.37 and remove steady state error. A root locus is plotted for the transfer function $G_{22}(s)$ and is shown in figure A.14:

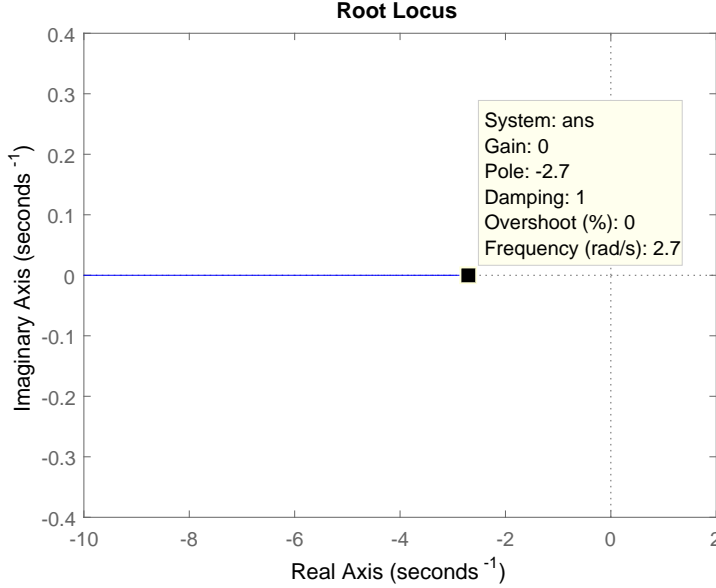


Figure A.14: Root locus of $G_{22}(s)$.

It can be seen from the figure that the pole is placed in -2.7. This pole needs to be canceled and will be done by the PI controller.

The OL_2 transfer function with PI is shown below:

$$OL_2(s) = D_{22}(s) \cdot G_{22}(s) \quad (\text{A.154})$$

$$= \left(K_P + \frac{K_i}{s} \right) \cdot \frac{0.049}{0.37s + 1}$$

By multiplying K_i outside the parenthesis the following OL_2 transfer function is given:

$$OL_2(s) = K_i \cdot \left(\frac{K_P}{K_i} + \frac{1}{s} \right) \cdot \frac{0.049}{0.37s + 1} \quad (\text{A.155})$$

Taking the ratio between K_P/K_i equal to 0.37 then the following OL_2 is given.

$$OL_2(s) = K_i \cdot \left(0.37 + \frac{1}{s} \right) \cdot \frac{0.049}{0.37s + 1} \quad (\text{A.156})$$

In figure A.15 the root locus can be seen for the OL_2 transfer function A.156.

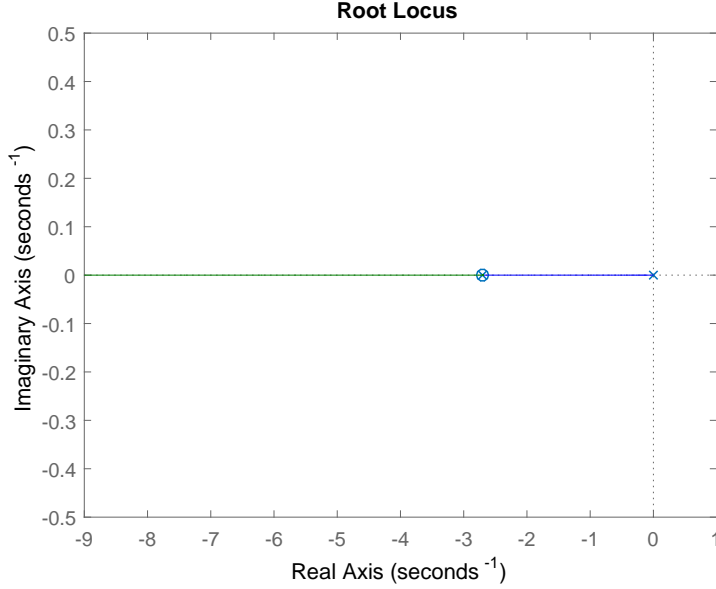


Figure A.15: Root locus of OL_2 transfer function A.156.

It can be seen that the pole and zero in -2.7 cancel each other out and therefore only one pole in zero is left. By reducing equation A.156 the following OL_2 transfer function is given:

$$OL_2(s) = \frac{0.049}{s} \quad (\text{A.157})$$

By increasing K_i the pole in zero will be moved to the left on figure A.15. Which also can be seen in equation A.158

$$\begin{aligned} CL_2(s) &= \frac{OL(s)}{1 + OL(s)} \\ &= \frac{\frac{0.049 \cdot Ki}{s}}{1 + \frac{0.049 \cdot Ki}{s}} \\ &= \frac{0.049 \cdot Ki}{s + 0.049 \cdot Ki} \end{aligned} \quad (\text{A.158})$$

The location where the pole have to be placed to get an rise time of 16.5 seconds is calculated in section 4.4 and is calculated to be -0.133. In figure A.16 the gain can be read.

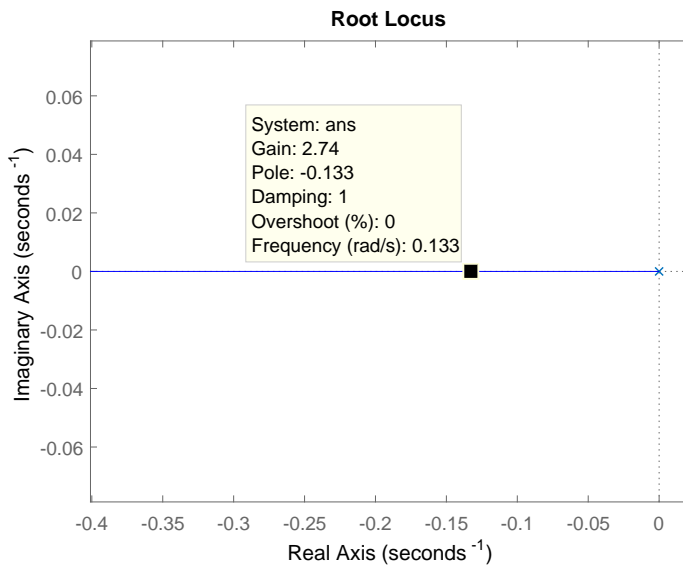


Figure A.16: Root locus for $G_{22}(s)$.

The gain can be read to be 2.74. With the gain known for K_i it will be used to find the controller for the hydraulic model.

$$\begin{aligned}
 CL_2(s) &= \frac{0.049 \cdot K_i}{s + 0.049 \cdot K_i} \\
 &= \frac{0.049 \cdot 2.74}{s + 0.049 \cdot 2.74} \\
 &= \frac{0.134}{s + 0.134}
 \end{aligned} \tag{A.159}$$

To verify that desired rise time is archived a step will be performed on this transfer function. In figure A.17 a step is performed on the $CL_2(s)$ transfer function from equation A.159.

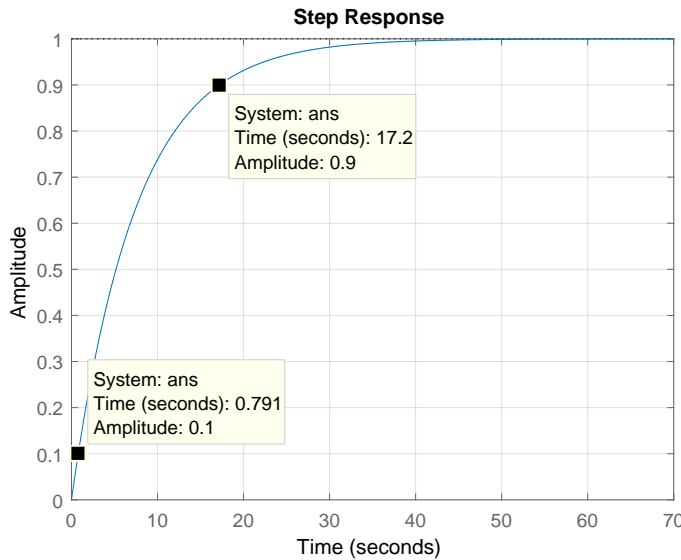


Figure A.17: Step response for $CL(s)$ transfer function A.159.

The rise time can be calculated from the figure.

$$\begin{aligned} tr &= 17.2 - 0.791 \\ &= 16.4 \approx 16.5 \end{aligned} \tag{A.160}$$

The rise time is faster than 16.5 the reason for this could be numbers have been round off. It is still deemed successful because it is a small deviation. In figure A.16 root locus will be used on the CL to see if the pole is placed at the correct location.

It can be seen that the $CL_2(s)$ is stable because the pole is placed in the left half plan and goes towards $-\infty$ when K increases. It can also be seen that the damping is equal to 1, which means that the system have no overshoot. This controller will still be used as it is a small deviation and therefore the controller design $D_{22}(s)$ for $G_{22}(s)$ is deemed successful.

$$D_{22}(s) = (0.37 + \frac{2.74}{s}) \tag{A.161}$$

A.3 Journals

This appendix contain the journals done throughout the report. The purpose is to document the measurement of the different tests.

A.3.1 Interconnection test

Purpose:

The purpose of the journal is to document the test and how the pressure at the end user behave when the velocity of the pumps are changed.

Equipment list:

- The water distribution network at the Dept. of Electronic Systems, Section for Automation and Control. (AAU no. 100911).
- MATLAB
- File: Simulink_for_distribution_network.mdl (CD [MATLAB/Simulink_for_distribution_network.mdl])

Measurement set up

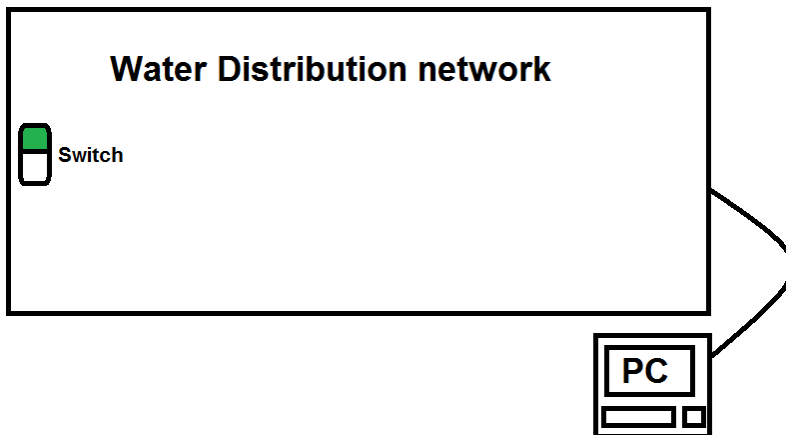


Figure A.18: Setup for the water distribution network.

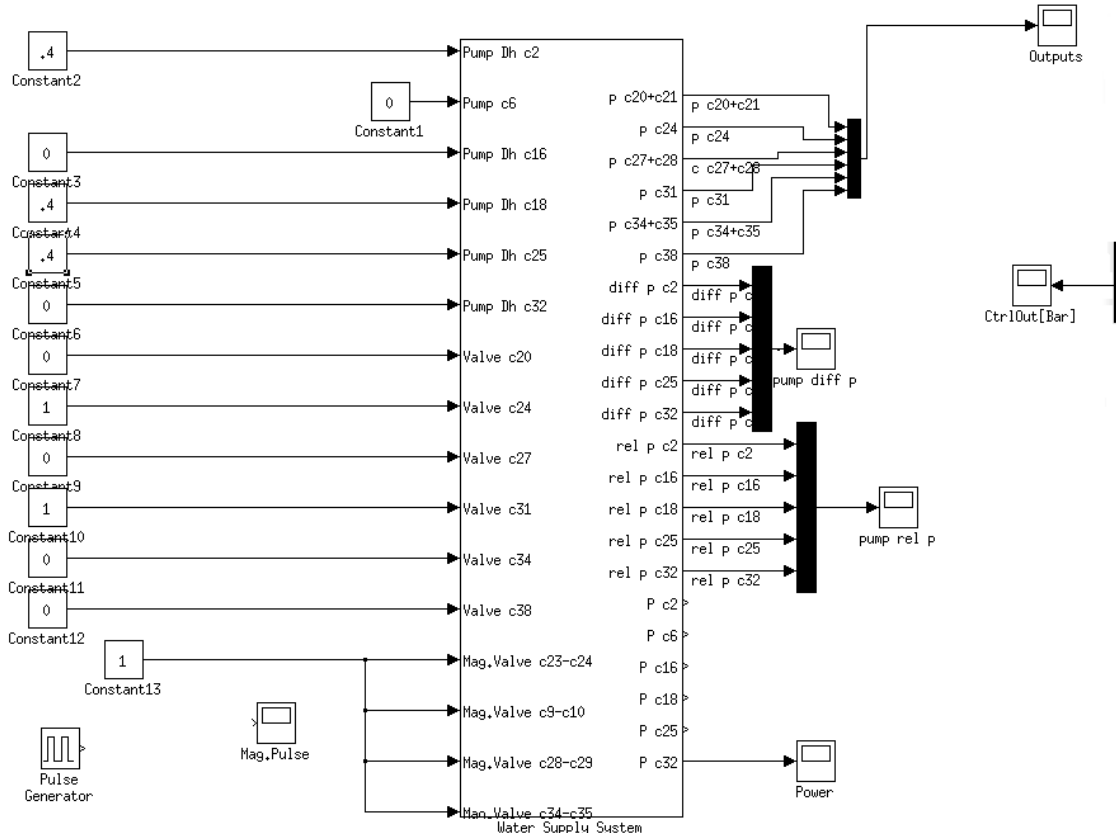


Figure A.19: Simulink.

Procedure:

- Turn on the water distribution network - Press the button on the wall. Green light indicate "on".
- Turn on the Computer next to the water distribution network.
- Start matlab.
- Load file: Simulink_for_distribution_network.mdl into MATLAB. This will start simulink.
- Compile the simulink file by pressing ctrl + b.
- Start the terminal.
 - Go to the folder where the file wss_system is placed inside the the terminal.
 - Write "sudo ./Simulink_for_distribution_network.mdl -tf inf -w"
 - Pres enter and go back to Simulink.
- Start simulating by pressing ctrl + t or go to the simulation button in the top and press "Connect To Target".
- Change the values in Simulink to (This is for the valves C_{24} and C_{31} when they are fully open, to do the same test for C_{20} and C_{27} change the value for constant8 and constant10 to 0 and constant7 and constant9 to 1):
 - Constant2 = 0.4
 - Constant1 = 0
 - Constant3 = 0
 - Constant4 = 0.2
 - Constant5 = 0.2
 - Constant6 = 0
 - Constant7 = 0

- Constant8 = 1
- Constant9 = 0
- Constant10 = 1
- Constant11 = 0
- Constant14 = 0
- Constant13 = 1
- Optional - Open the scope "outputs" to see the pressure output at the valves.
- Start the realtime workshop by pressing the same simulation button and pres "Start Real-Time Code".
- Now the water distribution network is "on".
- Wait 20 seconds.
- Change constant4 to 0.4
- Wait 20 seconds.
- Change constant5 to 0.4
- Wait 20 seconds.
- Turn the system off by pressing simulation and then "Stop Real-Time Code".
- Save the matlab file Simulink_for_distribution_network.mat.
- Used the MATLAB script on CD [MATLAB/Plot_for_c20_and_c27] or [MATLAB/Plot_for_c24_and_c31]

Measurement data:

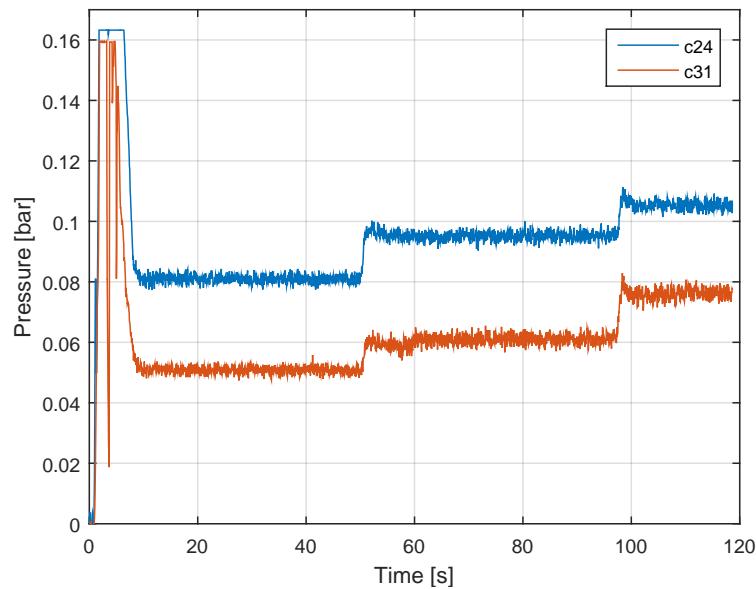
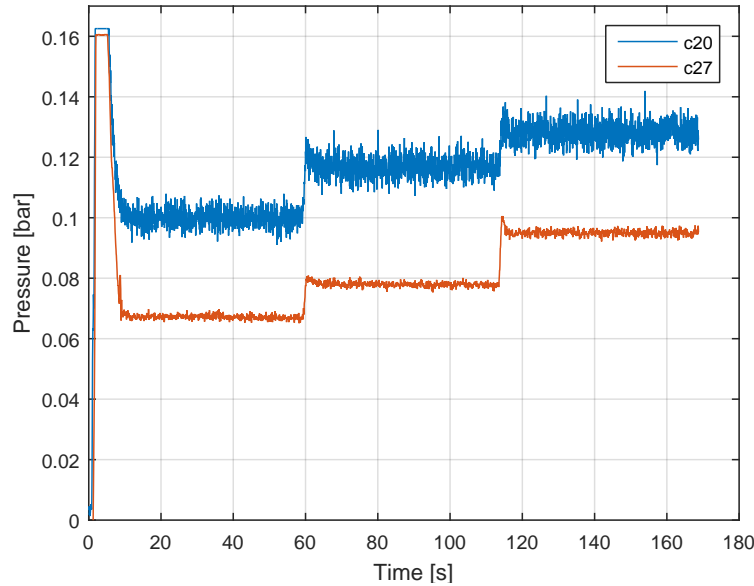


Figure A.20: Test for valve C_{24} and C_{31} .

Figure A.21: Test for valve C_{20} and C_{27} .**Results:**

From figure A.20, it can be seen that the pressure increases in both PMA's, when the pump (C_{18}) is increased in velocity. Furthermore the pressure increases most in the area closest to the pump. The same happens when pump C_{25} is increased in velocity. From figure A.21, the same results is given, the only difference is that the pressure is higher at these valves. The only difference is that the measurement for valve C_{20} variates more than the other measurements.

Source of error:

- Air in the system.
- Equipment tolerance.
- Noise from equipment.
- Ambient noise.

Conclusion:

From this journal, it can be concluded that both pumps cause an increase in pressure, when they are increased in velocity, this result in a pressure increase in both PMA's for each pump. The reason that the pressure is higher at $C_{20}C_{27}$ than $C_{24}C_{31}$ is because that the pipe before the pressure sensor is longer at $C_{24}C_{31}$ than $C_{20}C_{27}$ and therefore there is a pressure difference. The variation that comes from C_{20} could come from air in the pipes and cause this inaccuracy in pressure or it could be noise from the equipment.

A.3.2 Step response

Purpose:

The purpose of the journal is to document how the step response measurement were obtained. The data is used in chapter 2, section 2.8, to approximate the transfer functions for the physical system.

Theory:

Simulink Realtime workshop on the computer, perform a step response on the physical system, by sending signals that changes the parameters of the pumps and valves, which causing a change of the pressure in the system. Sensors measures this change and relay it back to the computer and store it in a file.

Equipment list:

- The water distribution network at the Department of Electronic Systems, Section for Automation and Control (AAU no. 100911).
- MATLAB
- File: Simulink_for_distribution_network.mdl (CD [MATLAB/Simulink_for_distribution_network.mdl])

Measurement set up

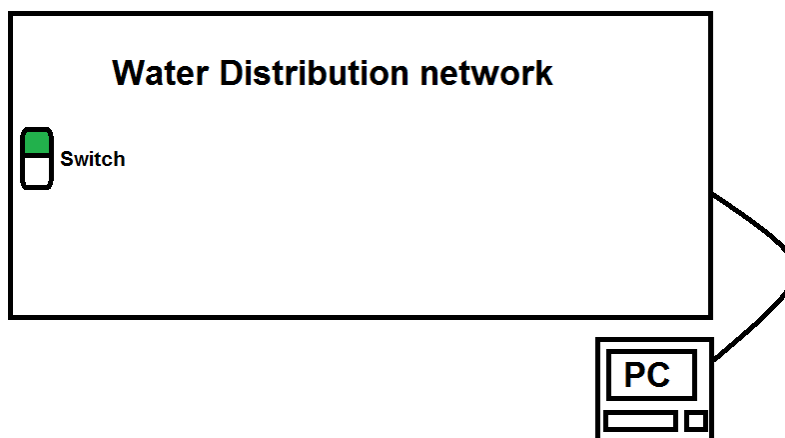


Figure A.22: Setup for the water distribution network.

Procedure:

- Turn on the water distribution network - Press the button on the wall. Green light indicate "on".
- Turn on the Computer next to the water distribution network.
- Start matlab.
- Load file: Simulink_for_distribution_network.mdl into MATLAB. This will start simulink.
- Compile the simulink file by pressing ctrl + b.
- Start the terminal.
 - Go to the folder where the file wss_system is placed inside the the terminal.
 - Write "sudo ./Simulink_for_distribution_network.mdl -tf inf -w"
 - Pres enter and go back to simulink.
- Connect to the physical system by pressing ctrl + t or go to the simulation button in the top and press "Connect To Target".

- Optional - Open the scope "outputs" to see the pressure output at the valves.
 - Start the realtime workshop by pressing the same simulation button and pres "Start Real-Time Code".
 - Now the water distribution network is "on".
 - The step will start after 40 seconds, starting from the operation point at 0.5 to the final value of 0.6.
 - Let it run for an additional 30 seconds after the step has started to ensure steady state have been achieved.
 - Turn the system off by pressing simulation and then "Stop Real-Time Code".
 - Save the data set as a .mat file.

The setup on the host computer can be seen on figure A.23.

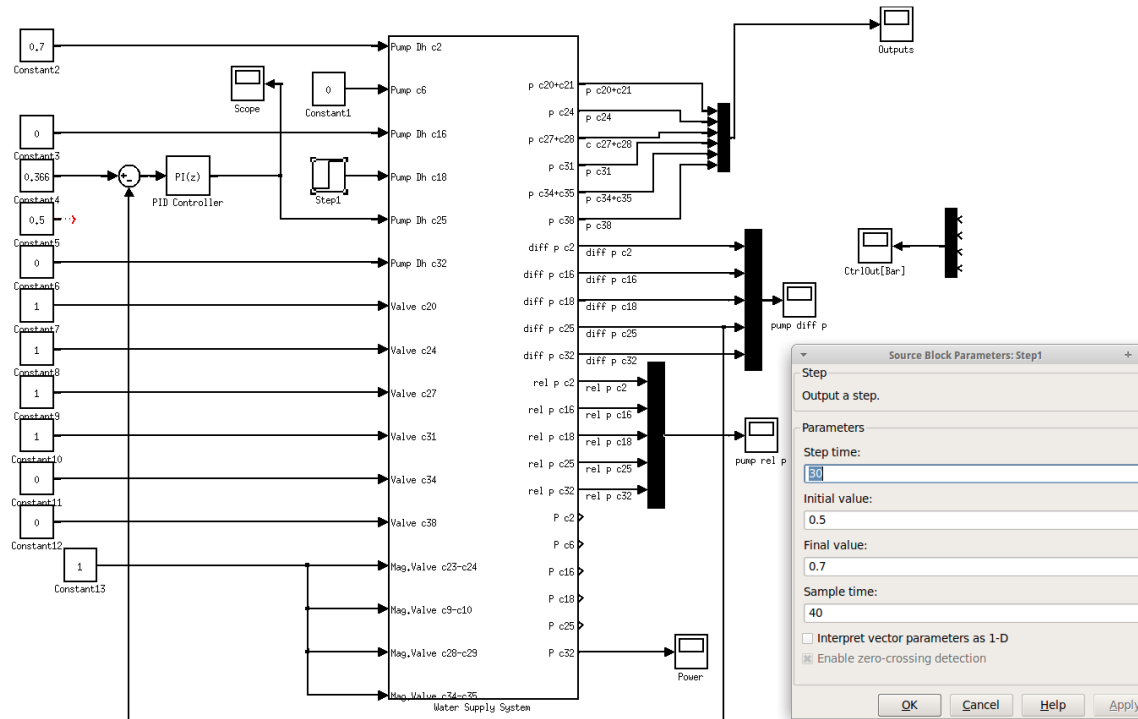


Figure A.23: Setup on the host computer, where a step is performed on one pump, while controlling the other pump to keep it in the operating point.

A integral controller is controlling the other pump to keep the differential pressure across it in steady state while doing the test. The difference pressure is measured on figure A.24.

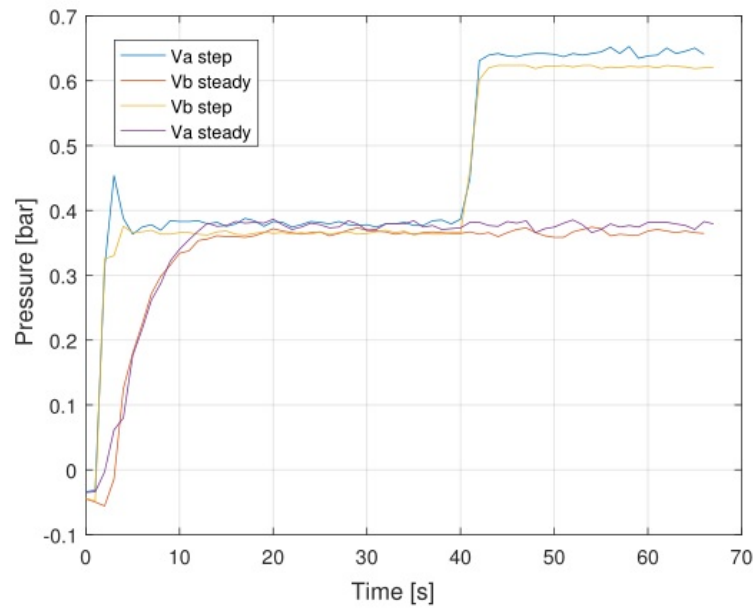


Figure A.24: The differential pressure across the pumps while doing a step on each of the pumps.

Measurement data:

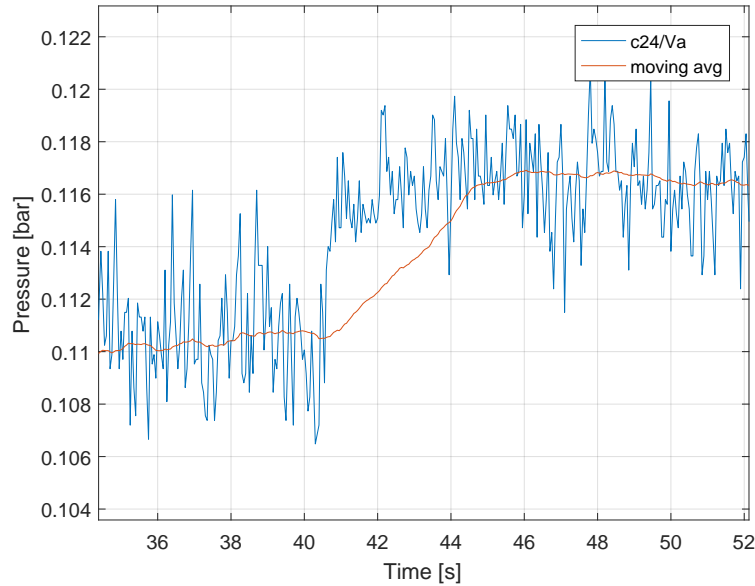


Figure A.25: Step response for G_{11} (C_{24}), were step is on C_{18} .

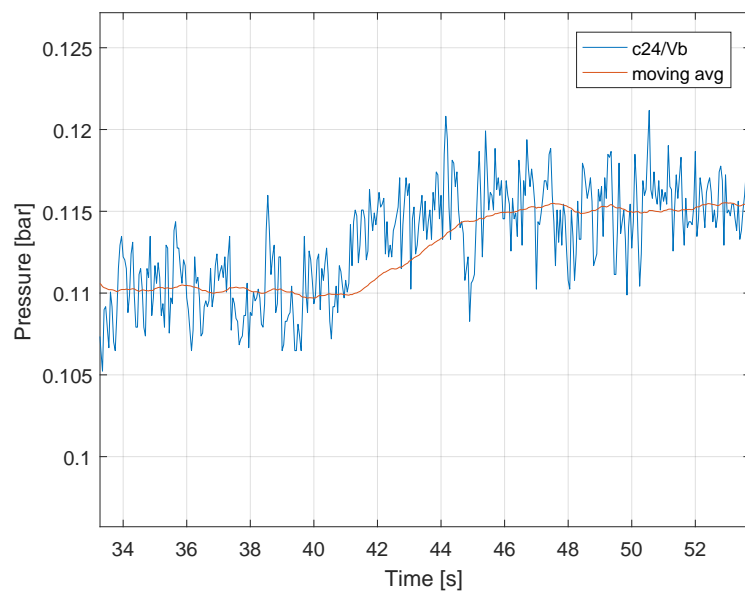


Figure A.26: Step response for G_{12} (C_{24}), were step is on C_{25} .

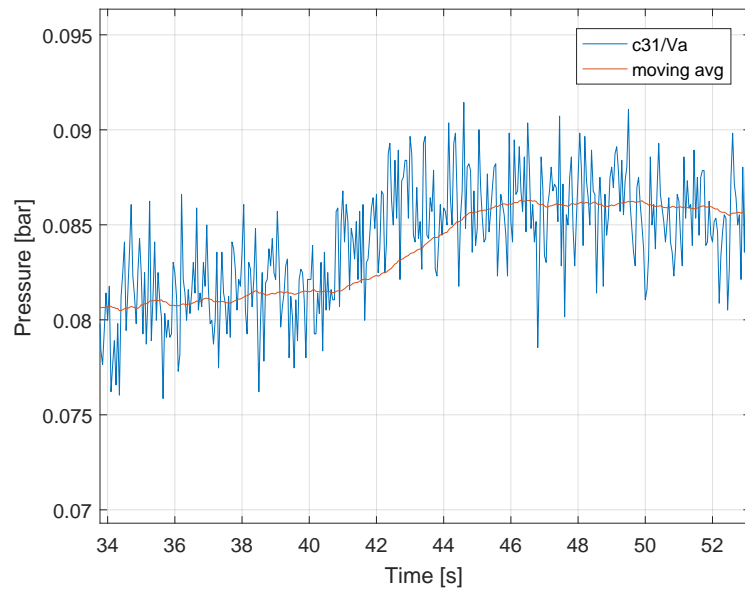


Figure A.27: Step response for G_{21} (C_{31}) where step is on C_{18} .

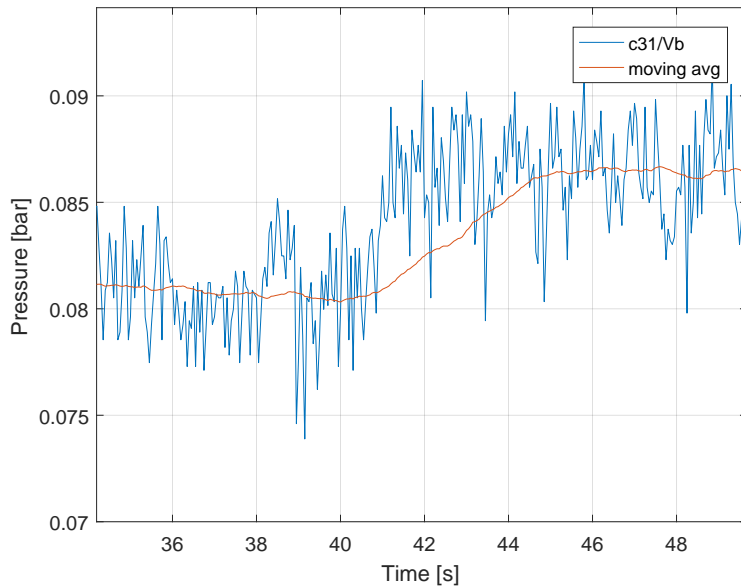


Figure A.28: Step response for G_{22} (C_{31}), were step is on C_{25} .

Results:

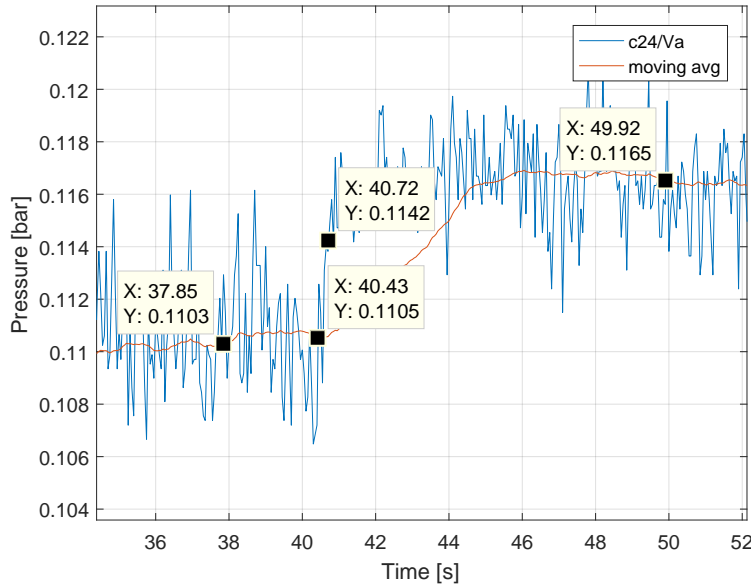


Figure A.29: Step response for G_{11} , with data set.

Steps to find the first order transfer function for G_{11} .

Calculate the range between the start value of the step to the steady state.

$$\begin{aligned} \text{range11} &= 0.1165 - 0.1103 \\ &= 0.0062 \end{aligned} \quad [\cdot] \quad (\text{A.162})$$

Take 63 % of the range to find the time constant τ .

$$\begin{aligned} \text{percent63} &= 0.63 \cdot \text{range11} \\ &= 0.0039 \end{aligned} \quad [\cdot] \quad (\text{A.163})$$

$$\begin{aligned} \text{Time } 63\% &= \text{percent63} + 0.1103 \\ &= 0.01142 \end{aligned} \quad [\cdot] \quad (\text{A.164})$$

$$\begin{aligned} \tau_{11} &= 40.72 - 40.33 \\ &= 0.39 \end{aligned} \quad [\text{s}] \quad (\text{A.165})$$

To find K the increment of the output is divide by increment of the input which is shown in the following equation:

$$K_{11} = \frac{\text{Output increment}}{\text{Input increment}} \quad [\cdot] \quad (\text{A.166})$$

$$\begin{aligned} &= \frac{0.0062}{0.1184} \\ &= 0.0524 \end{aligned} \quad (\text{A.167})$$

Now the first order transfer function can be deduced.

$$\begin{aligned} G_{11} &= \frac{K_{11}}{\tau_{11} \cdot s + 1} \\ &= \frac{0.05236}{0.39 \cdot s + 1} \end{aligned} \quad [\cdot] \quad (\text{A.168})$$

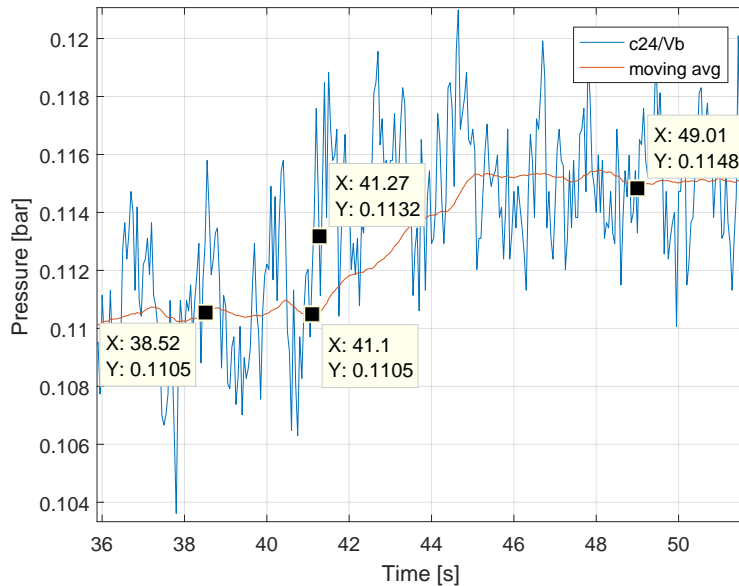


Figure A.30: Step response for G_{12} , with data set.

$$\begin{aligned} \text{range12} &= 0.1148 - 0.1105 \\ &= 0.0043 \end{aligned} \quad [\cdot] \quad (\text{A.169})$$

$$\begin{aligned} \text{percent63} &= 0.63 \cdot \text{range12} \\ &= 0.0027 \end{aligned} \quad [\cdot] \quad (\text{A.170})$$

$$\begin{aligned} \text{Time } 63 \% &= \text{percent63} + 0.1105 \\ &= 0.01132 \end{aligned} \quad [\cdot] \quad (\text{A.171})$$

$$\begin{aligned} \tau_{12} &= 41.24 - 41 \\ &= 0.24 \end{aligned} \quad [\text{s}] \quad (\text{A.172})$$

$$\begin{aligned} K_{12} &= \frac{\text{Output increment}}{\text{Input increment}} \\ &= \frac{0.0043}{0.1153} \\ &= 0.0373 \end{aligned} \quad [\cdot] \quad (\text{A.173})$$

$$\begin{aligned} G_{12} &= \frac{K_{12}}{\tau_{12} \cdot s + 1} \\ &= \frac{0.0373}{0.24 \cdot s + 1} \end{aligned} \quad [\cdot] \quad (\text{A.174})$$

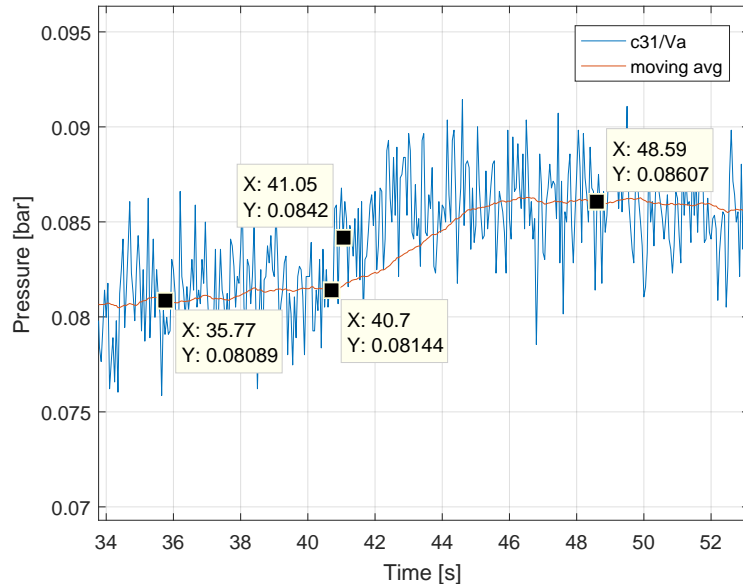


Figure A.31: Step response for G_{21} , with data set.

$$\begin{aligned} \text{range21} &= 0.08607 - 0.08089 \\ &= 0.0052 \end{aligned} \quad [\cdot] \quad (\text{A.175})$$

$$\begin{aligned} \text{percent63} &= 0.63 \cdot \text{range21} \\ &= 0.0033 \end{aligned} \quad [\cdot] \quad (\text{A.176})$$

$$\begin{aligned} \text{Time } 63 \% &= \text{percent63} + 0.08089 \\ &= 0.0842 \end{aligned} \quad [\cdot] \quad (\text{A.177})$$

$$\begin{aligned}\tau_{21} &= 41.05 - 40.7 \\ &= 0.35\end{aligned}\quad [\text{s}] \quad (\text{A.178})$$

$$\begin{aligned}K &= \frac{\text{Output increment}}{\text{Input increment}} \\ &= \frac{0.0052}{0.1184} \\ &= 0.0437\end{aligned}\quad [\cdot] \quad (\text{A.179})$$

$$\begin{aligned}G_{21} &= \frac{K_{21}}{\tau_{21} \cdot s + 1} \\ &= \frac{0.0437}{0.35 \cdot s + 1}\end{aligned}\quad [\cdot] \quad (\text{A.180})$$

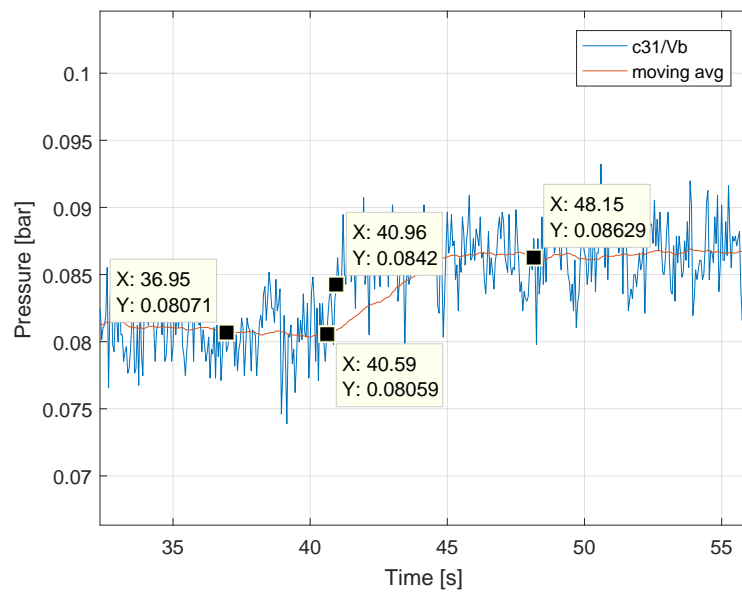


Figure A.32: Step response for G_{22} , with data set.

$$\begin{aligned}\text{range22} &= 0.08629 - 0.08071 \\ &= 0.0056\end{aligned}\quad [\cdot] \quad (\text{A.181})$$

$$\begin{aligned}\text{percent63} &= 0.63 \cdot \text{range22} \\ &= 0.0035\end{aligned}\quad [\cdot] \quad (\text{A.182})$$

$$\begin{aligned}\text{Time 63 \%} &= \text{percent63} + 0.08071 \\ &= 0.0842\end{aligned}\quad [\cdot] \quad (\text{A.183})$$

$$\begin{aligned}\tau_{22} &= 40.96 - 40.59 \\ &= 0.37\end{aligned}\quad [\text{s}] \quad (\text{A.184})$$

$$\begin{aligned}
 K_{22} &= \frac{\text{Output increment}}{\text{Input increment}} & [\cdot] & \quad (\text{A.185}) \\
 &= \frac{0.0056}{0.1153} \\
 &= 0.0484
 \end{aligned}$$

$$\begin{aligned}
 G_{22} &= \frac{K_{22}}{\tau_{22} \cdot s + 1} & [\cdot] & \quad (\text{A.186}) \\
 &= \frac{0.0484}{0.37 \cdot s + 1}
 \end{aligned}$$

$$G_1(s) = \begin{pmatrix} \frac{0.0524}{0.39 \cdot s + 1} & \frac{0.03729}{0.24 \cdot s + 1} \\ \frac{0.04375}{0.35 \cdot s + 1} & \frac{0.0484}{0.37 \cdot s + 1} \end{pmatrix} & [\cdot] & \quad (\text{A.187})$$

Source of error:

- Air in the system.
- Equipment tolerance.
- Noise from equipment.
- Ambient noise.

Conclusion:

In this journal four transfer functions was deduced from measured data from step responses performed on the pumps.

A.3.3 The water flow

Purpose:

The purpose of the journal is to document the test. Furthermore to find the flow in the distribution system by using the pressure sensors.

Equipment list:

- The water distribution network at the Dept. of Electronic Systems, Section for Automation and Control. (AAU no. 100911).
- MATLAB
- File: Simulink_for_distribution_network.mdl (CD [MATLAB/Simulink_for_distribution_network.mdl])

Measurement set up

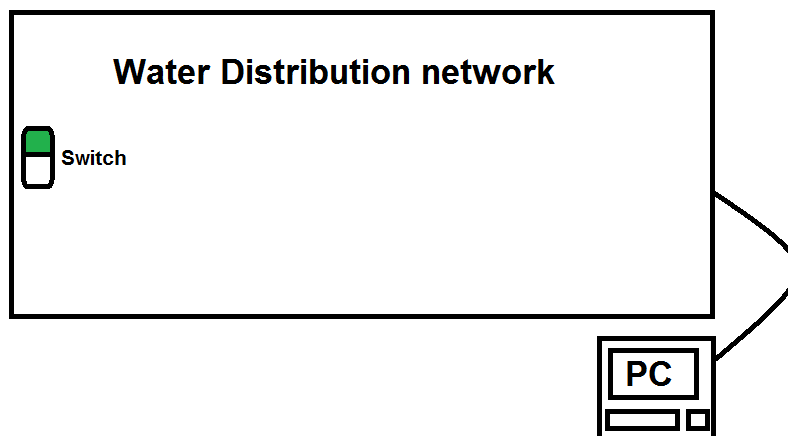


Figure A.33: Setup for the water distribution network.

Procedure:

- Turn on the water distribution network - Press the button on the wall. Green light indicate "on".
- Turn on the Computer next to the water distribution network.
- Start matlab.
- Load file: Simulink_for_distribution_network.mdl into MATLAB. This will start simulink.
- Compile the simulink file by pressing ctrl + b.
- Start the terminal.
 - Go to the folder where the file wss_system is placed inside the the terminal.
 - Write "sudo ./Simulink_for_distribution_network.mdl -tf inf -w"
 - Pres enter and go back to simulink.
- Start simulating by pressing ctrl + t or go to the simulation button in the top and press "Connect To Target".
- Change the values in simulink to:
 - Constant2 = 0.7
 - Constant1 = 0
 - Constant3 = 0
 - Constant4 = 0.5
 - Constant5 = 0.5
 - Constant6 = 0
 - Constant7 = 1

- Constant8 = 1
 - Constant9 = 1
 - Constant10 = 1
 - Constant11 = 0
 - Constant14 = 0
 - Constant13 = 1
- Optional - Open the scope "outputs" to see the pressure output at the valves.
 - Start the realtime workshop by pressing the same simulation button and pres "Start Real-Time Code".
 - Now the water distribution network is "on".
 - Wait 60 seconds.
 - Turn the system off by pressing simulation and then "Stop Real-Time Code".
 - Save the matlab file Simulink_for_distribution_network.mat.
 - Used the matlab script on CD [MATLAB/Water_flow_test_all_open.mat]

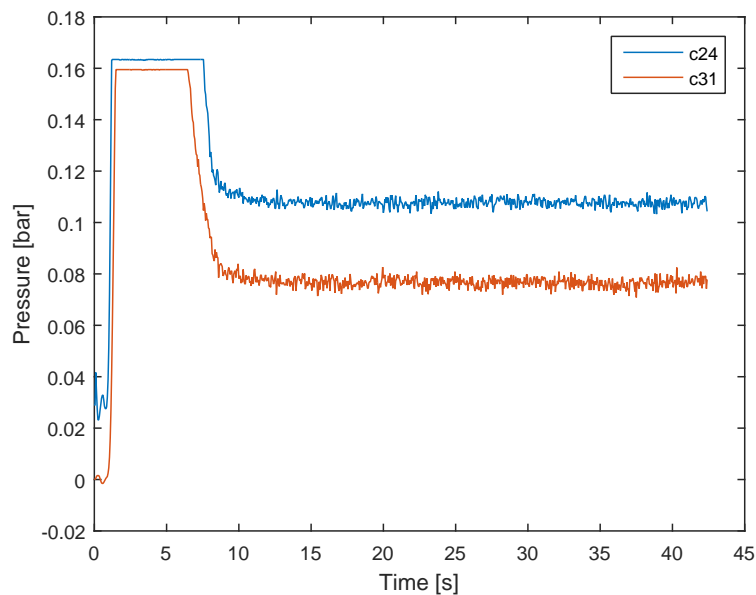
Measurement data:

Figure A.34: Pressure measurement for valve C_{24} and C_{31} .

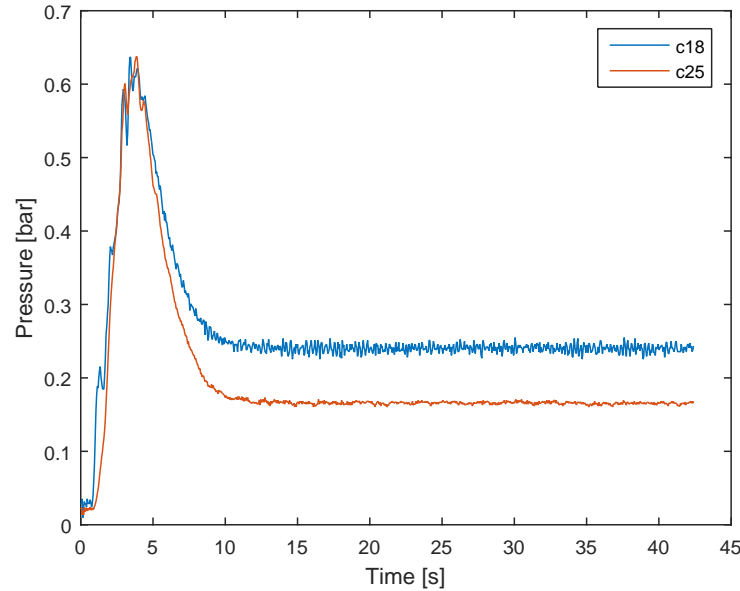


Figure A.35: Pressure measurement for valve C_{18} and C_{25} .

Results:

The results shows the pressure over time for valve C_{24} and C_{31} and the pressure at pumps C_{18} and C_{25} . On figure A.36 the average pressure for C_{24} and C_{31} can be seen.

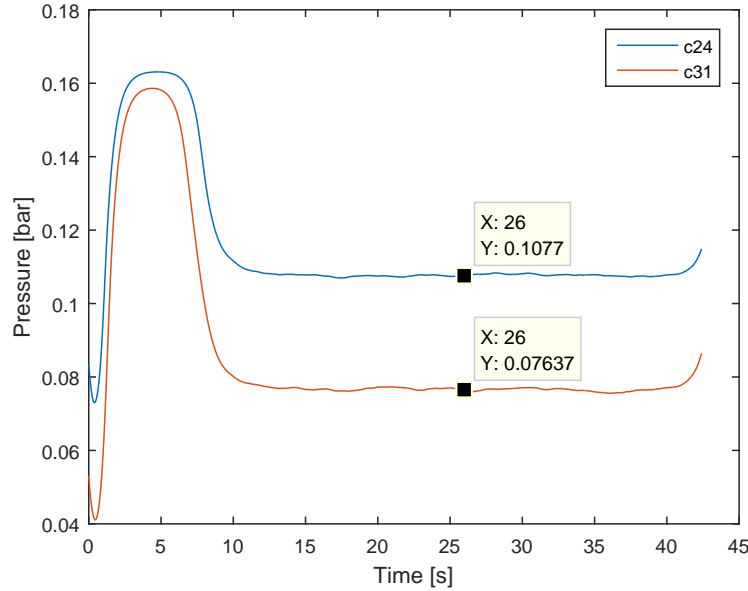


Figure A.36: Filtered MATLAB plot with the running average pressure over time for valve C_{24} and C_{31} .

A point have been taking out and will be used to calculate the flow in the distribution system.

On figure A.37 the average pressure for C_{18} and C_{25} can be seen.

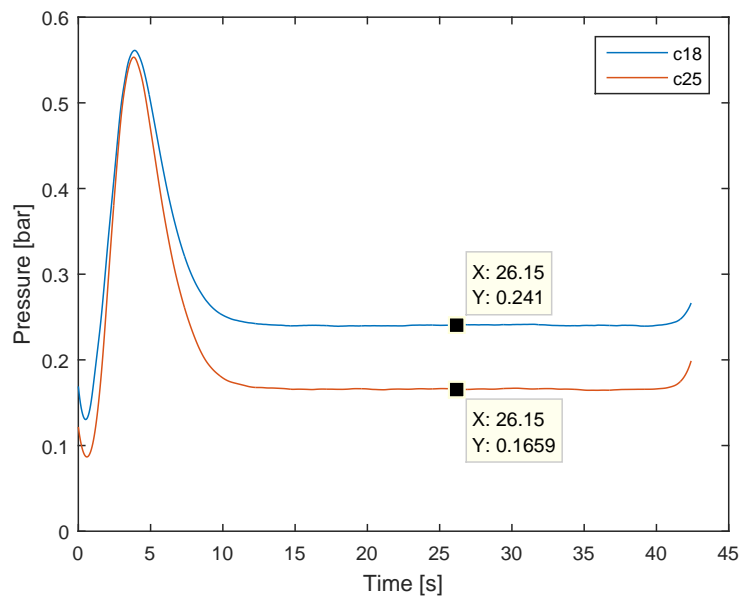


Figure A.37: Filtered MATLAB plot with the running average pressure over time at the pumps C_{18} and C_{25} .

A point have been taking out and will be used to calculate the flow in the distribution system.

Source of error:

- Air in the pipes can cause the measurements to be incorrect.
- Air in the system.
- Equipment tolerance.
- Noise from equipment.
- Ambient noise.

Conclusion:

The purpose of the journal has been fulfilled. The pressure measurements have been done and will be used to calculate the flow in the distribution system.

A.3.4 Relation between differential pressure and velocity

Purpose:

The purpose of the journal is to document how the measurement of the relation between the differential pressure and the velocity for the two pumps *c18* and *c25*, were obtained. The data is used in section 2.3. Furthermore it document the similar performance of the two pumps.

Theory:

The two pumps *c18* and *c25* changes the differential pressure in the system based on a velocity ω . Changing the velocity is done by a constant going from 0 to 1, this correspond to a change in the differential pressure. To determine the relation between the differential pressure and the velocity for the pump *c18*, the pump *c25* is kept at steady state by applying a constant. The constant for the pump *c18* is incremental increased and measured. If the measured data for each pump is consistent the pumps can be considered to have similar performance.

Equipment list:

- The water distribution network at the Department of Electronic Systems, Section for Automation and Control (AAU no. 100911).
- MATLAB
- File: speed_test.mdl (CD [MATLAB/speed_test.mdl])

Measurement set up

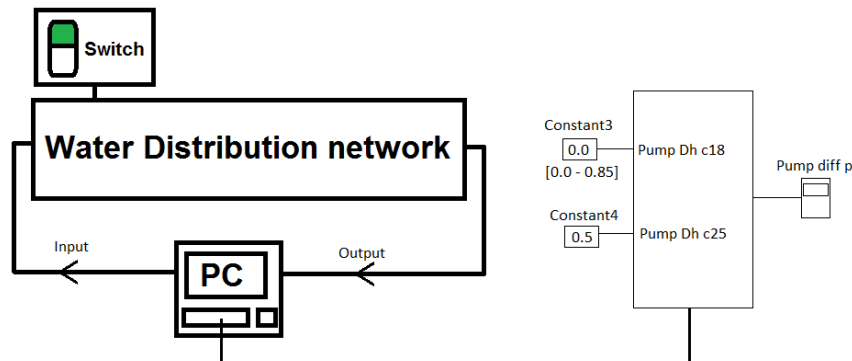


Figure A.38: Setup for the measurement performed on the water distribution network.

The setup for Simulink can be seen on figure A.39, the pump kept in steady state have a constant of 0.5.

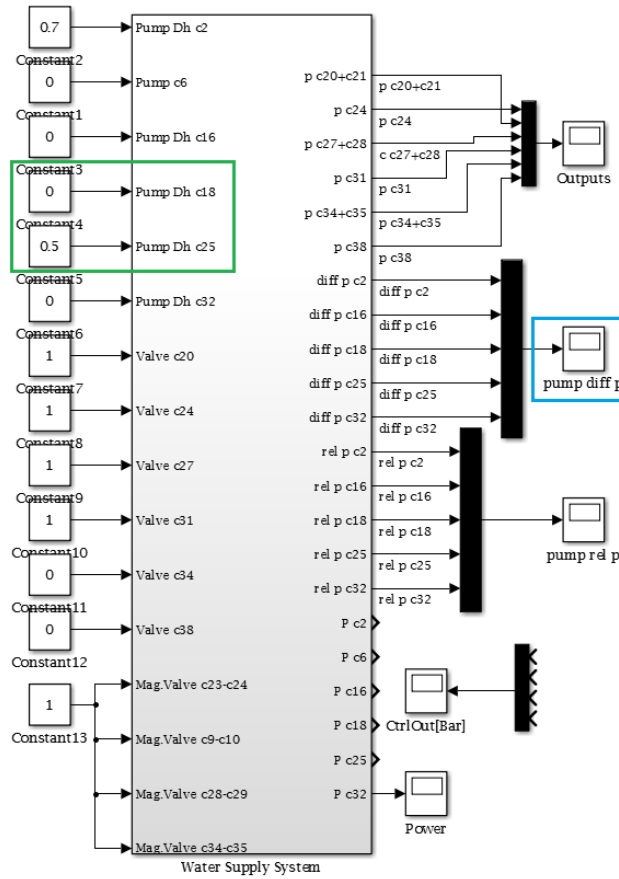


Figure A.39: Simulink setup, were constant 3 and 4 controls the velocity of the pumps $c18$ and $c25$ (green) and the differential pressure is measured on the scope (blue).

Procedure:

- Turn on the Water Distribution network - Button on the wall.
- Turn on the PC next to the Water Distribution network.
- Start MATLAB.
- Load file: speed_test.mdl into MATLAB. This will start Simulink.
- Compile the Simulink file by pressing **ctrl + b**.
- Start the terminal.
 - Go to the folder where the mdl file is placed inside the the terminal.
 - Write "sudo ./speed_test.mdl -tf inf -w"
 - Pres enter and go back to simulink.
- Start simulating by pressing **ctrl + t** or go to the simulation button in the top and press "Connect To Target".
- Start the Realtime workshop by pressing the same simulation button and pres "Start Real-Time Code".
- Let system run for 20 second, then increment constant 3 by 0.05 (see figure A.39).
- Repeat previous step until constant 3 is 0.85. Optionally it can be separated into two measurement, 0 to 0.45 and 0.45 to 0.85.
- Turn the system off by pressing simulation and then "Stop Real-Time Code".
- Data set is saved as speed_test.mat file.
- Swap $c18$ and $c25$, then redo the procedures

Measurement data:

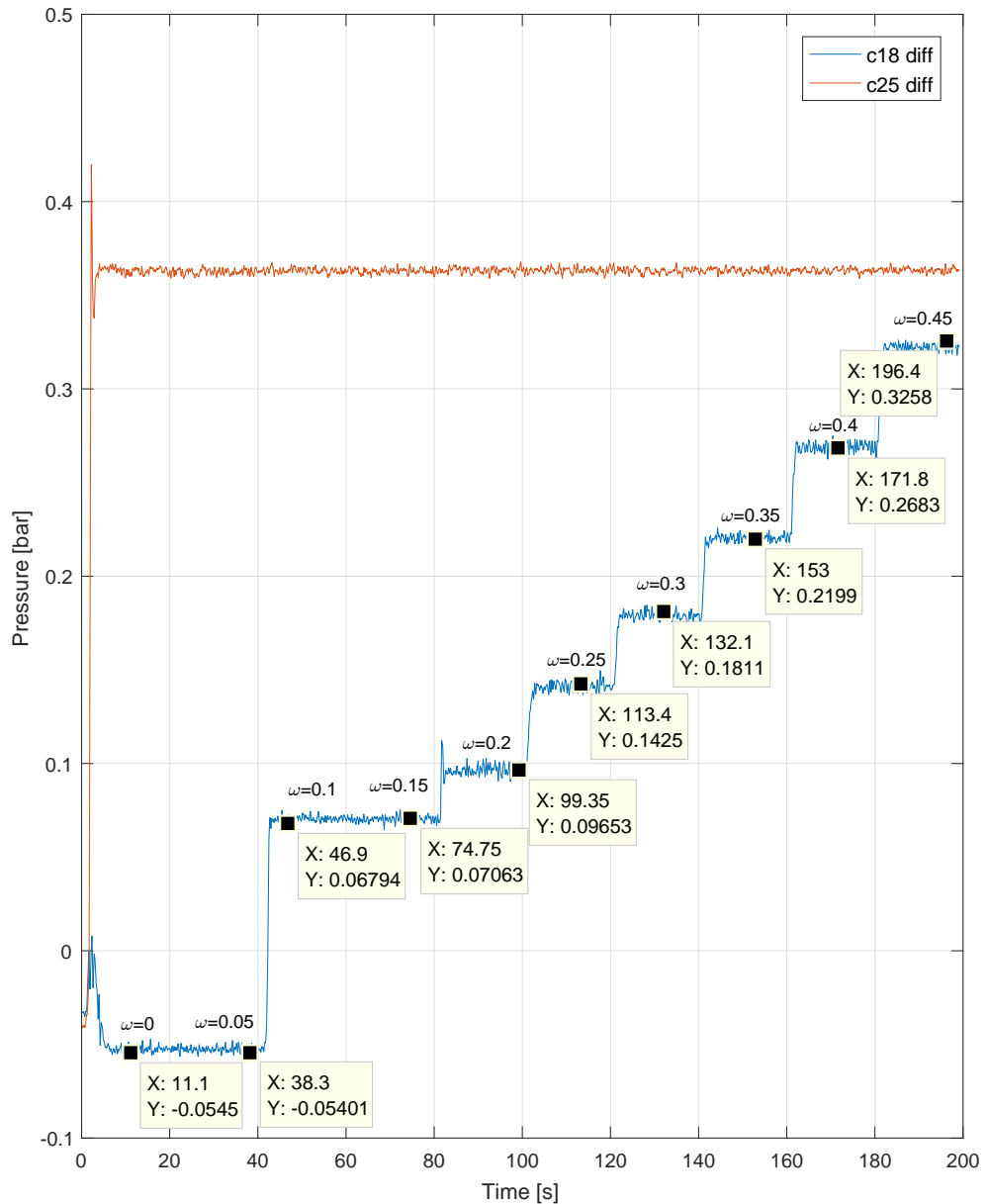


Figure A.40: Plot of measured pressure over time, were $c25$ is held in steady state and $c18$ is increment by 0.05 every 20 seconds, from 0 to 0.45.

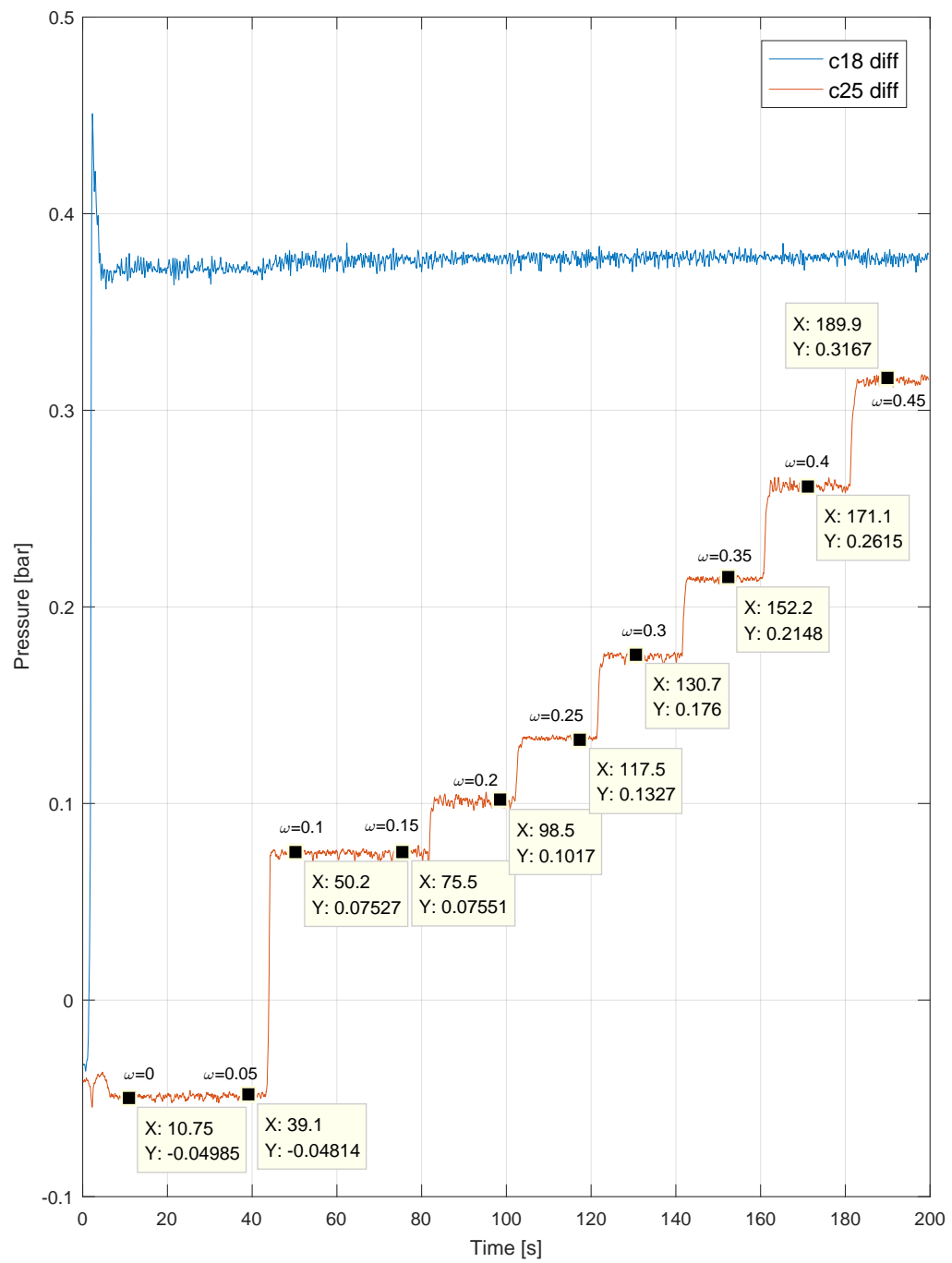


Figure A.41: Plot of measured pressure over time, were $c18$ is held in steady state and $c25$ is increment by 0.05 every 20 seconds, from 0 to 0.45.

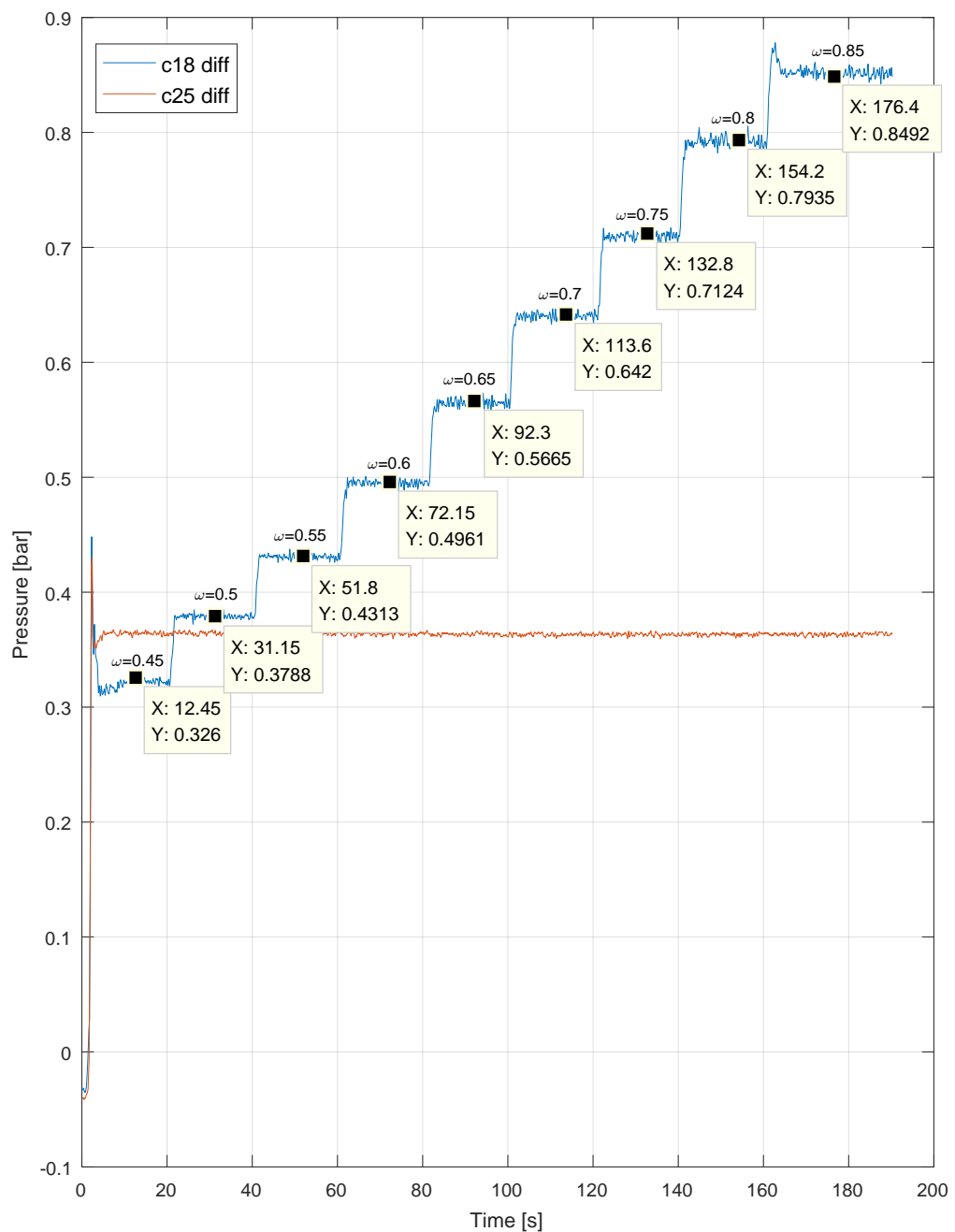


Figure A.42: Plot of measured pressure over time, were *c25* is held in steady state and *c18* is increment by 0.05 every 20 seconds, from 0.45 to 0.85.

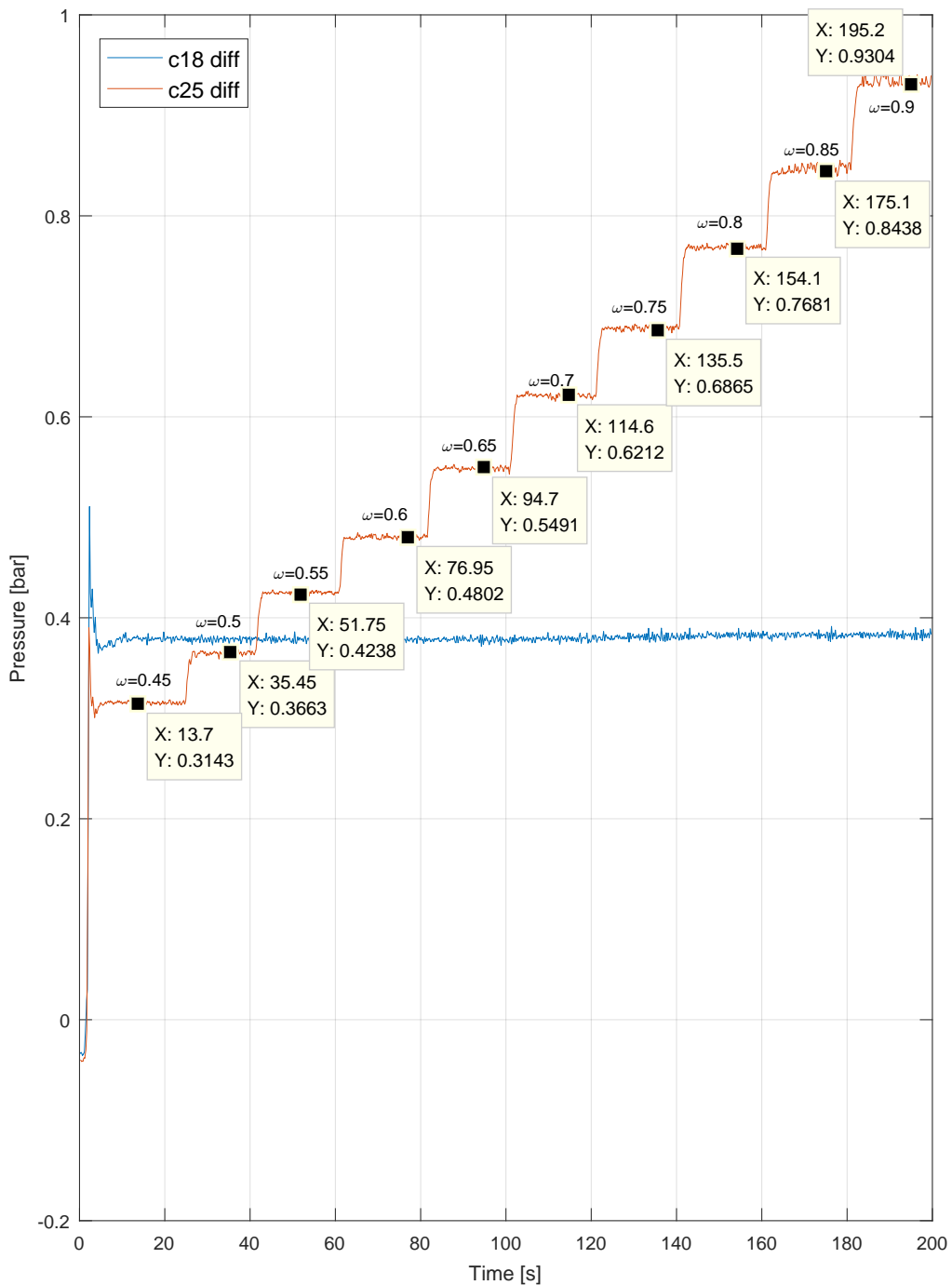


Figure A.43: Plot of measured pressure over time, were *c18* is held in steady state and *c25* is increment by 0.05 every 20 seconds, from 0.45 to 0.90.

Results:

Both pumps have a region of hysteresis, for velocity between 0 and 0.2 as seen on figure A.40 and A.41. The graphs follows relative close for each incrementation with a maximum difference of approximately 0.01 bar. The graphs in A.42 and A.43 deviated more, with upto approximately 0.03 bar. Generally both pumps is considered to perform close to identical, which is expected as they are of the same type.

Source of error:

- Air in the system.
- Equipment tolerance.
- Noise from equipment.
- Ambient noise.

Conclusion:

From this journal it can be concluded that the measurement for the relations between the differential pressure and the velocity for each of the pumps were obtained and the similarity in performance were verified.

A.3.5 Step response with different gains for pump

Purpose:

The purpose of the journal is to document how the measurement of different gains affects the pump *c18* response, were obtained. The data is used in section 4.2.

Theory:

An integrator multiplied a gain K and the pump model, is implemented in Simulink with a step. The measured step response from difference gain is stored and plotted together.

Equipment list:

- The water distribution network at the Department of Electronic Systems, Section for Automation and Control (AAU no. 100911).
- MATLAB
- File: gain_test.mdl (CD [MATLAB/gain_test.mdl])

Measurement set up

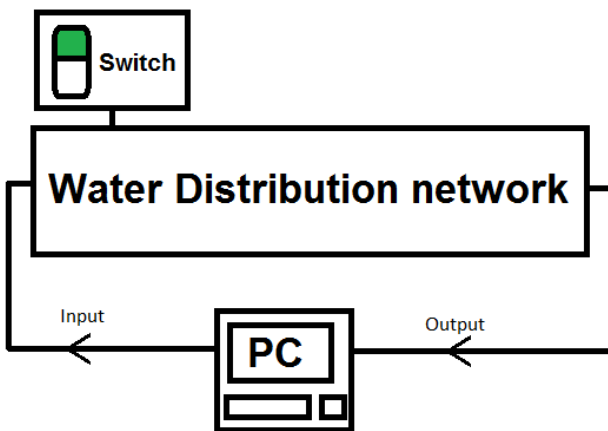


Figure A.44: Setup for the measurement performed on the water distribution network.

The setup for Simulink can be seen on figure A.45, the pump kept in steady state have a constant of 0.5. The step start at 40 seconds from steady state 0.377 to 0.5.

List of gain K to test:

1. Gain K = 1.
2. Gain K = 0.772.
3. Gain K = 0.643.
4. Gain K = 0.551.
5. Gain K = 0.482.
6. Gain K = 0.429.
7. Gain K = 0.386.

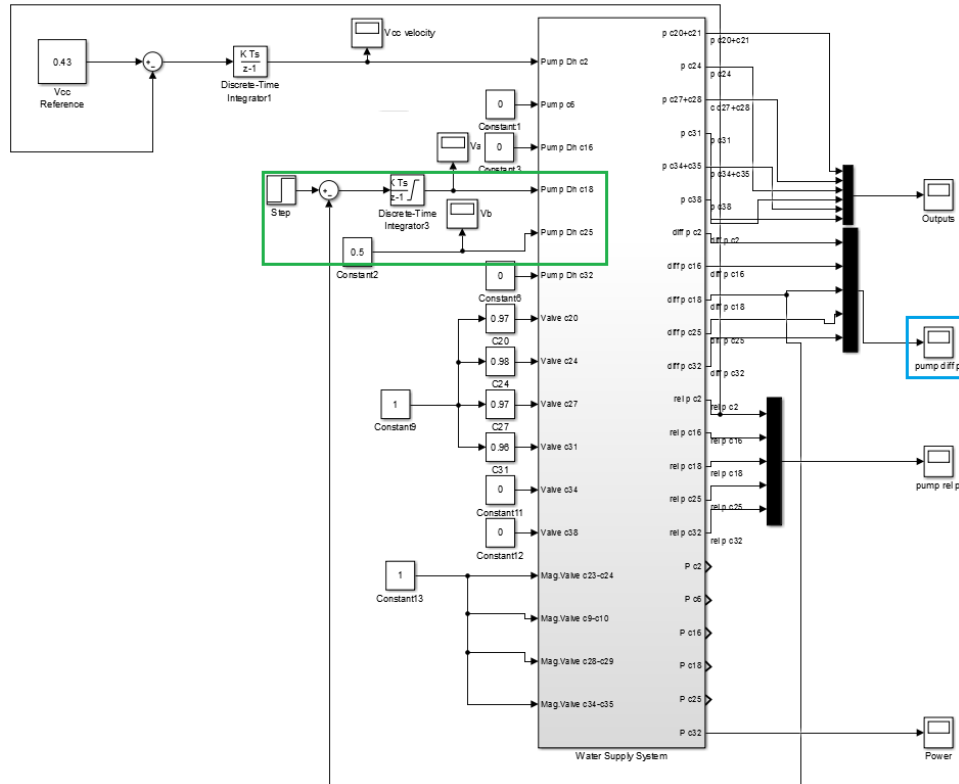


Figure A.45: Simulink setup, were a step is preformed on $c18$, while $c25$ is kept in steady state (green) and the differential pressure is measured on the scope (blue).

Procedure:

- Turn on the Water Distribution network - Button on the wall.
- Turn on the PC next to the Water Distribution network.
- Start MATLAB.
- Load file: gain_test.mdl into MATLAB. This will start Simulink.
- Compile the Simulink file by pressing **ctrl + b**.
- Start the terminal.
 - Go to the folder where the mdl file is placed inside the the terminal.
 - Write "sudo ./gain_test.mdl -tf inf -w"
 - Pres enter and go back to simulink.
- Start simulating by pressing **ctrl + t** or go to the simulation button in the top and press "Connect To Target".
- Start the Realtime workshop by pressing the same simulation button and pres "Start Real-Time Code".
- Let system run for 70 second.
- Turn the system off by pressing simulation and then "Stop Real-Time Code".
- Data set is saved as gain[K]_test.mat file.
- Enter a new gain K in the integrator, then redo the procedures until all gain K have been measured.

Measurement data:

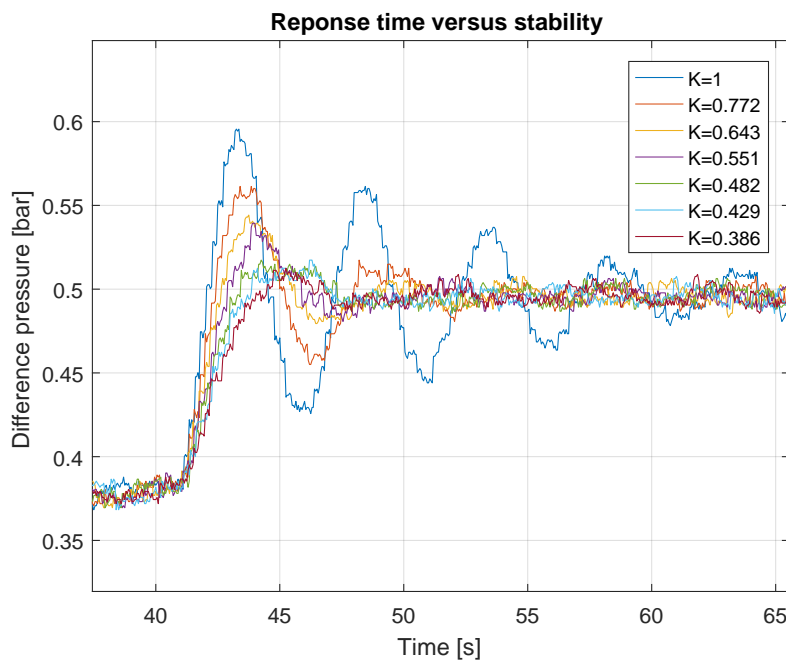


Figure A.46: Response time for gains of K , where a greater gain K give faster response time, but also longer settling time and larger overshoot. Plot is of all measured gains of K .

Results:

The measured data for all gains of K plotted together in figure A.46. It can be seen that when the gain is increased, the step response have larger overshoot and starts to oscillate, which increase the settling time. This is especially true for the gains 1, 0.772 and 0.643, were the last gains have a overshoot for which gain 0.482, 0.429 and 0.386 have similar overshoot.

Source of error:

- Dynamic in the pumps.
- Air in the system.
- Equipment tolerance.
- Noise from equipment.
- Ambient noise.

Conclusion:

From this journal it can be concluded that the measurement of the difference gains step response were obtained.

A.3.6 Test of steady state error

Purpose:

The purpose of the journal is to document how the steady state measurement were obtained. The data is used in chapter 6, section 6.1, to measure if the steady state of the output P2 and P4 is in between the steady state error requirement at $\pm 5\%$.

Theory:

Simulink Realtime workshop on the computer connected to the physical system, which are sending a reference signal into the designed control system and out to the physical system, which causing a change of parameters in the system. Sensors measures the output of P2 and P4 and relay it back to the computer and store it in a file.

Equipment list:

- The water distribution network at the Department of Electronic Systems, Section for Automation and Control (AAU no. 100911).
- MATLAB
- File: analyse_system.mdl (CD [MATLAB/analyse_system.mdl])

Measurement set up

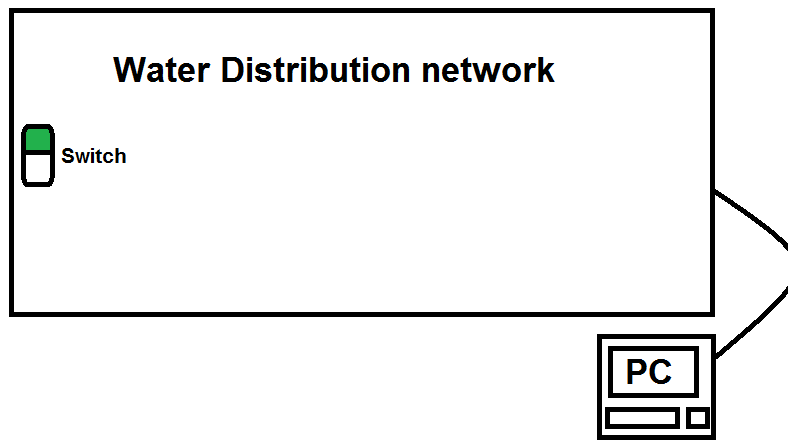


Figure A.47: Setup for the water distribution network.

Procedure:

- Turn on the water distribution network - Press the button on the wall. Green light indicate "on".
- Turn on the Computer next to the water distribution network.
- Start matlab.
- Load file: analyse_system.mdl into MATLAB. This will start simulink.
- Compile the simulink file by pressing **ctrl + b**.
- Start the terminal.
 - Go to the folder where the file wss_system is placed inside the the terminal.
 - Write "**sudo ./analyse_system.mdl -tf inf -w**"
 - Pres enter and go back to simulink.
- Connect to the physical system by pressing **ctrl + t** or go to the simulation button in the top and press "Connect To Target".
- Optional - Open the scope "outputs" to see the pressure output at the valves.
- Start the realtime workshop by pressing the same simulation button and pres "Start Real-Time Code".

- Now the water distribution network is "on".
- The system will startup at the design control system will regulate the outputs to their respective operation points.
- Turn the system off by pressing simulation and then "Stop Real-Time Code".
- Save the data set as a .mat file.

The setup on the host computer can be seen on figure A.48.

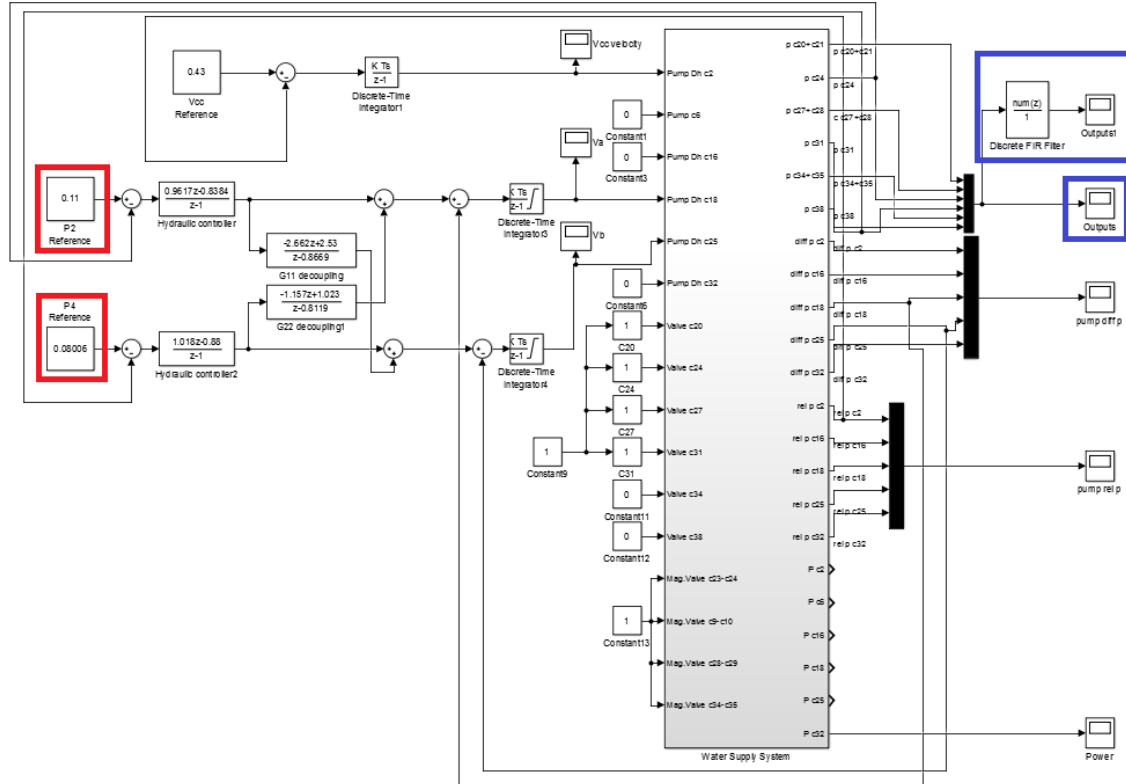


Figure A.48: Setup on the host computer, where the system regulating to keep the outputs P2 and P4 in steady state at the operation points.

The red boxes on figure A.48, is the reference for the output P2 and P4, where the output scopes is marked with blue boxes, both the regular output scope and a output with a FIR filter implemented.

Measurement data:

The test running in 626 seconds, where the data from the regular output scope for P2 and P4 is shown on figure A.49.

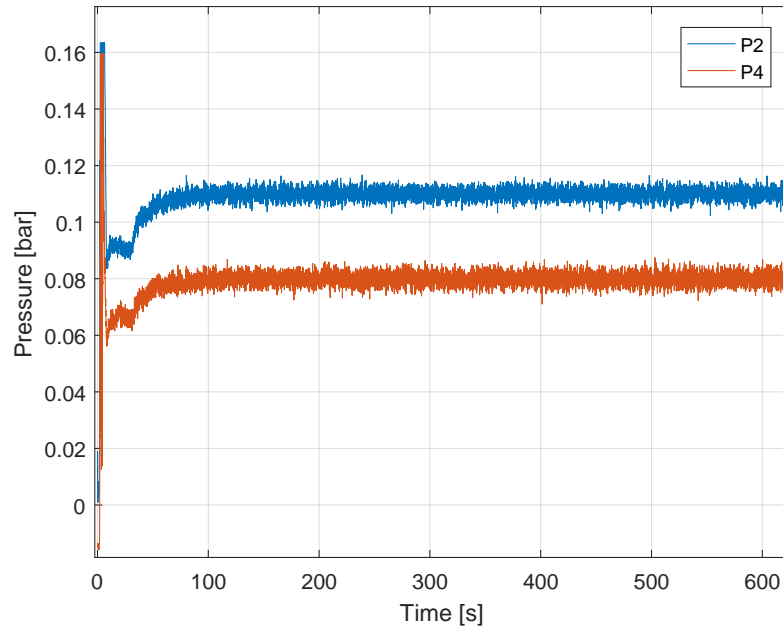


Figure A.49: Pressure at the regular outputs P2 and P4.

The output with a FIR filter implemented for P2 and P4 is shown on figure A.50.

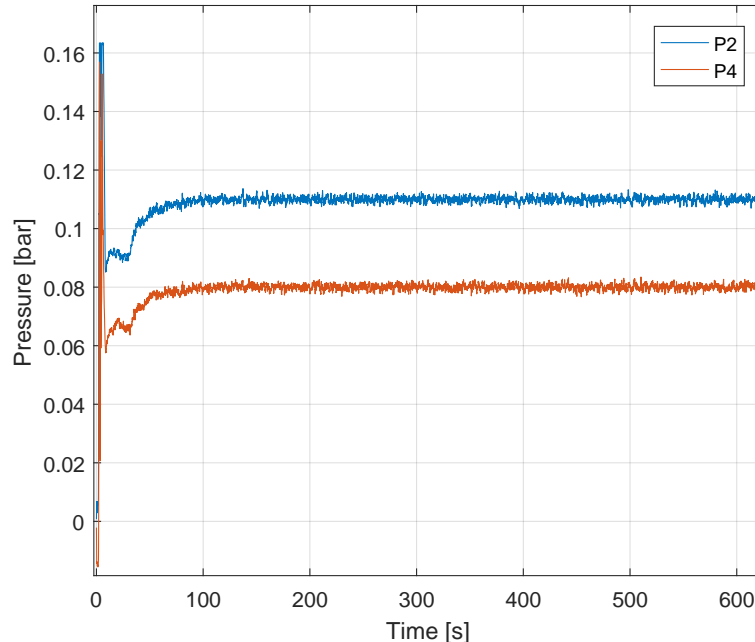


Figure A.50: Pressure at the outputs P2 and P4 with FIR filter.

Results:

The purpose of this test journal is to find out if the outputs is in between the steady state error requirement of $\pm 5\%$, therefore cutoff's of the regular output in figure A.49 and the FIR filtered output in A.50 is shown with red dashed lines, that indicate the 5% steady state error limit.

The cutoff of the regular output for P2 are shown on figure A.51, where it is seen that only a few spikes are crossing the limit, although this could be measurement noise.

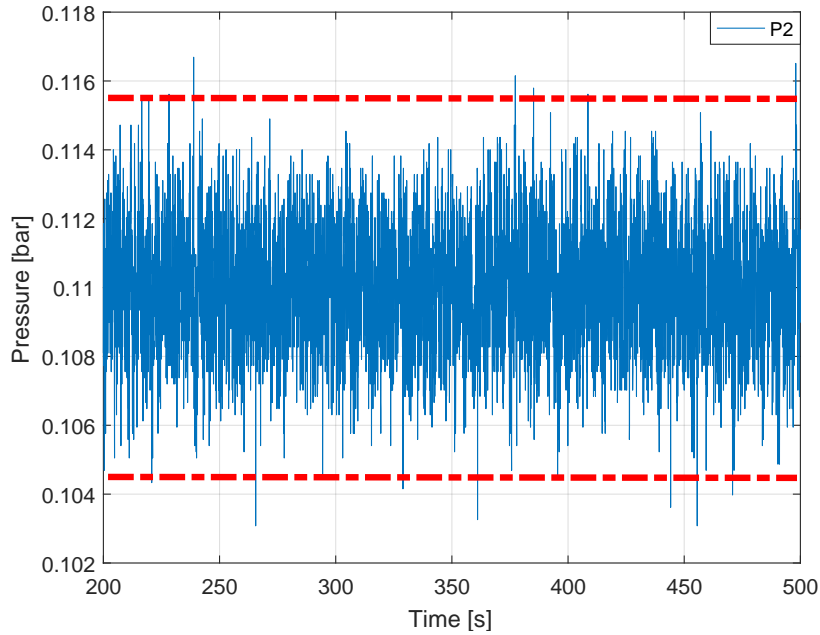


Figure A.51: Pressure at the output P2, where the red dashed lines indicate the limits.

The cutoff of the FIR filtered output for P2 are shown on figure A.52, where noise reduction done by a FIR filter is making a big difference.

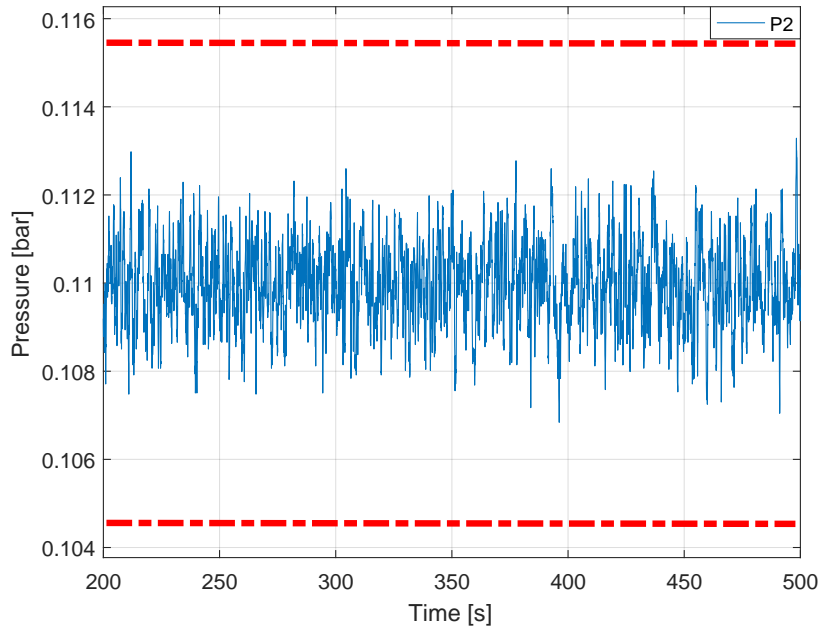


Figure A.52: Pressure at the output P2 with FIR filter, where the red dashed lines indicate the limits.

The cutoff of the regular output for P4 are shown on figure A.53, where it is seen that only a few spikes are crossing the limit, although this could be measurement noise.

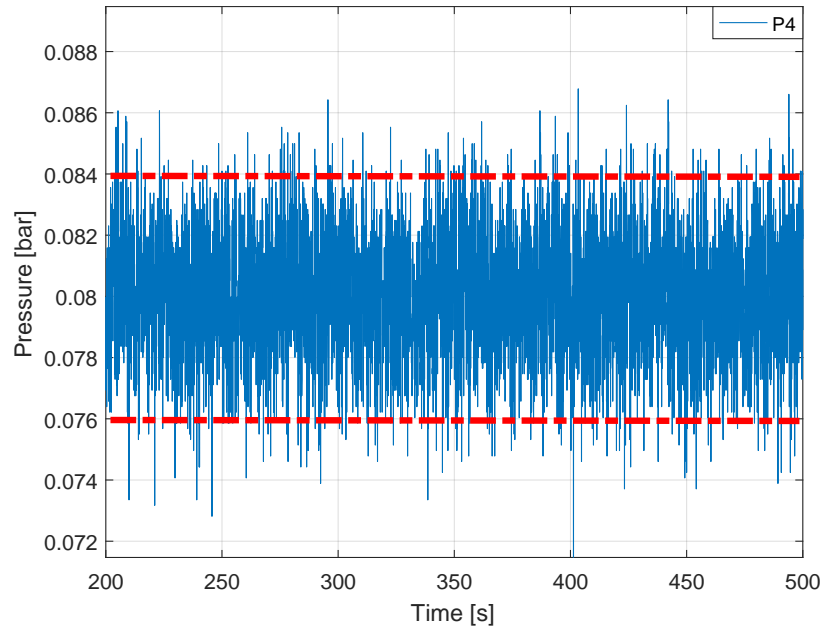


Figure A.53: Pressure at the output P4, where the red dashed lines indicate the limits.

The cutoff of the FIR filtered output for P4 are shown on figure A.54, where noise reduction done by a FIR filter is making a big difference.

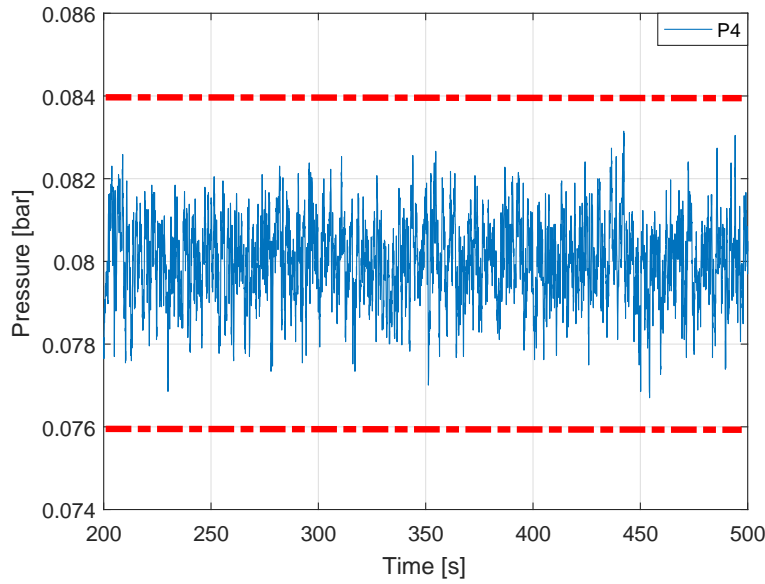


Figure A.54: Pressure at the output P4 with FIR filter, where the red dashed lines indicate the limits.

Source of error:

- Air in the system.
- Equipment tolerance.
- Noise from equipment.

- Ambient noise.

Conclusion:

In this journal four graphs with steady state limits inserted have been obtained at the outputs P2 and P4.

A.3.7 System response

Purpose:

The purpose of the journal is to document how the step response measurement were obtained for output P2 and P4. The data is used in chapter 6, section 6.2, to analyze the system response parameters such as rise time and overshoot.

Theory:

Simulink Realtime workshop on the computer, perform a step response on the physical system, by sending signals that changes the parameters of the pumps and valves, which causing a change of the pressure in the system. Sensors measures this change and relay it back to the computer and store it in a file.

Equipment list:

- The water distribution network at the Department of Electronic Systems, Section for Automation and Control (AAU no. 100911).
- MATLAB
- File: analyse_system.mdl (CD [MATLAB/analyse_system.mdl])

Measurement set up

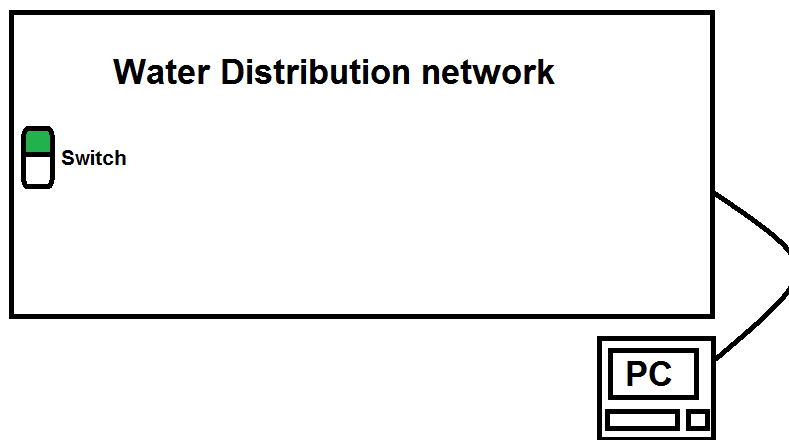


Figure A.55: Setup for the water distribution network.

Procedure:

- Turn on the water distribution network - Press the button on the wall. Green light indicate "on".
- Turn on the Computer next to the water distribution network.
- Start matlab.
- Load file: analyse_system.mdl into MATLAB. This will start simulink.
- Compile the simulink file by pressing ctrl + b.
- Start the terminal.
 - Go to the folder where the file wss_system is placed inside the the terminal.
 - Write "sudo ./analyse_system.mdl -tf inf -w"
 - Pres enter and go back to simulink.
- Connect to the physical system by pressing ctrl + t or go to the simulation button in the top and press "Connect To Target".
- Optional - Open the scope "outputs" to see the pressure output at the valves.
- Start the realtime workshop by pressing the same simulation button and pres "Start Real-Time Code".

- Now the water distribution network is "on".
- The system will startup at the design control system will regulate the outputs to their respective operation points.
- Turn the system off by pressing simulation and then "Stop Real-Time Code".
- Save the data set as a .mat file.

The setup on the host computer can be seen on figure A.48.

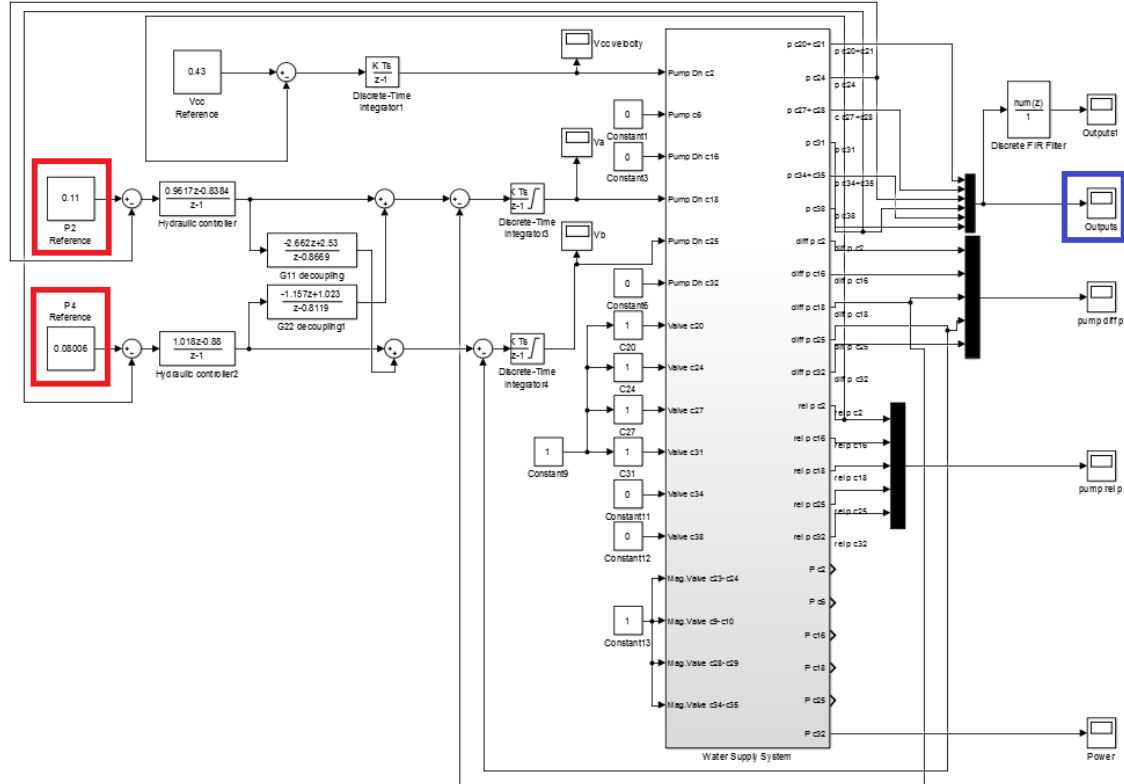


Figure A.56: Setup on the host computer, where a step is done on the reference for P2 and P4.

The red boxes on figure A.56, is the reference for the output P2 and P4, where the output scope is marked with a blue box.

Measurement data:

The test for performing a step on each reference, to see how the system response look like. First a step on the reference for P2 is performed from 0.1103 to 0.1165 bar, the output is shown in figure A.57.

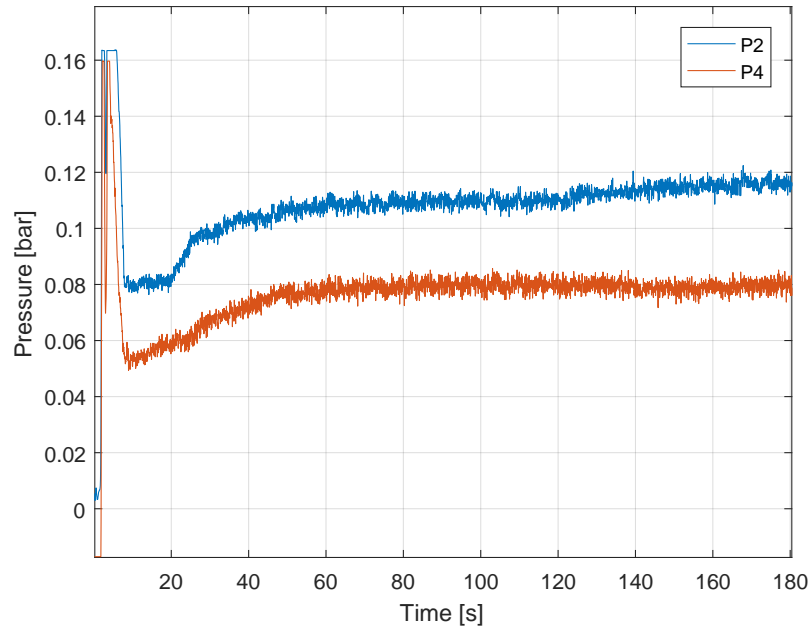


Figure A.57: Pressure at the output P2 and P4, where a step is performed at P2, while P4 is regulated to be steady.

Second test is where a step is performed on the reference for P4, a response from 0.08 to 0.08629 bar, as shown in figure A.58.

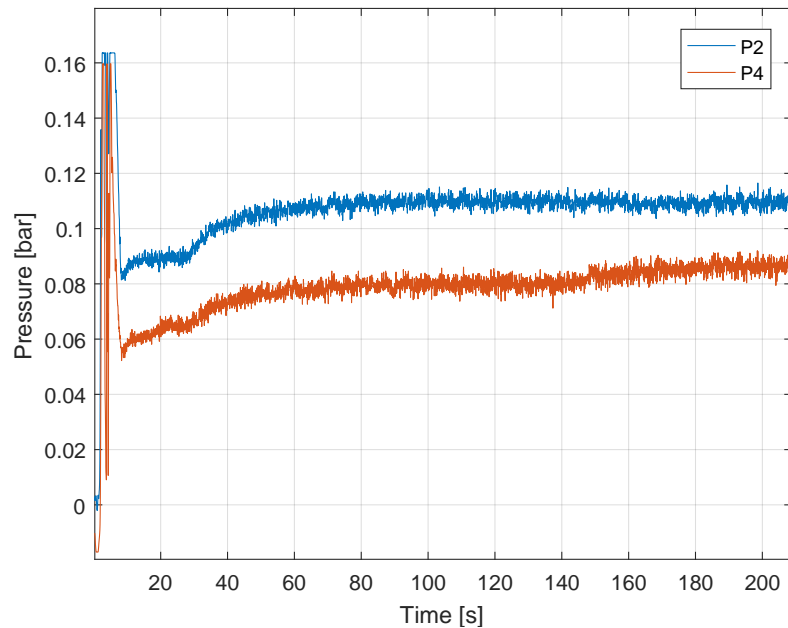


Figure A.58: Pressure at the output P2 and P4, where a step is performed at P4, while P2 is regulated to be steady.

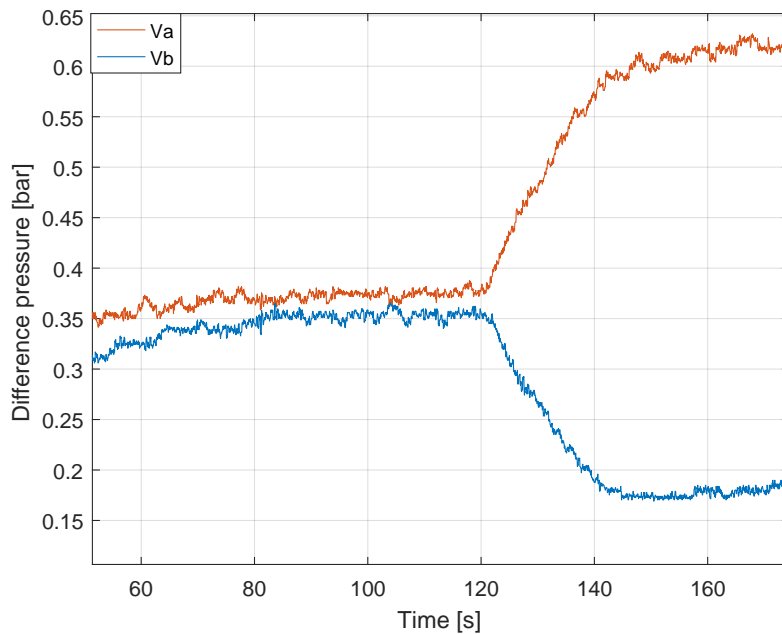


Figure A.59: Shows the decoupling when a step is applied on the output from 0.1103 to 0.1165 bar is applied to the reference value.

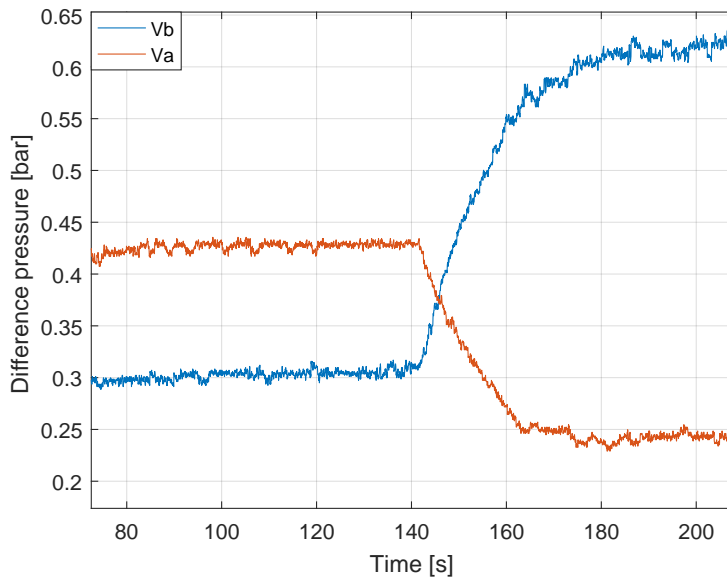


Figure A.60: Shows the decoupling when a step from 0.08 to 0.08629 bar is applied to the reference value.

Results:

The purpose of this test journal is to measure and therefore obtain the system response parameters, such as risetime, overshoot and also if the system is stable performing a step on the outputs P2 and P4.

The step for output P2 is shown in figure A.61, where the red dashed lines indicate the

5% steady state error limit for the desired pressure, which is 0.1165 bar. The green line indicate the desired pressure as the system response should reach.

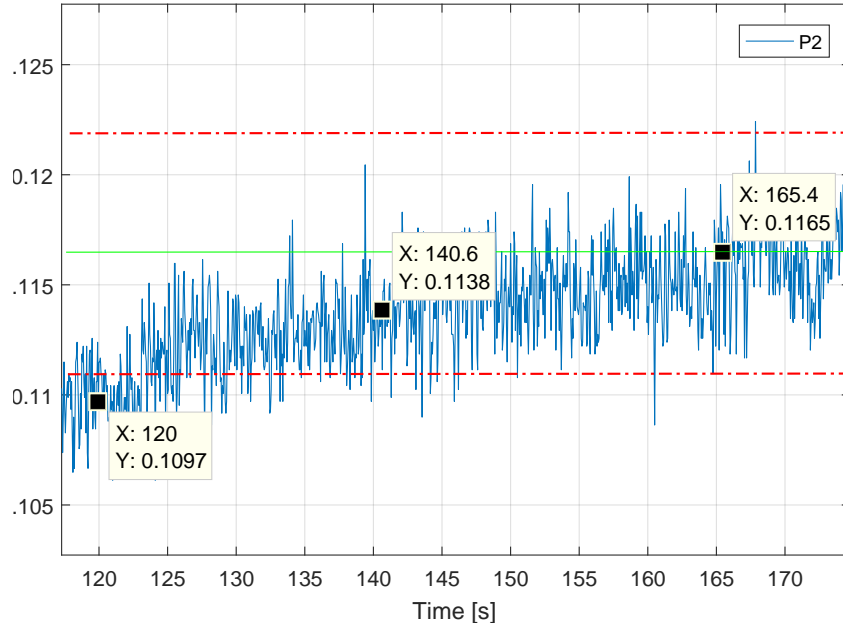


Figure A.61: Pressure at the output P2, while performing a step, the red dashed lines indicate the steady state limits.

The starting value is at 0.1103 where the step for P2 is performed at the time 120 seconds. The final/desired value is at 0.1165 at time 165.4 seconds. In equation A.188

$$\text{Increment} = \text{final value} - \text{starting value} \quad (\text{A.188})$$

$$= 0.1165 - 0.1103 \quad (\text{A.189})$$

$$= 0.0062 \quad (\text{A.190})$$

In equation A.191, the location of the time constant is found at 63% of the step response.

$$\text{Time_constant_location} = (\text{Increment} \cdot 0.63) + \text{starting value} \quad (\text{A.191})$$

$$= (0.0062 \cdot 0.63) + 0.1103 \quad (\text{A.192})$$

$$= 0.114 \quad (\text{A.193})$$

The time at 0.114 bar is approx 140.6 seconds as shown on figure A.61, the time constant τ can now be obtained:

$$\tau = \tau_{\text{time}} - \text{start}_{\text{time}} \quad (\text{A.194})$$

$$= 140.6 - 120 \quad (\text{A.195})$$

$$= 20.6 \text{ s} \quad (\text{A.196})$$

The rise time for the output P2 can then be found from the time constant:

$$t_r = \tau \cdot (\ln(0.9) - \ln(0.1)) \quad (\text{A.197})$$

$$= 20.6 \cdot (\ln(0.9) - \ln(0.1)) \quad (\text{A.198})$$

$$= 45.263 \text{ s} \quad (\text{A.199})$$

The rise time for output P2 is found to be approx 45.263 seconds from the response to reach 0.1165 bar from a starting pressure at 0.1103. the system response do not have overshoot and from the measurement is a nice stable response.

The step for output P4 is shown in figure A.62, where the red dashed lines indicate the 5% steady state error limit for the desired pressure, which is 0.1165 bar. The green line indicate the desired pressure as the system response should reach.

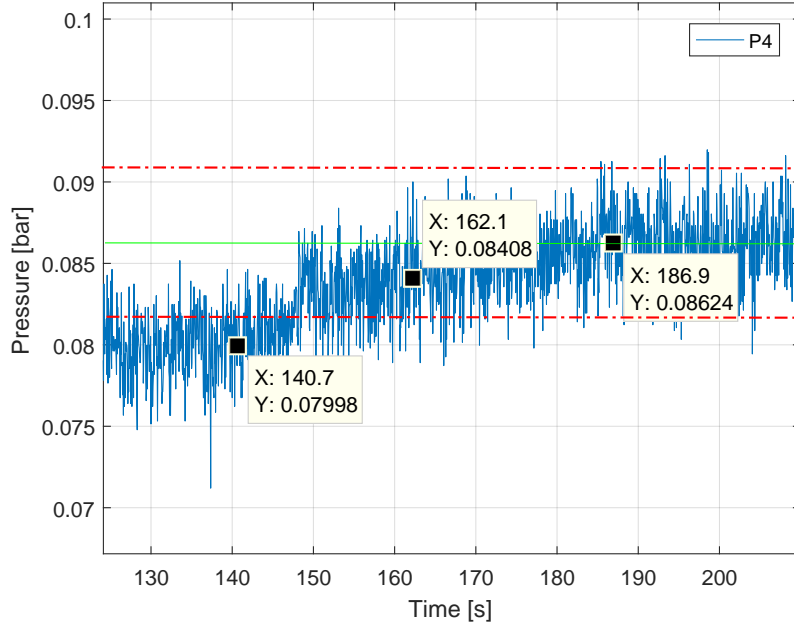


Figure A.62: Pressure at the output P4, while performing a step, the red dashed lines indicate the steady state limits.

The starting value is at 0.008 where the step for P4 is performed at the time 140 seconds. The final/desired value is at 0.08629 at time 186.9 seconds. In equation A.200

$$\text{Increment} = \text{final value} - \text{starting value} \quad (\text{A.200})$$

$$= 0.08629 - 0.08 \quad (\text{A.201})$$

$$= 0.00629 \quad (\text{A.202})$$

In equation A.203, the location of the time constant is found at 63% of the step response.

$$\text{Time_constant_location} = (\text{Increment} \cdot 0.63) + \text{starting value} \quad (\text{A.203})$$

$$= (0.00629 \cdot 0.63) + 0.08 \quad (\text{A.204})$$

$$= 0.084 \quad (\text{A.205})$$

The time at 0.084 bar is approx 162 seconds as shown on figure A.62, the time constant τ can now be obtained:

$$\tau = \tau_{\text{time}} - \text{start}_{\text{time}} \quad (\text{A.206})$$

$$= 162 - 140 \quad (\text{A.207})$$

$$= 22 \text{ s} \quad (\text{A.208})$$

The rise time for the output P4 can then be found from the time constant:

$$t_r = \tau \cdot (\ln(0.9) - \ln(0.1)) \quad (\text{A.209})$$

$$= 22 \cdot (\ln(0.9) - \ln(0.1)) \quad (\text{A.210})$$

$$= 48.339s \quad (\text{A.211})$$

The rise time for output P2 is found to be approx 48.339 seconds from the response to reach 0.08629 bar from a starting pressure at 0.08. the system response do not have overshoot and from the measurement is like P2 a nice stable response.

On figure A.59 the functionality of the decoupling is shown. It can be seen that when a step is performed on the output for P2, the difference pressure for Va is being compensated by Vb. The counter acting in the decoupling tries to keep the output pressure at P4 constant when the other output P2 is increasing to the new reference value. The output is shown on figure A.57.

The same is shown in figure A.60 just with a step applied to the reference value to P4. The output can be seen on figure A.58.

Source of error:

- Air in the system.
- Equipment tolerance.
- Noise from equipment.
- Ambient noise.

Conclusion:

In this journal two graphs with the system response for the output P2 and P4 have been obtained. This journal also shows the functionality of decoupling, which can be concluded to work.